

IMPLEMENTATION OF EUROCODES

HANDBOOK 5

DESIGN OF BUILDINGS FOR THE FIRE SITUATION



**Guide to basis of structural reliability and risk engineering
related to Eurocodes supplemented by practical examples**



LEONARDO DA VINCI PILOT PROJECT CZ/02/B/F/PP-134007

**DEVELOPMENT OF SKILLS FACILITATING IMPLEMENTATION
OF EUROCODES**



LEONARDO DA VINCI PILOT PROJECT CZ/02/B/F/PP-134007

DEVELOPMENT OF SKILLS FACILITATING IMPLEMENTATION OF EUROCODES

HANDBOOK 5

DESIGN OF BUILDINGS FOR THE FIRE SITUATION

PARTNERSHIP:

The Klokner Institute of the Czech Technical University in Prague (KI CTU),
convener, Prof. Milan Holický, Czech Republic
The Czech Chamber of Certified Engineers and Technicians Engaged in Construction
(CKAIT), Prof. Alois Materna, Czech Republic,
The Institute of Steel Constructions of the University of Technology Aachen (RWTH),
Prof. Gerhard Sedlacek, Germany, in cooperation with
Prof. Jean-Baptiste Schleich, Luxembourg
The Spanish Organisation for Scientific Research (IET), Spain, Dr. Angel Arteaga
The University of Pisa (UOP), Prof. Luca Sanpaolesi, Italy
The Netherlands Organisation for Applied Scientific Research (TNO), Prof. Ton
Vrouwenvelder, Netherlands
The Institute for Metal Constructions (IMK), Dr. Igor Kovse, Slovenia
The Building Research Establishment (BRE), Prof. Haig Gulvanessian, United
Kingdom

Luxembourg 10/2005

LEONARDO DA VINCI PILOT PROJECT CZ/02/B/F/PP-134007
DEVELOPMENT OF SKILLS FACILITATING IMPLEMENTATION
OF EUROCODES

HANDBOOK 5

DESIGN OF BUILDINGS FOR THE FIRE SITUATION

I	FIRE ACTIONS IN BUILDINGS (Pages I-1 to I-81)	
	Summary	I-1
1	INTRODUCTION	I-4
	1.1 General principles for conventional fires	I-4
	1.2 General principles for natural fires	I-7
	1.3 Methodology	I-14
2	CHARACTERISTICS OF THE FIRE COMPARTMENT	I-17
	2.1 Introduction	I-17
	2.2 Boundary elements of the compartment	I-17
	2.3 Thermal characteristics of boundaries	I-18
	2.4 Opening characteristics	I-19
	2.5 Mechanical ventilation	I-21
3	CHARACTERISTICS OF THE FIRE	I-22
	3.1 Introduction	I-22
	3.2 Fire load	I-22
	3.3 Type of fire	I-24
	3.4 Rate of heat release	I-25
	3.5 Design RHR evolution	I-26
	3.6 Experimental data	I-29
4	FIRE DEVELOPMENT MODELS	I-30
	4.1 Pre-flashover fires	I-30
	4.2 Fully developed fires	I-35
	4.3 Combination of 1-zone and 2-zone models	I-40
5	HEAT TRANSFER MODELS	I-43
	5.1 Heat flux	I-43
	5.2 Temperature development inside structural members	I-44
6	STRUCTURAL MODELS	I-50
	6.1 Introduction	I-50
	6.2 Mechanical actions	I-51
	6.3 Tabulated data	I-53
	6.4 Simple calculation models	I-59
	6.5 Advanced calculation models	I-72
	REFERENCES	I-79

II	ACCIDENTAL COMBINATIONS IN CASE OF FIRE (Pages II-1 to II-14)	
1	INTRODUCTION	II-1
1.1	Background documents	II-1
1.2	General principles	II-1
2	FUNDAMENTAL CASES OF STRUCTURAL RELIABILITY	II-2
2.1	General	II-2
2.2	Evaluation of the combination factor ψ for actions	II-2
	REFERENCES	II-8
	ATTACHMENT	II-10
III	CALIBRATION OF RELIABILITY PARAMETERS (Pages III-1 to III-30)	
1	INTRODUCTION	III-1
1.1	Background documents	III-1
1.2	General principles	III-1
2	FULL PROBABILISTIC APPROACH	III-3
2.1	General presentation	III-3
2.2	Applied structural safety on the basis of the probabilistic approach	III-7
3	SEMI-PROBABILISTIC APPROACH	III-14
3.1	Calibration of the global factor related to the fire load	III-14
3.2	Calibration of partial and differentiation factors related to the risk of fire activation and to the active fire safety measures	III-22
	REFERENCES	III-30
IV	LIFE SAFETY CONSIDERATIONS (Pages IV-1 to IV-9)	
1	INTRODUCTION	IV-1
1.1	Background documents	IV-1
1.2	General principles	IV-1
2	BAYESIAN NETWORK APPLIED TO LIFE SAFETY	IV-1
2.1	Introduction	IV-1
2.2	Probabilistic concepts	IV-2
2.3	Bayesian network	IV-3
2.4	Risk assessment	IV-6
2.5	Conclusions	IV-8
	REFERENCES	IV-8
V	PROPERTIES OF MATERIALS (PAGES V-1 to V-28)	
1	INTRODUCTION	V-1
2	THERMAL PROPERTIES OF CONCRETE	V-2
2.1	Normal weight concrete	V-2
2.2	Lightweight concrete	V-4
2.3	Density	V-4
3	THERMAL PROPERTIES OF STEEL	V-5
4	MECHANICAL PROPERTIES OF CONCRETE	V-7

4.1	Strength and deformation properties of concrete	V-7
4.2	Concrete stress-strain relationships adapted to natural fires with a decreasing heating branch for use in advanced calculation models	V-10
5	MECHANICAL PROPERTIES OF STEEL	V-11
5.1	Strength and deformation properties of structural steel	V-11
5.2	Strength and deformation properties of reinforcing steels	V-16
6	DETERMINATION OF MATERIAL PROPERTIES BY NUMERICAL SIMULATION OF REAL TESTS	V-15
6.1	Application to the thermal properties of concrete	V-15
6.2	Application to the mechanical properties of steel	V-25
	REFERENCES	V-28

VI EXAMPLE OF REINFORCED CONCRETE STRUCTURE (PAGES VI-1 to VI-13)

	Summary	VI-1
1	INTRODUCTION	VI-1
2	DESIGN CONDITIONS	VI-1
2.1	Building characteristics	VI-1
2.2	Structural characteristics	VI-2
2.3	Definition of the limit state equation	VI-2
2.4	Combination of actions	VI-3
3	DESIGN FIRE	VI-5
3.1	National requirements	VI-5
3.2	Equivalent time of fire exposure	VI-5
4	FIRE RESISTANCE DESIGN	VI-7
4.1	Tabulated data design	VI-7
4.2	Temperature analysis	VI-8
4.3	Cross-section resistance	VI-9
4.4	Conclusions	VI-13
	REFERENCES	VI-13

VII EXAMPLES OF STEEL AND COMPOSITE STRUCTURES (PAGES VII-1 to VII-48)

1	INTRODUCTION	VII-1
2	ISOLATED STRUCTURAL ELEMENTS	VII-5
2.1	Heating according to the standard fire	VII-5
2.2	Heating according to natural fires	VII-10
3	FRAME ANALYSIS FOR NATURAL FIRES	VII-18
3.1	School Campus "Geesseknäppchen" in Luxembourg	VII-18
3.2	Frame with composite columns and composite beams	VII-21
4	APPLICATION OF THE SEMI-PROBABILISTIC APPROACH	VII-23
4.1	Essentials	VII-23
4.2	Comparison between deterministic and semi-probabilistic approach	VII-24
4.3	Global fire safety concept applied to Banque Populaire	VII-39
4.4	Global fire safety concept applied to Chambre de Commerce	VII-43
	REFERENCES	VII-47

VIII CASE STUDIES OF REAL FIRES (PAGES VIII-1 to VIII-17)

1	INTRODUCTION	VIII-1
1.1	The great Lisbon fire - 1.11.1755	VIII-1
1.2	The great Boston fire - 20.3.1760	VIII-3
1.3	The great Chicago fire - 8.10.1871	VIII-4
2	RECENT CONFLAGRATIONS	VIII-6
2.1	Great fire, Chiado: Historical centre of Lisbon - 28.8.1987	VIII-6
2.2	Great fire, Duesseldorf Airport - 11.4.1996	VIII-9
2.3	Great fire, Göteborg Disco - 30.10.1998	VIII-12
2.4	Great fire, Windsor tower Madrid - 12.2.2005	VIII-15
2.5	Endless list.....	VIII-16
	REFERENCES	VIII-17

IX AVAILABLE SOFTWARE (PAGES IX-1 to IX-3)

	Summary	IX-1
1	FIRE RESISITANCE MODELS	IX-1
1.1	Simple calculation models	IX-1
1.2	Advanced calculation models	IX-2
2	FIRE DEVELOPMENT MODELS	IX-2
2.1	Simplified fire model	IX-2
2.2	Advanced fire model	IX-2
3	PROBABILISTIC MODEL	IX-2
	REFERENCES	IX-3

FOREWORD

The Leonardo da Vinci Pilot Project CZ/02/B/F/PP-134007, “Development of Skills Facilitating Implementation of Structural Eurocodes” addresses the urgent need to implement the new system of European documents related to design of construction works and products. These documents, called Eurocodes, are systematically based on recently developed Council Directive 89/106/EEC “The Construction Products Directive” and its Interpretative Documents ID1 and ID2. Implementation of Eurocodes in each Member State is a demanding task as each country has its own long-term tradition in design and construction.

The project should enable an effective implementation and application of the new methods for designing and verification of buildings and civil engineering works in all the partner countries (CZ, DE, ES, IT, NL, SI, UK) and in other Member States. The need to explain and effectively use the latest principles specified in European standards is apparent from various enterprises, undertakings and public national authorities involved in construction industry and also from universities and colleges. Training materials, manuals and software programmes for education are urgently required.

The submitted Handbook 5 is one of 5 upcoming handbooks intended to provide required manuals and software products for training, education and effective implementation of Eurocodes:

- Handbook 1: Basis of Structural Design
- Handbook 2: Reliability Backgrounds
- Handbook 3: Load Effects for Buildings
- Handbook 4: Load Effects for Bridges
- Handbook 5: Design of Buildings for the Fire Situation

It is expected that the Handbooks will address the following intents in further harmonisation of European construction industry

- reliability improvement and unification of the process of design;
- development of the single market for products and for construction services;
- new opportunities for the trained primary target groups in the labour market.

The Handbook 5 is based on structural reliability and risk engineering related to Eurocodes. The following topics are treated in particular:

- fire actions in buildings,
- accidental combinations in case of fire,
- calibration of reliability parameters,
- life safety considerations,
- properties of materials,
- examples of concrete structures,
- examples of steel and composite structures,
- case studies of real fires.

A CD added to this Handbook 5 provides a review of the available software frequently used in the text. The Handbook 5 is written in a user-friendly way employing only basic mathematical tools.

A wide range of potential users of the Handbooks and other training materials includes practising engineers, designers, technicians, officers of public authorities, young people - high school and university students. The target groups come from all territorial regions of the partner countries. However, the dissemination of the project results is foreseen to be spread into the other Member States of CEN and other interested countries..

CHAPTER I – FIRE ACTIONS IN BUILDINGS

Jean-Baptiste Schleich¹

¹ University of Technology Aachen, University of Liège

Summary

In addition to Chapter IV “General principles of fire safety-ID2” of Handbook 1 “Basis of structural design”, the objective of this handbook is to describe a performance based more realistic and credible approach to the analysis of structural safety in case of fire, which takes account of real fire characteristics and of active fire fighting measures .

This very general procedure, called “Global Fire Safety Concept” considers the following steps:

- take into account the building characteristics relevant to fire growth and its development: fire scenario, fire load, pyrolysis rate, compartment type, and ventilation conditions (see paragraphs 2 to 4),
- quantify the risk of a fire starting function of the size of the fire compartment considered and of the occupancy and take account of the influence of active fire fighting measures; this risk analysis is based on existing statistical data of real fires and on probabilistic procedures (see Chapter III),
- from the previous step establish the design value for the main parameter i.e. the fire load,
- determine the design heating curve as a function of the design fire load that takes implicitly into account the fire risk,
- simulate the global behaviour of the structure submitted to the design heating curve in combination with the static loads in case of fire (see paragraph 6 and Chapter VII),
- deduce the design fire resistance time $t_{fi,d}^{nat}$; this may often be unlimited when the structure is able to support the static loads beyond the end of the natural fire,
- verify the safety of the structure by comparing the design fire resistance time $t_{fi,d}^{nat}$ with the required time $t_{fi,requ}$ depending as well on the evacuation time for occupants as on the consequences of a failure; in most cases the required time $t_{fi,requ}$ is presently imposed in a prescriptive way by National Authorities.

This new concept has been applied to many new projects in Belgium, France, Italy, Luxembourg, The Netherlands, Spain, Switzerland, United Kingdom etc ; some of these newly constructed buildings are explained in detail in Chapters VI and VII.

It should be also underlined that the “Global Fire Safety Concept” is fully in line with the Interpretative Document on the Essential Requirement N°2 “Safety in case of fire” dated 1994 and fulfils the Commission Recommendation on the implementation and use of Eurocodes issued in 2003 [22, 51].

Furthermore a natural fire exposure is explicitly allowed to be used according to 5.1.4(3) of the Eurocode EN1990 [44] :

"The behaviour of the structure exposed to fire should be assessed by taking into account either nominal fire exposure, or modelled fire exposure as well as the accompanying actions. "

Finally explicit fire exposures are given in 3.1(10) of EN1991-1-2, [46]:

" Gas temperatures θ_g may be adopted as nominal temperature-time curves according to 3.2, or adopted according to the fire models in 3.3. "

This new approach is leading to both financial profits and enhanced safety. Instead to fulfil prescriptive ISO – fire resistance requirements, it is logical to focus on the active fire fighting measures that provide protection for people such as smoke detection, acoustic alarm, safe escape routes, automatic alarm transmission to the fire brigade, smoke exhaust systems and sprinklers.

The safety of people being ensured in an optimal way, the structure itself will of course also benefit from those measures that primarily aim to save occupants. Hence, costs needed to guarantee the stability of the structure in case of fire may be substantially reduced.

This new concept, illustrated in figures 1 & 2, has been elaborated through a long lasting and quite successful research effort undertaken in the field of fire resistance of structures since 1985 [32, 33, 36, 42, 47, 52]. It has been developed through a new methodology on the basis of statistical data and probabilistic procedures. This method, which may be used for all structural materials and for all types of buildings, is described in the following chapters.

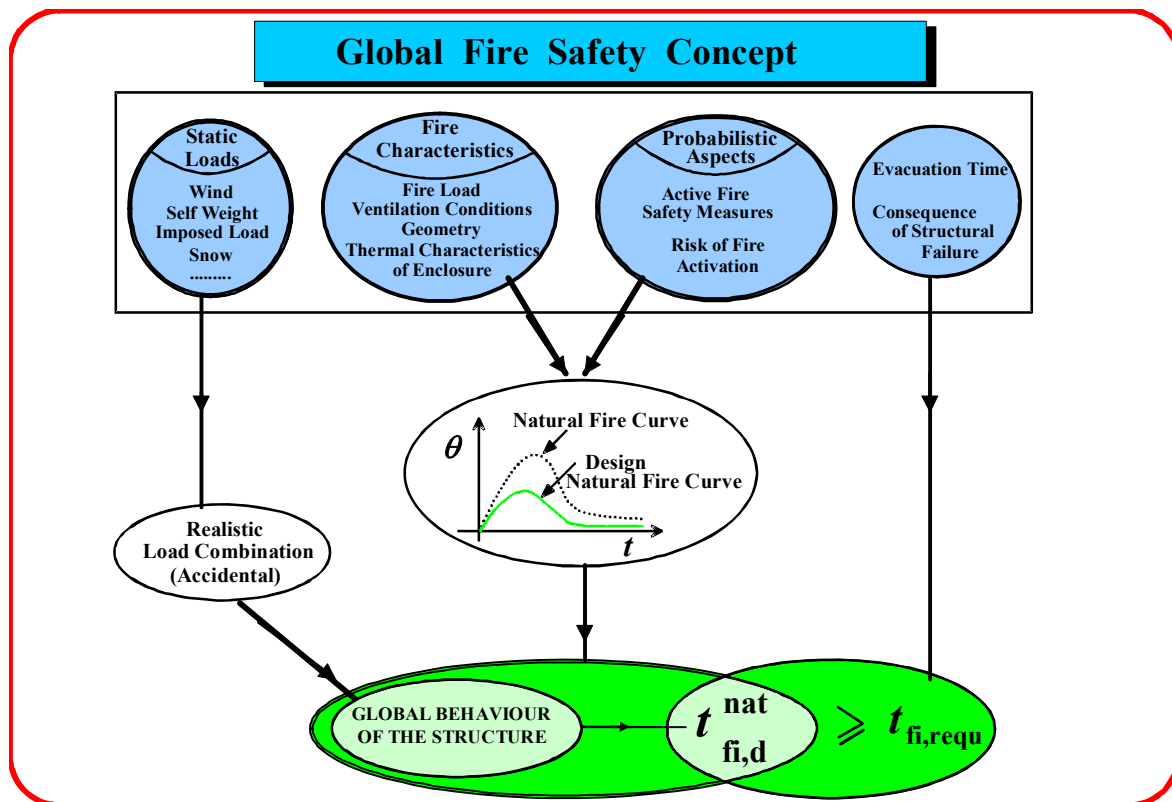


Figure 1. Successive steps of the " Global Fire Safety Concept ".

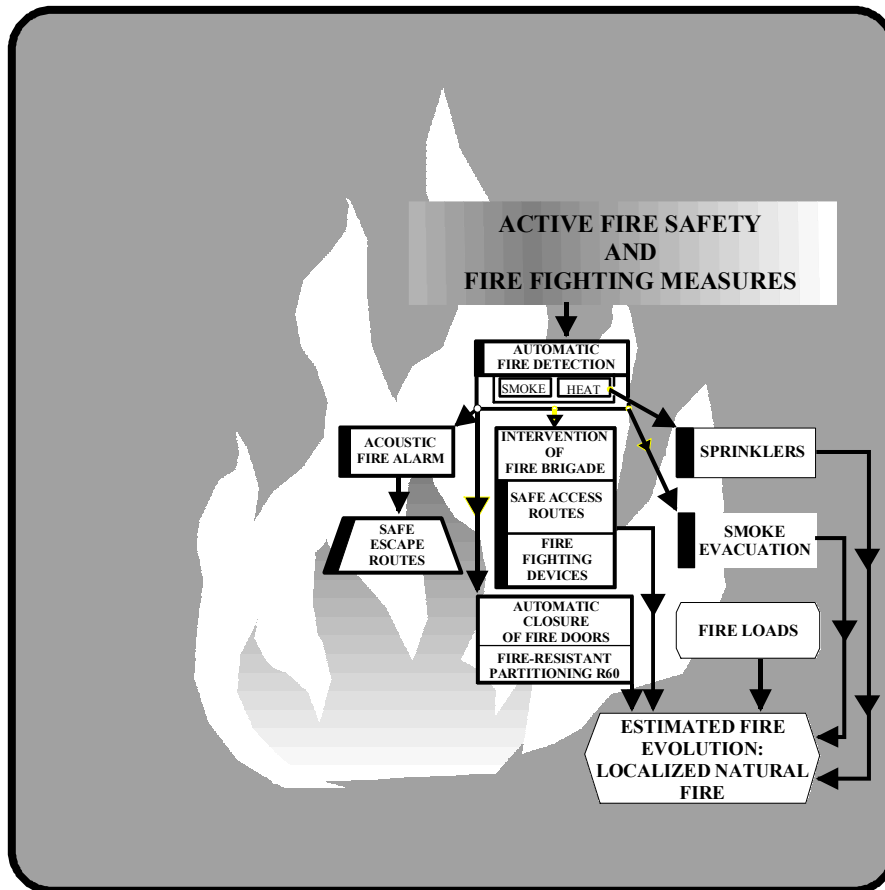


Figure 2. Active fire safety.

1 INTRODUCTION

1.1 General principles for conventional fires

In the sixties a number of dramatic fires, such as the fire at the supermarket “Innovation” in Brussels and the fire at the discotheque 'Le Cinq Sept' in Saint-Laurent-du-Pont in France, stimulated the drawing up of new regulations in European countries.

Those regulations specified

- the escape ways by prescribing the number of emergency exits, the characteristics of the exit signs, the number of staircases and the width of the doors,
- the prevention of fire spread by referring to the concepts of "fire resistance" and "reaction to fire":
 - compartments are limited by fire resistant walls and doors, the size of compartments is limited, minimum sill heights of windows are given in order to avoid fire spread from floor to floor,
 - the reaction to fire allows to limit the contribution of the material, within a given compartment, to the fire development,
- the fire resistance of the structure in terms of ISO-fire resistance periods, R30, 60, 90 or 120,
- the conditions for smoke and heat exhaust,
- the implementation of active fire fighting measures such as the number of hand extinguishers, smoke detectors and sprinklers,
- the access conditions for the fire brigade.

Each country defined its regulations generally based on its own perception of the fire safety problem. Which means that these prescriptive requirements have been based on historical considerations, experience, real fire lessons and mainly expert judgement. The main parameters influencing these requirements are the height of the building, the number of occupants and the type of occupancy.

Even if the general notions of fire safety are similar everywhere in Europe, the requirements concerning the ISO-fire resistance period vary in a substantial way from country to country. Figure 3 gives the structural requirements based on the standard fire, according to ISO-834, for different types of buildings as compiled in [47].

For example for a commercial centre with a single storey the required ISO-fire resistance is varying from R0 in Switzerland to R90 in Spain. In case of a medium rise office building protected by sprinklers the required ISO-fire resistance is R60 in the Netherlands, whereas it amounts to R120 in Finland.

Present regulations do not take proper account f.i. of the influence of sprinklers in suppressing or extinguishing the fire. Figure 3 shows that the present requirements are generally identical whether sprinklers are foreseen or not.

It is however known that the standard fire exposure, according to ISO-834 leads to a gas temperature θ in the fire compartment in °C which depends only on the elapsed time t in minutes.

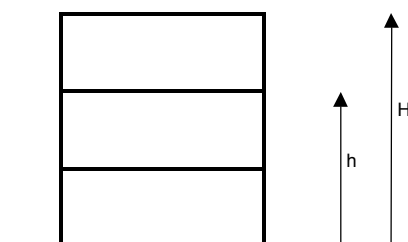
This standard temperature-time curve involves an ever increasing air temperature inside the considered compartment, even when later on all consumable materials have been destroyed. The application of this standard fire necessarily gives rise to important discrepancies in the fire resistance requirements existing in different countries for the same type of building like open car parks [20]. Furthermore it may be useful to know, that this so-called "standard and well defined fire" leads to a warming up of the structural element depending on the type of furnace used in order to perform the ISO fire test. Indeed, radiation conditions inside test furnaces have never been harmonised!

Chapter I – Fire actions in buildings

Minimum Periods (minutes) for elements of structure																		
in the following building types									according to the regulations of									
Building type	n	h	H	X	L	b	x(*)	S	B	CH	D	F	I	L	NL	FIN	SP	UK
Industrial Hall	1	0	10	20	100	50	2	YES	0	0	0	30 *2	0/60 (7)	0	0	0	-	0 *1
								NO	0	(1) *3	(1)	30 *2	30/90 (7)	0-60	0	0	-	0 *1
Commercial center and shop	1	0	4	500	80	80	4	YES	0	0	0	0 H 30 V	60/90 (7)	30	0	0	90	0 *1
								NO	(1)	(1) *3	(1)	30	90/120 (7)	(3)	0	30	90	0 *1
Dancing	2	5	9	1000	60	30	4	YES	0	0	(2)	60	(8) (9)	30	0	60 (4)	90	30
								NO	0	30	90	60	60	30	0	60 (5)	90	60
School	4	12	16	300	60	20	4	YES	60 (6)	0 30 *3	(2)	60	(8) (10)	90	60	60 (4)	60	60
								NO	60 (6)	60	90	60	60	90	60	60 (5)	60	60
Small rise Office Building	4	10	13	50	50	30	2	YES	60 (6)	0 30 *3	(2)	60	(8) (9)	90	60	60 (4)	60	30
								NO	60 (6)	(1) *3	90	60	60	90	60	60 (5)	60	60
Hotel	6	16	20	60	50	30	2	YES	60 (6)	30 60 *3	(2)	60	(8) (11)	90	60	60 (4)	90	60
								NO	60 (6)	60	90	60	60	90	60	60 (5)	90	60
Hospital	8	24.5	28	60	70	30	2	YES	120	60	(2)	60	(8) (12)	90/120	120	60 (4)	120	90
								NO	120	90	90	60	120	120	120	60 (5)	120	90
Medium rise Office Building	11	33	37	50	50	30	2	YES	120	60 90 *3	(2)	120	(8) (9)	90	60	120 (4)	120	120
								NO	120	90	90	120	90	120	90	120 (5)	120	(3)
High rise Office Building	31	90	93	100	50	50	2	YES	120	90	90	120	(8) (9)	120	90	120 (4)	120	120
								NO	120	90 (3)	(3)	120	120	(3)	90	120 (5)	120	(3)

n = Number of storeys, ground level included
 h = Height of top floor above ground
 H = Height of the roof above ground level
 X = Number of people to be evacuated by storey
 L = Length of the compartment
 b = Width of the compartment
 x = Number of exit routes (* indicate your requirement, in case of no requirement the values beneath may be considered)
 S = Sprinkler

- (1) compartment size too large
- (2) no regulation adopted
- (3) not allowed
- (4) $q > 600 \text{ MJ/m}^2$ floor
- (5) $q < 600 \text{ MJ/m}^2$ floor
- (6) new buildings + extension or structural charges of existing buildings
Periods usually required by local authority
(there'snt still national regulations)
- (8) Sprinkler is a possible alternative to other requirements
(case by case by authority)
- (9) Required for $q > 920 \text{ MJ/m}^2$
- (10) Required in underground rooms for $q > 550 \text{ MJ/m}^2$
- (11) Required over 1000 beds
- (12) Required over 300 beds



- *1 Roof structure & structure only supporting roof requires no fire resistance. Therefore single storey building structure normally has no requirement.
- *2 If $H < 10\text{m}$: no requirements (R0)
- *3 To be checked with SIA Doc 81

For FINLAND: for load bearing structures, not for separating structures
 For FRANCE : H = horizontal roof structure
 V = column

Figure 3. ISO-fire resistance requirements in Europe.

According to 3.2 of EN 1991-1-2, [46], conventional or nominal fires can be expressed by a simple formula and are assumed to be identical whatever is the size or the design of the building. Nominal fires are mainly the standard fire according to ISO-834 as given hereafter, the external fire used only for external walls, reaching practically a constant temperature of 680°C after 30 min and the hydrocarbon fire reaching practically a constant temperature of 1100°C after 30 min (see figure 4). They have to be used in order to prove that an element has the required level of fire resistance to fulfil national or other requirements expressed in terms of fire rating related to one of these nominal fires.

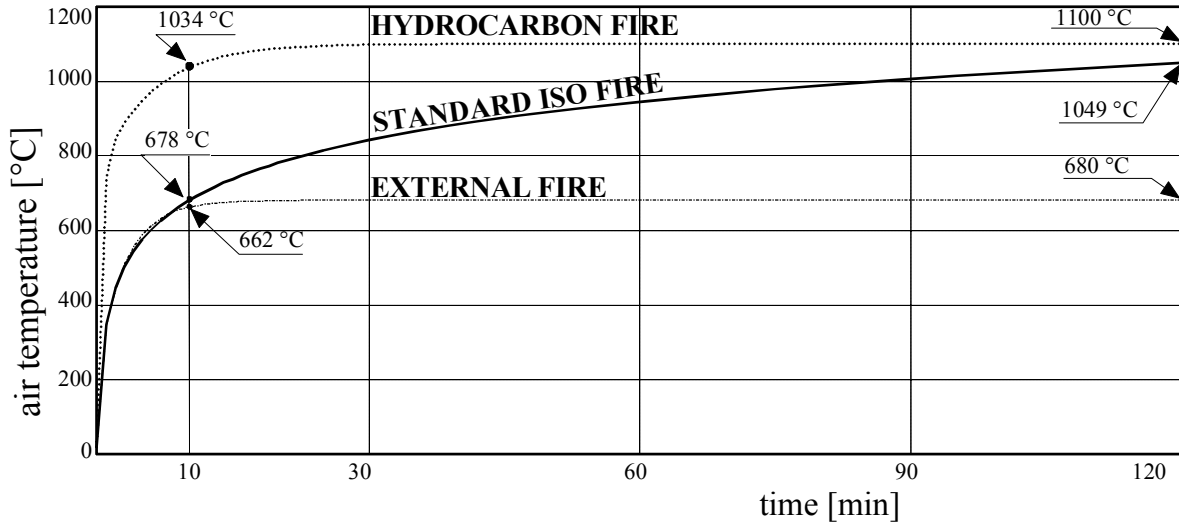


Figure 4 . Nominal temperature-time curves according to EN1991-1-2, [4].

The standard temperature-time curve is given by:

$$\Theta_g = 20 + 345 \log_{10} (8 t + 1)$$

where

Θ_g is the gas temperature in the fire compartment [°C]

t is the time [min].

The coefficient of heat transfer by convection in case of the standard temperature-time curve is:

$$\alpha_c = 25 \text{ [W/m}^2\text{K]}.$$

The external fire curve is given by :

$$\Theta_g = 660 (1 - 0,687 e^{-0,32 t} - 0,313 e^{-3,8 t}) + 20$$

where

Θ_g is the gas temperature near the member [°C]

t is the time [min].

The coefficient of heat transfer by convection in case of the external fire curve is:

$$\alpha_c = 25 \text{ [W/m}^2\text{K]}.$$

The hydrocarbon temperature-time curve is given by :

$$\Theta_g = 1\,080 (1 - 0,325 e^{-0,167 t} - 0,675 e^{-2,5 t}) + 20$$

where

Θ_g is the gas temperature in the fire compartment [$^{\circ}\text{C}$]

t is the time [min].

The coefficient of heat transfer by convection in case of the hydrocarbon temperature-time curve is:

$$\alpha_c = 50 \text{ [W/m}^2\text{K]}.$$

It has to be understood that these nominal fires correspond to a fully developed fire which means that the corresponding compartment is fully engulfed in fire. This clearly indicates that nominal fires do not correspond to any real fire situation, but practically exist only during fire tests in standard furnaces.

Hence the ISO-834 fire has to be ignored in any fire safety engineering.

1.2 General principles for natural fires

1.2.1 General

Fire resistance requirements should however be based on all parameters influencing the fire growth and its development such as:

- the probability of fire occurrence, the fire spread and its duration, the amount and distribution of the fire load, the severity of the fire i.e. the rate of heat release,
- the ventilation conditions,
- the size and geometry of the fire compartment,
- the importance of the structural element for the global stability of the whole structure,
- the evacuation conditions,
- the safety of the rescue teams,
- the risk for the neighbouring buildings and
- the active fire fighting measures.

A performance based analysis of the structural safety in case of fire considers all these physical factors in a systematic way i.e. active fire fighting measures and real fire characteristics are taken into account. This permits to evaluate for each compartment within a given building the natural fire curve to be used when designing for the fire situation.

Figure 5 shows a comparison between possible natural fire curves according to real fire tests with different values related to the compartment size, the fire loads etc and the standard ISO-fire curve. This demonstrates the difficulty in understanding the behaviour of elements in case of real fires, as such a real fire includes according to figure 6:

- ignition followed by a smouldering phase with very low temperatures and a duration that is difficult to estimate,
- a growing phase called pre-flashover with a localised fire and a duration depending mainly on the characteristics of the compartment; the fire remains localised up to a possible flashover,
- a flashover which represents the sudden outburst of the fire in the whole compartment; this phase is generally very short,
- a post flashover fire which corresponds to a fully developed fire in the whole compartment with increasing air temperatures for which the duration depends on the fire load and the ventilation conditions,
- a decreasing phase corresponding to air temperatures going down until all the combustible materials have completely burnt.

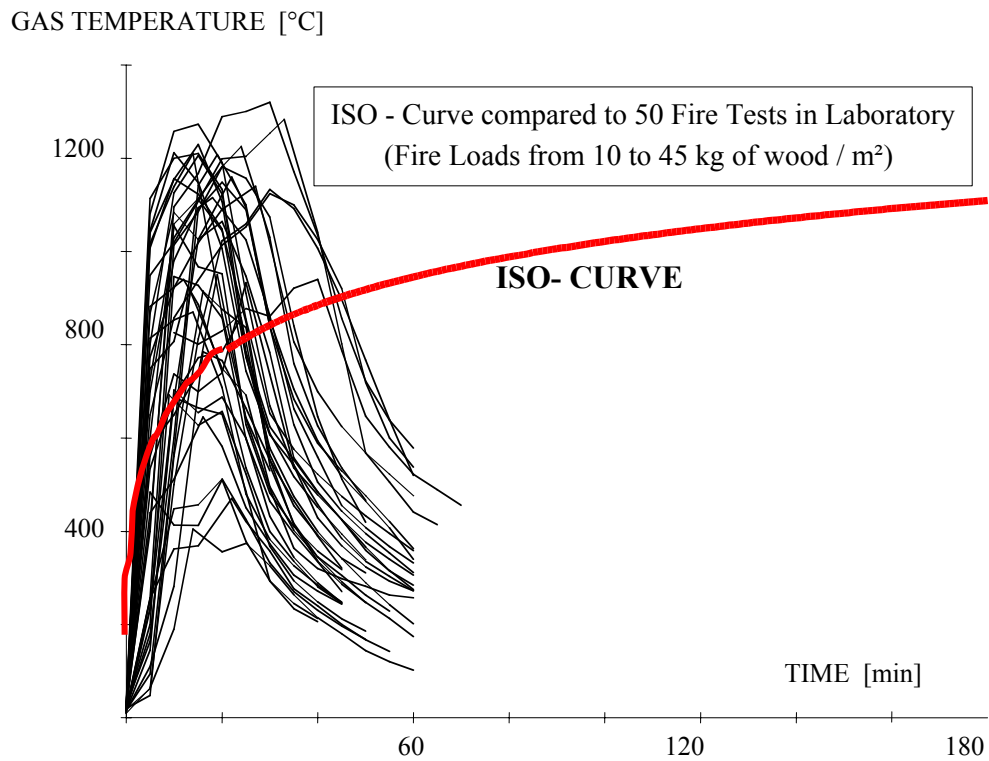


Figure 5. Natural fire curves and the ISO temperature-time curve.

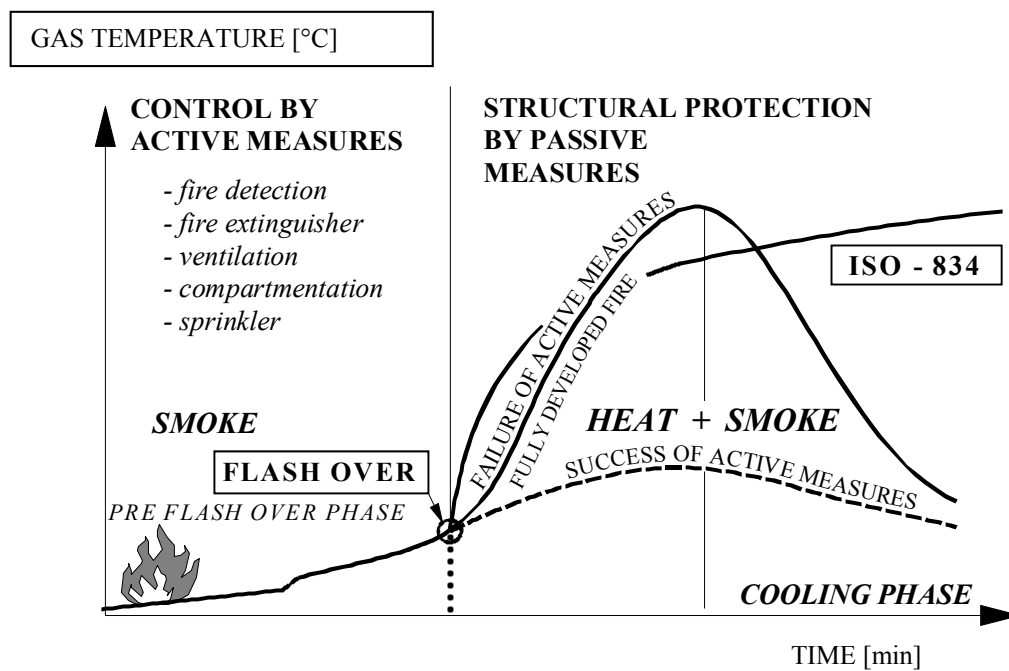


Figure 6. The various phases during the development of a natural fire.

1.2.2 Natural fire models

"Natural fire models" is a general term used to cover a fire evolution more in line with real fires expected to occur in buildings. They take into account the main parameters which influence the growth and development of fires. In this respect the temperature-time curve and subsequently the heat flux vary when the size of the building, the amount or kind of the fire load respectively the ventilation conditions vary.

This more realistic way of determining the thermal action due to an expected fire can only be used in association with an assessment by calculation. Due to the large variety of possible temperature-time curves in a building, the assessment method would have been very expensive if the only possibility was to test components in furnaces for each particular temperature-time fire curve.

Natural fire models according to 3.3 of EN 1991-1-2, [46], cover simplified and advanced models. **Simplified fire models** concern compartment fires where, for internal members of fire compartments, a method for the calculation of the uniform gas temperature in the compartment is given in Annex A, but concern also localised fires where a method for the calculation of thermal actions is given in Annex C. It should be noted that Annex B gives also a procedure for calculating the heating conditions of external members exposed to a fully developed compartment fire, through openings in the façade.

Annex A called "Parametric temperature time curves" gives, for elements inside the building, simplified formulas which take into account the following main parameters: the fire load, the opening factor $O = A_v \cdot \sqrt{h} / A_t$, (with A_v , area of vertical openings; h , height of vertical openings; A_t , total area of enclosure), and the thermal properties of the surrounding walls of the compartment. Furthermore the distinction is made between a fuel controlled and a ventilation controlled fire. Slow, medium and fast fire growth rates may also now be considered.

An example of the results when using these formulas with a fire load $q_{f,d} = 600 \text{ MJ/m}^2$, and an opening factor varying from $0,02 \text{ m}^{1/2}$ to $0,20 \text{ m}^{1/2}$ is shown in figure 7.

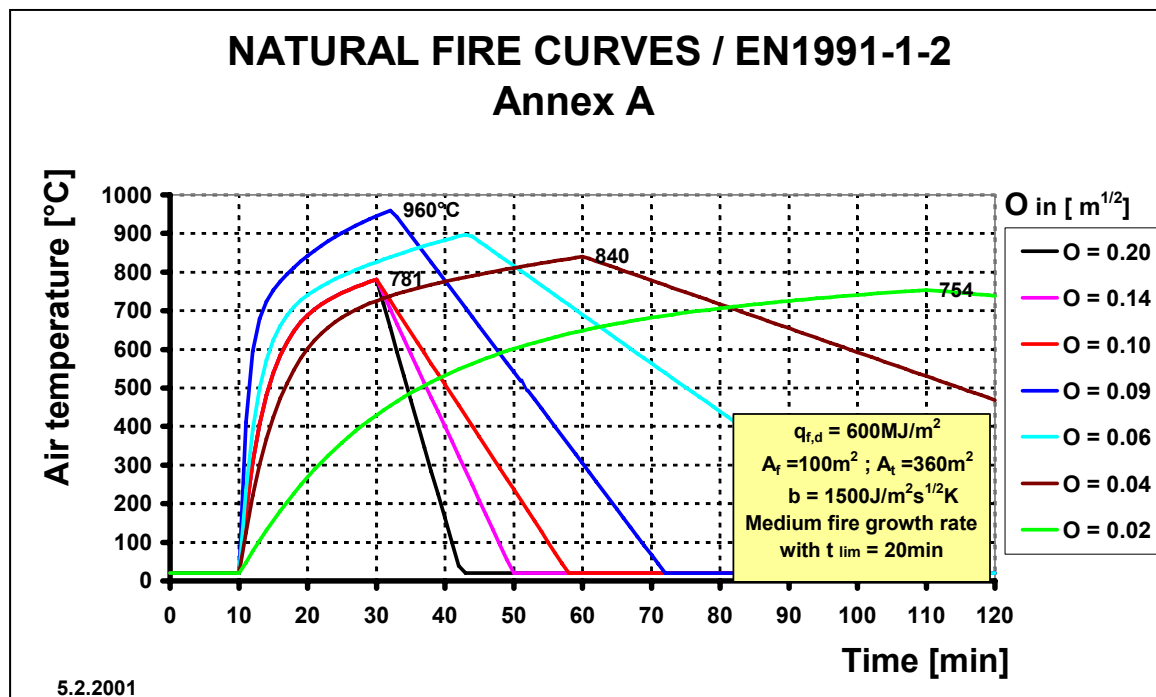


Figure 7.

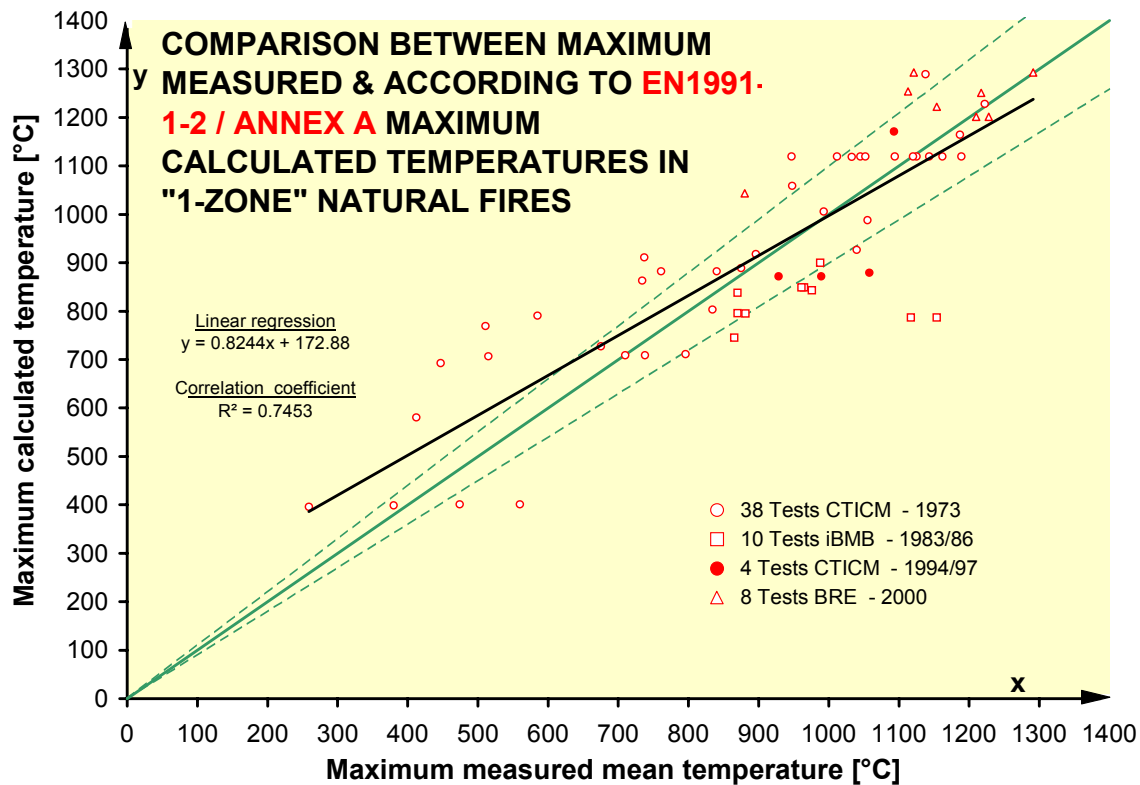


Figure 8.

The heating curves show that the fire is fuel-controlled for opening factors from $0,20 \text{ m}^{1/2}$ to $0,10 \text{ m}^{1/2}$ and becomes ventilation-controlled for smaller opening factors. These parametric temperature-time curves constitute a real progress compared to those given by ENV1991-2-2. This has been checked against real fire tests as shown in figure 8, where the maximum mean temperature measured in the fire compartment has been compared to the maximum temperature calculated according to Annex A. We must accept that the correspondance is far from being perfect, as the correlation coefficient is only 0,75. But we should not forget that the method of Annex A is based on a limited number of equations, hence may easily be covered by some EXCEL sheets. Furthermore the answer obtained is physically correct and therefore may surely be used in the frame of a predesign.

It has also to be understood that these parametric fires correspond to a fully developed fire which means that the corresponding compartment is fully engulfed in fire.

Advanced fire models take also into account gas properties, mass and energy exchanges. This allows to simulate a natural fire which first is localised, which means that the real fire area A_{fi} is limited compared to the total floor area A_f of the compartment. Normally a two zone situation is developing in the whole compartment i.e. an upper zone filled with smoke and having higher temperatures and a lower zone with low temperatures (see figure 11). As long as the lower zone remains sufficiently high, but above all as long as the upper zone gets not a temperature above 500°C , no flash-over takes place and the natural fire may remain localized in the compartment. Such a situation is given in open car parks, where on one side smoke and heat are escaping easily through the large openings provided in opposite façades, and where on the other side the heat source remains localised in the burning car [20].

This aspect of the evolution of a natural fire is being studied through calculation models like two-zone fire models, or quite advanced calculation models like multi-zone fire models or computational fluid dynamics (CFD) models (see Chapter IX).

Inside the European Research on the Natural Fire Safety Concept it's Working Group WG1, which was analysing natural fire models [47]. This development was confirmed by more than 100 new natural fire tests [52], consequently allowing to consider natural fire models when establishing EN1991-1-2.

When using, according to Annex D of EN1991-1-2, the two-zone fire model software called OZONE, established in the frame of these research projects by the University of Liège [49], and applying it to the same compartment as used in figure 7, the heating curves calculated are those given in figure 9.

These curves a priori seem more realistic as the heating up is more progressive and the cooling down not simply linear as given in figure 7 related to Annex A. In comparison to figure 7, the curves of figure 9 related to OZONE exhibit a clear advantage as for an opening factor O larger than $0,10 \text{ m}^{1/2}$ the maximum air temperature becomes significantly smaller. OZONE gives a maximum air temperature of 1009°C at $45'$ and for an opening factor O of $0,06 \text{ m}^{1/2}$, whereas Annex A has lead to a maximum air temperature of 960°C at $33'$ and for an opening factor O of $0,09 \text{ m}^{1/2}$. If the opening factor O is $0,02 \text{ m}^{1/2}$ a maximum air temperature of 812°C is obtained at $95'$ according to OZONE; a maximum air temperature of 754°C is given at $110'$ according to Annex A.

As a conclusion results produced on behalf of the software OZONE exhibit a high degree of credibility. Indeed these have been checked against real fire tests on figure 10, where maximum mean measured and calculated temperatures were compared; this time the correspondence is far better as the correlation coefficient is $0,89$.

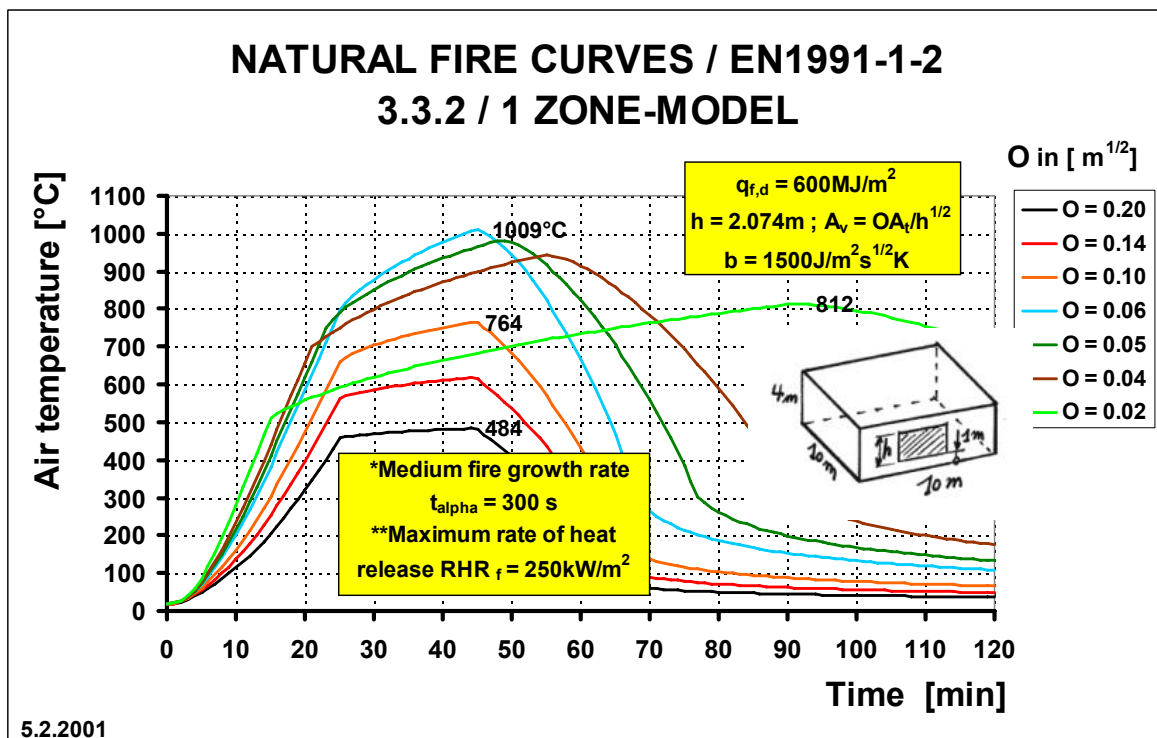


Figure 9.

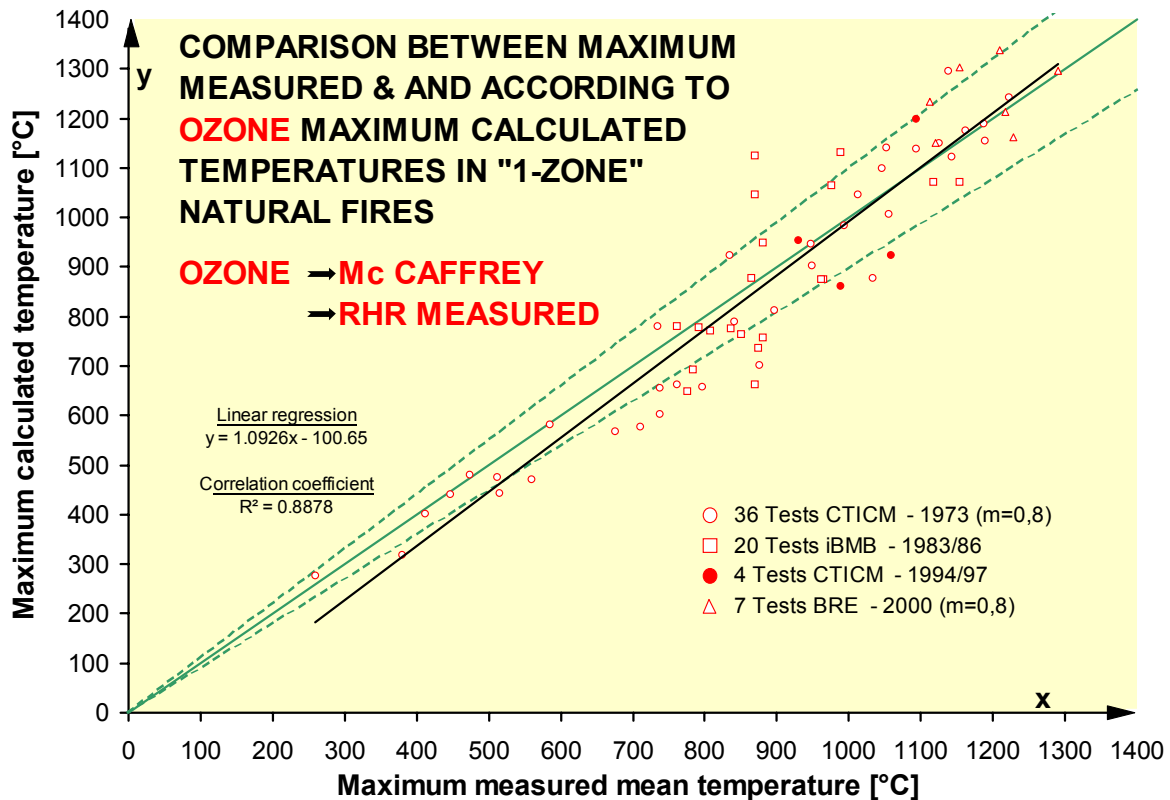


Figure 10.

1.2.3 Rules according to 3.3 of EN1991-1-2 for simplified fire models

Simple fire models are based on specific physical parameters with a limited field of application. For the calculation of the design fire load density $q_{f,d}$ a method is given in Annex E.

A uniform temperature distribution as a function of time is assumed for compartment fires. A non-uniform temperature distribution as a function of time is assumed in case of localised fires.

When simple fire models are used, the coefficient of heat transfer by convection should be taken as $\alpha_c = 35 \text{ [W/m}^2\text{K]}$.

Gas temperatures should be determined on the basis of physical parameters considering at least the fire load density and the ventilation conditions. For internal members of fire compartments, a method for the calculation of the gas temperature in the compartment is given in Annex A.

For external members, the radiative heat flux component should be calculated as the sum of the contributions of the fire compartment and of the flames emerging from the openings. For external members exposed to fire through openings in the facade, a method for the calculation of the heating conditions is given in Annex B.

Where flash-over is unlikely to occur, thermal actions of a localised fire should be taken into account. A method for the calculation of thermal actions from localised fires is given in Annex C.

1.2.4 Rules according to 3.3 of EN1991-1-2 for advanced fire models

Advanced fire models should take into account the gas properties, the mass exchange and the energy exchange. For the calculation of the design fire load density $q_{f,d}$ and of the rate of heat release \dot{Q} a method is given in Annex E. One of the following models should be used :

- One-zone models assuming a uniform, time dependent temperature distribution in the compartment;
- Two-zone models assuming an upper layer with time dependent thickness and with time dependent uniform temperature, as well as a lower layer with a time dependent uniform and lower temperature;
- Computational Fluid Dynamic models giving the temperature evolution in the compartment in a completely time dependent and space dependent manner.

A method for the calculation of thermal actions in case of one-zone, two-zone or computational fluid dynamic models is given in Annex D.

The coefficient of heat transfer by convection should be taken as $\alpha_c = 35 \text{ [W/m}^2\text{K]}$, unless more detailed information is available.

In order to calculate more accurately the temperature distribution along a member, in case of a localised fire, a combination of results obtained with a two-zone model and a localised fire approach may be considered. The temperature field in the member may be obtained by considering the maximum effect at each location given by the two fire models.

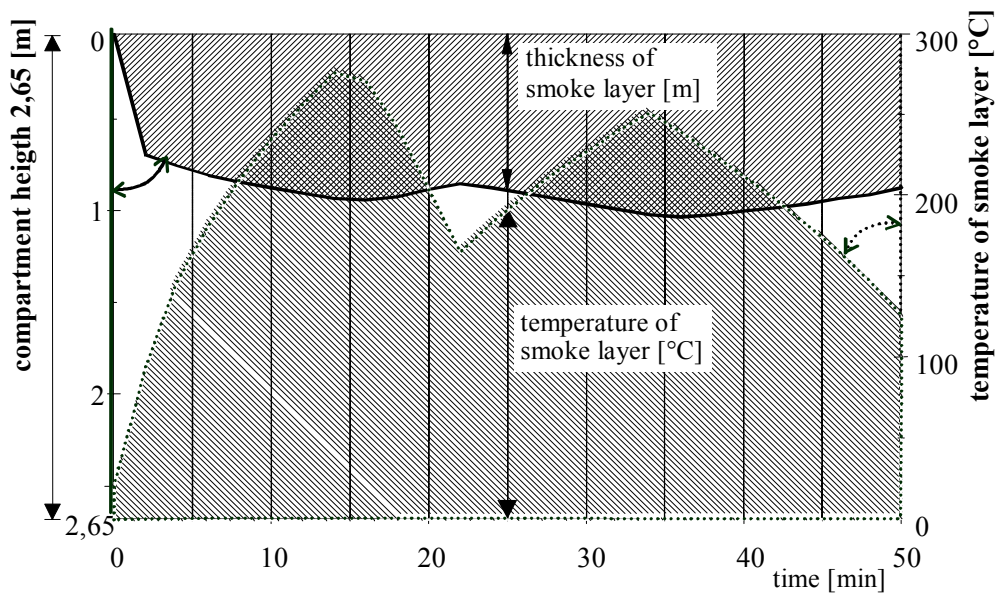
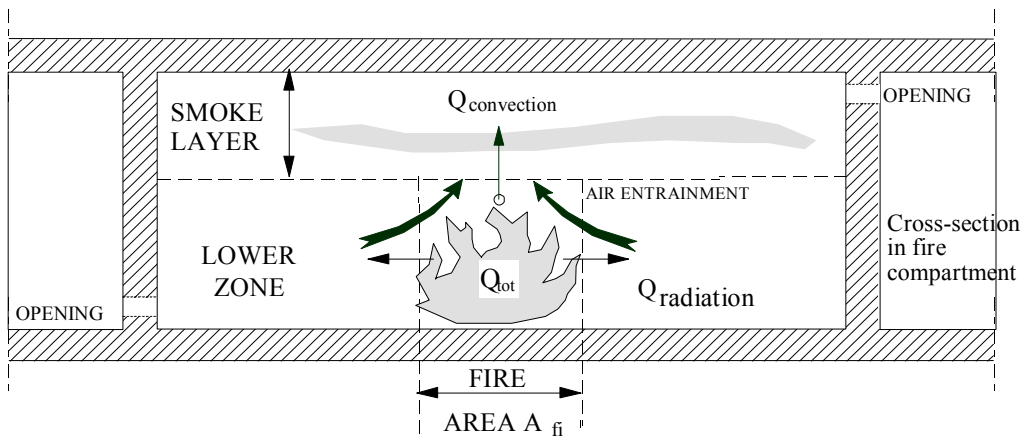


Figure 11. Calculation of the thickness of the smoke layer and its temperature in function of time, as it may happen in case of a burning car.

1.3 Methodology

1.3.1 General presentation

The evaluation of the fire development in a fire compartment requires knowledge on a large number of parameters. A given number of parameters are fixed through the characteristics of the building itself.

Nevertheless the main characteristic, the "fire load", is generally a function of the activity and further may not be the same during the life of the building. The fire load may however be defined as a statistical distribution in a similar way as the mechanical loads i.e. self-weight, imposed load and wind are defined for the structural design in normal conditions of use.

Consequently, it was decided to analyse the fire safety in a building taking advantage of the probabilistic approach. Therefore the target failure probability constitutes the main objective to be fulfilled by the global fire safety concept. In fact the safety level presently given in EN1990 [44] for normal conditions of use should be considered also for the fire situation. Furthermore active fire fighting measures may be considered in order to reach the required level of safety.

The general method of safety quantification is based on the procedure used for structural design at ambient temperature and defines a design fire load taking into account the probability of fire occurrence and the influence of active fire fighting measures.

That design fire load is taken into account in the fire models to assess the temperature evolution within the compartment. This permits to determine the temperature field in the structure and the corresponding structural response. The present handbook gives rules in paragraphs 4, 5 and 6 for assessing the various steps allowing to predict the behaviour of a structure in the fire situation.

Fire models and fire resistance models are described in Chapter IX. Fire models comprise simplified fire models, local fire models and advanced fire models. Fire resistance models may be either based on tabulated data, either constitute simple or advanced calculation models. For the evaluation of the global structural behaviour in the fire situation advanced models have to be used.

1.3.2 Performance based objective

The main objective is given by the acceptable safety level. This acceptable safety level may be defined by comparison to the different existing risks in life including the structural collapse of a building in normal conditions of use. The corresponding target failure probability not to be exceeded in normal conditions is given by $7,23 \cdot 10^{-5}$ for the building life of ~55 years.

Hence the objective for the fire situation should be also

$$P_f(\text{probability of failure}) \leq P_t (\text{target failure probability}) = 7,23 \cdot 10^{-5} \quad (1)$$

As defined in 3.2(2)P and 6.4.3.3(4) of the Eurocode – Basis of structural design, EN1990 [44], the fire is to be considered as an accidental action. An important statistical study has been performed in order to get credible data among others on the probability of a fire occurrence. Fire occurrence or ignition essentially is a function of the occupancy of the building. A quite good correspondence was found between statistics coming from different European countries; this is documented in [38] and [47].

When the fire has been ignited, collapse will only occur if the fire reaches severe conditions. Hence we have to establish the probability of the fire growing to a severe fire. In this phase active fire fighting measures, occupants and firemen have an important role to play.

Which means that in a large number of cases this fire may be stopped rather quickly, and will never grow to a severe fire. According to the previously named statistics, the effect of active measures and of the intervention of the fire brigade could be assessed; this permits to evaluate the probability of getting a severe fire.

So following the active fire fighting measures like sprinklers or smoke detection or the intervention of the fire brigade, the danger of fire activation given by the occupancy or the size of the compartments in the building, and given the target failure probability, the design fire load may be evaluated.

Two levels permitting the calculation of the design fire load are described:

- In Level 1 the probabilistic approach allows to use any target failure probability obtained through improved reliability considerations. This leads to a global factor γ_{qf} giving the design fire load according to

$$q_{f,d} = \gamma_{qf} \cdot q_{f,k} \quad [\text{MJ/m}^2] \quad (2)$$

The calibration of the global factor γ_{qf} is given in chapter III-3.1 for the target failure probability of $7,23 \cdot 10^{-5}$ for the building life.

- In Level 2 the design fire load is calculated by multiplying the characteristic fire load by the factors δ_{q1} , δ_{q2} and δ_n based on the target failure probability of $7,23 \cdot 10^{-5}$ for the building life according to

$$q_{f,d} = m \cdot \delta_{q1} \cdot \delta_{q2} \cdot \delta_n \cdot q_{f,k} \quad [\text{MJ/m}^2] \quad (3)$$

The calibration of the partial factors δ_{q1} and δ_{q2} related to the risk of fire activation and of the differentiation factors δ_{ni} related to the active fire fighting measures, is given in Chapter III-3.2.

The Level 2 method is of course an approximation which is on the safe side. For that reason the global combustion factor m may be taken as 0,8. This Level 2 method has the enormous advantage to be userfriendly as all the differentiation factors may be taken directly from Annex E of EN1991-1-2 [46].

1.3.3 Models for the fire development

Different levels of fire development models are available:

- simplified fire models like the parametric temperature-time curves given in Annex A of EN1991-1-2 [46] may be used for predesign calculation,
- zone-models take into account all main parameters influencing the fire,
- computational fluid dynamic models give the temperature evolution in a compartment in a completely time and space dependent manner; any fire sources and any geometry may be investigated.

First zone models i.e. both one-zone and two-zone models are analysed. The assumptions concerning the one-zone models are related to a generalised fire with uniform temperature in the compartment, while the two-zone models are related to a hot smoke layer and a colder lower layer generated from a localised fire, both layers having also uniform temperatures varying with time.

An essential parameter of the fire development is the rate of heat release (RHR). This rate of heat release is a function of the compartment size, of the occupancy and is a function of time. As described in figure 6 of paragraph 1.2 the initially localized fire goes through a growing phase called pre-flashover. The beginning of this phase is characterised by a fire growth quantified by a t^2 -fire which means, that the rate of heat release is given by a parabolic equation. Buildings are classified according to their occupancy into four categories related to

the fire growth rate which may be slow, medium, fast and ultra-fast. The rate of heat release will reach a maximum value corresponding to a steady state defined by fuel or ventilation controlled conditions.

The crucial assessment concerns the RHR evolution and the prediction whether the fire will grow to a flashover or will remain localized .

When the conditions of flashover or of a fully developed fire are not given, the fire remains localized. Two-zone models have to be used in order to estimate the evolution of the temperature of the smoke layer. The local heating effect due to the local fire source may be considered through the simplified fire models proposed by Heskestad [14] and Hasemi [29].

1.3.4 Models for the structural behaviour in the fire situation

Following the thermal action given in the previous chapter, the thermal transfer to the structural elements has to be evaluated. This leads to the temperature field in the structure, which in combination with the mechanical loads in case of fire finally allows to analyse the structural behaviour.

The procedure based on tabulated data needs only data in relation to geometry and loading, but unfortunately is exclusively applicable to ISO-fire requirements.

Simple calculation models applicable to the analysis of structural elements may be used. Quite often these models are based on the notion of critical temperature. If the temperature of the heated element is lower than the critical temperature no failure will occur, but if the heating goes beyond that critical temperature failure is imminent. The performance based objective is fulfilled if the time to reach the failure $t_{fi,d}^{nat}$ is higher than the required time $t_{fi,requ}$.

More sophisticated so-called advanced calculation models, based on finite differences or finite elements, may be used [11, 12, 13, 17]. The results produced by these models generally contain detailed informations on the deformation evolution of the complete structure during the whole fire duration. Full knowledge of the structural fire behaviour allows for an assessment against a range of performance criteria in terms of limited deformation or structural damage. The choice of the performance based objective for design purposes will be dependent on the consequences of a failure and on the function of the building. For a given multi-storey building this may mean that no structural failure should ever occur during and after the fire; in other words the fire resistance time $t_{fi,d}^{nat}$ should be unlimited.

1.3.5 Required data

In order to apply this methodology, the characteristics of the corresponding building have to be known. This methodology has to be applied to every compartment. The compartments have to be defined in terms not only of their geometry, but also of the thermal characteristics of the walls that are able to accumulate and to transfer a large part of the energy released by the fire. Furthermore the openings which allow the air exchange with the outside of the compartment have to be known. This will be the task of the following paragraph 2.

In order to estimate the probability of the fire to grow to a severe fire, the active measures selected for the building have to be known. The corresponding factors are elaborated in Chapters III-2 and III-3.

2 CHARACTERISTICS OF THE FIRE COMPARTMENT

2.1 Introduction

The objective of this handbook is to describe a performance based more realistic and credible approach to the analysis of structural safety in case of fire. Hence real fire characteristics shall be considered.

It is not astonishing at all, that the very first attempts to define realistic or natural fire conditions have been done even since 1958 [1, 2]. If a natural fire evolution is considered for which active measures have failed, the fully developed fire gives way to a heating phase with increasing air temperatures. However after a given time, depending on the fire load and the ventilation conditions, the air temperatures will necessarily decrease.

This important statement was recognized not later than 1987 to 1988, when first static calculations under natural fire conditions were undertaken and published [9, 13]. Frames were tested at the University of Braunschweig under natural fire conditions and a set of compartment temperature-time curves in function of the opening factor and the fire load were developed [16, 18]. Finally an European research program was undertaken in 1993 on natural fires in closed car parks and in large compartments [32, 33], followed in 1994 by the research project on the " Natural Fire safety concept " to which 11 European countries contributed [47, 52].

That development opened the way for the final version of EN1991-1-2 [4, 25, 34, 46] and to a global fire safety approach. As explained in paragraph 1 the first step of such a **"Global Fire Safety Concept"** consists in taking into account the building characteristics relevant to fire growth and its development, the compartment size, the possible fire scenario, the real fire load and rate of heat release as well as the ventilation conditions.

This means that the fire safety design is based on physically determined thermal actions. In contrast with conventional design, parameters like the amount of fire load, the rate of heat release and the degree of ventilation play an essential role in the natural fire development.

The specification of appropriate and realistic design fire scenarios is a crucial aspect of fire safety design. The design fire scenarios used for the analysis of a building have to be selected among possible fire scenarios. Only "credible worst case fire scenarios" should be considered.

The assumptions made with regard to all these factors have a major influence on the heating conditions in the compartment and have a significant impact on the fire resistance design. The following pages deal with the characteristics of the fire compartment and of the fire itself, as well as with the simplified and more advanced fire development models.

2.2 Boundary elements of the compartment

The development of a natural fire is assumed to occur in the corresponding compartment, without spreading to other compartments. Whether this is true, depends on the fire behaviour of the boundary parts i.e. the floor, the ceiling and the walls including doors etc.. It is necessary to understand this behaviour in order to assess the ability of the boundary parts to function as fire barriers.

Such an assessment is rather complex as a theoretical approach is not feasible at present and as experimental data mainly refer to standard fire conditions. The following options are available:

- proceed to furnace tests during which the boundary element may be exposed to temperature-time curves obtained from fire models using the worst case fire scenarios; however the number of fire tests needed may be very large.

- refer to expert judgement taking profit of available test-data related to ISO-fire resistance tests on separating elements. In combination with calculation procedures, the behaviour under natural fire conditions may be assessed for a limited number of simple elements like monolithic walls; for more complex wall constructions this approach is not feasible.
- use directly the ISO-fire requirements as given by the National Prescriptions for fire compartments. This assumes that the fire will not grow beyond the fire compartment for a time equal to the ISO rating.

In practice, very often the 3rd option is used. For the development of natural fires the compartment boundaries need normally not to comply with an ISO-fire rating higher than R60. If the fire starts in an enclosure without ISO-fire rating boundaries, it could however be assumed that the fire will stay in this enclosure for at least 15 minutes.

2.3 Thermal characteristics of boundaries

The heat loss outside of the compartment is an important factor for the determination of the evolution of temperatures inside of the compartment. Heat transfer to the compartment boundaries occurs by convection and radiation. The thermal properties of the walls have to be known in order to evaluate the heat transfer by conduction through the walls.

The three main parameters characterising the thermal properties of a material are the density ρ [kg/m³], the specific heat c [J/kgK] and the thermal conductivity λ [W/mK].

The specific heat and the thermal conductivity depend on the temperature of the material. In the case of zone or fluid dynamic models, the heat transfer through the walls is calculated through the resolution of thermal transfer equations. When the dependence on temperature is not known, the characteristics at ambient temperature may be used. It is suggested to neglect the effect of water content.

For simplified fire models, only the thermal inertia may be used. This so-called b-factor is given by:

$$b = \sqrt{\rho \cdot c \cdot \lambda} \quad [\text{J/m}^2\text{s}^{1/2} \text{ K}] \quad (4)$$

When the wall is composed of two materials, N°1 being in contact with the fire, it is suggested to establish the b-factor according to the following procedure:

- if $b_1 < b_2$, the b-factor is given by $b = b_1$,
- if $b_1 > b_2$, a limit thickness s_{lim} is calculated for the exposed material 1 according

$$s_{\text{lim}} = \sqrt{\frac{3600 \cdot t_{\text{max}} \cdot \lambda_1}{c_1 \rho_1}} \quad [\text{m}]$$

where t_{max} is the time in [h] when the highest temperature is obtained in the compartment; for more information see Annex A of EN1991-1-2, [46].

Finally the b-factor is determined as follows, s_1 being the thickness of material N°1:

$$\begin{aligned} &\text{if } s_1 > s_{\text{lim}} \quad \text{then } b = b_1, \\ &\text{if } s_1 < s_{\text{lim}} \quad \text{then } b = \frac{s_1}{s_{\text{lim}}} b_1 + \left(1 - \frac{s_1}{s_{\text{lim}}}\right) \cdot b_2. \end{aligned}$$

The following table 1 gives the thermal characteristics of the most commonly used materials for different temperatures.

Table 1. Thermal characteristics of commonly used materials.

material	Temperature [°C]	ρ [kg/m ³]	c [J/kgK]	λ [W/m/K]
Normal weight concrete	20	2300	900	1,95
	200	2300	1000	1,55
	500	2300	1100	1,04
	1000	2300	1100	0,62
Light weight concrete	20	1600	840	1
	200	1600	840	0,875
	500	1600	840	0,6875
	1000	1600	840	0,5
Steel	20	7850	440	53,3
	200	7850	530	47,3
	500	7850	667	37,3
	1000	7850	650	27,3
Gypsum insulating board	20/1000	800	1700	0,20
Vermiculite-cement spray	20/1000	350	1200	0,12
CaSi insulating board	20/1000	600	1200	0,15
Wood	20/1000	450	1100	0,1
Brick	20/1000	2000	1200	1,2
Glas	20/500	2500	720	1

To account for different b factors in walls, ceiling and floor, $b = \sqrt{(\rho c \lambda)}$ should be introduced as:

$$b = (\Sigma(b_j A_j)) / (A_t - A_v) \quad [\text{J/m}^2 \text{s}^{1/2} \text{ K}] \quad (5)$$

where

- A_j is the area of enclosure surface j , openings not included,
- b_j is the thermal inertia of enclosure surface j ,
- A_v is the total area of vertical openings on all walls,
- A_t is the total area of all enclosure surfaces.

2.4 Opening characteristics

The openings in an enclosure may consist of windows, doors and roof vents. The severity of the fire in a compartment depends among others on the degree of openings. The following rules are suggested:

- doors may be assumed to be closed if the enclosure has other openings,
- doors may be assumed to be opened if the enclosure has no other openings,
- glazing without ISO-Fire rating may be considered to brake as soon as the air temperature is reaching 200°C. If the size of the glazing in a certain wall is higher than 50% of the total surface of that wall surface, only 50% of that wall surface should be assumed to be broken which corresponds to the upper part of the glazing.

- glazing with an ISO-Fire rating may be considered to brake when the air temperature in the compartment under fire is reaching the temperature of the rating,
- simplified fire models may use the so-called opening factor O to model the openings in an enclosure. More complex models may use a gas flow calculation through the opening.
- the opening factor O may be calculated for enclosures with one vertical opening, with several vertical openings and with a combination of horizontal and vertical openings as described hereafter.

The opening factor O used in simplified fire models is defined according to the following equation for vertical openings

$$O = A_v \sqrt{h_{eq}} / A_t \quad [\text{m}^{1/2}] \quad (6)$$

where h_{eq} is the weighted average of window heights on all walls given by

$$h_{eq} = \left[\frac{\sum A_{vi} \sqrt{h_i}}{\sum A_{vi}} \right]^2 \quad [\text{m}] \quad (7)$$

with A_{vi} and h_i , the area respectively the height of the opening i .

Concerning **horizontal openings** the following methodology may be adopted to estimate the opening factor taking into account horizontal openings. For that case the opening factor is given by:

$$O = x (A_v \sqrt{h_{eq}} / A_t)$$

where x is a correction factor given by the following equations and figure 12.

$$x = (1 + 0,03(y-1)) \cdot y$$

$$\text{and } y = 2(A_h h_h^{1/2}) / (A_v h_{eq}^{1/2}) + 1$$

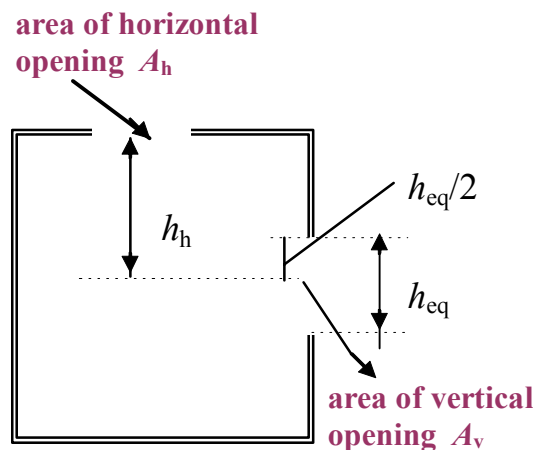


Figure 12. Vertical cross-section through enclosure with vertical and horizontal openings.

2.5 Mechanical ventilation

The use of pressurisation and mechanical ventilation is getting more frequent. However their interaction with other fire parameters needs some consideration.

It is assumed that an over-pressurised compartment will remain smoke free, if of course the compartment boundaries fulfil the load bearing and separating criteria R (resistance), E (integrity) and I (insulation).

The mechanical ventilation is also often used for smoke and heat extraction. Their effects on the fire development may be taken into account in advanced fire models.

The ventilation, used as air conditioning, will be ignored in fire development. Air conditioning should indeed be automatically stopped in case of fire alarm.

3 CHARACTERISTICS OF THE FIRE

3.1 Introduction

The aim of this chapter is to provide all information required for the evaluation of the parameters defining a fire. First data necessary for the design of a building against fire concern the heating energy going to affect the structure. A clear way of knowing this would be to perform a real fire test in the building. This is of course unreasonable, and besides would only provide information for one of the multiple fires that could occur in that building.

Knowledge from fire tests, from existing software models and from the theory of fire dynamics have been gathered so that a characterisation of the fire may now be obtained for different situations.

3.2 Fire load

The first problem consists in assessing the fire load to be considered for design. It is quite rare that the fire load is known in a deterministic way. Generally that has to be defined in a statistical manner.

3.2.1 Nature of fire load

The fire load Q in a fire compartment is defined as the total energy able to be released in case of fire. Part of the total energy will be used to heat the compartment (walls and internal gas), the rest of the energy will be released through openings. Building components such as construction elements, linings or finishings, and building contents due to the type of occupancy, such as furniture, constitute the fire load. Divided by the floor area, the fire load Q gives the fire load density q_f .

In EN1991-1-2 [11] the characteristic fire load density is defined by the following equation:

$$q_{f,k} = \frac{1}{A_f} \sum_i (\psi_i \cdot m_i \cdot H_{ui} \cdot M_{i,k}) \quad [\text{MJ/m}^2] \quad (8)$$

where:

- $M_{i,k}$ is the characteristic mass of the material i (kg)
- H_{ui} is the net calorific value of the material i (MJ/kg), (see table 2)
- m_i is the factor describing the combustion behaviour of the material i
- Ψ_i is the factor for assessing the material i as a protected fire load
- A_f is the floor area of the fire compartment [m^2].

$H_{ui} \cdot M_{i,k}$ represents the total amount of energy contained in material i and released assuming a complete combustion. The "m" factor is a non-dimensional factor between 0 and 1, representing the combustion efficiency: $m = 1$ corresponds to complete combustion and $m = 0$ to materials that do not contribute to the fire at all.

A value of $m = 0,8$ is suggested for standard materials. For wood, a value of 17,5 MJ/kg is suggested for H_u leading to 14 MJ/kg with $m=0,8$. For practical reasons this combustion factor is never considered on the level of the individual materials as shown in the previous equation, but is normally taken into account in a global way as proposed in equation (3) and in paragraph 1.3.

Fire loads in containments which are designed to survive fire exposure need not be considered, and are therefore associated with $\Psi_i = 0,0$. Fire loads in non-combustible containments with no specific fire design, but which remain intact during fire exposure, may be considered as follows.

The largest fire load, but at least 10% of the protected fire loads, is associated with

$\Psi_1 = 1,0$. If this fire load plus the unprotected fire loads are not sufficient to heat the remaining protected fire loads beyond ignition temperature, then the remaining protected fire loads may be associated with $\Psi_1 = 0,0$.

In all other situations Ψ_1 is to be taken as 1,0.

Table 2. Recommended net calorific values of combustible materials H_u (MJ/kg) for the calculation of fire loads.

Typical materials in buildings			
solids		Plastics	
Wood	~17,5	Polyurethane	~23-25
Cellulosic materials (clothes, cork, paper, cardboard, silk, straw)	~19-20	Polyurethane foam	26
Wool	~23	Polystyrene, polypropylene	~40
Linoleum	~20	Polyethylene	~40-44
Grease	41	Polyester	~30-31
Cotton	~20	Celluloid	19
Rubber tyre	~30-32	Melamine resin	18
Hydrocarbon			
gases		Liquids	
Methane, ethane	~50	Gasoline, petroleum, diesel	~44-45
Butane, propane	~46-50	Oil	41
Acetylene, ethylene, propylene	~45-48	Benzene	~40
		Benzyl alcohol	33
		Methanol, ethanol, spirits	~27-30
Others products			
Solids		Plastics	
Bitumen Asphalt	~40-41	ABS	~35-36
Leather	~20	Acrylic	28
Paraffin wax	47	PVC	~17-20
Coal, charcoal, anthracite	~30	Polycarbonate	29
Rubber isoprene	45	Epoxy	34

3.2.2 Amount of fire load

The fire load density may be estimated by summing up all the fire loads present in a building which represents the deterministic approach.

Some information is available on the fire load density for specific building types such as offices and schools. This statistical approach is only valid for building types where similar amounts of fire load can be expected. In those cases the characteristic fire load density may be given as a statistical distribution with a mean value and a standard deviation.

In table 3 these values are given for a number of building occupancies. The values for 80, 90 and 95% fractiles are calculated using a Gumbel type I distribution, assuming also a

variation coefficient V of 0,3. Mean values and standard deviations are derived from a compendium of commonly accepted values extracted from international documents [4, 25, 34,]; see also table E.4 of [46].

Table 3. Data on the characteristic fire load density for different occupancies [MJ/m²] fitting with a Gumbel type I distribution.

	Standard Deviation	Mean	80% fractile	90 % fractile	95 % fractile
Dwelling	234	780	948	1085	1217
Hospital	69	230	280	320	359
Hotel (room)	93	310	377	431	484
Library	450	1500	1824	2087	2340
Office (standard)	126	420	511	584	655
School	85,5	285	347	397	445
Shopping centre	180	600	730	835	936
Theatre (cinema)	90	300	365	417	468
Transport (public space)	30	100	122	139	156

Fire loads from the building i.e. construction elements, linings and finishings are not included in the classification of table 3, and should be established according to previous equation. Both components the fire load from the occupancy and the fire load from the building, if relevant, should be considered simultaneously.

3.3 Type of fire

Another question to be answered is what amount of the total fire load is going to burn in case of fire, and how will this affect the temperature-time curve occurring during the fire scenario.

Except for arson or explosion, which are not in the scope of this Handbook, fires never start at the same time in the whole fire compartment. They always start as a localized fire that will develop to a major fire depending on a series of conditions. Main differences between a localized and a fully developed fire are listed below in table 4.

In situations in which the whole compartment is involved in the fire, a uniform gas temperature may be assumed. In a fully developed fire all fire loads are burning so that the whole compartment is filled with smoke, combustion products and air that mix so well that the gas in the whole compartment may be considered as homogeneous and presenting everywhere the same uniform temperature.

Table 4. Differences between a localized and a fully developed fire.

	Fire load	Gas temperature
Localized fire	Only a part of the compartment is in fire	Two zones (two temperature-time curves)
Fully developed fire	All the fire loads distributed in the whole compartment are burning simultaneously	One zone (one temperature-time curve)

In the scope of [47] and [52] a method has been developed that allows to evaluate the temperature-time curves to be used for checking the structural behaviour, in case the fire is either localized or fully developed. This will be described in details in paragraph 4 on " fire development models".

3.4 Rate of heat release

The fire load having been characterised the next step consists in analysing at which rate this fire load will burn. This leads to the rate of heat release RHR.

The fire load defines the total available energy, but the maximum gas temperature in a fire depends also on the rate of heat release. The same fire load either burning very quickly or smouldering may lead to completely different gas temperature curves as shown in figure 13.

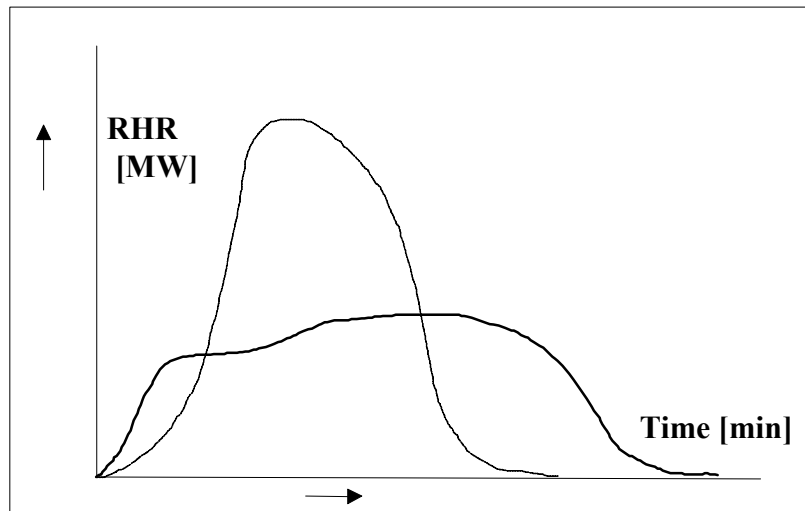


Figure 13. Two RHR curves corresponding to the same amount of fire load, as the surface beneath both curves is the same.

The RHR is the source of the gas temperature rise, and the driving force behind the spreading of gas and smoke. A typical fire starts small and goes through a growth phase. Two quite different scenarios may occur, depending whether or not during the growth process there is always enough oxygen to sustain combustion. Either the RHR reaches a maximum value without limitation of oxygen, so it is limited by the available fire load and the fire is called **fuel bed controlled fire**. Or if the size of openings in the compartment enclosure is too small to allow enough air to enter the compartment, the available oxygen limits the RHR and the fire is said to be **ventilation controlled**. Both ventilation and fuel-controlled fires may go through flashover.

This important phenomenon, flashover, marks the transition from a localised fire to a fire involving all the exposed combustible surfaces in the compartment. The two regimes, of fuel or ventilation controlled fire, are illustrated in Figure 14, which presents graphs of the rate of burning R_m , in kg of wood per hour, versus the ventilation parameter $O = A_v \sqrt{h_{eq}} / A_t$. Graphs are shown for different fire load densities. Starting on the left side of the figure in the ventilation controlled regime, with increasing ventilation parameter the rate of burning grows up to the limiting value determined by the fire load density and then remains approximately constant (fuel controlled region).

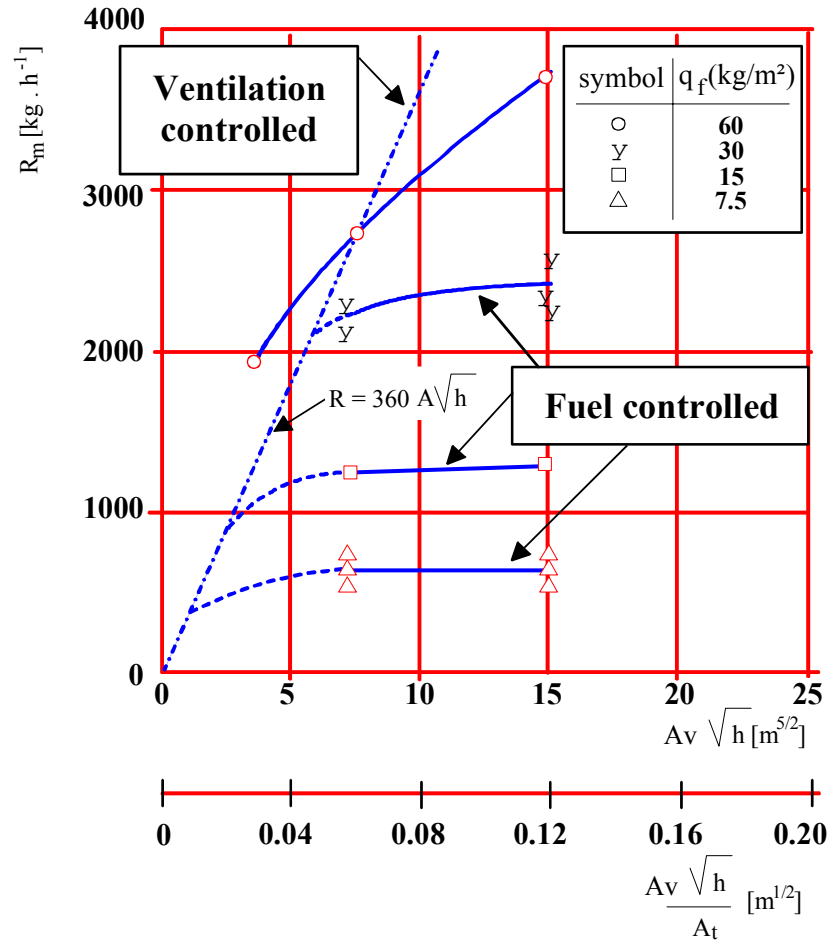


Figure 14. Rate of burning R_m , in kg of wood per hour, for different fire load densities in a compartment with $A_t = 125m^2$ and assuming a combustion factor $m = 1,0$.

3.5 Design RHR evolution

The rise of the rate of heat release up to its maximum value (see figure 15) may be given by a so-called t-square fire evolution:

$$RHR = (t / t_\alpha)^2 \quad [MW] \quad (9)$$

where:

RHR is the rate of heat release of the fire during the growth phase [MW]

t is the time [s]

t_α is the time constant [s] given in table 5 and corresponding to the time t needed to get $RHR=1MW$.

The fire growth parameters given in [34] and [46] vary according to the building occupancies and some guidance towards the classification and determination of these parameters is shown hereafter in table 5.

The growth rate "slow" corresponds to a low and discontinuously distributed fire load. The growth rate "medium" corresponds to a normal fire load which is more or less uniformly distributed. The growth rate "fast" corresponds to a fire due to densely packed materials or existing over the total height of the compartment. The growth rate "ultra fast" corresponds mainly to a pool fire initiated by alcoholic liquids rapidly spreading all over the compartment floor.

Table 5. Fire growth parameters depending on the building occupancy.

Occupancy/Activity	Fire growth rate	Time constant $t_a(s)$
Art-gallery; Public space for transport means	Slow	600
Storage building with few combustible materials	Slow	600
Dwelling; Hospital bedroom	Medium	300
Hotel bedroom; Hotel reception	Medium	300
Office building; School classroom	Medium	300
Storage building for cotton or polyester sprung mattresses...	Medium	300
Shopping centre; Library; Theatre; Cinema	Fast	150
Storage buildings with full mail bags, plastic foam, stacked timber...	Fast	150
Chemical Plant	Ultra fast	75
Storage buildings with alcoholic liquids or upholstered furniture...	Ultra fast	75

After this growing phase, the RHR curve follows a horizontal plateau with a maximum value of RHR corresponding to fuel bed or ventilation controlled conditions (see figure 15). In case of ventilation controlled conditions a proposal was established by Kawagoe.K. in [1] and [2] and has been adopted in [46] as follows:

$$RHR_{\max} = 0,10 \cdot m \cdot H_u \cdot A_v \cdot h_{eq}^{1/2} \quad [MW] \quad (10)$$

where

- A_v is the opening area [m^2]
- h_{eq} is the mean height of the openings [m]
- H_u is the net calorific value of wood with $H_u = 17,5$ [MJ/kg]
- m is the combustion factor with $m = 0,8$.

In case of fuel bed conditions the maximum value of RHR corresponds to:

$$RHR_{\max} = 0,001 \cdot A_{fi} \cdot RHR_f \quad [MW] \quad (11)$$

where

- A_{fi} is the maximum area of the fire [m^2], which is the fire compartment in case of uniformly distributed fire load, but which may be smaller in case of a localised fire,
- RHR_f is the maximum rate of heat release produced by 1 m^2 of fire in case of fuel controlled conditions [kW/m^2]. Some guidance towards the classification and determination of this parameter is shown hereafter in table 6.

In [24] and [34] the decay phase is assumed to show a linear decrease of the rate of heat release. Formulae are given to calculate the time of beginning of the decay period and the duration of the decay period. Based on test results, the decay phase may be estimated to start when approximately 70% of the total fire load has been consumed.

Table 6. Maximum rate of heat release [kW/m²] produced by 1 m² of fire in case of fuel controlled conditions depending on the building occupancy.

Occupancy/Activity	RHR_f [kW/m ²]
Art-gallery; Public space for transport means	250
Storage building with few combustible materials	
Dwelling; Hospital bedroom	
Hotel bedroom; Hotel reception	
Office building; School classroom	
Storage building for cotton or polyester sprung mattresses...	500
Shopping centre; Library; Theatre; Cinema	
Storage buildings for stacked timber pallets of 0,5m high	1250
Storage buildings for stacked PS insulation rigid foam boards; 4,3m high	2900
Storage buildings for stacked plastic bottles in cartoons; 4,6m high	4320
Storage buildings for stacked timber pallets of 3,0m high	6000

In the following figure 15 the RHR curve proposed in [47] and [52] is given. The curve includes the growing phase, steady state and the decay phase. It may be noted that this curve delimits a surface representing the total available energy given by:

$$\int RHR \cdot dt = A_{fi} \cdot q_{f,d} \quad [MJ] \quad (12)$$

with $q_{f,d}$ the design fire load density according to equation (2) or (3).

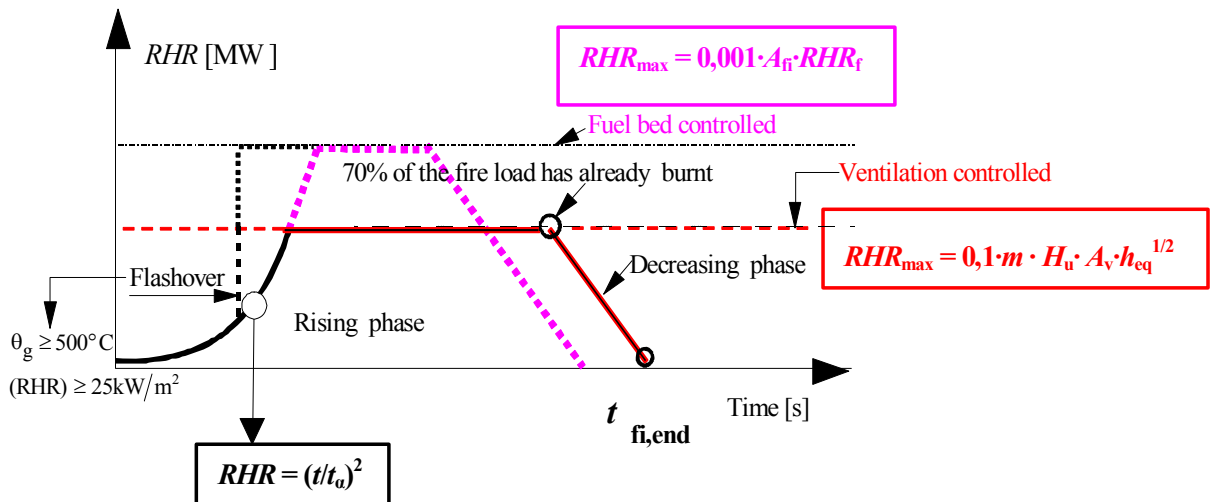


Figure 15. Design RHR curve versus time where three phases are recognised: a rising, steady state (post flashover) and decreasing phase.

3.6 Experimental data

The RHR curve may also be established through practical tests. Reliable techniques for measuring heat release rates were not available until, a few years ago, the oxygen depletion calorimeter was developed. Earlier attempts required the direct measurement of sensible enthalpy, which is very difficult to perform. The oxygen depletion technique, however, enables easy measurements together with a quite acceptable accuracy. The oxygen consumption principle states that, within a small uncertainty band, the heat released from the combustion of any common combustible is uniquely related to the mass of oxygen removed from the combustion flow stream. This technique has been used in order to establish a database of test results [26].

Different sources in the literature contain numerical values of heat release rates [3, 19, 21, 35].

The Hazard two-zone simulation model contains within its framework a database, where various items are laid out and information on the RHR is given [21]. These items tend to be only items related to the home, such as chairs, TV's, Christmas trees etc. This obviously leads to a limitation in the field of application. However in its particular area of use, it appears to be a very good source of information, since it includes every phase during a RHR curve. Argos contains another database within the framework of its fire simulation programme [19]. In Argos different equations are given for solid material fires, melting material fires, liquid fires and smouldering fires. These equations define the RHR as a function of the fire spread velocity in the horizontal and vertical directions. The numerical values valid for different materials and objects are given in the Argos database.

Another source of information on test results is the document called "Initial Fires", compiled by the University of Lund [3]. The latter has the same format as the Hazard database but contains more results. This document contains information not only on household objects but also on various vehicle types etc.

Furthermore new fire tests have been performed on real cars during the ECSC Research "Development of design rules for steel structures subjected to natural fires in closed car parks", which permitted to acquire a certain knowledge on the RHR during car fires [32].

CTICM in France has performed fire tests on new cars fabricated during the year 1996, on hotel rooms and on real furniture and the corresponding heat release rates were measured [31]. These experimental data are quite useful, because the majority of fire tests reported in the literature have been performed only on the basis of wood cribs.

4 FIRE DEVELOPMENT MODELS

When simulating numerically the fire development, different simplifications of fire dynamics are feasible. This part explains the models to apply in pre-flashover situation i.e. for a localised fire or for a 2 zone fire, and in post-flashover situation i.e. for a fully developed fire.

4.1 Pre-flashover fires

In a localised fire, there is an accumulation of combustion products in an upper layer beneath the ceiling, with an horizontal interface between this hot layer and the lower layer where the temperature of the gases remains much colder.

This situation is well represented by a two zone model, useful for all pre-flashover conditions. Besides calculating the evolution of gas temperatures, this model is used in order to know the smoke propagation in buildings and to estimate the level of life safety as a function of the smoke layer height, of toxic gas concentration and of radiative heat flux.

The thermal action on horizontal structural elements located above the fire depends on their distance from the fire. This can be assessed by specific, simplified models allowing to determine the effect on adjacent elements, such as the methods developed by Heskestad [14] and Hasemi [29]. Both procedures are presented in Annex C of EN1991-1-2 [41, 46].

The rules given hereafter for flames impacting or not impacting the ceiling are valid if the following conditions are met:

- ° the diameter of the fire is limited by $D \leq 10 \text{ m}$,
- °° the rate of heat release of the fire is limited by $Q \leq 50 \text{ MW}$.

4.1.1 Flame not impacting the ceiling / Heskestad's method

An empirical method, based on experiments, has been developed to determine the thermo-dynamic data of an open fire [14, 27]. These data are mainly temperature and velocity according to radial and axial distance along the flame and the plume of the open fire. The empirical equations finally elaborated form the basis for the equations (C1) to (C3) of EN1991-1-2 [46].

The first correlation obtained for an axisymmetric open fire is the flame length L_f (see figure 16) which is given by :

$$L_f = -1,02 D + 0,0148 Q^{2/5} \text{ [m]} \quad (13)$$

The second empirical correlation is given for the temperature $\theta_{(z)}$ along the axis of the plume when the flame is not impacting the ceiling of a compartment according to figure 16 with $L_f < H$ or in case of fire in open air:

$$\theta_{(z)} = 20 + 0,25 Q_c^{2/3} (z - z_0)^{-5/3} \leq 900 \text{ [}^\circ\text{C]} \quad (14)$$

where

- D is the diameter of the fire [m]
- Q is the rate of heat release of the localised fire [W]
- Q_c is the convective part of the rate of heat release [W], with $Q_c = 0,8 Q$ by default
- z is the height along the flame axis [m]
- H is the distance between the fire source and the ceiling [m].

The virtual origin z_0 of the axis is given by :

$$z_0 = -1,02 D + 0,00524 Q^{2/5} \text{ [m]}$$

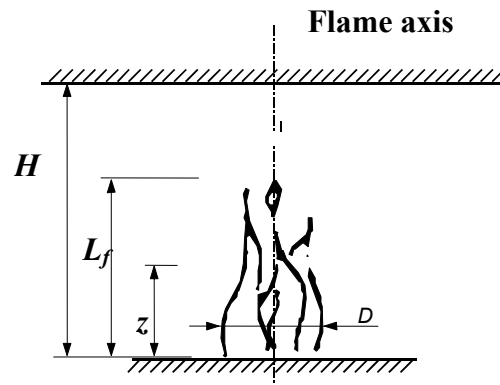


Figure 16. Flame not impacting the ceiling.

Several research projects on small scale tests, with a rate of heat release less than 1MW, had been carried out between 1979 and 1989 permitting to verify previous equations. More recently a validation could be carried out through two large scale tests leading to a maximum rate of heat release of about 20 MW and 66 MW.

This concerns the large scale test in Paris – Parc des expositions de Porte de Versailles – in 1994 [23, 28] and large scale tests in an industrial hall – in 1998 [37].

These experiments have shown that the mean temperature along the axis of a turbulent open fire is never higher than 900°C. Furthermore the correlation between the temperature predicted by the second empirical correlation and the recorded temperature along the axis of the flame, at the maximum rate of heat release (about 66 MW), is quite satisfying as shown in figure 17.

For the large scale test in Paris in 1994 the fire was a wood-crib fire with 3562 kg on 30 m². The wood-crib was weighted, thus leading to the mass loss versus time which reached a maximum of 3,8 kg of wood per seconde.

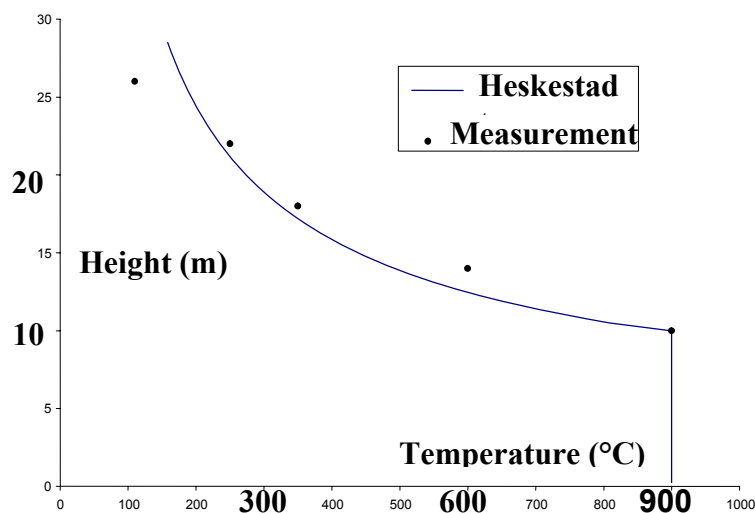


Figure 17. Comparison between the second empirical correlation and measured temperatures along the axis of the flame [23, 28].

4.1.2 Flame impacting the ceiling / Hasemi's method

Hasemi's method is a simple tool for the evaluation of the localised effect on horizontal elements located above the fire. It is based on the results of tests made at the Building Research Institute in Tsukuba, Japan [29].

When the flame is impacting the ceiling ($L_f \geq H$; see figure 16) the heat flux \dot{h} [W/m²] received by the fire exposed unit surface area at the level of the ceiling is given by :

$$\dot{h} = 100000 \quad \text{if } y \leq 0,30 \quad [\text{W/m}^2] \quad (15)$$

$$\dot{h} = 136300 - 121000 y \quad \text{if } 0,30 < y < 1,0$$

$$\dot{h} = 15000 y^{-3,7} \quad \text{if } y \geq 1,0$$

where

$$y \text{ is a parameter [-] given by : } y = \frac{r+H+z'}{L_h+H+z'}$$

r is the horizontal distance [m] between the vertical axis of the fire and the point along the ceiling where the thermal flux is calculated, see figure 18

H is the distance [m] between the fire source and the ceiling

L_h is the horizontal flame length given by the following relation:

$$L_h = (2,9 H (Q_H^*)^{0,33}) - H \quad [\text{m}]$$

with

Q_H^* a non-dimensional rate of heat release given by :

$$Q_H^* = Q / (1,11 \cdot 10^6 \cdot H^{2,5}) \quad [-]$$

z' is the vertical position of the virtual heat source [m] and is given by:

$$z' = 2,4 D (Q_D^{*2/5} - Q_D^{*2/3}) \quad \text{when } Q_D^* < 1,0$$

$$z' = 2,4 D (1,0 - Q_D^{*2/5}) \quad \text{when } Q_D^* \geq 1,0$$

where

$$Q_D^* = Q / (1,11 \cdot 10^6 \cdot D^{2,5}) \quad [-]$$

D is the diameter of the fire [m]

Q is the rate of heat release of the localised fire [W].

The net heat flux \dot{h}_{net} received by the fire exposed unit surface area at the level of the ceiling, is given by :

$$\dot{h}_{\text{net}} = \dot{h} - \alpha_c \cdot (\Theta_m - 20) - \Phi \cdot \varepsilon_m \cdot \varepsilon_f \cdot \sigma \cdot [(\Theta_m + 273)^4 - (293)^4] \quad [\text{W/m}^2] \quad (16)$$

where the various coefficients are given in paragraph 5 on heat transfer models and in [46].

In case of several separate localised fires, Hasemi's formula (15) for the heat flux \dot{h} [W/m²] may be used in order to get the different individual heat fluxes $\dot{h}_1, \dot{h}_2 \dots$ received by the fire exposed unit surface area at the level of the ceiling. The total heat flux may be taken as:

$$\dot{h}_{\text{tot}} = \dot{h}_1 + \dot{h}_2 \dots \leq 100\,000 \quad [\text{W/m}^2].$$

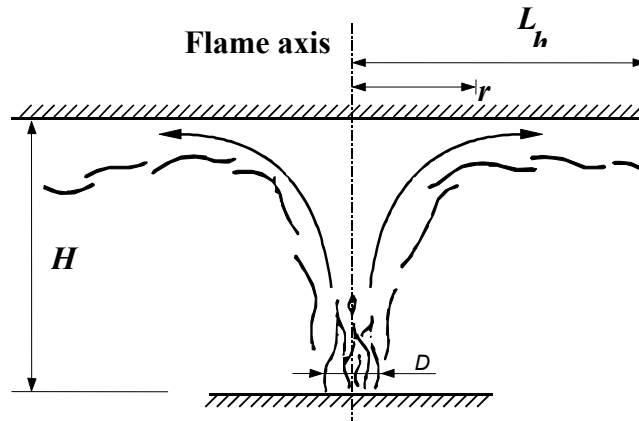


Figure 18. Flame impacting the ceiling.

The heat flux \dot{h} received by the ceiling decreases as a function of the ratio y and increases as a function of Q . In figure 19 these functions are shown for the case $r = 0$, $H = 5$ m and $D = 3$ m.

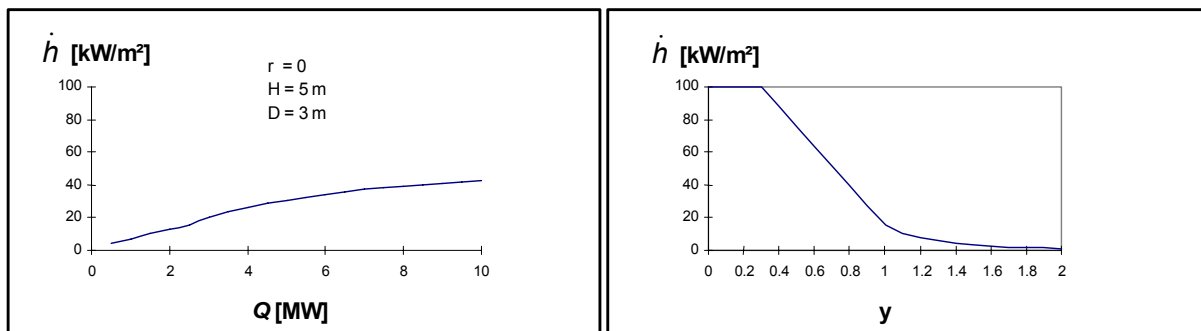


Figure 19. Heat flux \dot{h} [kW/m²] as a function of Q [MW] and y [-].

4.1.3 Two zone model, advanced calculation model

Zone model is the name given to numerical programs, which calculate the development of the temperature of the gases as a function of time, integrating the ordinary differential equations which express the mass balance and the energy balance for each zone of the compartment. They are based on the fundamental hypothesis that the temperature is uniform in each zone.

The data which have to be provided to a zone model are:

- geometrical data, such as the dimensions of the compartment, the openings and the partitions;
- material properties of the walls;
- fire data i.e. RHR curve, pyrolysis rate, combustion heat of fuel.

In a two zone model the equations expressing the mass balance and the energy balance for each zone of the compartment are written for each of the two layers and exchanges between the two layers are considered.

As a result of the simulation, the gas temperature is given in each of the two layers, as well as information on wall temperatures and mass or heat loss through the openings. An important result is the evolution, as a function of time, of the thickness of each layer. The thickness of the lower layer, which remains at rather low temperatures and contains no

combustion products, is very important to assess the tenability of the compartment for the occupants. Figure 20 shows how a compartment is modelled by a two zone model, with different terms of the energy and mass balance represented, as foreseen in the software OZONE [40, 49, 52].

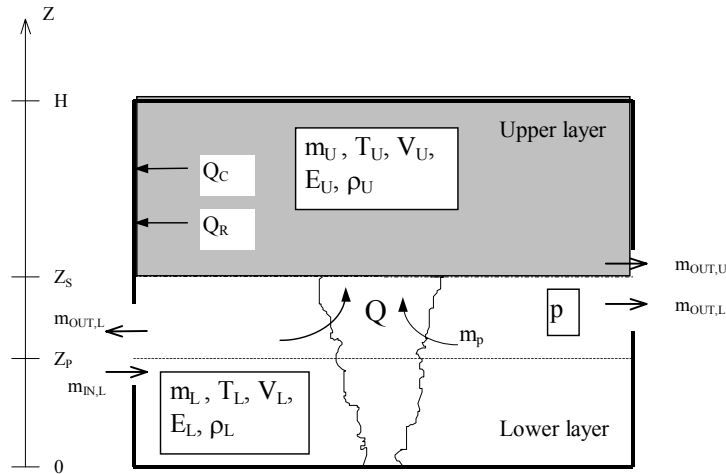


Figure 20. Compartment in a two zone model.

Figure 20 is typical of a simple situation where the compartment exchanges mass and energy only with the outside environment. These kind of models have the capability to analyse more complex buildings where the compartment of origin exchanges mass and energy with the outside environment but also with other compartments in the building. This is of particular interest to analyse the propagation of smoke from the compartment of origin towards other adjacent compartments where it can also be a threat to life. Such a situation, analysed by multi-compartment two zone models, is presented on figure 21.

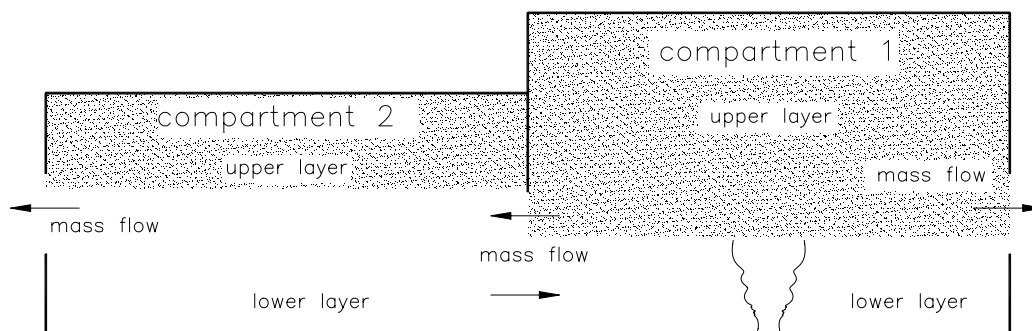


Figure 21. Compartment in a multi-compartment two zone model.

4.1.4 Combination between 2 zone model and localised fire model

In a localised fire the gas temperature distribution in the compartment may be estimated by a 2 zone model. In this model the gas temperature in each layer is calculated with the hypothesis that it is uniform in each layer. This average temperature in the hot zone is generally sufficiently accurate as far as global phenomena are considered: quantity of smoke to be extracted from the compartment, likelihood of flashover, total collapse of the roof or ceiling, etc.

When however the local behaviour of a structural element located just above the fire should be assessed, the hypothesis of a uniform temperature may be unsafe and the two zone model has to be combined with the localised fire formula given in the previous pages.

The temperatures close to the beam are obtained for each point alongside the beam by taking the highest temperature predicted by each of these two fire models.

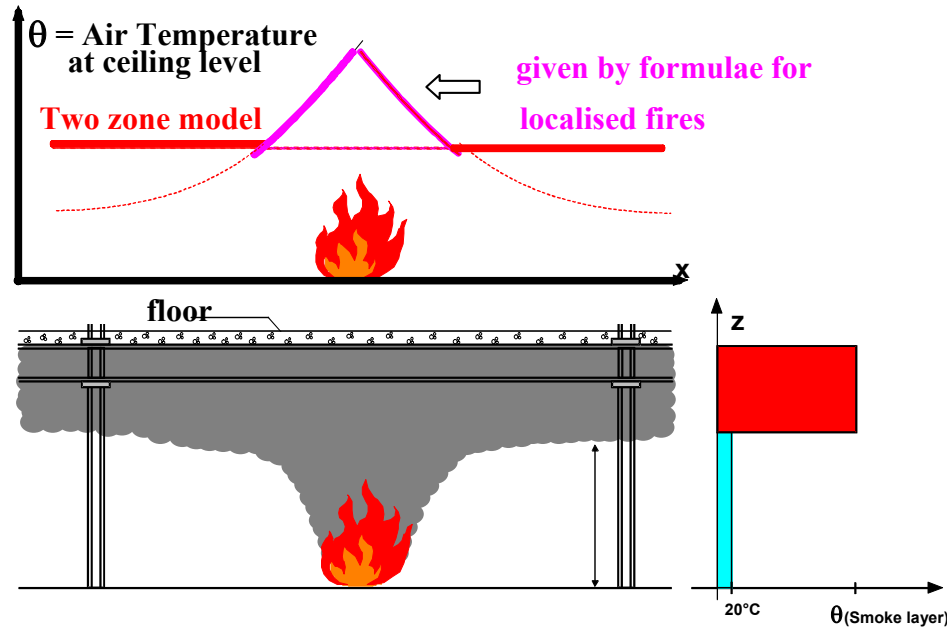


Figure 22. Combination of two zone model and Hasemi's method.

The height of the smoke zone and the temperatures of the hot gases at the level of the steel beams at different distances from the fire can be calculated by the **software TEFINAF** [32, 33]. This model combines a two zone model which provides the height and the mean temperature of the hot zone with the localised fire formula which gives the temperature peak just above the fire and at different distances from the fire.

4.2 Fully developed fires

A fully developed fire within a compartment means that this compartment is completely engulfed in fire, in other words flash-over has taken place and all combustible materials are simultaneously burning. The temperature inside that compartment is progressing in a more or less uniform way. The most widely used fire development models, able to simulate this situation, are described hereafter..

Some simplified and more advanced fire development models are given. However field models (CFD) are not included as these are too complex and need too much time and too many data in order to be used as practical engineering tools.

4.2.1 Natural fire curves NATFIR

This simplified fire model was developed during 1989 to 1990 in the frame of the ECSC Research 7210-SA/112 and constitutes the first practical software, called NATFIR, permitting to establish compartment temperature curves in function of the opening factor

$$O = A_v \sqrt{h_{eq}} / A_t \quad \text{and the fire load } q_f \text{ [18].}$$

These heating curves - see example in figure 23 - are available for all combinations between on one side 6 different **fire loads** varying from 100 to 1000 MJ/m² and on the other

side 13 opening factors varying from 0,02 to 0,32. The field of application is however limited to a compartment height of 3 to 4m, and to a floor area of 25 to 75 m².

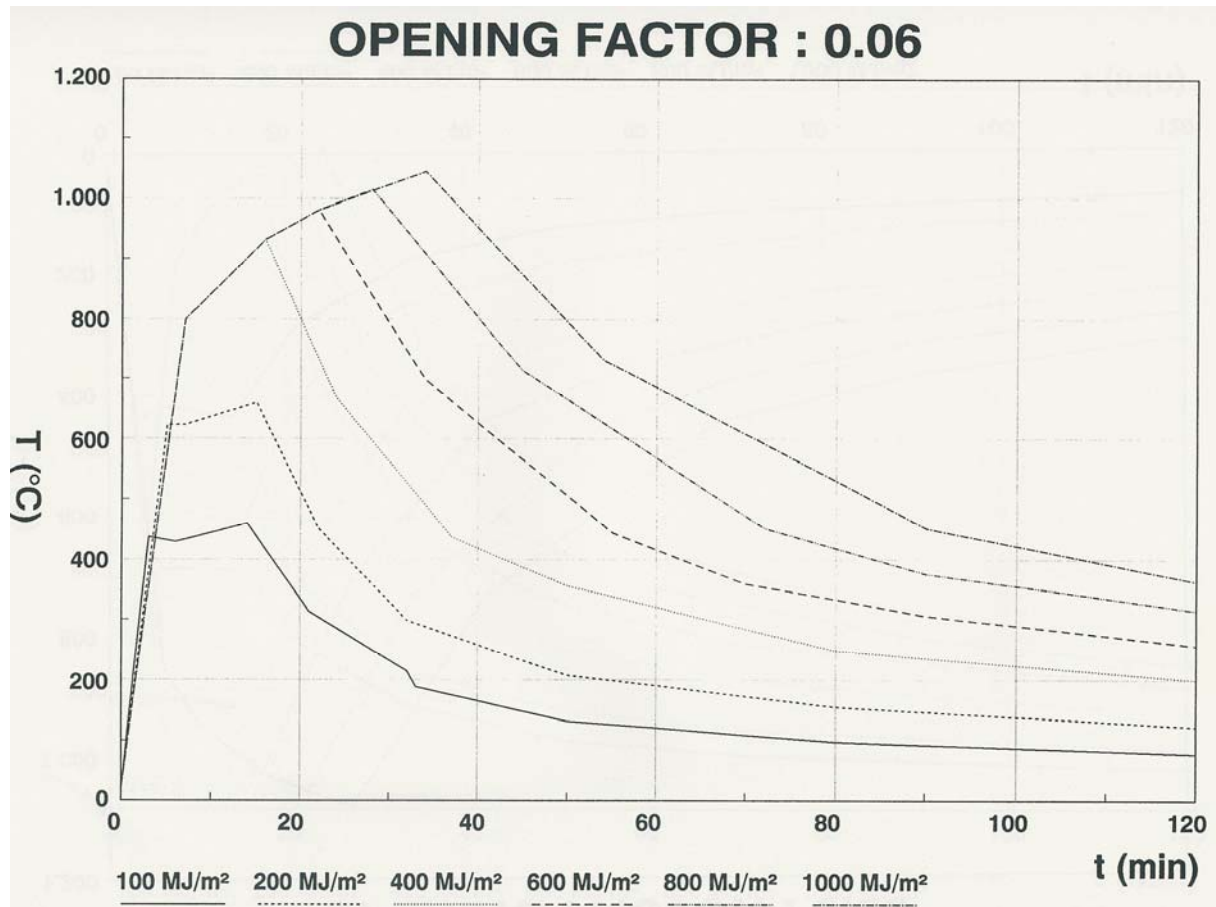


Figure 23. Set of heating curves for the opening factor $O = 0,06$.

4.2.2 Parametric fire according to ANNEX A of EN1991-1-2

Parametric fires provide a simple approach to take into account the most important physical aspects, which may influence the development of a fire in a particular building. Like nominal fires, they consist of time temperature relationships, but these relationships contain parameters deemed to represent particular aspects of real live like:

- the geometry of the compartment
- the fire load within the compartment,
- the openings within the walls and/or in the roof and
- the type and nature of the different construction elements forming the boundaries of the compartment.

Parametric fires are based on the hypothesis that the temperature is uniform in the compartment, which limits their field of application to post-flashover fires in compartments of moderate dimensions. They nevertheless constitute a significant step forward toward the consideration of the real nature of a particular fire when compared to nominal fires, while still having the simplicity of some analytical expressions, i.e. no sophisticated computer tool is required for their application.

A proposal is made in Annex A of EN1991-1-2 for such a parametric fire [39, 46]. It is valid for compartments up to 500 m² of floor area, without openings in the roof and for a

maximum compartment height of 4 m. It is assumed that the fire load of the compartment is completely burnt out.

Parameter b should be in the range from 100 to 2200 J/m²s^{1/2}K, and O should be comprised between 0,02 and 0,20. For an enclosure surface with different layers of material and for walls, ceiling and floor of different composition a method for the calculation of b is given in paragraph 2.3.

EN1991-1-2 contains some essential improvements, namely

- a more correct way to calculate the thermal diffusivity (b factor) in walls made of layers of different materials,
- the introduction of a minimum duration of the fire, t_{lim} , taking account of a fuel controlled fire when the fire load is low and the openings are large;
- a correction factor, k , which takes into account the large mass flow through openings in case of fuel controlled fires.

The temperature-time curves in the heating phase are given by :

$$\Theta_g = 20 + 1\,325 \left(1 - 0,324 e^{-0,2t^*} - 0,204 e^{-1,7t^*} - 0,472 e^{-19t^*} \right) \quad (17)$$

where

Θ_g is the temperature in the fire compartment [°C]

$$t^* = t \cdot \Gamma \quad [h] \quad (18a)$$

with

t time [h]

$$\Gamma = [O/b]^2 / (0,04/1\,60)^2 \quad [-]$$

$$b = \sqrt{(\rho c \lambda)}$$

with the following limits : $100 \leq b \leq 2\,200 \quad [J/m^2s^{1/2}K]$

ρ density of boundary of enclosure [kg/m³]

c specific heat of boundary of enclosure [J/kgK]

λ thermal conductivity of boundary of enclosure [W/mK]

O opening factor : $A_v \sqrt{h_{eq}} / A_t \quad [m^{1/2}]$

with the following limits : $0,02 \leq O \leq 0,20$

A_v total area of vertical openings on all walls [m²]

h_{eq} weighted average of window heights on all walls [m]

A_t total area of enclosure (walls, ceiling and floor, including openings) [m²]

Note that in case of $\Gamma = 1$, equation (17) approximates the standard temperature-time curve.

The maximum temperature Θ_{max} in the heating phase happens for $t^* = t_{max}^*$

$$t_{max}^* = t_{max} \cdot \Gamma \quad [h] \quad (19)$$

$$\text{with} \quad t_{max} = \max [(0,2 \cdot 10^{-3} \cdot q_{t,d} / O) ; t_{lim}] \quad [h] \quad (20)$$

where

$q_{t,d}$ is the design value of the fire load density related to the total surface area A_t of the enclosure whereby $q_{t,d} = q_{f,d} \cdot A_f / A_t$ [MJ/m²]. The following limits should be observed: $50 \leq q_{t,d} \leq 1\,000$ [MJ/m²].

$q_{f,d}$ is the design value of the fire load density related to the surface area A_f of the floor [MJ/m²]

t_{lim} is given hereafter in [h].

Note that the time t_{max} corresponding to the maximum temperature is given by t_{lim} in case the fire is fuel controlled. If t_{max} is given by $(0,2 \cdot 10^{-3} \cdot q_{t,d} / O)$, the fire is ventilation controlled.

When $t_{max} = t_{lim}$, which means that the fire is fuel controlled, t^* used in equation (17) is replaced by

$$t^* = t \cdot \Gamma_{lim} \quad [h] \quad (18b)$$

with
$$\Gamma_{lim} = [O_{lim}/b]^2 / (0,04/1\,160)^2 \quad (21)$$

and
$$O_{lim} = 0,1 \cdot 10^{-3} \cdot q_{t,d} / t_{lim} \quad (22)$$

and if ($O > 0,04$ and $q_{t,d} < 75$ and $b < 1\,160$), Γ_{lim} in (21) has to be multiplied by k :

$$k = 1 + \left(\frac{O - 0,04}{0,04} \right) \left(\frac{q_{t,d} - 75}{75} \right) \left(\frac{1160 - b}{1160} \right) \quad (23)$$

In case of slow fire growth rate, $t_{lim} = 25$ min; in case of medium fire growth rate, $t_{lim} = 20$ min and in case of fast fire growth rate, $t_{lim} = 15$ min.

The temperature-time curves in the cooling phase are given by :

$$\Theta_g = \Theta_{max} - 625 (t^* - t_{max}^* \cdot x) \quad \text{for } t_{max}^* \leq 0,5 \quad (24a)$$

$$\Theta_g = \Theta_{max} - 250 (3 - t_{max}^*) (t^* - t_{max}^* \cdot x) \quad \text{for } 0,5 < t_{max}^* < 2 \quad (24b)$$

$$\Theta_g = \Theta_{max} - 250 (t^* - t_{max}^* \cdot x) \quad \text{for } t_{max}^* \geq 2 \quad (24c)$$

where t^* is given by (18a)

$$t_{max}^* = (0,2 \cdot 10^{-3} \cdot q_{t,d} / O) \cdot \Gamma \quad (25)$$

and $x = 1,0$ if $t_{max} > t_{lim}$; or $x = t_{lim} \cdot \Gamma / t_{max}^*$ if $t_{max} = t_{lim}$.

An example of the results when using these formulas with a fire load $q_{f,d} = 600$ MJ/m², and an opening factor varying from $0,02 \text{ m}^{1/2}$ to $0,20 \text{ m}^{1/2}$ is shown in figure 7 .

The heating curves show that the fire is fuel-controlled for opening factors from $0,20 \text{ m}^{1/2}$ to $0,10 \text{ m}^{1/2}$ and becomes ventilation-controlled for smaller opening factors. These parametric temperature-time curves, by the way similar to those obtained in [18], constitute a real progress compared to those obtained by the prestandard ENV1991-2-2. This has been checked against real fire tests as shown in figure 8, where the maximum measured mean temperature in the fire compartment has been compared to the maximum temperature

calculated according to Annex A. We must accept that the correspondence is far from being perfect, as the correlation coefficient is only 0,75. But we should not forget that the method of Annex A is based on a limited number of equations, hence may easily be covered by some **EXCEL sheets for ANNEX A**. Furthermore the answer obtained is physically correct and therefore may surely be used in the frame of a predesign.

4.2.3 Zone model, advanced calculation model

Zone models have been already introduced in 4.1.3, where a short description of a two zone model was presented. The application field of a two zone model concerns the pre-flashover phase of a fire. For a fully engulfed fire a one zone model should be used.

The one zone model is based on the fundamental hypothesis that, during the fire, the gas temperature is uniform in the compartment. These models are valid for post-flashover conditions.

Data have to be supplied with a higher degree of detail than for the parametric curves and are the same as those required for a two zone model. Figure 24 shows how a compartment fire is modelled, with the different terms of the energy and mass balance represented.

During the Research Project presented in [47] the development of the one zone model called "OZONE", has been started at the University of Liège. This software OZONE has been further completed by a pre-flashover module which may be activated at the beginning of any fire before entering into post-flashover conditions [40, 49, 52].

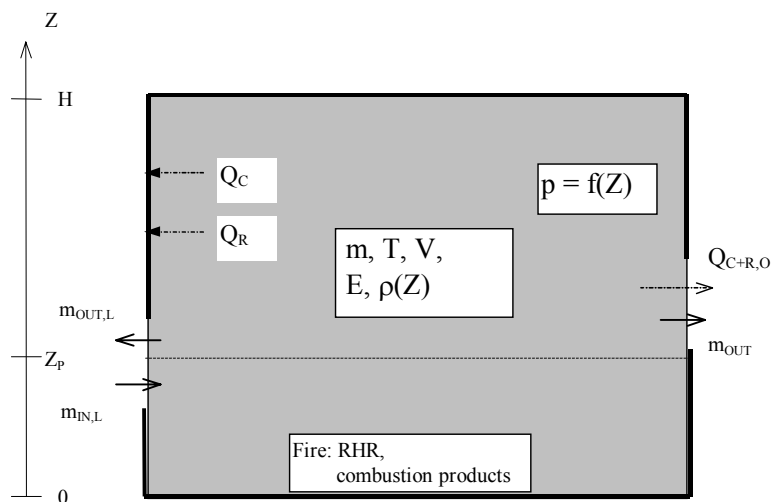


Figure 24. Vertical cross-section through a compartment in case of a one zone model.

An example of the results when using OZONE with a fire load $q_{f,d} = 600 \text{ MJ/m}^2$, an opening factor varying from $0,02 \text{ m}^{1/2}$ to $0,20 \text{ m}^{1/2}$ and applying it to the same compartment as used in figure 7, is shown in figure 9.

These curves a priori seem however more realistic as the heating up is more progressive and the cooling down not simply linear as given in figure 7 related to Annex A of EN1991-1-2. In comparison to figure 7, the curves of figure 9 related to OZONE exhibit a clear advantage as for an opening factor O larger than $0,10 \text{ m}^{1/2}$ the maximum air temperature becomes significantly smaller. OZONE gives a maximum air temperature of 1009°C at $45'$ and for an opening factor O of $0,06 \text{ m}^{1/2}$, whereas Annex A has led to a maximum air temperature of 960°C at $33'$ and for an opening factor O of $0,09 \text{ m}^{1/2}$. If the opening factor O is $0,02 \text{ m}^{1/2}$ a maximum air temperature of 812°C is obtained at $95'$ according to OZONE; a maximum air temperature of 754°C is given at $110'$ according to Annex A.

As a conclusion results produced on behalf of the **software OZONE** exhibit a high degree of credibility. Indeed this model has been **validated taking as reference the results of 106 experimental tests - showing two-zone or, and one-zone behaviour** - performed during the ECSC Research 7210-PR/060 [40, 52]. On figure 10, OZONE has been checked against 67 of these real fire tests with a clear one-zone behaviour; maximum mean measured and calculated temperatures were compared with this time a far better correspondence, as the correlation coefficient is 0,89 !

4.3 Combination of 1-zone and 2-zone models

After having defined the characteristics of the fire compartment as well as those of the fire itself, it is necessary to choose the natural fire model in accordance to the considered fire scenario. This choice should respect the application domain of the models.

In this consideration, it is assumed that the first application has to be a “two zone model” situation. The question is how and when the transition from the “two zone model” to a “one zone model” occurs.

The results of a “two zone model” are given in the form of two main variables:

- temperature of the upper zone T_u ,
- height of the interface i.e. lower layer H_i .

These two variables will mainly condition the simulation with the zone model as shown in figure 26. The following four conditions permit the transition from a “two zone” to a “one zone” behaviour:

- condition C1: $T_u > 500^\circ\text{C}$,
the temperature of combustion products, higher than 500°C , leads to a **flashover** by radiative flux to the other fire loads of the compartment;
- condition C2: $H_i < H_q$ and $T_u > T_{\text{ignition}}$,
the decrease of the interface height H_i is such that the combustible material enters into the smoke layer (H_q is the maximum height of combustible), and if the smoke layer has a temperature higher than T_{ignition} which is assumed to be 300°C , this leads to a sudden propagation of the fire to all the compartment by ignition of all the combustible material which corresponds to a **flashover**;
- condition C3: $H_i < 0,1 H$,
the interface height goes down and leads to a very small lower layer thickness (H is the compartment height), which is no more representative of a two zone phenomenon, hence the **one zone** model should now be applied;
- condition C4: $A_{fi} > 0,5 A_f$,
the fire area A_{fi} is too large compared to the floor surface A_f of the compartment so to consider still a localised fire and hence the **one zone** model should now be applied.

In fact the conditions C1 and C2 lead to a discontinuity in the evolution of the initial rate of heat release, which at time t_i jumps to the level of the horizontal plateau corresponding to the fuel bed or ventilation controlled conditions of figure 15. This sudden increase of the RHR is indicated in figure 25 and corresponds to the occurrence of a flashover.

The above approach is presented in the scheme of figure 27. In this scheme it is shown under which conditions, two- or one-zone modelling, the design temperature curves have to be determined. It is obvious that, if none of the four conditions C1 to C4 are fulfilled, the fire presents all the time a “two zone” behaviour.

Design of natural fire curves is being presented in Chapter VII on the basis of the software OZONE. Further results obtained are explained in [43], when dealing with the attack on the World Trade Centre through the impact of two “BOING 767”.

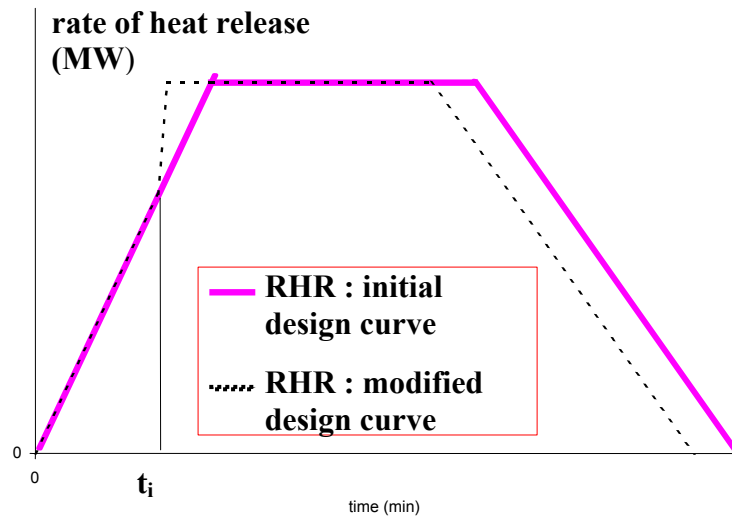


Figure 25. Design RHR curve versus time, showing the occurrence of flashover at time t_i .

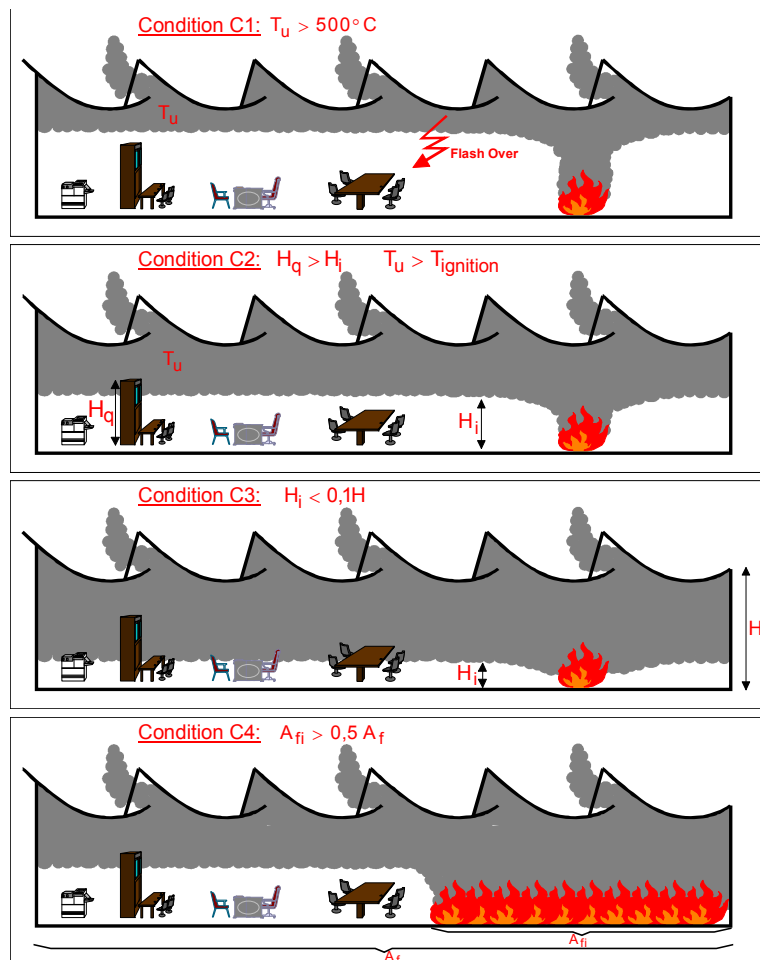


Figure 26. Conditions for the transition from a “two zone ” to a "one zone" behaviour.

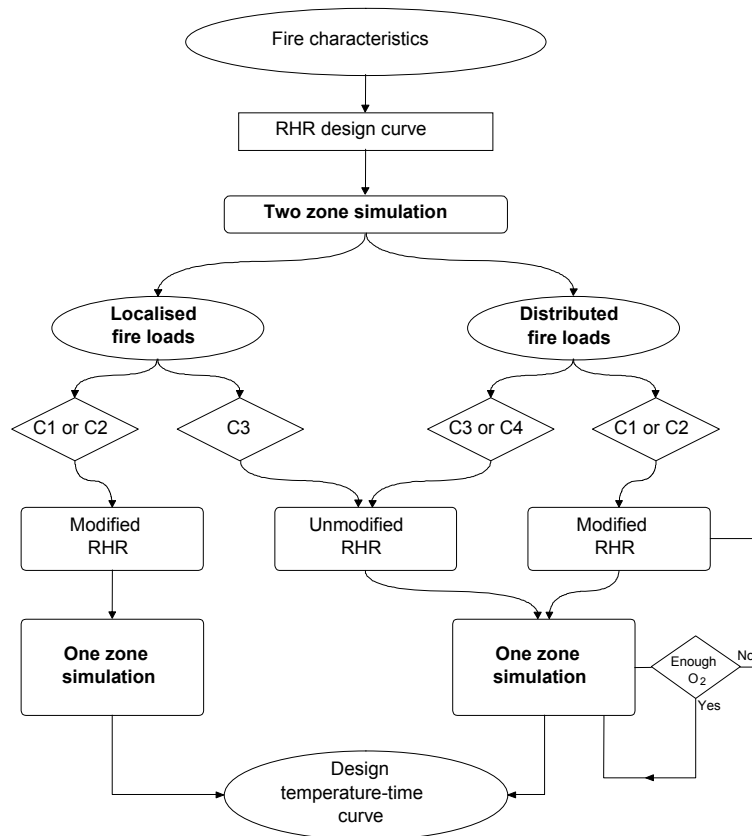


Figure 27. Scheme for the calculation of a design temperature curve.

5 HEAT TRANSFER MODELS

In previous chapters the various models, able to calculate the temperature inside a compartment as a function of time, were described. In order to know the temperature of the structural elements as a function of time, it is necessary to determine the heat flux transmitted to these elements.

Convective and radiative heat transfer occurs between the hot gases, the flame, the surrounding boundary construction and the structural element. Emissivity and convection govern the heat transfer.

The heating up of a structural element depends on the type of element (e.g. concrete, pure steel, composite-steel/concrete, timber or masonry) and of the nature and amount of the fire protection.

5.1 Heat flux

At a given time (t), during the fire, the net heat flux to a surface is determined by considering convection and thermal radiation from and to the fire environment:

$$\dot{h}_{net} = \dot{h}_{net,c} + \dot{h}_{net,r} \quad [\text{W/m}^2] \quad (26)$$

The net convective heat transfer is mainly a function of the gas movement around the structural element and is given by:

$$\dot{h}_{net,c} = \alpha_c \cdot (\theta_g - \theta_m) \quad [\text{W/m}^2] \quad (27)$$

where:

α_c is the coefficient of heat transfer by convection $[\text{W/m}^2\text{K}]$

θ_g is the gas temperature in the vicinity of the fire exposed member $[\text{°C}]$

θ_m is surface temperature of the structural element $[\text{°C}]$

The net radiative heat transfer is given by:

$$\dot{h}_{net,r} = \Phi \varepsilon_f \varepsilon_m \sigma \left[(\theta_r + 273)^4 - (\theta_m + 273)^4 \right] \quad [\text{W/m}^2] \quad (28)$$

where:

Φ is the configuration factor

ε_f is the emissivity of the fire compartment (gas+boundaries)

ε_m is the surface emissivity of the structural member

σ is the Stephan Boltzmann constant given by $5,67 \cdot 10^{-8} \quad [\text{W}/(\text{m}^2 \cdot \text{K}^4)]$

θ_r is the effective radiation temperature of the fire environment $[\text{°C}]$

θ_m is the surface temperature of the structural member $[\text{°C}]$

In case of fully fire engulfed members, the radiation temperature θ_r may be represented by the gas temperature θ_g around that member.

The emissivity coefficient for steel and concrete related to the surface of the structural member should be $\varepsilon_m = 0,7$. For all other materials a value of $\varepsilon_m = 0,8$ is proposed.

Regarding the emissivity of the fire a value of $\varepsilon_f = 1,0$ may be taken.

Regarding the coefficient of heat transfer by convection a value of $\alpha_c = 25 \quad [\text{W/m}^2\text{K}]$ should be taken in case of the standard temperature-time curve.

Concerning the convection heat transfers in a natural fire, the speed distribution provided by the pressure and density differences can be strongly non-uniform. It is quite

difficult to evaluate one global coefficient of heat transfer by convection. Nevertheless, some experimental studies point out that in case of a furniture fire the maximum convective transfer coefficient is about 35 [W/m² K].

On the unexposed side of separating members, the net heat flux $\dot{h}_{net,c}$ should be determined with $\alpha_c = 4$ [W/m²K]. The coefficient of heat transfer by convection should be taken as $\alpha_c = 9$ [W/m²K], when assuming it contains the effects of heat transfer by radiation.

The configuration factor Φ allows to consider that some parts of the structural element may be eventually shielded from the radiation. By definition, the value of the configuration factor is taken between 0 and 1. Where no specific data are available, the configuration factor can be conservatively taken as $\Phi = 1$. The real value depends of the distance between the emitting and receiving surfaces, the size of surfaces and their relative orientation. A corresponding method is given in Annex G of EN1991-1-2 [46].

5.2 Temperature development inside structural members

5.2.1 General

The calculation of the development of a temperature field in the cross section of a structural member exposed to fire involves solving Fourier's differential equation:

$$\frac{\partial}{\partial x} \left(\lambda_{\theta} \frac{\partial \theta}{\partial x} \right) + \frac{\partial}{\partial y} \left(\lambda_{\theta} \frac{\partial \theta}{\partial y} \right) + \frac{\partial}{\partial z} \left(\lambda_{\theta} \frac{\partial \theta}{\partial z} \right) + Q = \rho c_{\theta} \frac{\partial \theta}{\partial t} \quad (29)$$

where Q is the internal heat source that is equal to 0 in case of non-combustible members. The boundary condition is expressed in terms of the net heat flux \dot{h}_{net} .

Simple models for the calculation of the steel temperature development are based on the hypothesis of a uniform temperature distribution in the global cross section or in the parts of the cross-section of the structural member, as presented in EN1993-1-2 [53] and EN1994-1-2 [55].

Outside of these assumptions, advanced calculation models may be used for the determination of the distribution of the temperature within structural members. In this case the thermal response model has to consider:

- the realistic thermal action due to the fire,
- the variation of the thermal properties of the materials in function of the temperature produced in the materials.

5.2.2 Simple calculation model for unprotected steelwork

When calculating the temperature distribution of the steel section, the cross section may be divided into various parts according to Figure 28.

It is assumed that no heat transfer takes place between these different parts nor between the upper flange and the concrete slab.

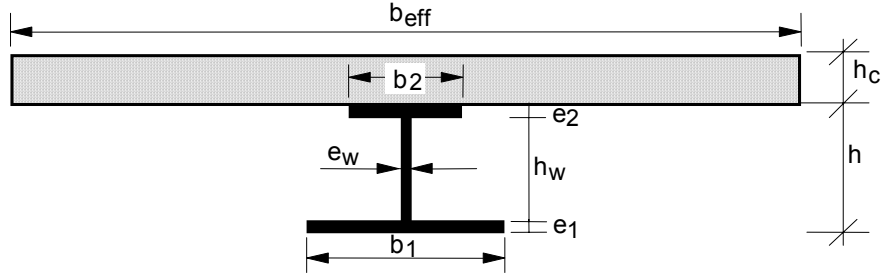


Figure 28. Elements of a cross-section.

The increase of temperature $\Delta\theta_{a,t}$ of the various parts of an unprotected steel beam during the time interval Δt may be determined from:

$$\Delta\theta_{a,t} = k_{shadow} \left(\frac{1}{c_a \rho_a} \right) \left(\frac{A_i}{V_i} \right) \dot{h}_{net} \cdot \Delta t \quad [^{\circ}\text{C}] \quad (30)$$

where

k_{shadow} is a correction factor for the shadow effect

c_a is the specific heat of steel in accordance with Chapter V [J/kgK]

ρ_a is the density of steel in accordance with Chapter V [kg/m³]

A_i is the exposed surface area of the part i of the steel cross-section per unit length [m²/m]

A_i/V_i is the section factor of the part i of the steel cross-section [m⁻¹]

V_i is the volume of the part i of the steel cross-section per unit length [m³/m]

\dot{h}_{net} is the net heat flux per unit area in accordance with equation (26)

$\theta_{a,t}$ is the steel temperature at time t supposed to be uniform in each part of the steel cross-section [°C]

Δt is the time interval which should not be taken as more than 5 seconds [sec]

The shadow effect may be determined from:

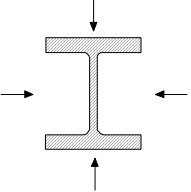
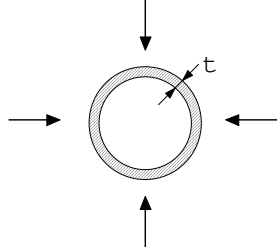
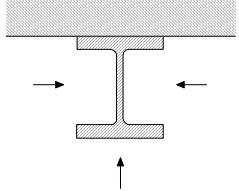
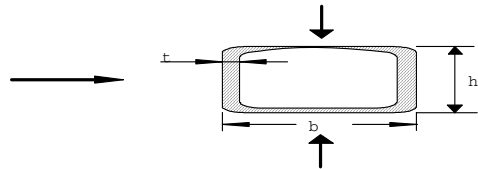
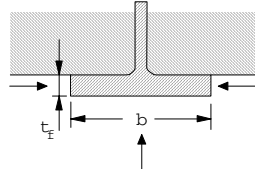
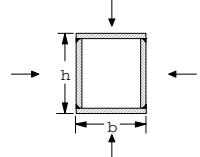
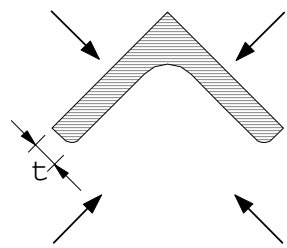
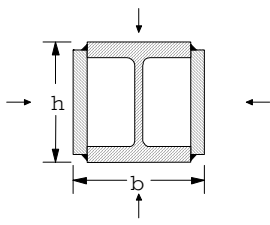
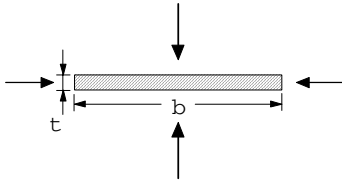
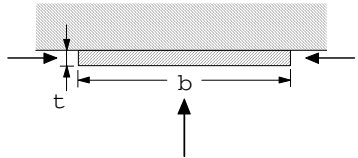
$$k_{shadow} = 0,9 \left(\frac{e_1 + e_2 + 1/2 \cdot b_1 + \sqrt{h_w^2 + 1/4 \cdot (b_1 - b_2)^2}}{h_w + b_1 + 1/2 \cdot b_2 + e_1 + e_2 - e_w} \right) \quad (31)$$

with $e_1, b_1, e_w, h_w, e_2, b_2$ according to figure 28.

Note: Equation (31) giving the shadow effect is an approximation, based on the results of a large amount of systematic calculations. For more refined calculations, the concept of the configuration factor Φ as presented in Annex G of EN1991-1-2 should be applied [46].

Some expressions for calculating the section factor A_m/V for unprotected steel members are given hereafter in table 7.

Table 7. Section factor A_m/V for unprotected steel members.

<p><i>Open section exposed to fire on all sides:</i></p> $\frac{A_m}{V} = \frac{\text{perimeter}}{\text{cross-section area}}$ 	<p><i>Tube exposed to fire on all sides: $A_m/V = 1/t$</i></p> 
<p><i>Open section exposed to fire on three sides:</i></p> $\frac{A_m}{V} = \frac{\text{surface exposed to fire}}{\text{cross-section area}}$ 	<p><i>Hollow section (or welded box section of uniform thickness) exposed to fire on all sides:</i> If $t \ll b$: $A_m/V \cong 1/t$</p> 
<p><i>I-section flange exposed to fire on three sides:</i> $A_m/V = (b + 2t_f)/(bt_f)$ If $t \ll b$: $A_m/V \cong 1/t_f$</p> 	<p><i>Welded box section exposed to fire on all sides:</i></p> $\frac{A_m}{V} = \frac{2(b + h)}{\text{cross-section area}}$ 
<p><i>Angle (or any open section of uniform thickness) exposed to fire on all sides:</i> $A_m/V = 2/t$</p> 	<p><i>I-section with box reinforcement, exposed to fire on all sides</i></p> $\frac{A_m}{V} = \frac{2(b + h)}{\text{cross-section area}}$ 
<p><i>Flat bar exposed to fire on all sides:</i> $A_m/V = 2(b + t)/(bt)$ If $t \ll b$: $A_m/V \cong 2/t$</p> 	<p><i>Flat bar exposed to fire on three sides:</i> $A_m/V = (b + 2t)/(bt)$ If $t \ll b$: $A_m/V \cong 1/t$</p> 

5.2.3 Simple calculation model for steelwork insulated by fire protection material

The increase of temperature $\Delta\theta_{a,t}$ of various parts of an insulated steel beam during the time interval Δt may be obtained from:

$$\Delta\theta_{a,t} = \left[\left(\frac{\lambda_p/d_p}{c_a \rho_a} \right) \left(\frac{A_{p,i}}{V_i} \right) \left(\frac{1}{1+w/3} \right) (\theta_g - \theta_{a,t}) \Delta t \right] - \left[\left(e^{w/10} - 1 \right) \Delta\theta_g \right] \quad (32)$$

with

$$w = \left(\frac{c_p \rho_p}{c_a \rho_a} \right) d_p \left(\frac{A_{p,i}}{V_i} \right)$$

where

λ_p is the thermal conductivity of the fire protection material [W/mK]

d_p is the thickness of the fire protection material [m]

$A_{p,i}$ is the area of the inner surface of the fire protection material per unit length of the part i of the steel member [m²/m]

c_p is the specific heat of the fire protection material [J/kgK]

ρ_p is the density of the fire protection material [kg/m³]

θ_g is the ambient gas temperature at time t [°C]

Δt is the time interval which should not be taken as more than 30 seconds [sec]

$\Delta\theta_g$ is the increase of the ambient gas temperature during the time interval Δt [°C].

Any negative temperature increase $\Delta\theta_{a,t}$ obtained by equation (32) should be replaced by zero.

For non protected members and members with contour protection, the section factor A_i/V_i or $A_{p,i}/V_i$ should be calculated as follows:

for the lower flange

$$A_i/V_i \text{ or } A_{p,i}/V_i = 2(b_1 + e_1)/b_1 e_1 \quad (33a)$$

for the upper flange, when at least 85% of the upper flange of the steel profile is in contact with the concrete slab or, when any void formed between the upper flange and a profiled steel deck is filled with non-combustible material:

$$A_i/V_i \text{ or } A_{p,i}/V_i = (b_2 + 2e_2)/b_2 e_2 \quad (33b)$$

for the upper flange when used with a composite floor when less than 85% of the upper flange of the steel profile is in contact with the profiled steel deck:

$$A_i/V_i \text{ or } A_{p,i}/V_i = 2(b_2 + e_2)/b_2 e_2 \quad (33c)$$

If the beam depth h does not exceed 500 mm, the temperature of the web may be taken as equal to that of the lower flange.

For members with box-protection, a uniform temperature may be assumed over the height of the profile when using equation (32) together with A_p/V

where

A_p is the area of the inner surface of the box protection per unit length of the steel beam [m²/m]

V is the volume of the complete cross-section of the steel beam per unit length [m³/m]

Protection of a steel beam bordered by a concrete floor on top, may be achieved by a **horizontal screen** below, and its temperature development may be calculated assuming that the ambient gas temperature θ_g is given by the temperature in the void. The performance of the heat screen and the temperature development in the void should be determined from measurements according to EN13381-1 [56].

When the performance of the heat screen is known, the temperature development in the void may also be evaluated on behalf of an advanced calculation model.

The **moisture content** of fire protection materials applied to steelwork may be used to increase the fire resistance time by taking advantage of the evaporation time t_v given by:

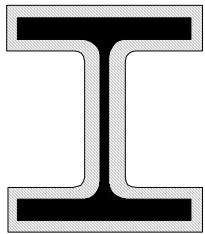
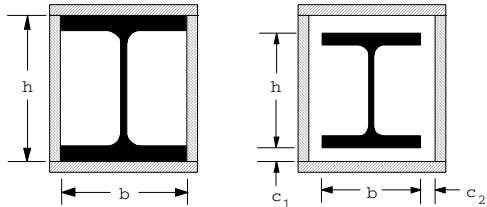
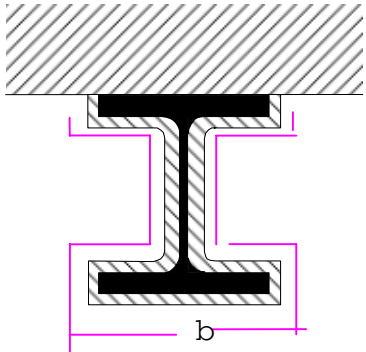
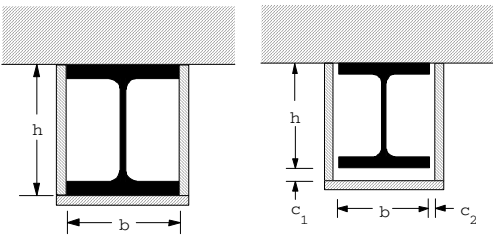
$$t_v = (p \cdot \rho_p \cdot d_p^2) / 5\lambda_p \quad [\text{min}] \quad (34)$$

where

p is the moisture content of the fire protection material [%].

Some design values of the section factors A_p/V for insulated steel members are given in table 8.

Table 8. Section factor A_p/V for steel members insulated by fire protection material.

Sketch	Description	Section factor (A_p/V)
	Contour encasement of uniform thickness	$\frac{\text{steel perimeter}}{\text{steel cross-section area}}$
	Hollow encasement ¹⁾ of uniform thickness	$\frac{2(b + h)}{\text{steel cross-section area}}$
	Contour encasement of uniform thickness, exposed to fire on three sides	$\frac{\text{steel perimeter} - b}{\text{steel cross-section area}}$
	Hollow encasement ¹⁾ of uniform thickness, exposed to fire on three sides	$\frac{2h + b}{\text{steel cross-section area}}$
¹⁾ The clearance dimensions c_1 and c_2 should normally not exceed $h/4$.		

6 STRUCTURAL MODELS

6.1 Introduction

The objective of this Handbook is to describe a performance based more realistic and credible approach to the analysis of structural safety in case of fire, which of course takes also account of structural models, which should be as realistic as possible.

Within structural models, it is necessary to differentiate the schematisation of the structure to be checked from calculation models allowing to assess the mechanical resistance of this schematised structure.

6.1.1 Schematisation of the structure

The behaviour of a structure in the fire situation may be performed:

- either as a **global structural analysis** dealing with the entire structure, which should take into account the relevant failure mode under fire, the temperature dependent material properties and member stiffnesses, the effects of thermal expansions, thermal gradients and thermal deformations.

- or as an **analysis of parts of the structure**. In this case, appropriate subassemblies should be selected on the basis of the potential thermal expansions and deformations, such that their interaction with other parts of the structure may be approximated by time-independent support and boundary conditions during fire exposure. The design effects of actions at supports and boundaries of subassemblies applicable at time $t = 0$, $E_{fi,d,t} = 0$, are assumed to remain unchanged throughout the fire exposure.

- or as a **member analysis**. In this case also the support and restraint conditions of the member, applicable at time $t = 0$, may generally be assumed to remain unchanged throughout the fire exposure. The buckling length ℓ_θ of any compression member for the fire design situation should generally be determined as for normal temperature design. However, for continuous columns in braced frames, the buckling length ℓ_θ may be reduced. In the case of a steel frame in which each level may be considered as a fire compartment with sufficient fire resistance, the buckling length of a continuous column ℓ_θ is equal to $0,5L$ for an intermediate storey, whereas for the top storey the buckling length ℓ_θ is equal to $0,7L$. It may be noted that L is the system length in the relevant storey.

As mentioned in EN1992-1-2 [54], EN1993-1-2 [53] and EN1994-1-2 [55], member analysis is mainly used when verifying standard fire resistance requirements. When dealing with a real fire development, combined with the purpose to have a realistic evaluation of the fire behaviour of a real building, it is generally necessary to consider the interaction between members. Hence it is required to perform a global structural analysis of the entire structure including the parts of the structure directly exposed to fire and those which are not exposed.

6.1.2 Design procedures

The load-bearing function of a structure, of a part of it or of a member shall be maintained up to the required fire resistance time t so that:

$$E_{fi,d,t} \leq R_{fi,d,t} \quad (35)$$

where:

- $E_{fi,d,t}$ is the design effect of actions for the fire situation at time t , according to EN1991-1-2 [46], including all indirect fire actions (see also 6.2),
- $R_{fi,d,t}$ is the corresponding design resistance of a structure, of a part of it or of a member, for the fire situation at time t .

The corresponding design resistance should be based on the recommended value of the partial material factor for the fire situation $\gamma_{M,fi} = 1,0$ to be applied to mechanical properties of steel and concrete [53, 54, 55].

According to EN1992-1-2, EN1993-1-2 and EN1994-1-2 the assessment of structural behaviour in a fire design situation shall be based on one of the following permitted design procedures:

- recognized design solutions **called tabulated data** for specific types of structural members,
- **simple calculation models** for specific types of structural members,
- **advanced calculation models** able to deal with any kind of schematisation of the structure.

Tabulated data and simple calculation models should give conservative results compared to relevant tests or advanced calculation models.

Where no tabulated data nor simple calculation models are applicable, it is necessary to use either a method based on an advanced calculation model or a method based on test results.

6.2 Mechanical actions

Regarding mechanical actions, it is commonly agreed that the probability of the combined occurrence of a fire in a building and an extremely high level of mechanical loads is very small. In fact the load level to be used to check the fire resistance of elements refers to other safety factors than those used for normal design of buildings. The general formula proposed to calculate the relevant effects of actions is according to EN 1990 and EN1991-1-2 [44, 46]:

$$\sum G_{k,j} + (\psi_{1,1} \text{ or } \psi_{2,1})Q_{k,1} + \sum \psi_{2,i} Q_{k,i} + \sum A_{d(t)} \equiv \text{Static Actions} + \text{Accidental Action} \quad (36)$$

where:

$G_{k,j}$ is the characteristic value of the permanent action ("dead load")

$Q_{k,1}$ is the characteristic value of the main variable action

$Q_{k,i}$ is the characteristic value of the other variable actions

$\psi_{1,1}; \psi_{2,1}; \psi_{2,i}$ is the combination factors for buildings according to table 9,

$A_{d(t)}$ is the design value of the accidental action resulting from the fire exposure.

The accidental action is represented by:

- * the temperature effect on the material properties and
- * the indirect thermal actions created either by deformations and expansions caused by the temperature increase in the structural elements, where as a consequence internal forces and moments may be initiated, P- δ effect included, either by thermal gradients in cross-sections leading to internal stresses.

For instance in a domestic, residential or an office building with imposed loads as the main variable action ($Q_{k,1}$) and wind or snow as the other variable actions, the formula concerning static actions is, in case $\psi_{1,1}$ is chosen,

$$G_k + 0,5 Q_{k,1} \quad (36a)$$

since for wind ψ_2 equals zero, and for snow ψ_2 equals also zero if the altitude $H \leq 1000$ m.

However for the altitude $H > 1000$ m or in Finland, Iceland, Norway and Sweden snow shall be considered as follows

$$G_k + 0,5 Q_{k,1} + 0,2 S_{k,2} \quad (36b)$$

Table 9. Recommended values for combination factors ψ , [5].

Action	ψ_0	ψ_1	ψ_2
Imposed loads in buildings, category (see EN 1991-1-1)			
Category A : domestic, residential areas	0,7	0,5	0,3
Category B : office areas	0,7	0,5	0,3
Category C : congregation areas	0,7	0,7	0,6
Category D : shopping areas	0,7	0,7	0,6
Category E : storage areas	1,0	0,9	0,8
Category F : traffic area, vehicle weight $\leq 30\text{kN}$	0,7	0,7	0,6
Category G : traffic area, $30\text{kN} < \text{vehicle weight} \leq 160\text{kN}$	0,7	0,5	0,3
Category H : roofs	0	0	0
Snow loads on buildings (see EN 1991-1-3)*			
Finland, Iceland, Norway, Sweden	0,70	0,50	0,20
Remainder of CEN Member States, for sites located at altitude $H > 1000\text{ m a.s.l.}$	0,70	0,50	0,20
Remainder of CEN Member States, for sites located at altitude $H \leq 1000\text{ m a.s.l.}$	0,50	0,20	0
Wind loads on buildings (see EN 1991-1-4)	0,6	0,2	0
Temperature (non-fire) in buildings (see EN 1991-1-5)	0,6	0,5	0
NOTE The ψ values may be set by the National annex.			
* For countries not mentioned below, see relevant local conditions.			

When in a domestic, residential or an office building, the main variable action is considered to be the wind load ($Q_{k,1} \equiv W_{k,1}$) and the imposed load ($Q_{k,2}$ in this case) is the other variable action, the formula is, in case $\psi_{1,1}$ is chosen,

$$G_k + 0,2 W_{k,1} + 0,3 Q_{k,2} \quad (36c)$$

since for snow ψ_2 equals zero if the altitude $H \leq 1000\text{ m}$.

But for the altitude $H > 1000\text{ m}$ or in Finland, Iceland, Norway and Sweden we get

$$G_k + 0,2 W_{k,1} + 0,3 Q_{k,2} + 0,2 S_{k,3} \quad (36d)$$

In the case of snow as the main variable action ($Q_{k,1} = S_{k,1}$), the formula becomes

$$G_k + 0,2 S_{k,1} + 0,3 Q_{k,2} \quad (36e)$$

But for the altitude $H > 1000\text{ m}$ or in Finland, Iceland, Norway and Sweden we get

$$G_k + 0,5 S_{k,1} + 0,3 Q_{k,2} \quad (36f)$$

Generally this leads in the fire situation to a loading which corresponds approximately to 50 % of the ultimate load bearing resistance at room temperature for structural elements.

6.3 Tabulated data

The tables have been developed on an empirical basis, confirmed by the evaluation of tests and calibrated by theoretical calculations. At the time being they give design solutions only valid for the standard fire exposure.

6.3.1 Concrete structural elements

Tables for **beams** have been published in EN1992-1-2 [54]. These beams may be exposed to fire on three sides, i.e. the upper side is insulated by slabs or other elements which keep their insulation function during the whole fire resistance period. Typical cross-sections are shown in figure 29.

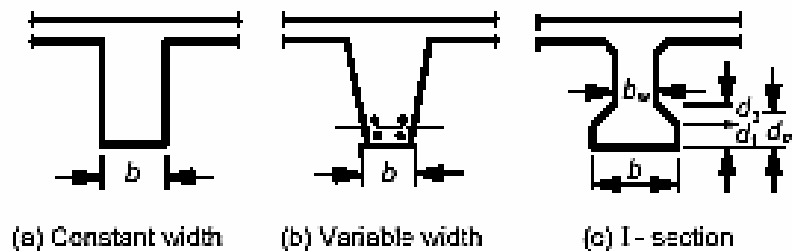


Figure 29. Definition of dimensions for different types of beams.

The effective height d_{eff} of the bottom flange of I-shaped beams should not be less than

$$d_{eff} = d_1 + 0,5d_2 \geq b_{min}$$

where b_{min} is the width of the beam given in table 10.

Table 10. Minimum dimensions and axis distances for simply supported beams of reinforced or prestressed concrete.

Standard fire resistance	Minimum dimensions (mm)						
	Possible combinations of a and b_{min} where a is the average axis distance and b_{min} is the width of beam				Web thickness b_w		
					Class WA	Class WB	Class WC
1	2	3	4	5	6	7	8
R 30	$b_{min}= 80$ $a = 25$	120 20	160 15*	200 15*	80	80	80
R 60	$b_{min}= 120$ $a = 40$	160 35	200 30	300 25	100	80	100
R 90	$b_{min}= 150$ $a = 55$	200 45	300 40	400 35	110	100	100
R 120	$b_{min}= 200$ $a = 65$	240 60	300 55	500 50	130	120	120
R 180	$b_{min}= 240$ $a = 80$	300 70	400 65	600 60	150	150	140
$a_{sd} = a + 10\text{mm}$							
a_{sd} is the axis distance to the side of beam for the corner bars (or tendon or wire) of beams with only one layer of reinforcement. For values of b_{min} greater than that given in Column 4 no increase of a_{sd} is required.							
* Normally the cover required by EN 1992-1-1 will control.							

Note that table 10 is based on the assumption that $E_{fi,d} = 0,7 \cdot E_d$
where

$E_{fi,d}$ is the design effect of actions for the fire situation,

E_d is the design effect of actions for normal temperature conditions.

Similar tables exist for rectangular or circular **columns** shown in figure 30.

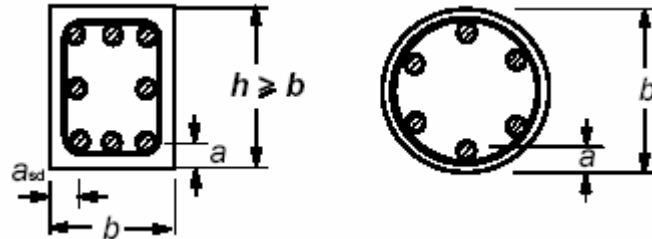


Figure 30. Definition of dimensions for different types of columns, showing the axis distance a.

Note that table 11, which gives design solutions for columns mainly submitted to compression in braced frames, is based on the load level for fire design given by

$$\eta_{fi,t} = E_{fi,d} / R_d = N_{Efi,d} / N_{Rd}$$

where

R_d is the design resistance for normal temperature conditions

$N_{Efi,d}$ is the design axial load in the fire situation

N_{Rd} is the design resistance under axial loads for normal temperature conditions.

The buckling length should be limited to 3m, the load eccentricity to 0,15 (b or h) and the reinforcement A_s to $0,04 \cdot A_c$.

Table 11. Minimum dimensions and axis distances for columns with rectangular or circular cross section.

Standard fire resistance	Minimum dimensions (mm) Column width b_{min} /axis distance a of the main bars			
	Column exposed on more than one side			Exposed on one side
	$\mu_{fi} = 0.2$	$\mu_{fi} = 0.5$	$\mu_{fi} = 0.7$	$\mu_{fi} = 0.7$
1	2	3	4	5
R 30	200/25	200/25	200/32 300/27	155/25
R 60	200/25	200/36 300/31	250/46 350/40	155/25
R 90	200/31 300/25	300/45 400/38	350/53 450/40**	155/25
R 120	250/40 350/35	350/45** 450/40**	350/57** 450/51**	175/35
R 180	350/45**	350/63**	450/70**	230/55
** Minimum 8 bars				

Note that in this table

° $\mu_{fi} \equiv \eta_{fi,t}$

°° $\alpha_{cc} = 1,0$ according to the recommendation given in 3.1.6.1(P) of EN1992-1-1, [45].

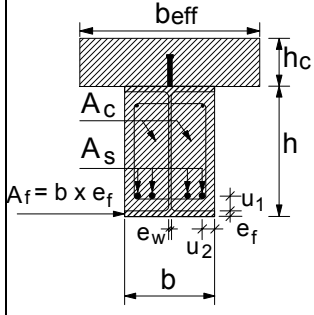
6.3.2 Composite steel-concrete structural elements

The design solutions presented in the following tables 12, 13 and 14 were published in prEN1994-1-2 [55]. They correspond to standard fire resistance classes for which the design resistance in the fire situation $R_{fi,d,t}$ has decreased to the level of the design effect of actions $E_{fi,d,t}$ in the fire situation such as $E_{fi,d,t} = R_{fi,d,t}$.

This means however that the load level for fire design is given by $\eta_{fi,t} = R_{fi,d,t} / R_d$. Hence the load level for fire design $\eta_{fi,t}$ given in these tables allows also to calculate the design resistance in the fire situation $R_{fi,d,t}$ by the relation $R_{fi,d,t} = \eta_{fi,t} \cdot R_d$, provided the design resistance for normal temperature conditions R_d is calculated.

6.3.2.1 Composite beam comprising steel beam with partial concrete encasement

Table 12. Minimum cross-sectional dimensions b and minimum additional reinforcement, for composite beams comprising steel beams with partial concrete encasement.

		Standard Fire Resistance				
		R30	R60	R90	R120	R180
1	Minimum cross-sectional dimensions for load level $\eta_{fi,t} \leq 0,3$					
	min b [mm] and additional reinforcement A_s in relation to the area of flange A_s / A_f					
1.1	$h \geq 0,9 \times \min b$	70/0,0	100/0,0	170/0,0	200/0,0	260/0,0
1.2	$h \geq 1,5 \times \min b$	60/0,0	100/0,0	150/0,0	180/0,0	240/0,0
1.3	$h \geq 2,0 \times \min b$	60/0,0	100/0,0	150/0,0	180/0,0	240/0,0
2	Minimum cross-sectional dimensions for load level $\eta_{fi,t} \leq 0,5$					
	min b [mm] and additional reinforcement A_s in relation to the area of flange A_s / A_f					
2.1	$h \geq 0,9 \times \min b$	80/0,0	170/0,0	250/0,4	270/0,5	-
2.2	$h \geq 1,5 \times \min b$	80/0,0	150/0,0	200/0,2	240/0,3	300/0,5
2.3	$h \geq 2,0 \times \min b$	70/0,0	120/0,0	180/0,2	220/0,3	280/0,3
2.4	$h \geq 3,0 \times \min b$	60/0,0	100/0,0	170/0,2	200/0,3	250/0,3
3	Minimum cross-sectional dimensions for load level $\eta_{fi,t} \leq 0,7$					
	min b [mm] and additional reinforcement A_s in relation to the area of flange A_s / A_f					
3.1	$h \geq 0,9 \times \min b$	80/0,0	270/0,4	300/0,6	-	-
3.2	$h \geq 1,5 \times \min b$	80/0,0	240/0,3	270/0,4	300/0,6	-
3.3	$h \geq 2,0 \times \min b$	70/0,0	190/0,3	210/0,4	270/0,5	320/1,0
3.4	$h \geq 3,0 \times \min b$	70/0,0	170/0,2	190/0,4	270/0,5	300/0,8

Composite beams comprising a steel beam with partial concrete encasement may be classified in function of the load level $\eta_{fi,t}$, the beam width b and the additional reinforcement A_s related to the area of the bottom flange A_f of the steel beam as given in table 12.

The values given in table 12 are valid for simply supported beams. When determining R_d and $R_{fi,d,t} = \eta_{fi,t} R_d$ in connection with table 12, the following conditions should be observed:

- the thickness of the web e_w does not exceed 1/15 of the width b ;
- the thickness of the bottom flange e_f does not exceed twice the thickness of the web e_w ;
- the thickness of the concrete slab h_c is at least 120 mm;
- the additional reinforcement area related to the total area between the flange $A_s / (A_c + A_s)$ does not exceed 5 %;
- the value of R_d is calculated on the basis of EN 1994-1-1, [48], provided that the effective slab width b_{eff} does not exceed 5 m and the additional reinforcement A_s is not taken into account.

6.3.2.2 Composite columns

The design tables 13 and 14 are valid for braced frames and for columns with a maximum length of 30 times the minimum external dimension of the cross-section chosen.

Tables 13 and 14 are valid both for concentric axial or eccentric loads applied to columns. When determining R_d , the design resistance for normal temperature design, the eccentricity of the load has to be considered.

Load levels $\eta_{fi,t}$ in those tables are defined assuming pin-ended supports of the column for the calculation of R_d , provided that both column ends are rotationally restrained in the fire situation. This is generally the case in practice when assuming that only the level under consideration is submitted to fire.

In general, when using tables 13 or 14, R_d has to be based on twice the buckling length used in the fire design situation.

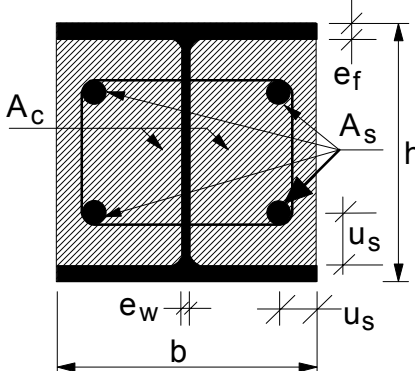
6.3.2.3 Composite columns with partially encased steel sections

Composite columns made of partially encased steel sections may be classified in function of the load level $\eta_{fi,t}$, the depth b or h , the minimum axis distance of the reinforcing bars u_s , the ratio of reinforcement $A_s / (A_c + A_s)$ in % and the ratio between the web thickness e_w and the flange thickness e_f as given in table 13.

When determining R_d and $R_{fi,d,t} = \eta_{fi,t} R_d$, in connection with table 13, reinforcement ratios $A_s / (A_c + A_s)$ higher than 6 % or lower than 1 %, should not be taken into account.

Table 13 may be used for the structural steel grades S 235, S 275 and S 355.

Table 13. Minimum cross-sectional dimensions, minimum axis distance and minimum reinforcement ratios of composite columns made of partially encased steel sections.

		Standard Fire Resistance			
		R30	R60	R90	R120
	Minimum ratio of web to flange thickness e_w/e_f	0,5	0,5	0,5	0,5
1	Minimum cross-sectional dimensions for load level $\eta_{fi,t} \leq 0,28$				
1.1	minimum dimensions h and b [mm]	160	200	300	400
1.2	minimum axis distance of reinforcing bars u_s [mm]	-	50	50	70
1.3	minimum ratio of reinforcement $A_s/(A_c+A_s)$ in %	-	4	3	4
2	Minimum cross-sectional dimensions for load level $\eta_{fi,t} \leq 0,47$				
2.1	minimum dimensions h and b [mm]	160	300	400	-
2.2	minimum axis distance of reinforcing bars u_s [mm]	-	50	70	-
2.3	minimum ratio of reinforcement $A_s/(A_c+A_s)$ in %	-	4	4	-
3	Minimum cross-sectional dimensions for load level $\eta_{fi,t} \leq 0,66$				
3.1	minimum dimensions h and b [mm]	160	400	-	-
3.2	minimum axis distance of reinforcing bars u_s [mm]	40	70	-	-
3.3	minimum ratio of reinforcement $A_s/(A_c+A_s)$ in %	1	4	-	-

6.3.2.4 Composite columns with concrete filled hollow sections

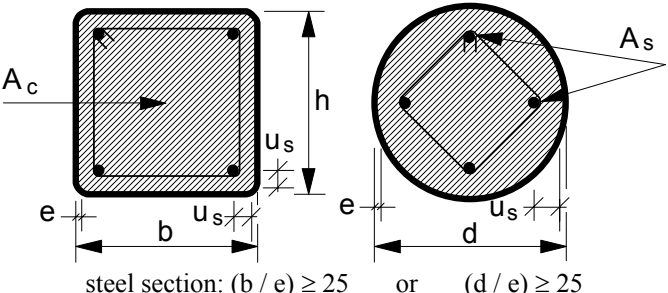
Composite columns made of concrete filled hollow sections may be classified as a function of the load level $\eta_{fi,t}$, the cross-section size b, h or d, the ratio of reinforcement $A_s / (A_c + A_s)$ in % and the minimum axis distance of the reinforcing bars u_s according to table 14.

When calculating R_d and $R_{fi,d,t} = \eta_{fi,t} R_d$, in connection with table 14, following rules apply:

- irrespective of the steel grade of the hollow sections, a nominal yield point of 235 N/mm² is taken into account;
- the wall thickness e of the hollow section is considered up to a maximum of 1/25 of b or d;
- reinforcement ratios $A_s / (A_c + A_s)$ higher than 3 % are not taken into account and
- the concrete strength is considered as for normal temperature design.

The values given in table 14 are valid for the steel grade S 500 used for the reinforcement A_s .

Table 14. Minimum cross-sectional dimensions, minimum reinforcement ratios and minimum axis distance of the reinforcing bars of composite columns made of concrete filled hollow sections.

 steel section: $(b / e) \geq 25$ or $(d / e) \geq 25$		Standard Fire Resistance				
		R30	R60	R90	R120	R180
1	Minimum cross-sectional dimensions for load level $\eta_{fi,t} \leq 0,28$					
1.1	Minimum dimensions h and b or minimum diameter d [mm]	160	200	220	260	400
1.2	Minimum ratio of reinforcement $A_s / (A_c + A_s)$ in (%)	0	1,5	3,0	6,0	6,0
1.3	Minimum axis distance of reinforcing bars u_s [mm]	-	30	40	50	60
2	Minimum cross-sectional dimensions for load level $\eta_{fi,t} \leq 0,47$					
2.1	Minimum dimensions h and b or minimum diameter d [mm]	260	260	400	450	500
2.2	Minimum ratio of reinforcement $A_s / (A_c + A_s)$ in (%)	0	3,0	6,0	6,0	6,0
2.3	Minimum axis distance of reinforcing bars u_s [mm]	-	30	40	50	60
3	Minimum cross-sectional dimensions for load level $\eta_{fi,t} \leq 0,66$					
3.1	Minimum dimensions h and b or minimum diameter d [mm]	260	450	550	-	-
3.2	Minimum ratio of reinforcement $A_s / (A_c + A_s)$ in (%)	3,0	6,0	6,0	-	-
3.3	Minimum axis distance of reinforcing bars u_s [mm]	25	30	40	-	-

NOTE: Alternatively to this method, the design rules of table 11 may be used, when neglecting the steel tube.

6.4 Simple calculation models

6.4.1 Concrete structural elements

6.4.1.1 Temperature profiles

The temperature profiles given hereafter in figures 31, 32 and 33 constitute a selection of temperature profiles contained in Annex A of EN1992-1-2 [54]. They may be used to determine the temperature in cross-sections with siliceous aggregate exposed to a standard fire up to the time corresponding to the different ISO-fire classes. The profiles are conservative for most other aggregates.

These figures are based on a moisture content of 1,5% as well as on the lower limit of the thermal conductivity of concrete (see Chapter V, paragraph 6.1).

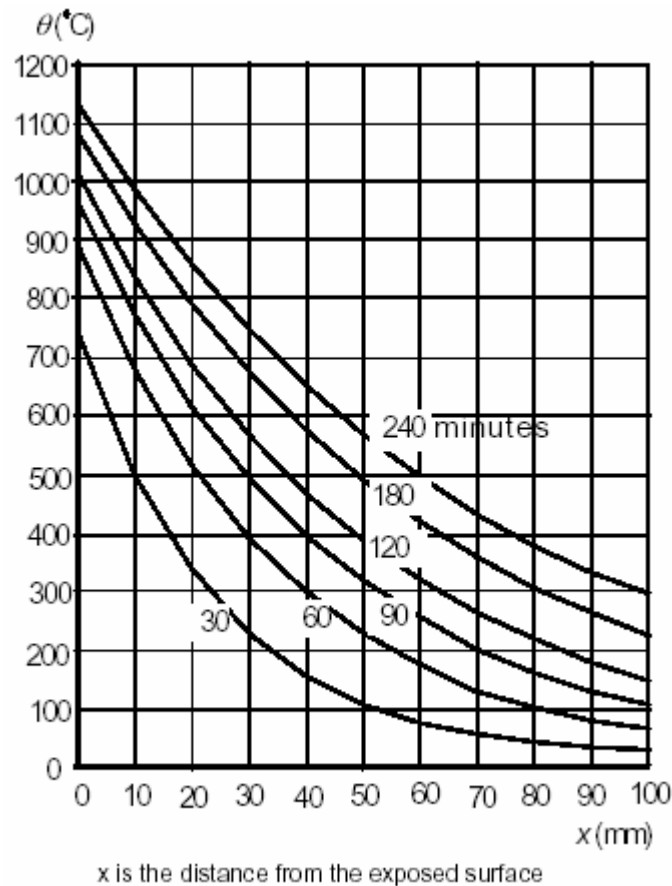
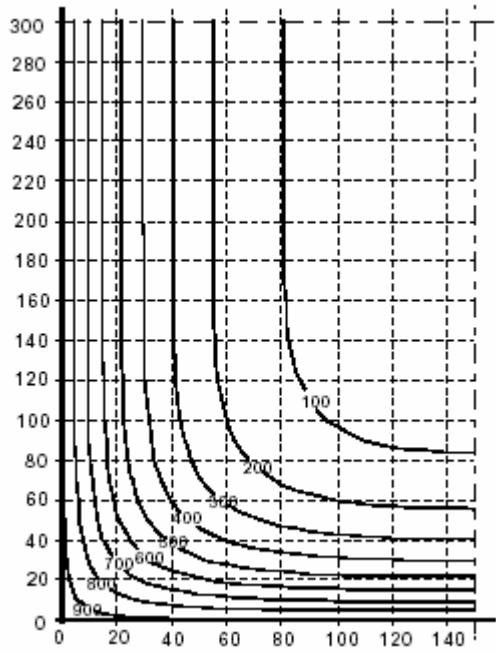
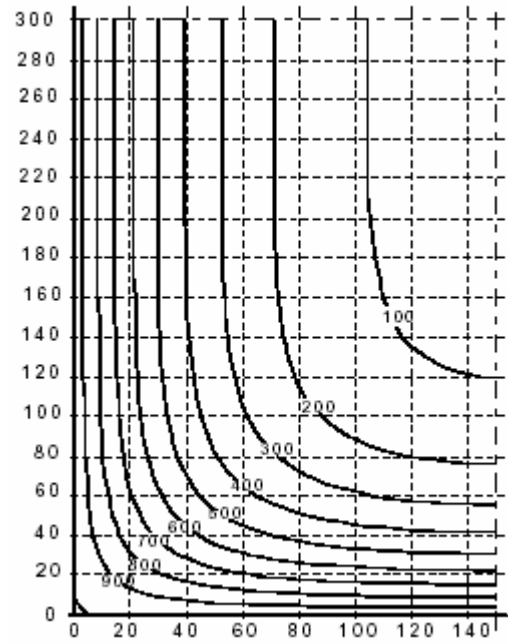


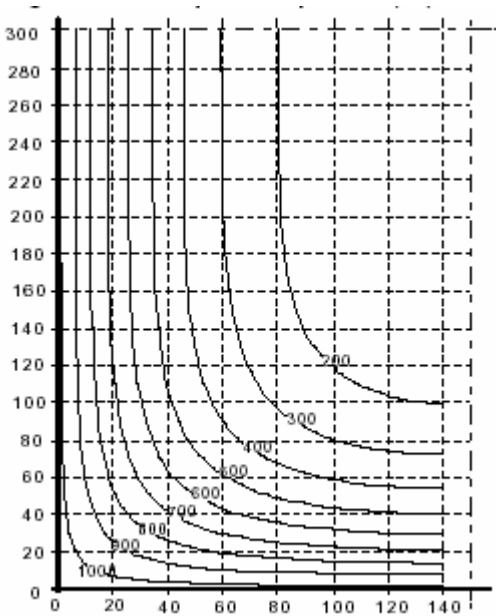
Figure 31. Temperature profiles at 30 to 240 minutes for concrete slabs of 200 mm height, heated from below by the standard fire.



a) at 60 minutes

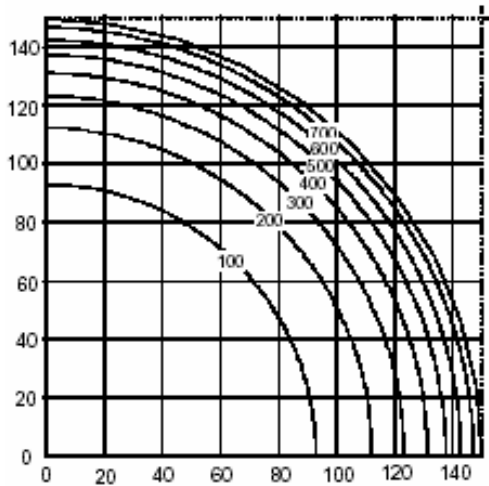


b) at 90 minutes

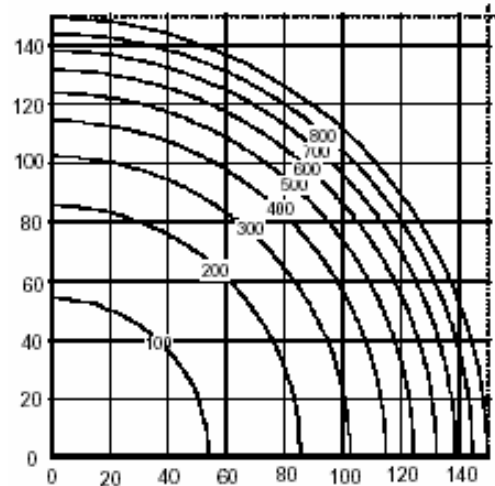


c) at 120 minutes

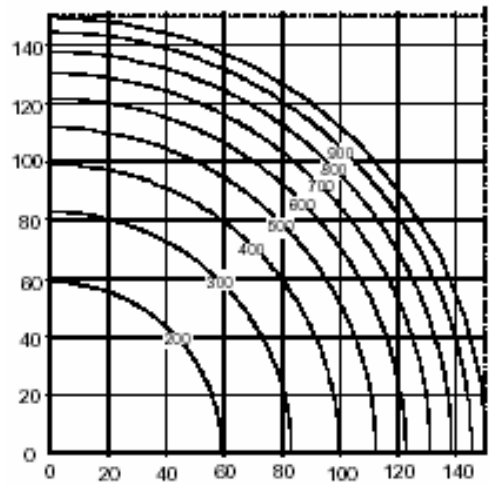
Figure 32. Temperature profiles (°C) for a concrete beam $h \cdot b = 600\text{mm} \cdot 300\text{mm}$, heated all around by the standard fire.



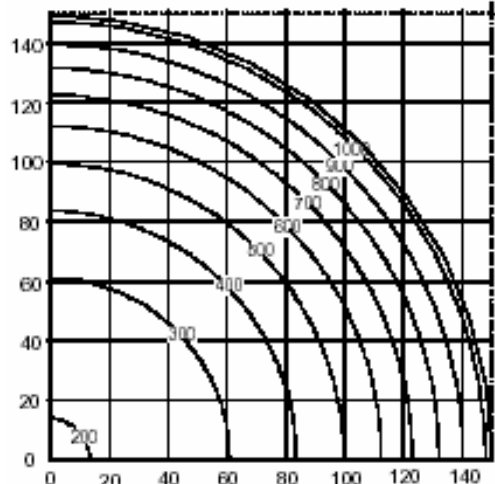
a) R30



b) R60



c) R90



d) R120

Figure 33. Temperature profiles (°C) for a circular column, Ø 300mm, heated all around by the standard fire.

6.4.1.2 Models based on a reduced cross-section

A first model is based on the assumption that concrete at a temperature of more than 500°C may be neglected when calculating the design resistance, while concrete at a temperature below 500°C is considered without strength reduction. This method is applicable to a reinforced or prestressed concrete section with respect to axial or eccentric load N_{sd} or bending moment M_{sd} (see Annex B.1 of EN1992-1-2, [54]). This model is valid for the standard fire exposure as well as for a parametric fire.

A second model consists in subdividing the cross-section into zones of equal thickness parallel to the heated surfaces. For each zone the mean temperature θ and the corresponding compressive strength of concrete $f_{c,\theta}$ are assumed for the different ISO-fire classes (see Annex B.2 of EN1992-1-2, [54]).

6.4.1.3 Assessment of a reinforced concrete cross-section exposed to bending moment and axial load by the curvature method.

This model explained in Annex B.3 is the basis for tables given in Annex C of EN1992-1-2, [54]. These permit to assess columns in braced frames, with a maximum slenderness of $\lambda = l_{\text{buckling}} / i = 80$, and for standard fire conditions (see model table 15).

Table 15. Minimum dimensions and axis distances for rectangular or circular reinforced concrete columns; reinforcement ratio is 1%; moderate first order moments are considered i.e. $e = 0,25b < 100\text{mm}$; n is the load level at normal temperature conditions.

Standard fire resistance	λ	Minimum dimensions (mm) Column width b_{min} /axis distance a			
		Column exposed on more than one side			
		$n = 0,15$	$n = 0,3$	$n = 0,5$	$n = 0,7$
1	2	3	4	5	6
R 30	30	150/25*	150/25*	150/25*	200/30:300/25
	40	150/25*	150/25*	150/25*	250/30:450/25*
	50	150/25*	150/25*	200/25*	300/35:500/25*
	60	150/25*	150/25*	200/30:250/25*	400/40:550/25*
	70	150/25*	150/25*	250/35:300/25*	500/35:600/30
	80	150/25*	150/30:250/25*	300/35:500/25*	500/60:600/35
R 60	30	150/25*	150/30:200/25*	200/40:400/25*	300/50:600/30
	40	150/25*	150/40:250/25*	250/40:500/25*	400/50:600/35
	50	150/25*	200/35:400/25*	300/40:600/25*	500/45:600/40
	60	150/30:200/25*	200/40:450/25*	400/40:600/30	550/40:600/40
	70	150/35:200/25*	240/40:550/25*	450/45:500/35	600/60
	80	200/30:250/25	300/40:550/25	500/50:600/40	600/80
R 90	30	200/25*	200/40:300/25*	250/40:550/25*	500/50:600/45
	40	200/30:250/25*	200/50:400/25*	300/50:600/35	500/60:600/50
	50	200/35:300/25*	250/50:550/25*	400/50:600/40	600/55
	60	200/40:400/25	300/45:600/25*	500/50:600/45	600/70
	70	200/45:450/25*	300/50:600/35	550/55:600/50	(1)
	80	200/50:500/25*	400/50:600/35	600/55	(1)
R 120	30	200/40:250/25	250/50:400/25*	450/45:600/30	600/60
	40	200/45:300/25*	300/40:500/25*	500/50:600/35	(1)
	50	250/40:400/25*	400/40:550/25*	550/50:600/45	(1)
	60	250/50:450/25*	400/50:500/35	600/55	(1)
	70	300/40:500/25*	500/45:600/35	(1)	(1)
	80	300/50:550/25*	500/60:600/40	(1)	(1)
R 180	30	300/35:400/25*	450/50:550/25*	500/60:600/45	(1)
	40	300/40:450/25*	500/40:600/30	550/65:600/60	(1)
	50	400/40:500/25*	500/45:600/35	600/75	(1)
	60	400/45:550/25*	500/55:600/45	(1)	(1)
	70	400/50:600/30	500/65:600/50	(1)	(1)
	80	500/45:600/35	600/70	(1)	(1)
R 240	30	400/45:500/25*	500/40:600/30	600/60	(1)
	40	450/45:550/25*	500/55:600/40	600/80	(1)
	50	450/50:600/25*	500/65:600/45	(1)	(1)
	60	500/45:600/35	550/70:600/55	(1)	(1)
	70	500/50:600/40	600/75	(1)	(1)
	80	500/60:600/45	(1)	(1)	(1)

* Normally the cover required by EN 1992-1-1 will control.
 (1) Requires a width greater than 600 mm. Particular assessment for buckling is required.

6.4.2 Steel structural elements

6.4.2.1 Introduction

For pure steel members (tensile members, columns, beams) the EN1993-1-2 [53] gives simple calculation models for determining the load bearing resistance for a standard fire exposure of:

- tension members with uniform temperature distribution across the cross-section;
- compression members with uniform temperature distribution,
- beams with uniform or non-uniform temperature distribution, taking into account the risk of lateral-torsional buckling,
- members subjected to bending and axial compression, with uniform temperature distribution.

For the purpose of simple calculation models the steel cross-sections may be classified as for normal temperature design with a reduced value for ε as given hereafter

$$\varepsilon = 0,85 [235 / f_y]^{0,5} \quad (37)$$

where:

f_y is the yield strength at 20 °C.

6.4.2.2 Resistance of tension members

The design resistance $N_{fi,\theta,Rd}$ of a tension member with a uniform temperature θ_a should be determined from:

$$N_{fi,\theta,Rd} = k_{y,\theta} N_{Rd} [\gamma_{M,0} / \gamma_{M,fi}] \quad (38)$$

where:

$k_{y,\theta}$ is the reduction factor for the yield strength of steel at temperature θ_a reached at time t (see Chapter V)

N_{Rd} is the design resistance of the cross-section $N_{pl,Rd}$ for normal temperature design, according to EN 1993-1-1, [50] .

6.4.2.3 Resistance of compression members with Class 1, Class 2 or Class 3 cross-sections

The design buckling resistance $N_{b,fi,t,Rd}$ at time t of a compression member with a Class 1, Class 2 or Class 3 cross-section with a uniform temperature θ_a , and submitted to axial compression should be determined from:

$$N_{b,fi,t,Rd} = \chi_{fi} (A k_{y,\theta} f_y) / \gamma_{M,fi} \quad (39)$$

where:

χ_{fi} is the reduction factor for flexural buckling in the fire design situation.

The value of χ_{fi} should be taken as the lesser of the values of $\chi_{y,fi}$ and $\chi_{z,fi}$ determined according to:

$$\chi_{fi} = \frac{1}{\varphi_{\theta} + \sqrt{\varphi_{\theta}^2 - \bar{\lambda}_{\theta}^2}} \quad (40)$$

with

$$\varphi_{\theta} = \frac{1}{2} [1 + \alpha \bar{\lambda}_{\theta} + \bar{\lambda}_{\theta}^2]$$

and

$$\alpha = 0,65 \sqrt{235 / f_y}$$

The non-dimensional slenderness $\bar{\lambda}_\theta$ for the temperature θ_a , is given by:

$$\bar{\lambda}_\theta = \bar{\lambda} [k_{y,\theta} / k_{E,\theta}]^{0,5} \quad (41)$$

where:

$k_{E,\theta}$ is the reduction factor for the slope of the linear elastic range at the steel temperature θ_a reached at time t ;

$\bar{\lambda}$ is the non-dimensional slenderness according 6.3.1.2 of EN1993-1-1, [50].

The buckling length l_θ of a column for the fire design situation should generally be determined as for normal temperature design. However, in a braced frame the buckling length l_θ of a column length may be determined by considering it as fixed, at continuous or semi-continuous connections, to the column lengths in the fire compartments above and below, provided that the fire resistance of the building components that separate these fire compartments is not less than the fire resistance of the column.

In the case of a braced frame in which each storey comprises a separate fire compartment with sufficient fire resistance, in an intermediate storey the buckling length l_θ of a continuous column may be taken as $l_\theta = 0,5L$ and in the top storey the buckling length may be taken as $l_\theta = 0,7L$, where L is the system length in the relevant storey (see figure 34).

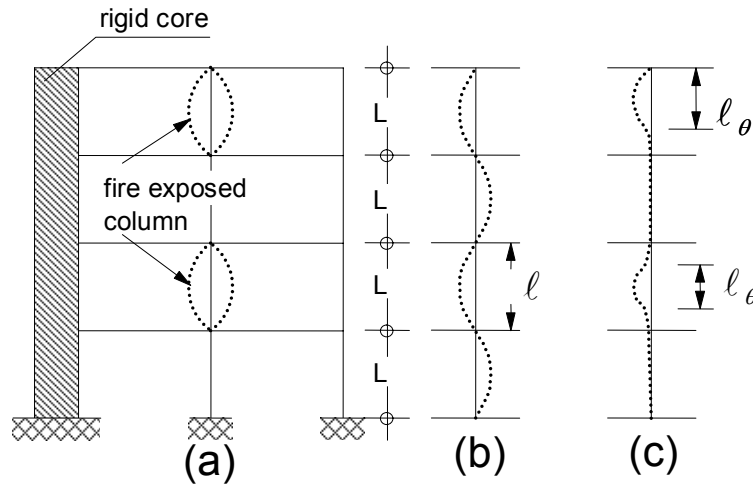


Figure 34. Buckling lengths l_θ of columns in braced frames with a) section through the building, b) deformation mode at room temperature and c) deformation mode at elevated temperature.

6.4.2.4 Resistance of beams with Class 1 or Class 2 cross-sections

The design moment resistance $M_{fi,\theta,Rd}$ of a Class 1 or Class 2 cross-section with a uniform temperature θ_a should be determined from:

$$M_{fi,\theta,Rd} = k_{y,\theta} M_{Rd} [\gamma_{M,0} / \gamma_{M,fi}] \quad (42)$$

where:

M_{Rd} is the plastic moment resistance of the cross-section $M_{pl,Rd}$ for normal temperature design, according to EN 1993-1-1 or the reduced moment resistance for normal temperature design, allowing for the effects of shear if necessary, according to EN 1993-1-1;

$k_{y,\theta}$ is the reduction factor for the yield strength of steel at temperature θ_a reached at time t (see Chapter V).

The design moment resistance $M_{fi,t,Rd}$ at time t of a Class 1 or Class 2 cross-section in a member with a **non-uniform temperature distribution**, may be determined from:

$$M_{fi,t,Rd} = M_{fi,\theta,Rd} / \kappa_1 \kappa_2 \quad (43)$$

where:

$M_{fi,\theta,Rd}$ is the design moment resistance of the cross-section for a uniform temperature θ_a in a cross-section which is not thermally influenced by the support;

κ_1 is the adaptation factor for non-uniform temperature in the cross-section,

κ_2 is the adaptation factor for non-uniform temperature along the beam.

The value of the adaptation factor κ_1 for non-uniform temperature distribution in the cross-section should be taken as follows:

- for a beam exposed on all four sides: $\kappa_1 = 1,0$
- for an unprotected beam exposed on three sides,
with a composite or concrete slab on top $\kappa_1 = 0,70$
- for a protected beam exposed on three sides,
with a composite or concrete slab on top $\kappa_1 = 0,85$

For a non-uniform temperature distribution along a beam the adaptation factor κ_2 should be taken as follows:

- at the supports of a statically indeterminate beam: $\kappa_2 = 0,85$
- in all other cases: $\kappa_2 = 1,0$.

The design **lateral torsional buckling resistance** moment $M_{b,fi,t,Rd}$ at time t of a laterally unrestrained member with a Class 1 or Class 2 cross-section should be determined from:

$$M_{b,fi,t,Rd} = \chi_{LT,fi} W_{pl,y} (k_{y,\theta,com} \cdot f_y) / \gamma_{M,fi} \quad (44)$$

where:

$\chi_{LT,fi}$ is the reduction factor for lateral-torsional buckling in the fire situation;

$k_{y,\theta,com}$ is the reduction factor for the yield strength of steel at the maximum temperature in the compression flange $\theta_{a,com}$ reached at time t .

The value of $\chi_{LT,fi}$ should be determined according to the following equations:

$$\chi_{LT,fi} = \frac{1}{\phi_{LT,\theta,com} + \sqrt{[\phi_{LT,\theta,com}]^2 - [\lambda_{LT,\theta,com}]^2}} \quad (45)$$

with

$$\phi_{LT,\theta,com} = \frac{1}{2} \left[1 + \alpha \bar{\lambda}_{LT,\theta,com} + (\bar{\lambda}_{LT,\theta,com})^2 \right]$$

and

$$\alpha = 0,65 \sqrt{235 / f_y}$$

$$\bar{\lambda}_{LT, \theta, com} = \bar{\lambda}_{LT} [k_{y, \theta, com} / k_{E, \theta, com}]^{0,5}$$

where:

$k_{E, \theta, com}$ is the reduction factor for the slope of the linear elastic range at the maximum steel temperature in the compression flange $\theta_{a, com}$ reached at time t ,

$\bar{\lambda}_{LT}$ is the non-dimensional slenderness related to lateral torsional buckling according 6.3.2.2 of prEN1993-1-1, [50].

6.4.2.5 For beams with Class 3 cross-sections, and members with Class 1, 2 or 3 cross-sections subject to combined bending and axial compression reference is done to 4.2.3.4 and 4.2.3.5 of prEN1993-1-2 [53].

6.4.2.6 Nomogram for protected or unprotected beams and columns

On the basis of the previously explained procedures the nomogram given in figure 35 was established [30], allowing to predict the ISO-fire resistance of steel beams and steel columns provided:

- the adaptation factors κ_1 and κ_2 are known; for instability aspects κ equals 1,2
- the degree of utilisation μ_0 of a member, just at the beginning of the fire, is given by

$$\mu_0 = E f_{t,d} / R_{f,t,d,0} \quad (46)$$

where:

- $E f_{t,d}$ is the design effect of actions in the fire situation,
- $R_{f,t,d,0}$ is the design resistance for the fire situation at time $t = 0$, which means that $\gamma_M = \gamma_{M,fi} = 1,0$ and buckling lengths l_{θ} are chosen according to figure 34,
- for an unprotected steel member the section factor is calculated according to (A_m / V) in $[m^{-1}]$ and
- for a protected steel member the equivalent section factor is calculated according to $(A_p \cdot \lambda_p) / (V \cdot d_p)$ in $[W/m^3K]$

with

A_m the surface area of the member per unit length $[m^2/m]$

V the volume of the member per unit length $[m^3/m]$

A_p the inner surface of fire protection material per unit length of the member $[m^2/m]$

λ_p the thermal conductivity of the fire protection $[W/mK]$

d_p the thickness of the fire protection material $[m]$.

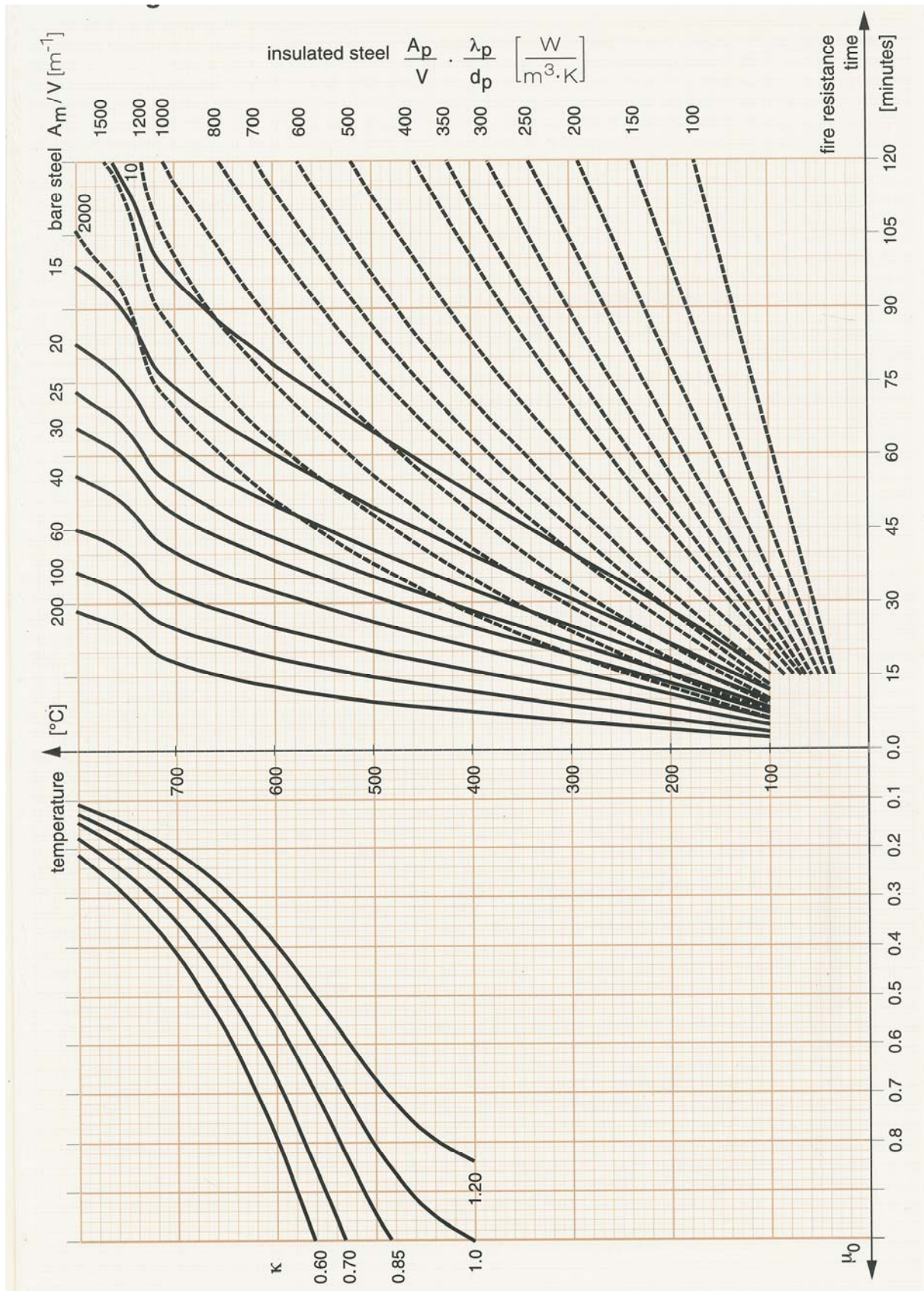


Figure 35. Design graph for steel beams and columns submitted to the standard fire.

6.4.3 Composite steel-concrete structural elements

6.4.3.1 Introduction

For composite members, some simple calculation models given in the prEN1994-1-2 [55] have been established for the standard fire situation. They are dealing with:

- composite slabs, for which the load-bearing resistance of simply supported or continuous slabs is obtained by applying the theory of plasticity, taking into account the temperature of reinforcement bars and of the concrete. If a protection system is used to slow down the heating of the slab, it is assumed that the load-bearing criterion (R) is fulfilled as long as the temperature of the steel sheet is lower or equal to 350°C. This model is detailed in Annex D of prEN1994-1-2.
- composite beams, for which the load-bearing capacity is determined by considering a critical temperature or by calculating the bending moment resistance based on simple plastic theory. Corresponding models are given in Annexes E and F of prEN1994-1-2.
- composite columns with partially encased steel sections, and concrete filled hollow sections are dealt with in Annexes G and H of prEN1994-1-2. These models shall only be used for braced frames and in the fire situation the ratio between bending moment and axial force, $M/N = \delta$, shall not exceed 0,5 times the size b or d of the column cross-section.

6.4.3.2 Composite beams comprising steel beams with partial concrete encasement

The model given in Annexe F of prEN1994-1-2, [55], permits to calculate the fire resistance of a composite beam, comprising a steel beam with partial concrete encasement. This is applicable to simply supported or continuous beams including cantilever parts. The rules apply to composite beams heated from below by the standard temperature-time curve.

The effect of temperatures on material characteristics is taken into account either by reducing the dimensions of the parts composing the cross section or by multiplying the characteristic mechanical properties of materials by a reduction factor as given in Annex F and illustrated in figures 36 and 37.

The slab thickness h_c should be greater than the minimum slab thickness given in table 16. This table may be used for solid and steel deck-concrete slab systems.

Table 16. Minimum slab thickness.

Standard Fire Resistance	Minimum Slab Thickness h_c [mm]
R30	60
R60	80
R90	100
R120	120
R180	150

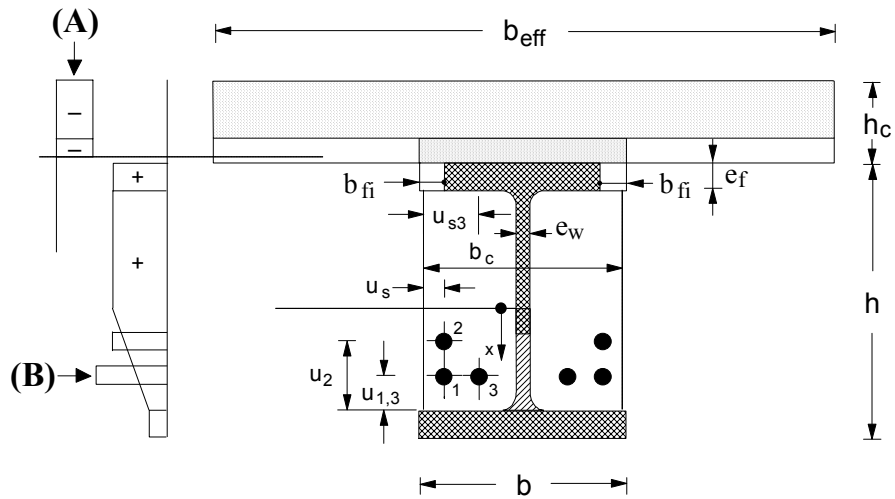


Figure 36. Elements of a cross-section for the calculation of the sagging moment resistance with (A), example of stress distribution in concrete and (B), example of stress distribution in steel.

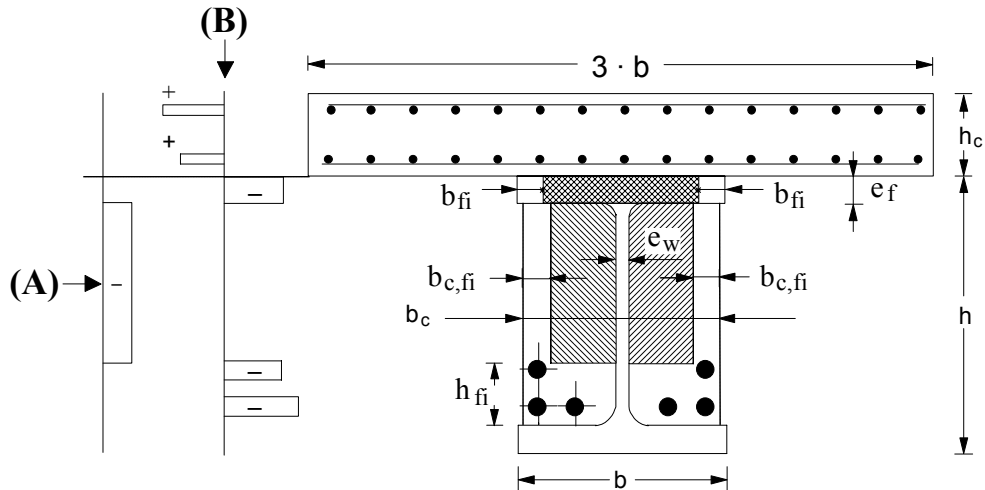


Figure 37. Elements of a cross-section for the calculation of the hogging moment resistance with (A), example of stress distribution in concrete and (B), example of stress distribution in steel.

6.4.3.3 Composite columns with partially encased steel sections

The model for columns heated all around by the standard fire, given in Annexe G of prEN1994-1-2, [55], permits to calculate the design buckling load in axial compression (see model figure 38), on the basis of buckling curve c given in 6.3.1.2 of EN1993-1-1 as follows:

$$N_{fi,Rd,z} = \chi_z N_{fi,pl,Rd} \quad (47)$$

For the calculation procedure in the fire situation, the cross-section is divided into the four components, the flanges of the steel profile, the web of the steel profile, the concrete contained by the steel profile and the reinforcing bars as shown in figure 39.

Each component is evaluated on the basis of a reduced characteristic strength, a reduced modulus of elasticity and a reduced cross-section in function of the standard fire resistance times 30, 60, 90 or 120 minutes.

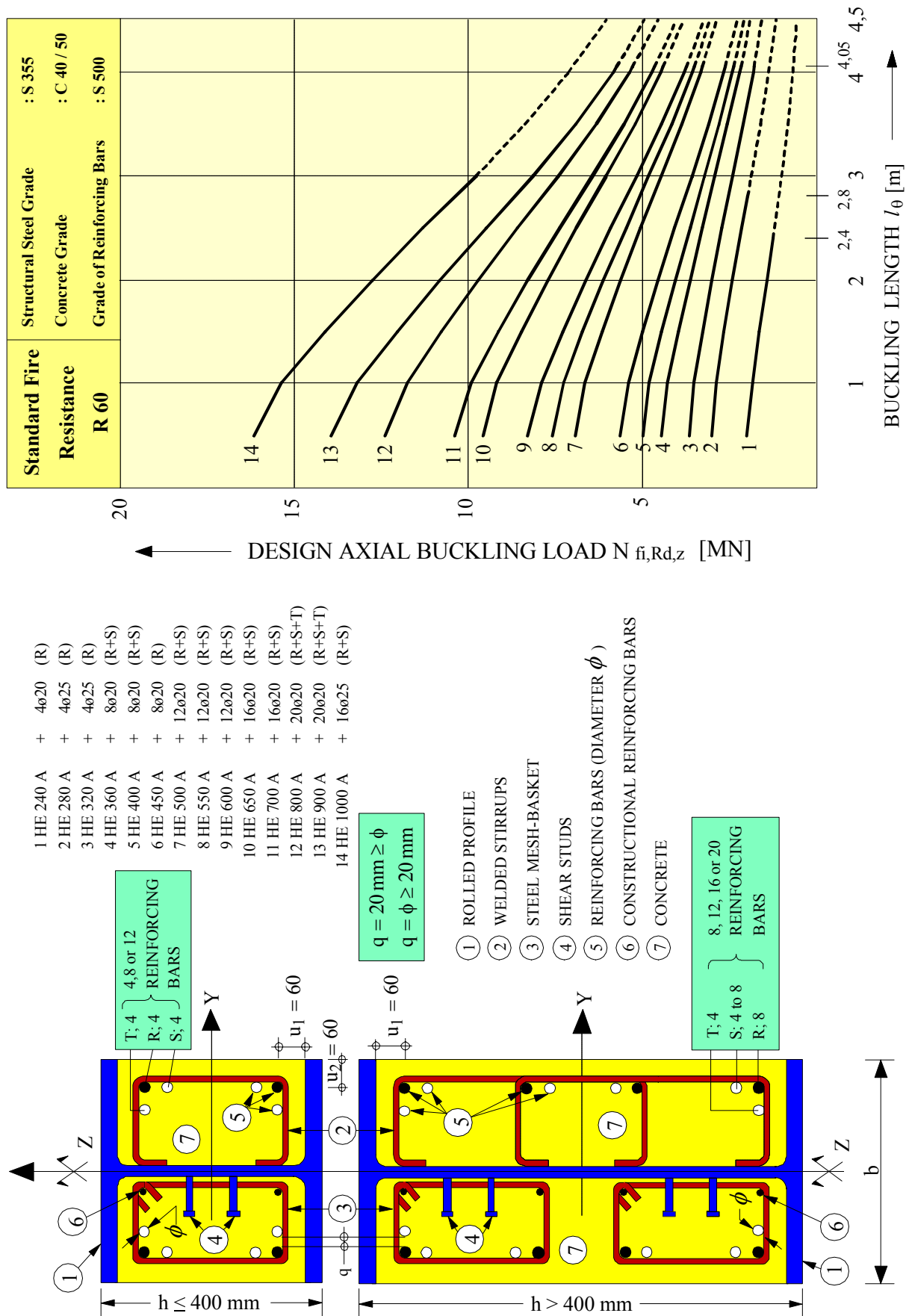


Figure 38. Example of design graph R60 for partially encased steel sections.

The design value of the plastic resistance to axial compression and the effective flexural stiffness of the cross-section are obtained by a balanced summation of the corresponding values of the four components.

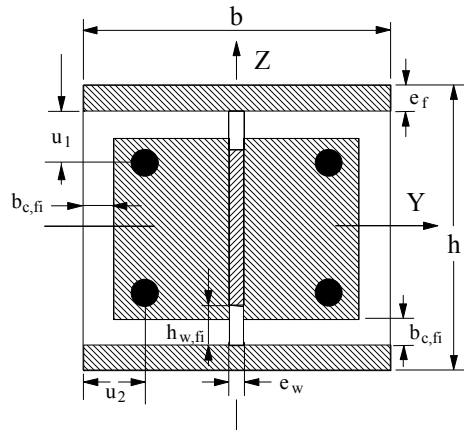


Figure 39. Reduced cross-section for structural fire design. It may be noted that this model was first published in 1988 through ECCS [15].

6.4.3.4 Composite columns with concrete filled hollow sections

The model for columns heated all around by the standard fire, given in Annexe H of prEN1994-1-2, [55], permits to determine the design value of the resistance of a concrete filled hollow section column in axial compression. This model is divided in two steps:

- calculation of the field of temperature in the composite cross-section and
- calculation of the design axial buckling load $N_{fi,Rd}$ for this field of temperature.

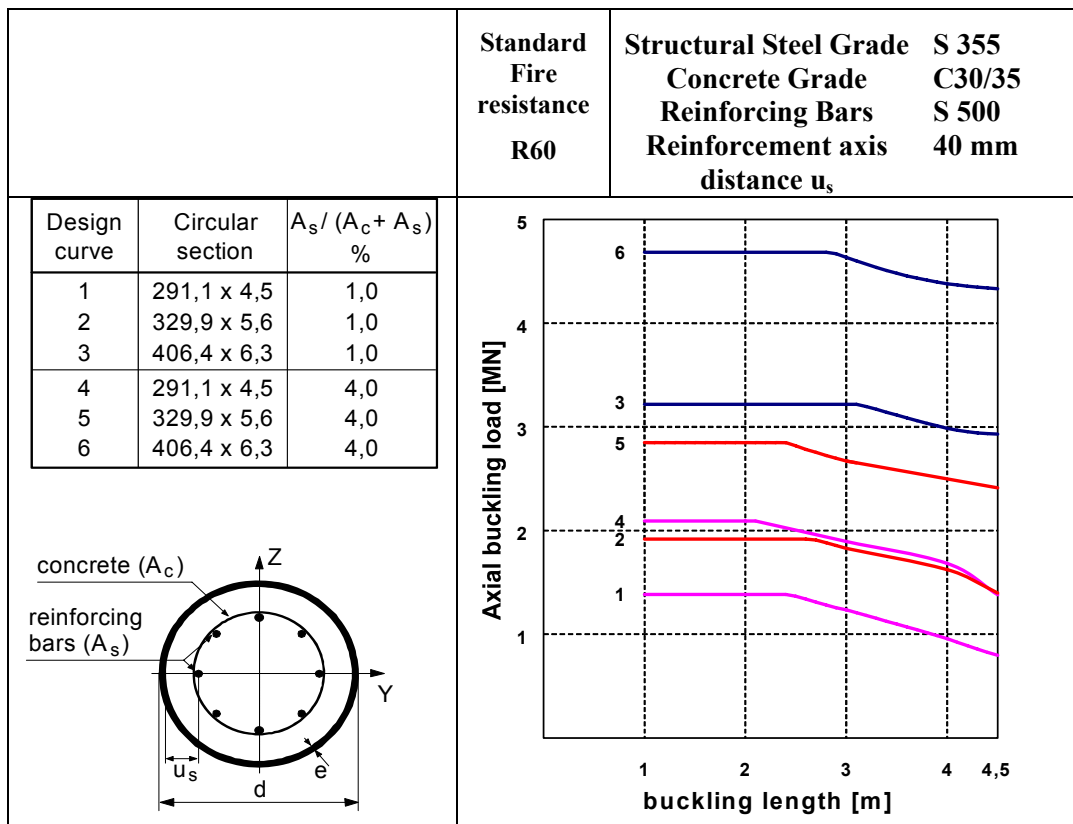


Figure 40. Example of design graph R60 for circular hollow sections.

6.5 Advanced calculation models

6.5.1 Introduction

As mentioned in EN1992-1-2 [54], EN1993-1-2 [53] and EN1994-1-2 [55], advanced calculation models are based on fundamental physical principles leading to a reliable approximation of the expected behaviour of the structure under fire conditions.

They may be **used in association with any temperature-time heating curve**, provided that the material properties are known for the relevant temperature range. Furthermore they are **used for individual members, for subassemblies or for entire structures**, and are able to deal with **any type of cross section**.

Regarding the mechanical models, they have to be based on the acknowledged principles and assumptions of the theory of structural mechanics, taking into account the effects of temperature. Where relevant, the models shall also take account of:

- the combined effects of mechanical actions, geometrical imperfections and thermal actions,
- the temperature dependent mechanical properties of materials,
- the effects of thermally induced strains and stresses, both due to temperature rise and due to temperature differentials,
- geometrical non-linear effects,
- the effects of non-linear material properties, including the effects of loading and unloading on the structural stiffness.

The deformations at ultimate limit state, given by advanced calculation models, shall be limited as necessary to ensure that compatibility is maintained between all parts of the structure. It is possible to include the effects of non-uniform thermal exposure and of heat transfer to adjacent building components. The influence of any moisture content and of any migration of the moisture within the concrete and the fire protection material, may be also considered.

Any potential failure modes not covered by an advanced calculation method (for instance, local buckling and failure in shear) shall be eliminated, in the design of the structure by appropriate means or detailing.

In general the advanced numerical models require a division of the structural element under consideration into small elements. The size of these finite elements shall be chosen such that further refining will not significantly influence the general results. In general mesh refinement will lead to more accurate results.

It is known however that advanced numerical models based upon the finite element method suffer from so-called mesh-dependence, i.e. the results may be influenced significantly by size and orientation of the finite elements. This problem arises in cases where local phenomena like plastic hinges and concrete cracking occur. These local phenomena are generally “smeared” over the length of a finite element. Although overall structural behaviour may be simulated in a quite good agreement with test results, locally predicted strains / stresses may become unrealistic. This problem is especially relevant in cases where rotation capacity governs the ultimate load bearing capacity such as the large rotations occurring at internal supports of continuous slabs and beams.

Advanced models will, in general, be based on a so-called incremental iterative solution procedure. It shall be verified that time and/or load increments are chosen such that in each increment a properly converged solution is obtained.

The validity of any advanced calculation model shall be verified by applying the following rules:

- a verification of the calculation results shall be made on basis of relevant test results,

- calculation results may refer to temperatures, deformations and fire resistance times,
- the critical parameters shall be checked, by means of a sensitivity analysis, to ensure that the model complies with sound engineering principles,
- these critical parameters may refer to the buckling length, the size of the elements, the load level, etc.

6.5.2 Application examples

The examples presented hereafter have been produced through the thermo-mechanical soft CEFICOSS. This software, extensively used during ~ 15 research projects and for the design of ~ 300 buildings, is accepted by engineering experts throughout Europe and worldwide. It was developed during the C.E.C. Research REFAO-CAFIR, which was published in 1987 [11].

A verification of calculation results was undertaken on behalf of the set of 15 ISO-fire resistance tests performed in the frame of this first research [5, 6, 7]. Figure 41 shows the quite good correspondence between failure times measured and calculated in the time domain 40 to 240 minutes. But further comparisons were done up to 1990 for more than 50 real fire tests on columns and beams covering steel and composite steel-concrete construction.

In order to deal properly with the differential temperature evolution in cross-sections, these have to be discretized through a mesh able to represent the various parts composed eventually of different materials like concrete or steel. Such a discretization is shown in figure 42. Temperatures are established in the middle of the patches as indicated in figure 43 by applying the "method of the finite differences". Figure 44 gives the temperatures in an octagonal cross-section of a composite column heated all around by the standard fire. The temperature fields are shown at 30, 60, 90 and 120 minutes.

In order to define stresses and deformations of the structure loaded and subject to heating effects, structural elements are divided into finite elements - normally beam elements - and the structure is analysed by the " finite element method ". An example of discretization into finite elements is produced in figure 45.

Of course the deformation behaviour up to the failure time during the heating has to be simulated in a correct physical way. For columns this means that the typical combined buckling aspects i.e. the horizontal accelerating movement at mid-height and the vertical column elongation changing into a shortening of the column at failure shall be demonstrated (see figure 46).

For beams this means that the formation of plastic hinges, leading at failure to a mechanism, shall be simulated. However in practical tests this situation is never attained, as on one side the quite large vertical displacements do not allow hydraulic presses to maintain loading and on the other side possible vertical collapse of the tested beam might endanger that same test equipment!! For those reasons it is recognized to consider for test beams, under heating conditions, a maximum vertical deformation of $L/30$, L representing the span of the beam.

In real frames the global behaviour is of course more complex, but continuity shall always be observed except where buckling or a plastic hinge occurs at an early stage. **It is essential to observe the deformation history of the structure**, like shown in figure 47, and to **compare this physical behaviour with the stiffness evolution expressed on the mathematical level by the " minimum proper value MPV connected to the determinant of the matrix " of the structural system**. A corresponding example of the MPV evolution related to figure 47 is given in figure 48.

Further to the verification up to 1990 of the calculation results made on the basis of relevant test results, sensitivity studies were undertaken, which underlined the **strong duality**

of this thermo-mechanical soft CEFICOSS, concerning on one side the mathematical behaviour and on the other side the corresponding physical explanation [8, 9, 10, 12, 17].

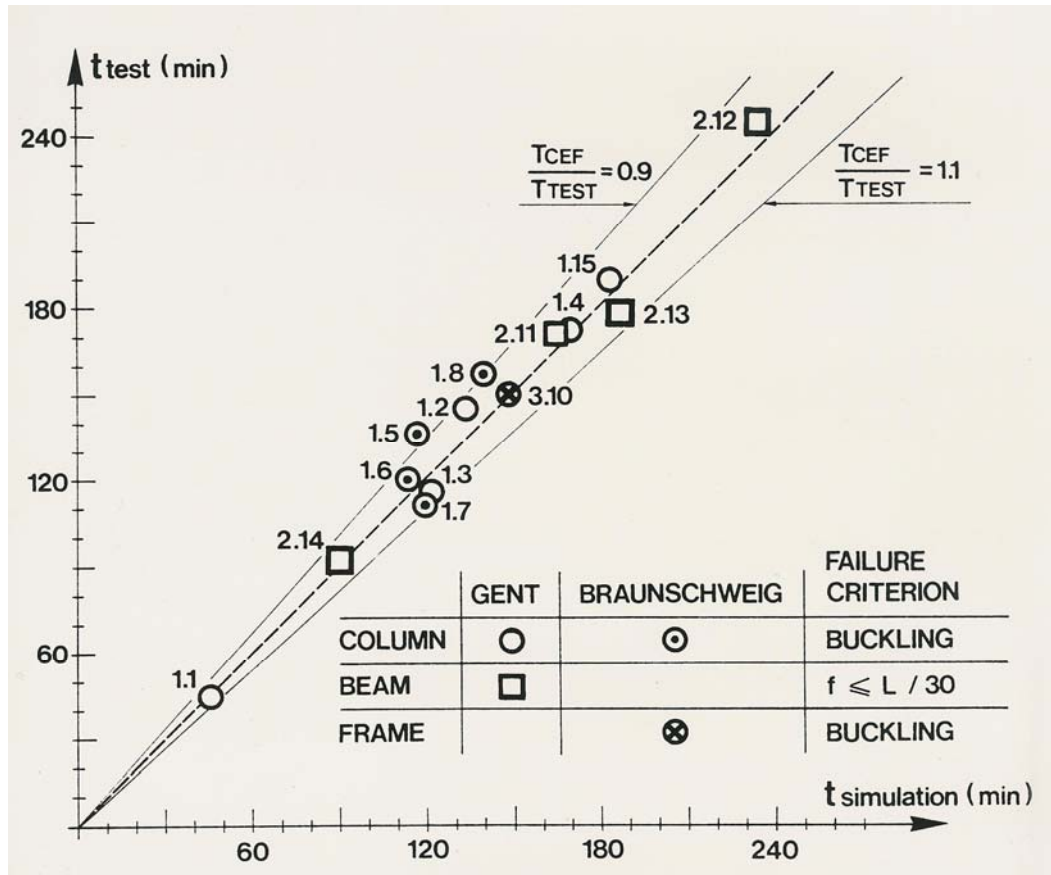


Figure 41. ISO-fire resistance times calculated by CEFICOSS ($t_{\text{simulation}}$) compared to the measured times (t_{test}) during the practical fire tests for steel and composite columns, beams and frames as illustrated in [5, 6, 7 and 11].

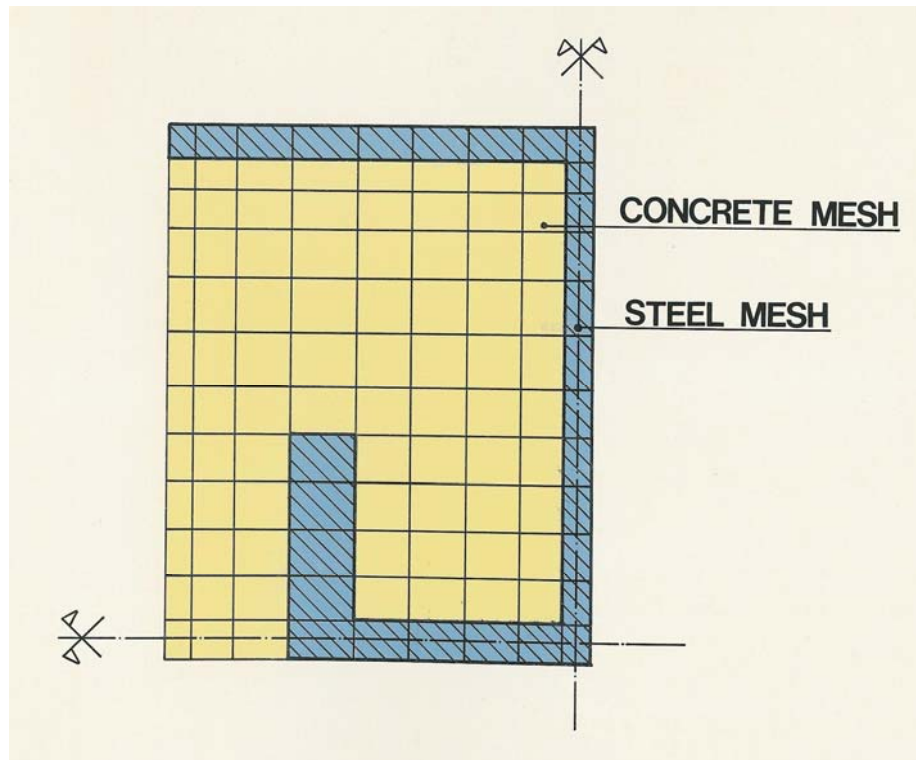


Figure 42. Concrete and steel mesh of a quarter of the column cross-section.

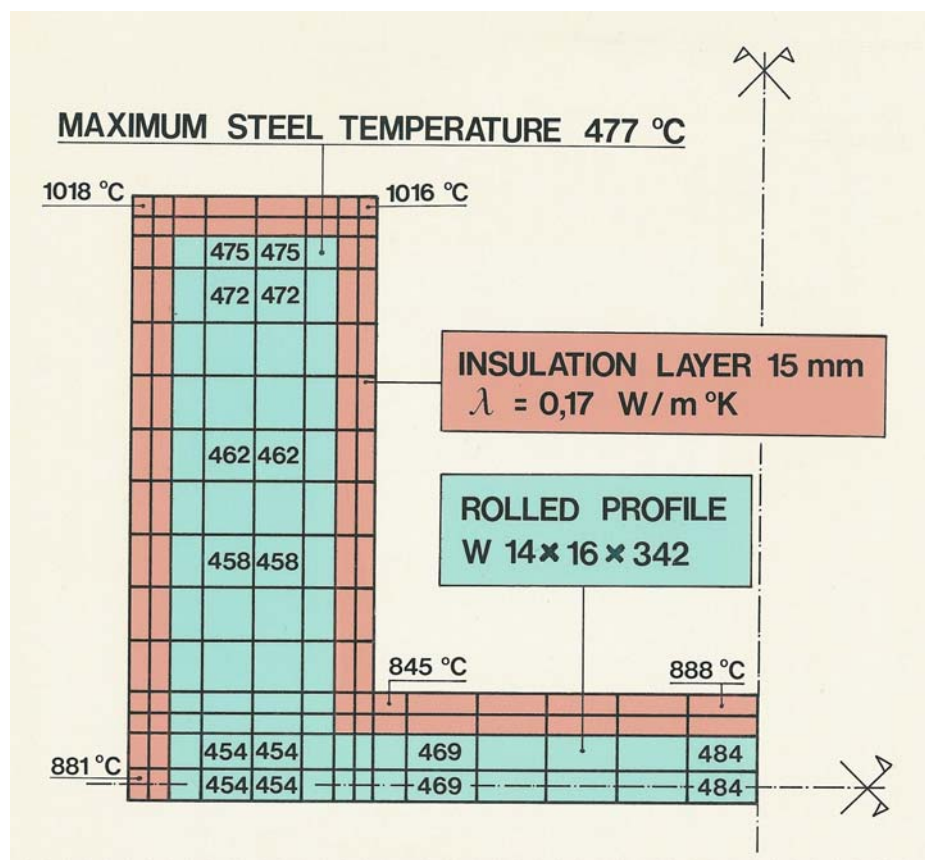


Figure 43. Temperature field of an insulated steel column after 120 minutes of ISO-fire.

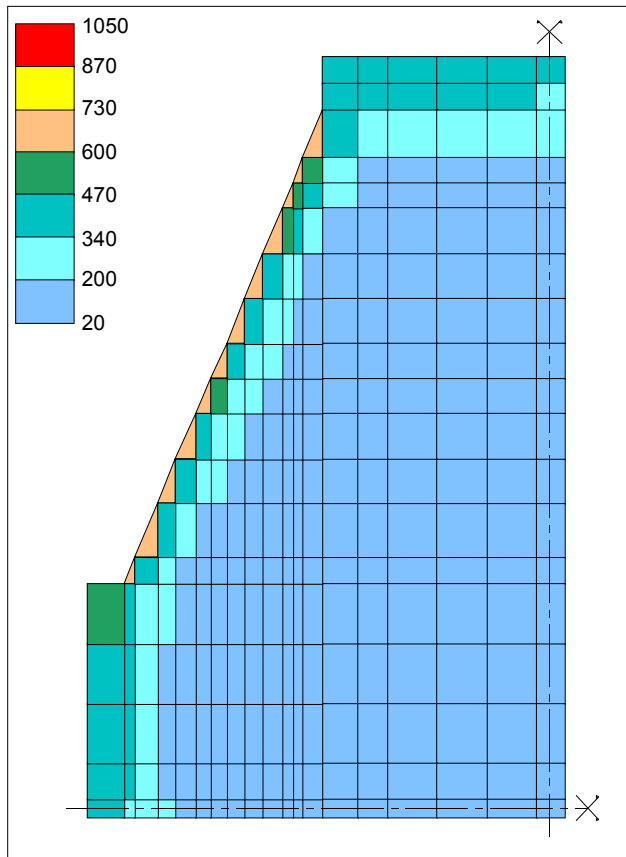


Figure 44a: Temperature field in the section after 30'

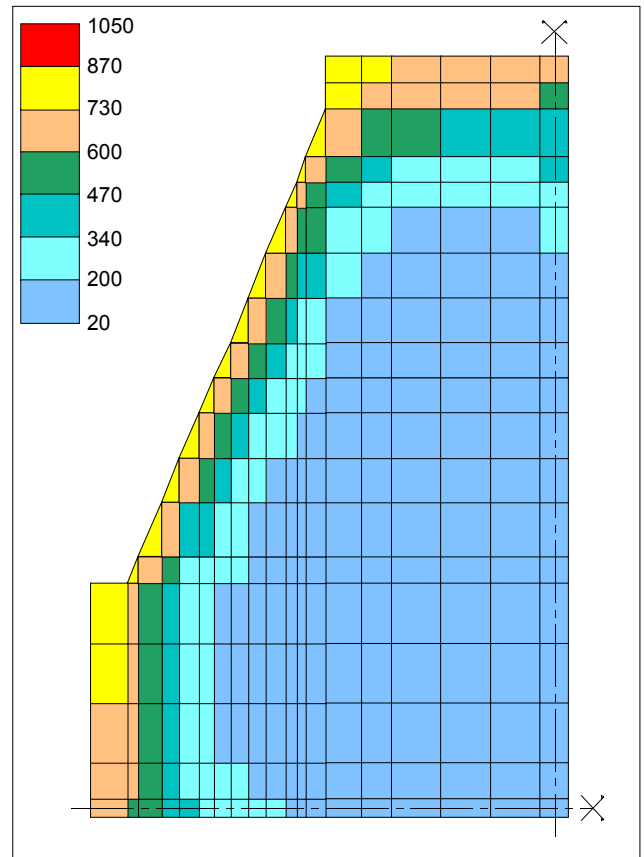


Figure 44 b: Temperature field in the section after 60'

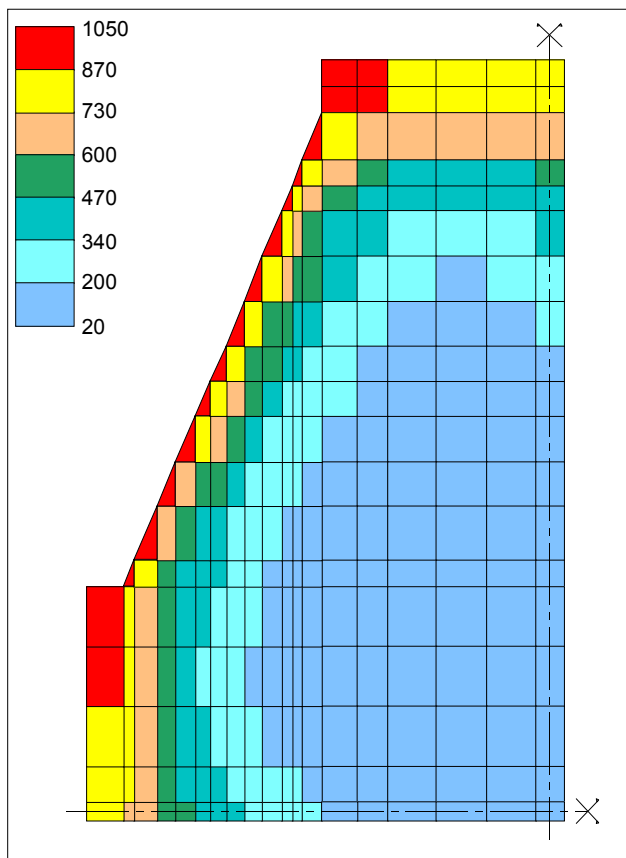


Figure 44 c: Temperature field in the section after 90'

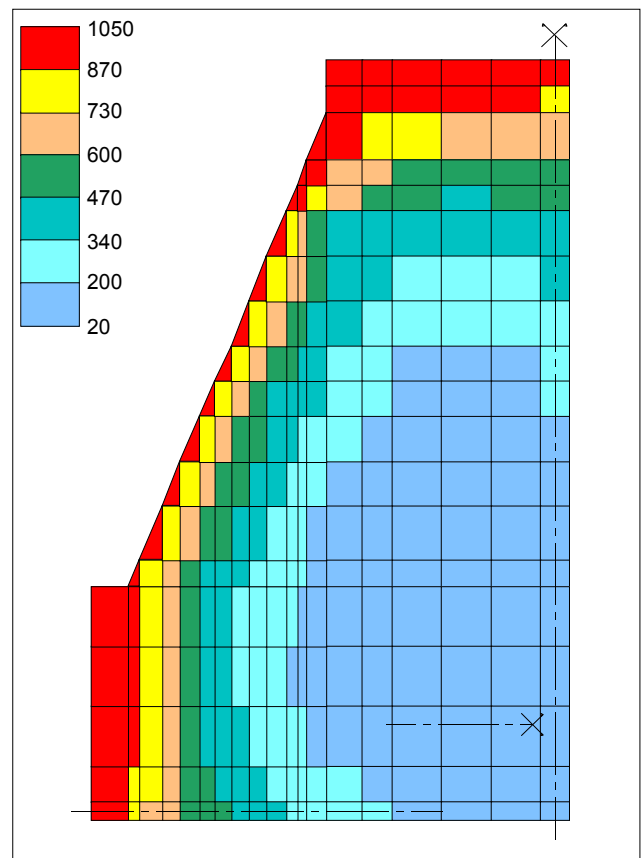


Figure 44 d: Temperature field in the section after 120'

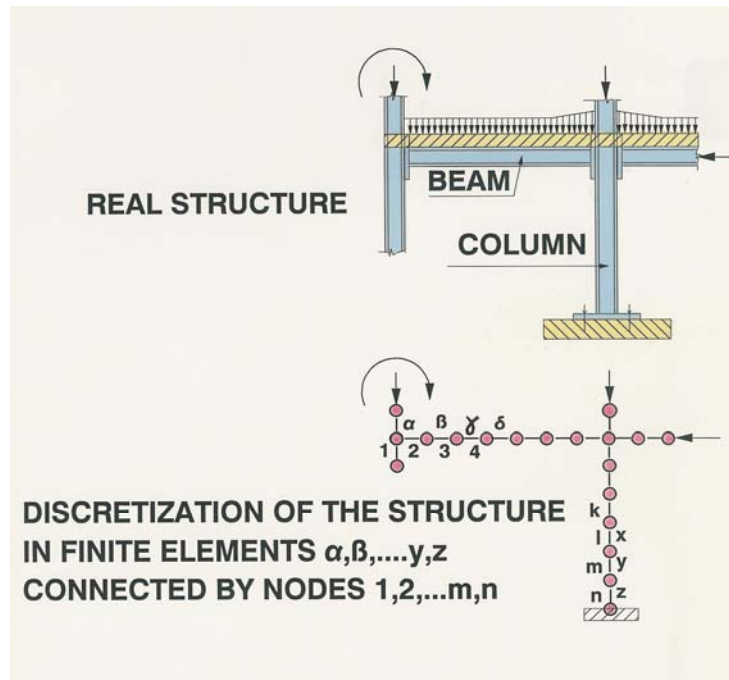


Figure 45.

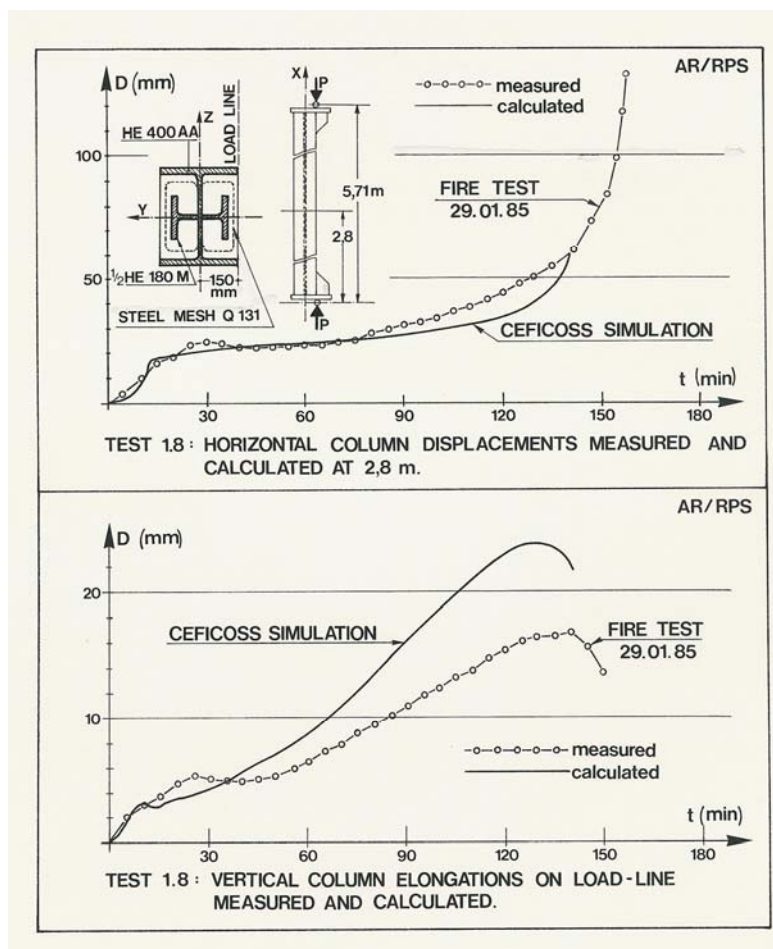


Figure 46. Deformation behaviour during ISO-heating up to the failure time at 157 minutes by buckling of column C 1.8 according [5] and [11]; note the typical combined buckling aspects i.e. the horizontal accelerating movement at mid-height and the vertical column elongation changing into a shortening of the column.

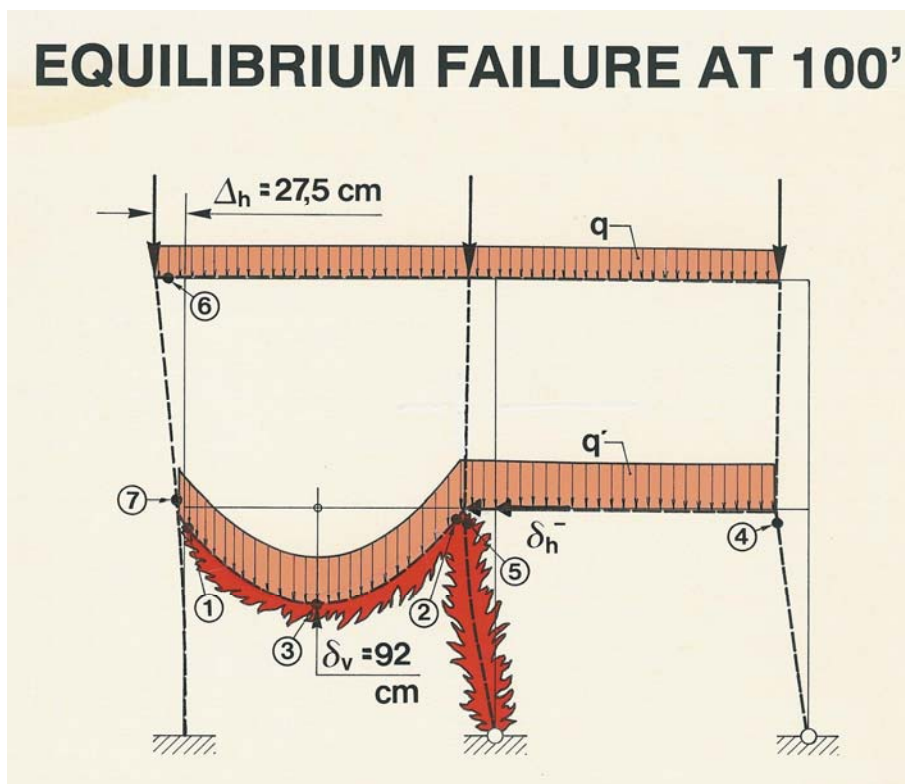


Figure 47. Equilibrium failure by successive plastic hinge formations.

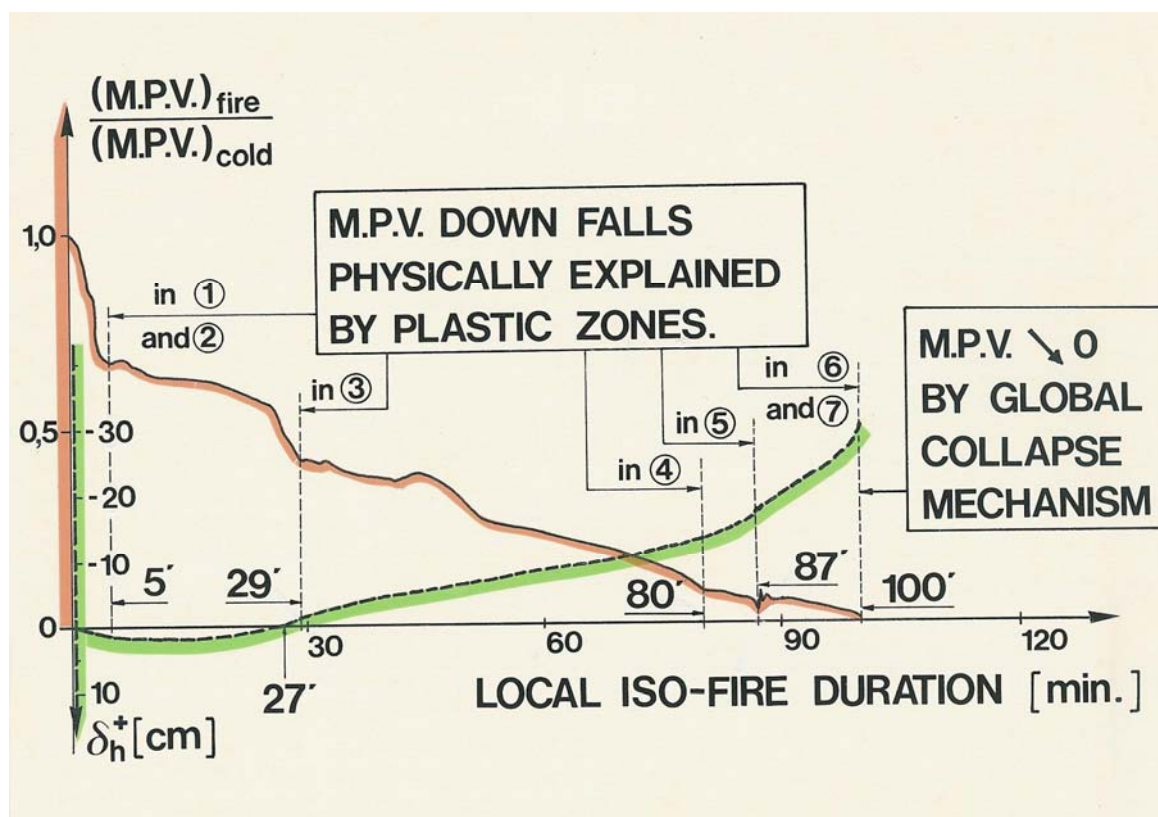


Figure 48. MPV evolution of the matrix of the structural system compared to the horizontal displacement δ_h of the frame given in figure 47.

REFERENCES

- [1] Kawagoe K.; Fire behaviour in rooms. Japanese Building Research Institute, Report N° 27, Tokyo, 1958.
- [2] Kawagoe K., Sekine T; Estimation of fire temperature-time curve in rooms. Japanese Building Research Institute, Occasional Reports N° 11 and 17, Tokyo, 1963/64.
- [3] Lund University – Institute of Fire Safety Engineering; Initial Fires. ISSN 1102-8246 / ISRN LUTVDG/TVBB-3070-SE, Sweden, April 1973.
- [4] SIA; Brandrisikobewertung, Berechnungsverfahren. Dokumentation SIA 81, Zürich, 1984.
- [5] Kordina K., Hass R.; Untersuchungsbericht N°85636, Amtliche Materialprüfanstalt für das Bauwesen. TU Braunschweig 1985.
- [6] Kordina K., Wesche J., Hoffend F.; Untersuchungsbericht N°85833, Amtliche Materialprüfanstalt für das Bauwesen. TU Braunschweig 1985.
- [7] Minne R., Vandevelde R., Odou M.; Fire test reports N° 5091 to 5099, Laboratorium voor Aanwending der Brandstoffen en Warmte-overdracht. Gent University 1985.
- [8] Baus R. Schleich J.B.; Résistance au feu des constructions mixtes acier-béton, détermination d'un niveau précis de sécurité / Mémoire C.E.R.E.S. N°59. Université de Liège, 1986.
- [9] Schleich J.B.; Numerische Simulation - zukunftsorientierte Vorgehensweise zur Feuersicherheitsbeurteilung von Stahlbauten / Allianz Versicherungs-AG, Berlin und München. Der Maschinenschaden 60, Heft 4, S. 169-176, 1987.
- [10] Schleich J.B.; CEFICOSS, a computer program for the fire engineering of steel structures / International Conference on mathematical models for metals and materials applications, Sutton Coldfield, 12-14.10.1987. Institut of Metals, London, 1987.
- [11] Schleich J.B.; REFAO-CA FIR, Computer assisted analysis of the fire resistance of steel and composite concrete-steel structures / C.E. C. Research 7210-SA/502 1982/85. Final Report EUR10828 EN, Luxembourg 1987.
- [12] Schleich J.B.; Numerische Simulation: Zukunftsorientierte Vorgehensweise zur Feuersicherheitsbeurteilung von Stahlbauten / Springer Verlag. Bauingenieur 63, S. 17-26, 1988.
- [13] Schleich J.B.; The effect of local fires on overall structural behavior. AISC National Steel Construction Conference, Miami, 1988, Proceedings p. 42-1 to 42-13.
- [14] Heskestad G.; Fire plumes. The Society of fire protection engineers / Handbook of Fire Protection Engineering, September, 1988.
- [15] ECCS-TC3; Calculation of the fire resistance of centrally loaded composite steel-concrete columns exposed to the standard fire, Technical Note N° 55/ECCS. Brussels, 1988.
- [16] Schleich J.B., Lickes J.P.; Simulation of test frames A2/I and A2/II. ECSC Research 7210-SA/112, Activity A2/B1 / RPS Report N°04/90, Luxembourg, 26.11.1990.
- [17] Cajot L.G., Franssen J.M. and Schleich J.B.; Computer Model CEFICOSS for the fire resistance of composite structures. IABSE Symposium, Mixed Structures including New Materials, Brussels 1990, IABSE Volume 60, p. 395-400.
- [18] Schleich J.B., Scherer M.; Compartment temperature curves in function of opening factor and fire load. ECSC Research 7210-SA/112, Activity C1 / RPS Report N°08/90, Luxembourg, 02.02.1991.
- [19] ARGOS; Theory Manual, Draft 5. Danish Institute of Fire Technology, 22.7.1992.
- [20] ECCS-TC3; Fire Safety in Open Car Parks. Technical Note N° 75/ECCS, Brussels, 1993.

- [21] Peacock R.D. et al.; An update guide for HAZARD I, Version 1.2, NISTIR 5410. National Institute of Standards and Technology, Gaithersburg, May 1994.
- [22] Interpretative Document, Essential Requirement No 2 "Safety in case of fire", Official Journal of the European Communities, No C 62/23, 1994.
- [23] H. Leborgne : Research Report n°94-R-242. CTICM, Maizières-les-Metz, 1994.
- [24] NKB; Performance and requirements for fire safety and technical guide for verification by calculation. Nordic Committee on Building Regulations, Work Report 1994:07E.
- [25] Thomas P.H.; Design guide on structural fire safety. Workshop CIB W14, February 1995.
- [26] Babrauskas V; Burning rates. SFPE Handbook of Fire Protection Engineering, Section 3 / Chapter 1, NFPA Publication , Quincy-Massachusetts, June 1995.
- [27] Audouin L. and Most J.M.; Average centreline temperatures of a buoyancy pool fire by image processing of video recordings. Fire Safety Journal - Vol 24 n°2, 1995
- [28] D. Joyeux : "Simulation of the test of Parc des expositions de Versailles" - INC-95/34-DJ/IM- 1995. CTICM, St.-Remy les Chevreuse, 1995.
- [29] Hasemi Y., Yokobayashi Y. , Wakamatsu T., Ptchelintsev A.; Fire Safety of Building Components Exposed to a Localized Fire - Scope and Experiments on Ceiling/Beam System Exposed to a Localized Fire. ASIAFLAM's 95, Hong Kong, 1995.
- [30] ECCS-TC3; Fire resistance of steel structures-Nomogram, Technical Note N° 89/ECCS. Brussels, 1995.
- [31] Joyeux D; Car fire tests. Rapport CTICM INC-96/294-DJ/VG, Maizières-les-Metz, 1996.
- [32] Schleich J.B., Cajot L.G; Natural fires in closed car parks. ECSC Research 7210-SA/518 etc., B-E-F-L-NL, 1993-96, Final report EUR 18867 EN, 1997.
- [33] Schleich J.B., Cajot L.G.; Natural fires in large compartments. ECSC Research 7210-SA/517 etc., B-E-F-L-NL, 1993-96, Final report EUR 18868 EN, 1997.
- [34] BSI; DD 240 - Fire Safety Engineering in Building, Part 1, Guide to the Application of Fire Safety Engineering Principles, London, 1997.
- [35] DIN; DIN 18230-1;Baulicher Brandschutz im Industriebau - Teil 1: Rechnerisch erforderliche Feuerwiderstandsdauer. Beuth Verlag , Berlin , Mai 1998.
- [36] Schleich J.B.; Influence of active fire protection on the safety level & its consequence on the design of structural members. « Abschlussarbeit Nachdiplomkurs Risiko & Sicherheit », ETHZ, Zuerich 1.09.1998.
- [37] H. Leborgne : Research Report N°98-R-406. CTICM, Maizières-les-Metz, 1998.
- [38] Fontana M., Favre J.P., Fetz C.: A survey of 40000 building fires in Switzerland. Fire Safety Journal 32 (1999) p. 137-158.
- [39] CEN; Background Document CEN/TC250/SC1/N298A - Parametric temperature-time curves according to Annex A of EN1991-1-2, 9.11.2001.
- [40] CEN; Background Document CEN/TC250/SC1/N299A- Advanced fire models according to 3.3.2 of EN1991-1-2, 9.11.2001.
- [41] CEN; Background Document CEN/TC250/SC1/N339 – Localised fires according to Annex C of EN1991-1-2, 9.11.2001.
- [42] Schleich J.B.; The design fire load density $q_{f,d}$, function of active fire safety measures-the probabilistic background. Reliability based code calibration / JCSS Workshop, Zuerich, 21/22.3.2002.
- [43] Schleich J.B.; Auswirkungen des WTC-Schocks auf den europäischen Stahlgeschossbau. Ernst & Sohn, Stahlbau, Heft 4, April 2002, S. 289-293.
- [44] CEN; EN1990, Eurocode – Basis of Structural design. CEN Central Secretariat, Brussels, DAV 24.4.2002.

[45] CEN; EN1992-1-1, Eurocode 2 – Design of concrete structures, Part1.1 – General rules and rules for buildings. CEN Central Secretariat, Brussels, 2004.

[46] CEN; EN1991-1-2, Eurocode 1 – Actions on structures , Part 1.2 – Actions on structures exposed to fire. CEN Central Secretariat, Brussels, DAV 20.11.2002.

[47] Schleich J.B., Cajot L.G.; Natural fire safety concept. ECSC Research 7210-SA/522 etc.,B-D-E-F-I-L-NL-UK & ECCS, 1994-98, Final Report EUR 20360EN, 2002.

[48] CEN; prEN1994-1-1, Eurocode 4 - Design of composite steel and concrete structures, Part 1.1 - General rules and rules for buildings. CEN Central Secretariat, Brussels, Final draft, May 2003.

[49] Cadorin J.F.; Compartment Fire Models for Structural Engineering. Thèse de doctorat, Université de Liège, 17.6.2003.

[50] CEN; prEN1993-1-1, Eurocode 3 – Design of steel structures, Part1.1 – General rules and rules for buildings. CEN Central Secretariat, Brussels, Final draft, November 2003.

[51] EC; Commission Recommendation on the implementation and use of Eurocodes for construction works and structural construction products, dated 11.12.2003, C(2003)4639. Official Journal of the European Union, L 332/62, Luxembourg, 19.12.2003.

[52] Schleich J.B.,Cajot L.G.; Natural Fire Safety Concept / Full scale tests, Implementation in the Eurocodes & Development of userfriendly design tools. ECSC Research 7210-PR/060 etc., D,F,FI,L,NL & UK,1997-2000, Final Report EUR 20580EN, 2003.

[53] CEN; prEN1993-1-2, Eurocode 3 – Design of steel structures, Part1.2 – General rules – Structural fire design. CEN Central Secretariat, Brussels, Stage 49 draft, June 2004.

[54] CEN; EN1992-1-2, Eurocode 2 – Design of concrete structures, Part1.2 – General rules – Structural fire design. CEN Central Secretariat, Brussels, December 2004.

[55] CEN; prEN1994 -1-2, Eurocode 4 – Design of composite steel and concrete structures, Part1.2 – General rules – Structural fire design. CEN Central Secretariat, Brussels, Stage 49 draft, December 2004.

[56] CEN; EN13381-1, Fire tests on elements of building construction, Part 1 - Test method for determining the contribution to the fire resistance of structural members by horizontal protective membranes. CEN Central Secretariat, Brussels, Final Draft, 2005.

CHAPTER II – ACCIDENTAL COMBINATIONS IN CASE OF FIRE

Milan Holický¹ and Jean-Baptiste Schleich²

¹Klockner Institute, Czech Technical University in Prague, Czech Republic

² University of Technology Aachen, University of Liège

1 INTRODUCTION

1.1 Background documents

Safety in case of fire is one of the essential requirements imposed on construction products and works by the Council Directive [2]. In accordance with the essential requirement No. 2 [6], “the construction works must be designed and built in such a way that in the event of an outbreak of fire the load bearing capacity of the construction works can be assumed for a specific period of time”.

Thus the Eurocodes EN 1990 [13] and EN 1991-1-2 [15] are used as basic background materials in this contribution. General information concerning fire actions is available in the important international documents [3, 4, 5, 12], which have been used as background materials for the development of EN1991-1-2 [15]. In addition to the above mentioned materials, relevant findings provided in the previous investigations [8, 9, 10, 14] for fire actions and combinations of actions during the accidental design situations due to fire are taken into account.

The reliability analysis is further based on basic laws of the theory of probability [1] and common procedures of the structural reliability [7].

1.2 General principles

Regarding mechanical actions, it is commonly agreed that the probability of the combined occurrence of a fire in a building and an extremely high level of mechanical loads is very small. In fact the load level to be used to check the fire resistance of elements refers to other safety factors than those used for normal design of buildings. The general formula proposed to calculate the relevant effects of actions is according to EN 1990 and EN1991-1-2 [13, 15]:

$$\sum G_{k,j} + (\psi_{1,1} \text{ or } \psi_{2,1})Q_{k,1} + \sum \psi_{2,i} Q_{k,i} + \sum A_{d(t)} \equiv \text{Static Actions} + \text{Accidental Action} \quad (1)$$

where:

$G_{k,j}$ is the characteristic value of the permanent action ("dead load")

$Q_{k,1}$ is the characteristic value of the main variable action

$Q_{k,i}$ is the characteristic value of the other variable actions

$\psi_{1,1}; \psi_{2,1}; \psi_{2,i}$ are the combination factors for buildings according to table 9 of

Chapter I, Fire actions in buildings

$A_{d(t)}$ is the design value of the accidental action resulting from the fire exposure.

One of the key discussion items is the value of the combination factor ψ . In particular an alternative use of the value ψ_1 (for a frequent combination value) or ψ_2 (for a quasi permanent combination value) used in accidental load combinations is discussed. A possible decrease of the original value of ψ_1 used in ENV 1991-2-2 (for the imposed load equal to 0,5)

or complete avoidance of the variable action in the accidental combination due to fire (thus to consider $\psi = 0$) is considered.

EN1991-1-2 [15] recommends in 4.3.1(2) the quasi-permanent value ψ_2 that corresponds to 0,3 for buildings of category A or B. This recommendation was first suggested by Prof. M.H. Faber in April 2001 [11]. Later on a second study was performed by the present authors in 2002 [14].

2 FUNDAMENTAL CASES OF STRUCTURAL RELIABILITY

2.1 General

The calibration study of the factor ψ used in the combination of actions for accidental design situations due to fire is based on the procedure recommended in EN 1990 Basis of Structural Design and EN 1991-1-2 Actions on Structures Exposed to Fire. The bearing capacity of a **steel member** exposed to a permanent load G and one variable action Q is verified using expression (1) given in EN 1990. It appears that the combination factor ψ used in the combination of actions should depend on the type and extent of the compartment area A , on active and passive measures, and generally also on the load ratio $\chi = Q_k/(G_k+Q_k)$ of the characteristic variable action Q_k and the total load G_k+Q_k . It is further shown that the optimum combination factor ψ may be found by minimizing the total expected cost. A special purpose software tool enables further calibration studies

It is obvious that **further comprehensive calibration studies are needed to specify the load combination factor ψ also for fire design of concrete and timber structural members.**

The developed special purpose software tool may be effectively used to take into account particular conditions of different types of buildings.

2.2 Evaluation of the combination factor ψ for actions

2.2.1 Introduction

In particular the recent study [14] on the calibration of the combination factor for a fire design situation of a steel member is enhanced and extended in the following contribution.

2.2.2 Probabilistic requirements

The target probability of structural failure given the fire is fully developed $P_t(\text{failure}/\text{fire})$ may be derived from a specified target probability of structural failure under a persistent design situation $P_t(\text{failure})$, commonly taken as 0,0000723 with $\beta = 3,8$, by using the law of full probability [1] that can be approximated by the following expression

$$P_t(\text{failure}/\text{fire}) = P_t(\text{failure}) / P(\text{fire}) \quad (2)$$

However, the probability $P(\text{fire})$ may vary widely depending on the particular conditions of the construction work. The following factors seem to be most significant [9, 10]

- type of the occupancy,
- compartment area A and
- active and passive measures to extinguish or resist the fire.

Table 1 indicates informative values of involved probabilities for an office area provided with sprinklers [9, 10] and the target reliability index β under a fire design situation assumed for ~55 years $P_t(\text{failure})=0,0000723$, which corresponds to the reliability index $\beta=3,8$.

Table 1. Informative values of probabilities

Area A	P(fire starts)	$P(\text{fire})$	$P_t(\text{failure/fire})$	β_t
25 m ²	0,01	0,0002	0,36	0,4
100 m ²	0,04	0,0008	0,09	1,3
250 m ²	0,1	0,002	0,036	1,8
1000 m ²	0,4	0,008	0,009	2,4

The target index β_t under a fire situation may be expressed in terms of β for a persistent situation

$$\beta_t = -\Phi^{-1}(\Phi(-\beta)/P(\text{fire})) \quad (3)$$

where $\Phi()$ denotes a standardised normal distribution. It follows from the above table 1 that $\beta_t = 1,0$, indicated in figure 1 by the dashed line, may be considered as a reasonable requirement for a compartment area up to 100 m². Then it follows from figure 1 that the combination factor ψ (for an imposed load), used in the fire design situation, should be at least 0,3, for which the reliability index is almost independent of the load ratio χ (the values $\psi_0 = 0,7$, $\psi_1 = 0,5$ and $\psi_2 = 0,3$ are indicated in EN 1990 [13], for buildings of category A or B).

2.2.3 Design procedure using the partial factor method

Only one permanent load G having the characteristic value G_k and one variable (imposed) load Q having the characteristic value Q_k are considered. Following the general rules specified in EN 1990 [13] and EN 1991-1-2 [15], the design expression for a steel element (beam, rod) may be then written as

$$R_{0k} \cdot k_y / \gamma_M = \gamma_G \cdot G_k + \gamma_Q \cdot \psi \cdot Q_k \quad (4)$$

Here R_{0k} denotes the characteristic value of the resistance (bending moment, axial force) at a normal temperature, k_y denotes the reduction factor due to an elevated temperature, γ_M the material factor, γ_G and γ_Q the load factors. The characteristic values of both actions G_k and Q_k in equation (4) further satisfy the load ratio

$$\chi = Q_k / (G_k + Q_k) \quad (5)$$

which is used to study the effect of mutual proportion of Q_k and G_k . The factors γ_M , γ_G , γ_Q , χ , and ψ can be considered as parameters of the design.

The design relationship (4) used in this study can be normalised choosing, for example, $R_{0k} k_y = 1$ (kNm, kN). Thus the absolute value of $R k_y$ is irrelevant to the following reliability analysis.

Furthermore, as fire corresponds to an accidental situation, the load factors γ_G and γ_Q are put equal to 1.0 in the following development. In the same context, γ_M is also assumed to be 1.0. Under these conditions and considering equations (4) and (5), the probabilistic analysis of the following limit state function (6) may be undertaken.

2.2.4 Reliability analysis

The limit state function $g(\mathbf{X})$, where \mathbf{X} denotes the vector of basic variables, used to analyse the probability of failure, follows from equation (4) for tension elements or beams without instability risks

$$g(\mathbf{X}) = \xi_R \cdot R_0 \cdot k_y - \xi_E \cdot (G + Q) \quad (6)$$

where ξ_R denotes the model uncertainty factor of the resistance R , ξ_E denotes the model uncertainty factor of the load effect $E = G + Q$. Probabilistic models of the basic variables are summarised in table 2.

Table 2. Probabilistic models of basic variables.

Basic variable	Symbol X	Distribution	The mean μ_X	Coefficient of variation V
Resistance	R_0	LN	1	0,08
Reduction factor	k_y	LN	1	0,20*
Permanent load	G	N	G_k	0,10
Variable load	Q	GUM	$0.2 Q_k$	1,1
Uncertainty of R	ξ_R	LN	1,1	0,05
Uncertainty of E	ξ_E	LN	1	0,10

* Alternatively 0,30 is considered.

An important assumption concerns the coefficient of variation of the reduction factor k_y , which further depends on the assumed temperature time curve and a number of other factors. It should be mentioned that the value 0,20 considered in this study is "a reasonable estimate" based on a more detailed probabilistic analysis. However, depending on actual structural conditions and the temperature of the structural steel the coefficient of variation of k_y may be expected in a broad range from 0,10 to approximately 0,5.

An auxiliary software tool "PsiFire3.mcd" (attached to this contribution), which has been developed using the mathematical language MATHCAD, is applied for a reliability analysis of the limit state function (6). Figure 1 shows the variation of the reliability index β with the load ratio χ assuming the probabilistic models of basic variables specified in table 2.

It appears that for $\psi = 0,3$ the reliability index β is almost independent of the load ratio χ and approximately equal to 1, which is the required target value mentioned above. It also follows from figure 1 that $\psi < 0,3$ may lead to an unsatisfactory low reliability, particularly for a load ratio χ greater than 0,3.

Figure 2 shows the variation of the reliability index β with the load ratio χ and the combination factor ψ for the same assumption as in figure 1. The plane in figure 2 corresponds to the reliability index level $\beta \approx 1$, obtained for the load ratio $\chi = 0$ (thus for a permanent load only). It is apparent from figure 2 that the combination $\psi = 0,3$ provides the most uniform and satisfactory reliability level.

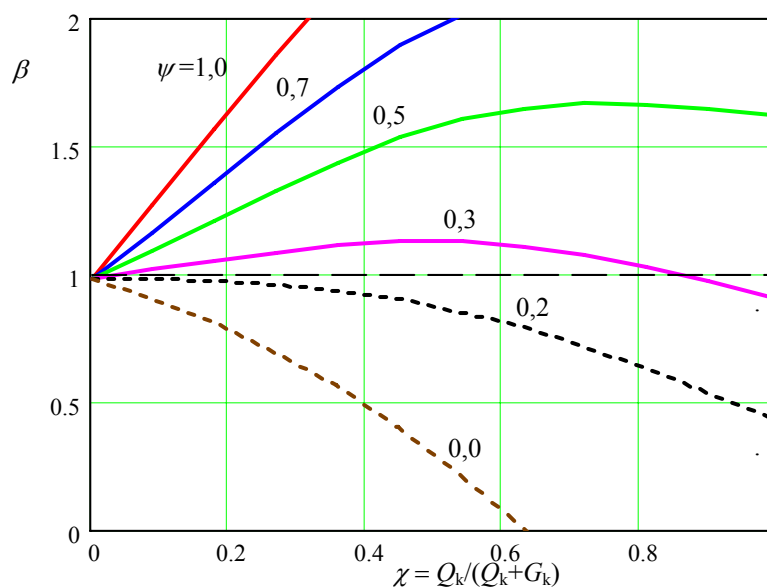


Figure 1. Variation of the reliability index β with the load ratio χ for selected combination factors ψ assuming the probabilistic models given in table 2.

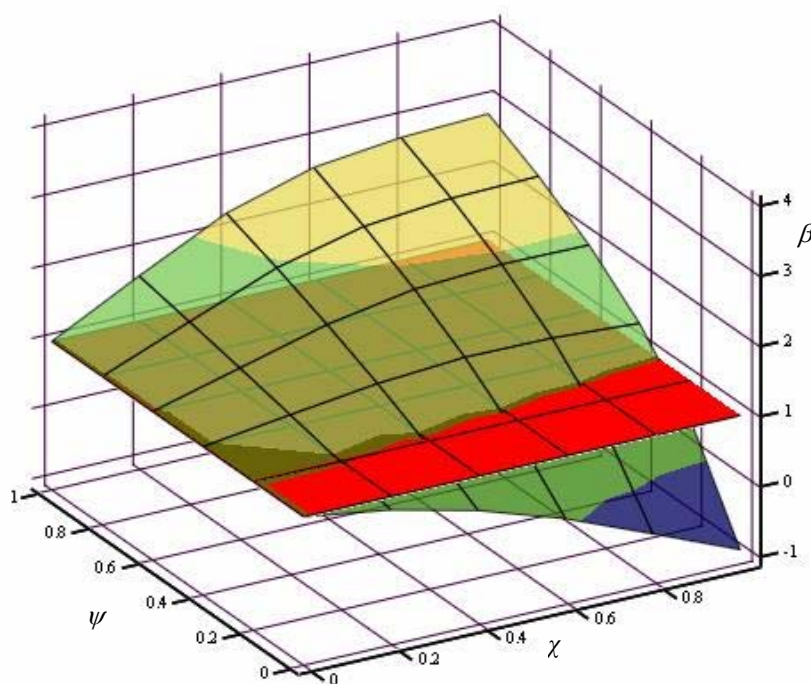


Figure 2. Variation of the reliability index β with the load ratio χ and the combination factor ψ for the same assumptions as in figure 1.

The attached software tool “PsiFire3.mcd” has been used for extensive parametric studies. Similar results have been obtained for slightly different theoretical models for all the basic variables than those indicated in table 2. It appears that the reliability index level β may be most significantly affected by the assumed variability of the coefficient of variation V of the reduction factor k_y . Figure 3 indicates the variation of the reliability index β with the load ratio χ for the same theoretical models as given in table 2, except the coefficient of variation V of the reduction factor k_y , for which the value 0,3 (instead of the original 0,2) is considered.

Obviously due to the increased variability of the coefficient of variation V of the reduction factor k_y , the reliability index decreased by about 0,3 (the reliability index level $\beta \approx 0,7$ for the load ratio $\chi = 0$). However the combination factor $\psi = 0,3$ seems to provide still the most uniform reliability level.

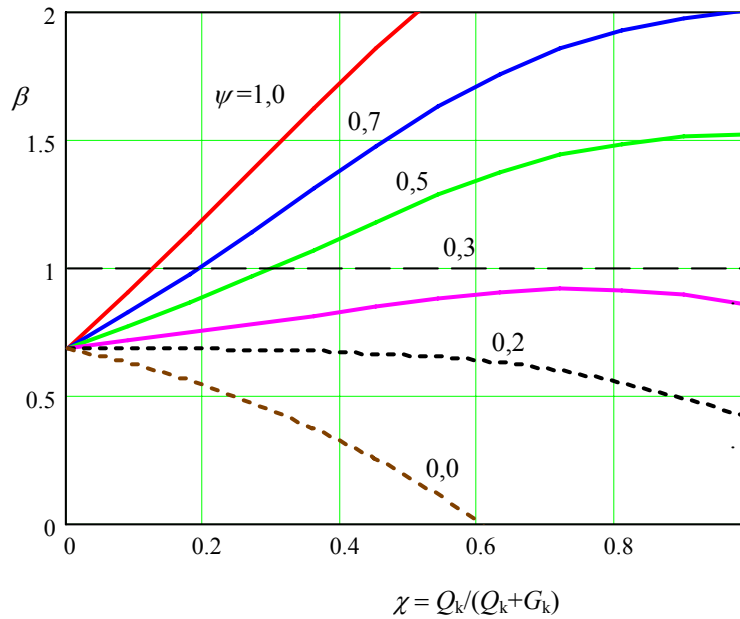


Figure 3. Variation of the reliability index β with the load ratio χ for selected combination factors ψ , assuming the probabilistic models given in table 2, but for a coefficient of variation V of k_y equal to 0,30.

2.2.5 Optimisation

It is expected that with an increasing factor ψ the failure probability $P_f(\psi)$, which is dependent on the combination factor ψ , will decrease, while the cost of the structure will increase. Therefore, it may be interesting to search for the minimum (if it exists) of the total expected cost of a structure including its possible failure. Such a consideration may provide further valuable information for choosing an appropriate value of the factor ψ with regard to an accidental design situation due to fire.

The total expected cost $C_{tot}(\psi)$, which is considered as an objective function, may be approximately expressed as the sum

$$C_{tot}(\psi) = C_0 + \psi \cdot C_m + P_f(\psi) \cdot H \quad (7)$$

where C_0 denotes the initial cost, C_m the marginal cost, $P_f(\psi)$ the probability of failure and H is the cost due to malfunctioning or failure of the structure. Note that the marginal cost C_m corresponds to an increase of the total structural cost due to the combination factor $\psi = 1,0$. It

is therefore assumed that the structural cost is linearly dependent on the combination factor ψ that is considered as the decision variable.

Equation (7) represents a simplified model of the total expected costs that neglects many factors including capitalisation and cost of various passive and active measures, which may affect the probability $P_f(\psi)$. The following results should be therefore considered only as indicative.

Note that unlike the total expected cost $C_{\text{tot}}(\psi)$, the partial costs C_0 , C_m and H are assumed to be independent of ψ . Then the minimum of the total cost $C_{\text{tot}}(\psi)$ will be achieved for the same combination factor ψ as the minimum of the relative cost $\kappa(\psi) = (C_{\text{tot}}(\psi) - C_0)/H$. It follows from equation (7) that the relative cost $\kappa(\psi)$ can be expressed as

$$\kappa(\psi) = (C_{\text{tot}}(\psi) - C_0) / H = \psi \cdot C_m / H + P_f(\psi) \quad (8)$$

The cost ratio C_m/H (which is independent of the currency unit) is expected to be within the interval $<0, 1>$. As a first approximation the value $C_m/H \approx 0,5$ may be expected. In particular situations, however the relevant cost ratio C_m/H should be determined taking into account actual economic conditions and consequences of a possible failure.

The minimum cost $\kappa(\psi)$ may be achieved for such a value of the combination factor ψ , for which the first derivative of $\kappa(\psi)$ vanishes. It follows from equation (8) that this condition is fulfilled when the first derivative of the probability $P_f(\psi)$ attains the value

$$\frac{dP_f(\psi)}{d\psi} = -C_m / H \quad (9)$$

Considering the load ratio $\chi = 0,5$ and the basic variables having the probabilistic models given in table 2, figure 4 shows the relative total cost $\kappa(\psi) = (C_{\text{tot}}(\psi) - C_0) / H$ as a function of the combination factor ψ for selected cost ratios C_m/H , whereas the dots in figure 4 indicate the minimum values for C_m/H .

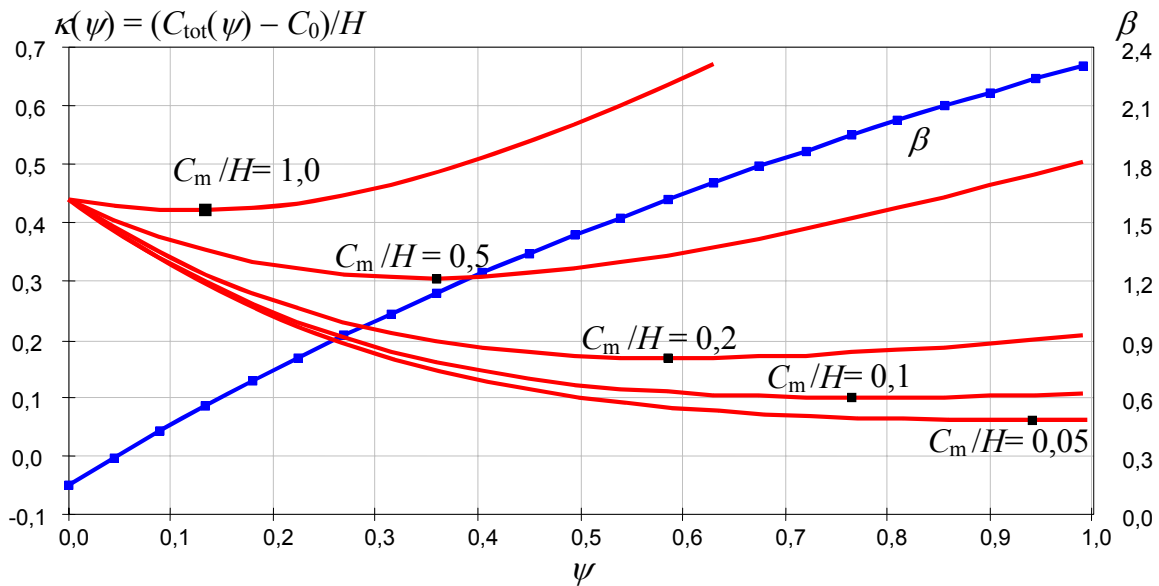


Figure 4. The relative cost $\kappa(\psi) = (C_{\text{tot}}(\psi) - C_0) / H$ and the reliability index β versus ψ for the load ratio $\chi = 0,5$ and selected values of the cost ratio C_m/H .

It follows from figure 4 that, with the increasing cost ratio C_m/H , both the optimum combination factor ψ and the corresponding reliability index β decrease. For the cost ratio $C_m/H = 1$ (the marginal cost C_m is high and equals the cost of failure H), the optimum factor ψ is about 0,13 and the corresponding reliability index β is about 0,6, which may not be sufficient due to probabilistic requirements ($\beta = 1,0$ is mentioned above as a required value). For a low cost ratio, say $C_m/H = 0,1$ (the cost of failure H is ten times greater than the marginal cost C_m), the optimum ψ is about 0,77 and the corresponding reliability index β is about 2,0. On the other hand, if the failure cost H is less than the marginal cost C_m and $C_m/H > 1$ (a very unrealistic condition), then the optimum factor ψ approaches zero.

Note that for a reasonable cost ratio C_m/H around 0,5 the optimum combination factor ψ may be expected within the interval from 0,3 to 0,4, which is an interval corresponding well to the results of the reliability consideration described above (see figure 1).

2.2.6 Conclusions

The following conclusions, concerning the factor ψ used in a load combination for a fire design situation, may be drawn from obtained results of the reliability analysis and optimisation of a steel element in an office area:

- the factor ψ should depend on the type and extent of the compartment area A , on active and passive measures, and on the load ratio χ ,
- the factor ψ should increase with increasing the compartment area A ,
- the factor ψ should be at least 0,3, for which β is about 1,
- the optimum factor ψ depends on the cost ratio C_m/H of the marginal cost C_m and the failure cost H ; for $C_m/H \approx 0,5$ the optimum factor $\psi \approx 0,35$.

Thus, the combination factor ψ for a fire design situation should be specified taking into account actual structural conditions including the load ratio χ , the compartment area A and the cost ratio C_m/H .

REFERENCES

- [1] A.H.-S. Ang and W.H. Tang; Probabilistic concepts in engineering planning and design. John Wiley and Sons, New York, 1975.
- [2] Construction Product Directive, dated 21.12.1988, 89/106/EEC. Official Journal of the European Communities, N° L40/12, Luxembourg, 11.02.1989.
- [3] ISO 834 Part 1; Fire resistance tests - Elements of building construction, 1992.
- [4] CIB Report, Publication 166; Action on Structures, Fire, September 1993.
- [5] Schleich J.-B. et al.; Fire engineering design for steel structures. State of the Art Report. International Iron and Steel Institute, Brussels, 1993.
- [6] Interpretative Document N°2, Essential Requirement "Safety in case of fire". Official Journal of the European Communities, N° C62/23-72, Luxembourg 28.02.1994.
- [7] Schneider, J.; Introduction to safety and reliability of structures. Structural Engineering Documents, N°5, International Association for Bridge and Structural Engineering, IABSE, Zurich, 138p., 1997.
- [8] Gulvanessian H., Holický M., Cajot L.G., Schleich J.-B.; Probabilistic Analysis of Fire Safety using Bayesian Causal Network. Proc of ESREL99, Muenchen, A.A. Balkema, Rotterdam, pp. 725-730, 1999.

[9] Holický M. and Schleich J.-B.; Estimation of risk under fire design situation. Proc. of Risk Analysis 2000 Conference, Bologna, 11/13.10.00, WITpress, Southampton, Boston, pp. 63-72, ISBN 1-85312-830-9, 2000.

[10] Holický M. & Schleich J.-B.; Modelling of a Structure under Permanent and Fire Design Situation. Proc. of Safety, Risk and Reliability - Trends in Engineering. International Conference, Malta, 21/23.3.01, A.A. Balkema, Rotterdam, pp. 789-794, ISBN 3-85748-120-4, 2001.

[11] CEN; Background document CEN/TC250/SC1/N337- Background document on combination rules for actions according to 4.3 of EN1991-1-2, 9.11.2001.

[12] Schleich J.B. et al; Model Code on Fire Engineering. ECCS-Technical Committee 3, ECCS Publication N°111, Brussels, 2001.

[13] CEN; EN1990, Eurocode – Basis of Structural design. CEN Central Secretariat, Brussels, DAV 24.4.2002.

[14] Holický M. & Schleich J.-B.; Calibration of the Combination Factor for the Fire Design Situation. Third European Conference on Steel Structures, EUROSTEEL 3, Coimbra, pp. 1421-1426, ISBN 972-98376-3-5, 19-20.9. 2002.

[15] CEN; EN1991-1-2, Eurocode 1 – Actions on structures, Part 1.2 – Actions on structures exposed to fire. CEN Central Secretariat, Brussels, DAV 20.11.2002

ATTACHMENT

A special purpose software tool, based on the mathematic language MATHCAD, has been developed for the calibration study of the combination factor ψ .

Mathcad sheet "Psi Fire 3" is developed to study the effect of the factor ψ used in the accidental (fire) combination provided in EN 1991-1-2, clause 4.3.1. MH, October 2004.

1. Definition of the study

Design expression: $R0k \cdot ky / \gamma_M = \gamma_G \cdot Gk + \gamma_Q \cdot \psi \cdot Qk$

Limit state function: $g(X) = \rho \cdot R0 \cdot ky - \theta \cdot (G + Q)$

Parameters of the study: action ratio $\chi = Qk/(Gk+Qk)$, factors γ_M, ψ (γ_Q)

The resistance (bending moment, axial or shear force) $R = \rho \cdot R0 \cdot ky$ is described by a three parameter lognormal distribution (shifted lognormal distribution) $LN(\mu_R, \sigma_R, \alpha_R)$.

Resistance variables: $R0$: $LN(\mu_R, 0.08\mu_R)$, ρ : $LN(1.0, 0.15)$, ky : $GUM(kynom, 0.15 kynom)$.

The load effect $E = \theta \cdot (G+Q)$ described by a three parameter lognormal distribution (shifted lognormal distribution) $LN_s(\mu_E, \sigma_E, \alpha_E)$.

Action variables: G : $N(Gk, 0.1 \cdot Gk)$, Q : $GUM(0.25Qk, 0.75Qk, 1.14)$, θ : $N(1.0, 0.1)$.

2. Definition of the parameters χ, γ_M, γ_G and $\gamma_Q = \psi$

Parameters as range variables: $\chi := 0, 0.09.. 0.99$ $\gamma_M := 1, 1.05.. 1.15$ $\gamma_G := 1, 1.05.. 1.35$ $\gamma_Q := 0.0, 0.10.. 1.0$

3. The characteristic values of the actions $Gk = \mu_G$ and Qk

Assuming $Ed = Rd$ (economic design) then $\gamma_G \cdot Gk + \gamma_Q \cdot Qk = Rd$ $Rd := 1$ (normalised value)

$$\mu_G(\chi, \gamma_G, \gamma_Q) := \frac{Rd}{\left(\gamma_G + \frac{\chi \cdot \gamma_Q}{1 - \chi}\right)} \quad Qk(\chi, \gamma_G, \gamma_Q) := \frac{\chi \mu_G(\chi, \gamma_G, \gamma_Q)}{1 - \chi} \quad \text{Check: } \boxed{\mu_G(0.3, 1, 0.7) = 0.769}$$

$$\boxed{Qk(0.3, 1, 0.7) = 0.33}$$

4. Theoretical models for the resistance variables $R0, \rho$ and ky

$$\omega := \frac{280}{235}$$

The mean of $R0$ assumed as $\mu_{R0} = \omega \cdot R0k$ $\mu_{R0}(\gamma_M) := \omega \cdot Rd \cdot \gamma_M$ $w_{R0} := 0.08$ $\alpha_{R0} := 3 \cdot w_{R0} + w_{R0}^3$

Model uncertainty ρ : $\mu_\rho := 1.10$ $w_\rho := 0.05$ $\alpha_\rho := 3 \cdot w_\rho + w_\rho^3$

Reduction factor due to elevated temperature (normalised value) $\mu_{ky} = ky$, Gumbel distribution :

$$\mu_{ky} := 1 \quad w_{ky} := 0.30 \quad \alpha_{ky} := 0.927$$

5. Theoretical models for the resistance $R = \rho \cdot ky \cdot R0$

The mean μ_R : $\mu_R(\gamma_M) := \mu_\rho \cdot \mu_{ky} \cdot \mu_{R0}(\gamma_M)$ Check: $\boxed{\mu_R(1.0) = 1.311}$

$$\text{Coefficient of v. } w_R := \sqrt{w_{R0}^2 + w_\rho^2 + w_{ky}^2 + w_{R0}^2 \cdot w_\rho^2 + w_{R0}^2 \cdot w_{ky}^2 + w_\rho^2 \cdot w_{ky}^2 + w_{R0}^2 \cdot w_\rho^2 \cdot w_{ky}^2}$$

$$\sigma_R(\gamma_M) := w_R \cdot \mu_R(\gamma_M) \quad w_{R1} := \sqrt{w_\rho^2 + w_{ky}^2 + w_\rho^2 \cdot w_{ky}^2} \quad \alpha_{R1} := \frac{(w_\rho^3 \cdot \alpha_\rho + w_{ky}^3 \cdot \alpha_{ky} + 6w_\rho^2 \cdot w_{ky}^2)}{w_{R1}^3}$$

$$\alpha_R := \frac{(w_{R1}^3 \cdot \alpha_{R1} + w_{R0}^3 \cdot \alpha_{R0} + 6w_{R1}^2 \cdot w_{R0}^2)}{w_R^3} \quad \alpha_R = 0.955$$

6 A three parameter lognormal distribution of R

Parameter CR:

$$CR := 2^{\frac{-1}{3} \cdot \left(\sqrt{\alpha_R^2 + 4 + \alpha_R} \right)^{\frac{1}{3}} - 2^{\frac{-1}{3} \cdot \left(\sqrt{\alpha_R^2 + 4 - \alpha_R} \right)^{\frac{1}{3}}}$$

Parameters of a transformed variable:

$$mR(\gamma M) := -\ln(|CR|) + \ln(\sigma R(\gamma M)) - (0.5) \cdot \ln(1 + CR^2) \quad sR(\gamma M) := \sqrt{\ln(1 + CR^2)} \quad xR(\gamma M) := \mu R(\gamma M) - \frac{1}{CR} \sigma R(\gamma M)$$

Probability distribution of R for arbitrary αR approximated by a three parameter lognormal distribution:

$$R \ln(x, \gamma M) := \begin{cases} \text{plnorm}(x - xR(\gamma M), mR(\gamma M), sR(\gamma M)) & \text{if } \alpha R > 0 \\ 1 - \text{plnorm}(xR(\gamma M) - x, mR(\gamma M), sR(\gamma M)) & \text{otherwise} \end{cases}$$

$xR(1) = -0.03$

$R \ln(0.0, 1) = 0$

7. Theoretical models of action variables G and Q

Normal distribution of G: $wG := 0.10 \quad \sigma G(\chi, \gamma G, \gamma Q) := wG \cdot \mu G(\chi, \gamma G, \gamma Q) \quad \sigma G(0.3, 1.0, 0.7) = 0.077$

Gumbel distribution of Q: $mQ := 0.20 \quad mQ \text{ is } \mu Q / Q_k \quad \mu Q(\chi, \gamma G, \gamma Q) := mQ \cdot Q_k(\chi, \gamma G, \gamma Q)$

$wQ := 1.1 \quad \sigma Q(\chi, \gamma G, \gamma Q) := wQ \cdot \mu Q(\chi, \gamma G, \gamma Q) \quad \alpha Q := 1.14$

Model uncertainty θ , normal distribution: $\mu \theta := 1.0 \quad w \theta := 0.10 \quad \alpha \theta := 3 \cdot w \theta + w \theta^3 \quad \mu Q(0.3, 1, 0.7) = 0.066$

8. Theoretical models of the load effect E = $\theta \cdot (G + Q)$

Load effect E: $\mu E(\chi, \gamma G, \gamma Q) := \mu G(\chi, \gamma G, \gamma Q) + \mu Q(\chi, \gamma G, \gamma Q) \quad \mu E(\chi, \gamma G, \gamma Q) := \mu \theta \cdot \mu E0(\chi, \gamma G, \gamma Q)$

The coefficient of variation of E0 (without model uncertainty θ): $wE0(\chi, \gamma G, \gamma Q) := \frac{(\sqrt{\sigma G(\chi, \gamma G, \gamma Q)^2 + \sigma Q(\chi, \gamma G, \gamma Q)^2})}{\mu E0(\chi, \gamma G, \gamma Q)}$

The coefficient of variation E (including θ) $wE(\chi, \gamma G, \gamma Q) := \sqrt{wE0(\chi, \gamma G, \gamma Q)^2 + w \theta^2 + wE0(\chi, \gamma G, \gamma Q)^2 \cdot w \theta^2}$

The standard deviation of E (including θ) $\sigma E(\chi, \gamma G, \gamma Q) := \mu E(\chi, \gamma G, \gamma Q) \cdot wE(\chi, \gamma G, \gamma Q)$

9. A three parameter lognormal distribution for the load effect E

A three parameter lognormal distribution of E with a general lower bound (shifted lognormal distribution)

Skewness of E0: $\alpha E0(\chi, \gamma G, \gamma Q) := \frac{\sigma Q(\chi, \gamma G, \gamma Q)^3 \cdot \alpha Q}{(\sqrt{\sigma G(\chi, \gamma G, \gamma Q)^2 + \sigma Q(\chi, \gamma G, \gamma Q)^2})^3}$

Skewness of E:
$$\alpha E(\chi, \gamma G, \gamma Q) := \frac{\mu E0(\chi, \gamma G, \gamma Q)^3 \cdot \mu \theta^3 \cdot \left[\frac{w \theta^3 \cdot \alpha \theta + (\sqrt{\sigma G(\chi, \gamma G, \gamma Q)^2 + \sigma Q(\chi, \gamma G, \gamma Q)^2})^3 \cdot \alpha E0(\chi, \gamma G, \gamma Q)}{\mu E0(\chi, \gamma G, \gamma Q)^3} + 6 \cdot w \theta^2 \cdot wE0(\chi, \gamma G, \gamma Q)^2 \right]}{\sigma E(\chi, \gamma G, \gamma Q)^3}$$

Parameter C:
$$C(\chi, \gamma G, \gamma Q) := \frac{\left(\sqrt{\alpha E(\chi, \gamma G, \gamma Q)^2 + 4 + \alpha E(\chi, \gamma G, \gamma Q)} \right)^{\frac{1}{3}} - \left(\sqrt{\alpha E(\chi, \gamma G, \gamma Q)^2 + 4 - \alpha E(\chi, \gamma G, \gamma Q)} \right)^{\frac{1}{3}}}{\frac{1}{2^{\frac{1}{3}}}}$$

Parameters of transformed variable:

$mE(\chi, \gamma G, \gamma Q) := -\ln(|C(\chi, \gamma G, \gamma Q)|) + \ln(\sigma E(\chi, \gamma G, \gamma Q)) - (0.5) \cdot \ln(1 + C(\chi, \gamma G, \gamma Q)^2) \quad \alpha E(0.5, 1.35, 1.5) = 1.173$

$sE(\chi, \gamma G, \gamma Q) := \sqrt{\ln(1 + C(\chi, \gamma G, \gamma Q)^2)} \quad x(\chi, \gamma G, \gamma Q) := \mu E(\chi, \gamma G, \gamma Q) - \frac{1}{C(\chi, \gamma G, \gamma Q)} \sigma E(\chi, \gamma G, \gamma Q)$

Probability density function (PDF) of E, an approximation by a three parameter lognormal distribution:

$$Eln(x, \chi, \gamma G, \gamma Q) := dlnorm(x - x0(\chi, \gamma G, \gamma Q), mE(\chi, \gamma G, \gamma Q), sE(\chi, \gamma G, \gamma Q))$$

10. The failure probability pf and the reliability index β using integration

Probability of failure
$$pfln(\chi, \gamma M, \gamma G, \gamma Q) := \int_0^\infty Eln(x, \chi, \gamma G, \gamma Q) Rln(x, \gamma M) dx$$

Reliability index β : $\beta ln(\chi, \gamma M, \gamma G, \gamma Q) := -qnorm(pfln(\chi, \gamma M, \gamma G, \gamma Q), 0, 1)$ Check: $\beta ln(0.0, 1.0, 1, 1) = 0.685$

11. A parametric study of the index β versus the action ratio χ Target probability $\beta_t := 1.0$

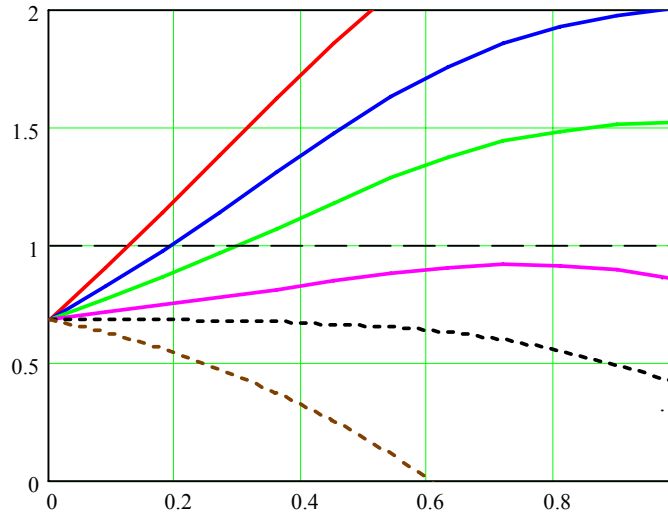


Figure 1. The Reliability index β versus $\chi = Qk/(Gk+Qk)$ for $\psi = \gamma Q = 0, 0.2, 0.3, 0.5, 0.7, 1.0$.

12. A Parametric study of the reliability index β versus the combination factor ψ

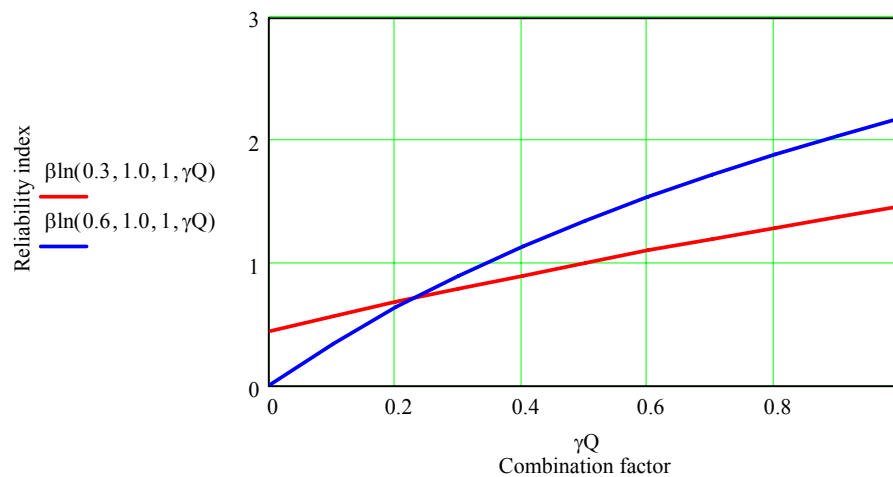


Figure 2. The reliability index β versus combination factor ψ for $\chi = 0.3$ and 0.6 .

The load ratio χ is commonly between 0.3 and 0.6. The following Figure 2 shows the reliability index β versus the combination factor ψ for these two boundary values $\chi = 0.3$ and 0.6 . Figure 2 confirms the above finding that the index β is about 1 for $\psi = 0.3$ in both cases when $\chi = 0.3$ and 0.6 .

13. Discussion

Note 1: The target probability of structural failure given the fire is fully developed $P_t(\text{failure/fire})$ may be derived from a specified target probability of structural failure under persistent design situation $P_t(\text{failure})$ (commonly 0.000072, $\beta = 3.8$) using an approximate expression

$$P_t(\text{failure/fire}) = P_t(\text{failure}) / P(\text{fire})$$

However, the probability $P_t(\text{fire})$ may very widely depend on a particular condition of the construction work. The following factors seem to be most significant

- type of the space,
- compartment area A ,
- active and passive measures to exiting the fire.

The following table indicates informative values of the involved probabilities for an office area provided with sprinklers (see Holicky & Schleich, 2000) and the target reliability index β_t under a fire design situation assuming $P_t(\text{failure})=0.000072$ for 50 years, which corresponds to the reliability index $\beta = 3.8$.

Area	$P(\text{fire starts})$	$P(\text{fire})$	$P_t(\text{failure/fire})$	β_t
25 m ²	0.01	0.0002	0.36	0.4
100 m ²	0.04	0.0008	0.09	1.3
250 m ²	0.1	0.002	0.036	1.8
1000 m ²	0.4	0.008	0.009	2.4

The target index β_t under a fire situation may be expressed in terms of β for persistent situation

$$\beta_t = -\Phi^{-1}(\Phi(-\beta)/P(\text{fire}))$$

where $\Phi()$ denotes the standardised normal distribution. It follows from the above Table that $\beta_t = 1.0$, indicated in Figure 1 by the dashed line may be considered as a reasonable requirement for a compartment area up to 100 m². Then it follows from figure 1 that the combination factor ψ (for imposed load) used in the fire design situation should be at least 0.3, for which the reliability index is almost independent of the load ratio χ (the values $\psi_0 = 0.7$, $\psi_1 = 0.5$ and $\psi_2 = 0.3$ are indicated in prEN 1990).

Note 2: An important assumptions concerns the coefficient of variation of the reduction factor k_y , which further depends on the assumed temperature time curve and a number of other factors. It should be mentioned that the value 0.20 is considered in this study as "a reasonable estimate" based on more detailed probabilistic analysis. With the increasing coefficient of variation of k_y the failure probability increases and, therefore, the required factor ψ should also increase.

14. Preliminary conclusions

The following preliminary conclusions concerning the factor ψ used in a load combination under fire design situation may be drawn from the limited results of the reliability analysis of a steel element in an office area:

- the factor ψ should depend on the type and extent of the compartment area A , on active and passive measures, and on the load ratio χ ,
- the factor ψ should increase with increasing the compartment area A ,
- the factor ψ should be at least 0.3, for which β is about the same as for a loading with only a permanent load.

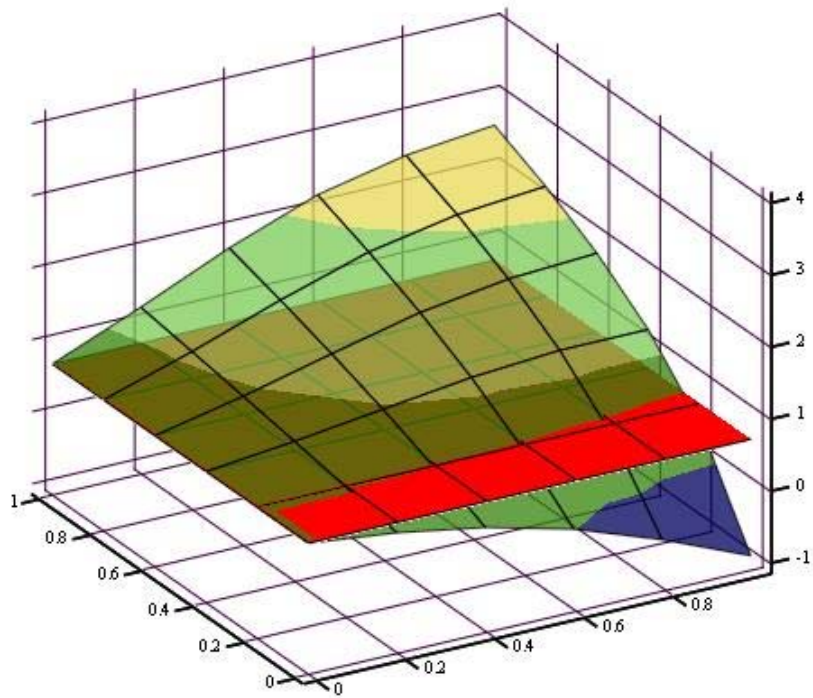
15. Two parameters study

Definition of the function: $\chi := 0, 0.045.. 0.99$

$$\beta(\chi, \gamma Q) := \beta \ln(\chi, 1.0, 1, \gamma Q)$$

Check: $\beta(0.0, 0.) = 0.685$

$$\beta_0(\chi, \gamma Q) := \beta \ln(0, 1.0, 1, \gamma Q)$$



β, β_0

CHAPTER III – CALIBRATION OF RELIABILITY PARAMETERS

Jean-Baptiste Schleich¹

¹ University of Technology Aachen, University of Liège

1 INTRODUCTION

1.1 Background documents

The Eurocodes EN 1990 [15] and EN 1991-1-2 [16] are used as basic background materials in this contribution. General information concerning reliability is available in the important international publications [3, 6, 8, 9, 10, 14], which have been used as background materials for the development of EN1991-1-2 [16]. In addition to the above mentioned materials, relevant findings described in various documents [1, 2, 4, 5, 11, 12, 13, 18, 20] have influenced the analysis of the relevant reliability parameters.

1.2 General principles

The target failure probability not to be exceeded in normal conditions is given by $7,23 \cdot 10^{-5}$ for the building life of ~55 years [15]. Hence the objective for the fire situation should also be

$$p_{f,55}(\text{probability of failure}) \leq p_{t,55}(\text{target failure probability}) = 7,23 \cdot 10^{-5} \quad (1)$$

The first method of safety quantification is given by a **full probabilistic approach (LEVEL 0)**, which requires to establish the limit state function and hence the mathematical expression of the probability of the physically relevant failure in the fire situation. This limit state function shall be given by a continuous algebraic function and the corresponding probability of failure determined by a software able to deal with a set of variables given by different statistical distributions [3, 9, 11].

In this procedure the characteristic fire load $q_{f,k}$ [MJ/m²] is considered when establishing the limit state function, and the danger of fire activation as well as the influence of active fire fighting measures are taken into account when evaluating the probability of getting a fully fire engulfed compartment or a severe fire [7, 10].

Of course the establishment of the limit state function gets difficult if not impossible for structures larger than one beam or one column, so that this approach is actually not feasible for practical engineering.

Hence the use of a **semi-probabilistic approach (LEVEL 1 or LEVEL 2)** is suggested, which is based on the procedure for structural design at ambient temperature and which defines a design fire load $q_{f,d}$ [MJ/m²] taking into account the danger of fire activation and the influence of active fire fighting measures [6, 17].

That design fire load is directly considered - in a deterministic way - in the fire development models, in order to assess the temperature evolution within the compartment. This permits to determine the temperature field in the structure and the corresponding structural response, again in a deterministic way. Fire development models and fire resistance models have been discussed in Chapter I-4 and in Chapter I-6. Fire models comprise localised fires and fully developed fires. Fire resistance models may either constitute simple

or advanced calculation models. For the evaluation of the global structural behaviour in the fire situation advanced models should be used.

Two levels permitting the calculation of the design fire load are described:

° In LEVEL 1 the probabilistic approach allows to use any target failure probability obtained through improved reliability considerations. This leads to a global factor γ_{qf} giving the design fire load according to

$$q_{f,d} = \gamma_{qf} \cdot q_{f,k} \quad [\text{MJ/m}^2] \quad (2)$$

The calibration of the global factor γ_{qf} is given hereafter in paragraph 3.1 for the target failure probability of $7,23 \cdot 10^{-5}$ for the building life.

°° In LEVEL 2 the design fire load is calculated by multiplying the characteristic fire load by the partial factors δ_{q1} and δ_{q2} , and the differentiation factor δ_n based on the target failure probability of $7,23 \cdot 10^{-5}$ for the building life according to

$$q_{f,d} = m \cdot \delta_{q1} \cdot \delta_{q2} \cdot \delta_n \cdot q_{f,k} \quad [\text{MJ/m}^2] \quad (3)$$

The calibration of the partial factors δ_{q1} and δ_{q2} related to the risk of fire activation and the calibration of the differentiation factors δ_{ni} related to the active fire safety measures is given hereafter in paragraph 3.2.

The Level 2 method is of course an approximation which is on the safe side. For that reason the global combustion factor m may be taken as 0,8. This Level 2 method has the enormous advantage to be quite userfriendly as all the partial and differentiation factors may be taken directly from Annex E of EN1991-1-2 [16].

2 FULL PROBABILISTIC APPROACH

2.1 General presentation

" The general method of safety quantification is given by a full probabilistic approach (LEVEL 0), which requires to establish the limit state function and hence the mathematical expression of the probability of the physically relevant failure in the fire situation. This limit state function shall be given by a continuous algebraic function and the corresponding probability of failure determined by a software able to deal with a set of variables given by different statistical distributions [3, 9, 11] ".

The verification of structural safety leads to various factors connected to loads, to the resistance of the structure and to the calculation models which introduce into the design procedure a lack of precision and hence random aspects. The origin and the nature of the essential imperfections are:

- **Lack of precision due to loads.** Among loads acting on structures, some are relatively well known (proper weight, permanent loads). On the contrary variable actions like those for instance resulting from wind or snow can't be established with high precision for any location; their value is fixed thanks to measurements and on the basis of experience and observation. Consequently we have a certain probability that, during the whole service life of the structure, the real action effects are at a given moment higher than those supposed for the design calculations.
- **Lack of precision connected to the resistance of the structure.** The properties of materials, defined by tests, vary from one specimen to the next one, or even from one point to another for the same specimen. The composition and hence the mechanical characteristics of steel or concrete constitute data comprising a certain dispersion. Furthermore the real dimensions of elements don't fully correspond to the theoretical dimensions, due to tolerances in fabrication or during concreting. Finally we should also consider the lack of precision due to the erection methods (tolerances in execution, difference between drawings and the execution).
- **Lack of precision due to the calculation models.** Calculation is indeed based on analytical and mathematical models simulating approximately the real behaviour of a structure. Results based on these incomplete models contain necessarily a lack of precision.

Let's analyse in a most simple way how we should consider the random nature of the resistance of the structure and of actions. By using the notations R and S for the description of the resistance of the structure and the action effect of loads on the structure, it is possible to represent in a graphical way those parameters and to take account of their statistical distribution. The Standard Normal distribution, i.e. the law of Gauss, may be used to define the probabilistic distribution of a variable (figure 1)

- m_S , mean value of the action effect,
- m_R , mean value of the resistance,
- σ_S , standard deviation of the action effect,
- σ_R , standard deviation of the resistance.

This representation might be correct for certain variables, but may be too clumsy for others. This distribution is relatively easy to handle compared to other probabilistic distributions, but should be used with great care and if needed replaced by the other more realistic distribution types. Let's remember that the law of Gauss is symmetrical and that the mean value has the highest probability to occur, as m_S and m_R given in figure 1. It can be seen that both curves S and R intersect; hence a certain probability p_f exists that the action effect S becomes larger than the resistance of the structure R .

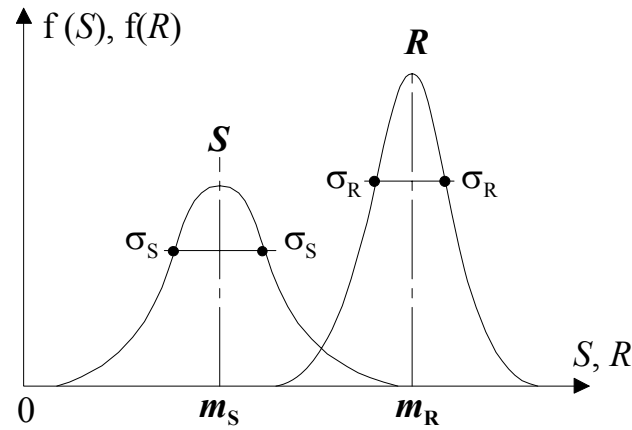


Figure 1. Scheme of the probabilistic distribution of the action effect and of the resistance of a structure.

The design of a structure always requires to compare the value S of the action effect to the value R of the resistance, in other words requires to verify the general relation :

$$S \leq R \quad (4)$$

which may also be written as the **limit state function F**

$$F = R - S \geq 0 \quad (5)$$

The distribution of the new variable $F = R - S$ is represented in figure 2. This curve shows clearly that a certain probability of failure p_f of the structure exists, due to the fact that it is possible that resistance R gets inferior to the action effect S . This failure probability corresponds to the hatched surface and is given by

$$p_f = 1 - p((R - S) \geq 0) = p((R - S) \leq 0) \quad (6)$$

with $p(\dots)$, probability of occurrence .

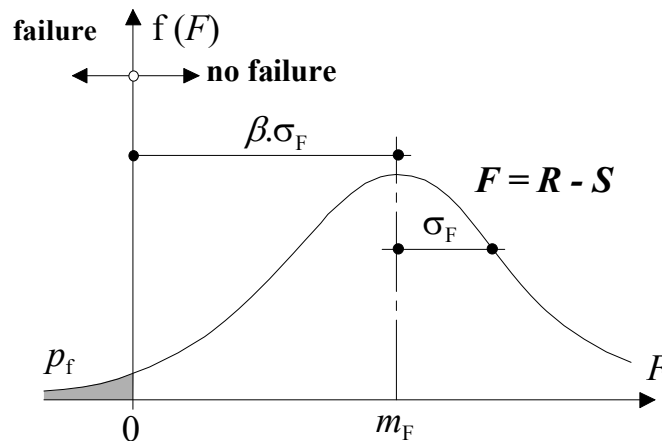


Figure 2. Limit state function and probability that resistance R gets inferior to the action effect S , i.e. failure probability or probability that the limit state function becomes negative.

Chapter III - Calibration of reliability parameters

When defining the safety index β as the number of standard deviations σ_F separating the mean value m_F from the origin,

$$\beta \cdot \sigma_F = m_F \quad (7)$$

with m_F mean value of the limit state function and σ_F standard deviation of the limit state function, the failure probability p_f may be given by

$$p_f = \Phi(-\beta) \quad (8)$$

with Φ , Standard Normal cumulative distribution function given in table 1.

Table 1. Standard Normal cumulative distribution function, $p_f = \Phi(-\beta)$.

β	p_f	β	p_f
.0	.50000		
.1	.46017	2.6	.0246612
.2	.42074	2.7	.0246612
.3	.38209	2.8	.0225551
.4	.34458	2.9	.0218658
.5	.30854	3.0	.0213499
.6	.27425	3.1	.0396760
.7	.24196	3.2	.0368714
.8	.21186	3.3	.0348342
.9	.18406	3.4	.0333693
1.0	.15866	3.5	.0323263
1.1	.13567	3.6	.0315911
1.2	.11507	3.7	.0310780
1.3	.096800	3.8	.0472348
1.4	.080757	3.9	.0448096
1.5	.066807	4.0	.0431671
1.6	.054799	4.1	.0420658
1.7	.044565	4.2	.0413346
1.8	.035930	4.3	.0585399
1.9	.028717	4.4	.0554125
2.0	.022750	4.5	.0533977
2.1	.017864	4.6	.0521125
2.2	.013903	4.7	.0513008
2.3	.010724	4.8	.0679333
2.4	.0281975	4.9	.0647918
2.5	.0262097		

Note that the table gives $\beta \in [4,9 ; 0]$ for $p_f \leq 0,5$ and larger probabilities are obtained by:

$$\begin{aligned} \Phi[-(\beta = -a)] &= 1 - \Phi[-(\beta = +a)] \\ \text{f.i: } 0,95 &= 1 - (0,05) \\ \beta &= -1,645 \quad \downarrow \quad \downarrow \beta = +1,645 \end{aligned}$$

This is illustrated in figure 3.

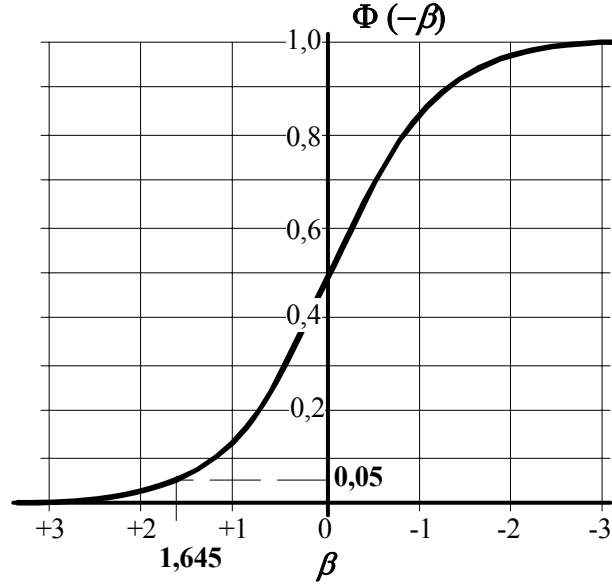


Figure 3. Complete Standard Normal cumulative distribution function with $0,0 \leq p_f = \Phi(-\beta) \leq 1,0$.

Note that a safety index β of 3,8 corresponds to a failure probability p_f of $7,23 \cdot 10^{-5}$, and a safety index β of 4,7 represents in fact a failure probability of $1,3 \cdot 10^{-6}$!!!

Every structure has necessarily a failure probability, as one hundred percent safety is not existing; this fact has to be accepted. However the problem consists in selecting the reasonable failure probability. We may underline that an order of magnitude of $p_f = 10^{-5}$ to 10^{-6} is readily accepted as failure probability for civil engineering structures, which corresponds approximately to a safety index of $\beta = 4,2$ à $4,7$.

A probabilistic analysis of structural safety would allow to obtain, when choosing a safety index β larger or equal to a limit value β_0 , design values S_d of the action effect and R_d of the resistance. In case the variables S and R correspond to a Standard Normal distribution, we have :

$$m_F = m_R - m_S \text{ and} \quad (9)$$

$$\sigma_F = (\sigma_R^2 + \sigma_S^2)^{0,5} \quad (10)$$

which permits, when requiring that the safety index β given in (7) be larger or equal to β_0 , to define the design values S_d of the action effect and R_d of the resistance in the following way:

$$S_d = m_S (1 + \beta_0 \alpha_S V_S) \quad (11)$$

$$R_d = m_R (1 - \beta_0 \alpha_R V_R) \quad (12)$$

with

$$\alpha_S \text{ weighting factor of } S \text{ given by } \alpha_S = \sigma_S / (\sigma_R^2 + \sigma_S^2)^{0,5} \quad (13)$$

$$\alpha_R \text{ weighting factor of } R \text{ given by } \alpha_R = \sigma_R / (\sigma_R^2 + \sigma_S^2)^{0,5} \quad (14)$$

$$V_S \text{ variation coefficient of } S \text{ obtained from } V_S = \sigma_S / m_S \quad (15)$$

$$V_R \text{ variation coefficient of } R \text{ obtained from } V_R = \sigma_R / m_R \quad (16)$$

Note that $\sum \alpha_i^2 = 1$, and that in general the verification of the structural stability formulated in (4) may be expressed with the results of a probabilistic approach as follows:

$$S_d \leq R_d \quad (17)$$

In case of other distribution types, as well as when more variables have to be activated, theoretical procedures given in the literature have to be used.

In the frame of this Handbook 5, this more complex aspect is covered in the next chapter through the examples dealing with civil engineering applications.

2.2 Applied structural safety on the basis of the probabilistic approach

Reality is more complex than previous developments, as the number of variables as well on the side of actions as on the side of resistance is often quite large. Hence the use of probabilistic procedures gets very quickly time consuming for everyday's practical engineering. For this reason we should take advantage of computer programs able to deal with a number of variables embedded in a well defined analytical limit state function. That's the case with the software VaP "Variables Processor" developed by Professor Jörg Schneider at the ETHZ [9]. This software is being used hereafter when analysing practical applications.

First we should express the limit state function F , given by equation (5), in an analytical and continuous manner.

As next we should define for all variables X the type of distribution, the mean m_x and the standard deviation σ_x . Note that the selection of the type of distribution is more or less imposed by the physical type of variable. Here we refer to the literature and to table 2, which proposes the type of distribution, nominal resp. characteristic values X_k (fractile) as well as the variation coefficient V_x given by

$$V_x = \sigma_x / m_x \quad (18)$$

Table 2. Proposals for type of distribution, fractile and variation coefficient of variables X according to experience & literature.

Type of variable X	Type of distribution	Fractile of X_k	Variation coefficient V_x
Proper weight G	Normal (Gauss)	50%	0,1
Life load Q	GUMBEL Type I	95%	0,3
Resistance R	LOGNORMAL	5%	0,05 \rightarrow 0,10
Strenght of concrete f_c	LN	5%	0,17
Yield point of steel f_y	LN	2%	0,05 \rightarrow 0,08
Thermal characteristic of a wall $b = (\rho.c.\lambda)^{0,5}$	BETA or DETERMINED	50%	0,05
Opening factor $\theta = Av(h)^{0,5}/At$	LN or D	50%	0,1
Fire load q_f	GL or BETA	50%	0
Geometrical dimensions	GL or BETA	80 %	0,3
	NORMAL or D	50%	0,05 \rightarrow 0,10 !
			0,005 \rightarrow 0,03
			0

Knowing for a given variable X , X_k as well as V_x , it is possible to calculate m_x and σ_x in function of the type of distribution as indicated in table 3 and by using equation (18).

Table 3. Design value and characteristic value of variable X for different types of distribution.

Type of distribution	Design value X_d / γ_{Sd}	Characteristic value X_k	Explanations
NORMAL	$m_x - \alpha_x \cdot \beta \cdot \sigma_x$	$m_x - \beta_k \cdot \sigma_x$	m = mean; σ = standard deviation
LOGNORMAL	$m_x \cdot e^{(-\alpha_x \cdot \beta \cdot V_x)}$	$m_x \cdot e^{(-\beta_k \cdot V_x)}$	for $V_x = (\sigma_x / m_x) < 0,2$
GUMBEL	$u - a^{-1} \cdot \ln[-\ln\Phi(-\alpha_x \beta)]$	$u - a^{-1} \cdot \ln[-\ln\Phi(-\beta_k)]$	$u = m_x - 0,577216/a$ and $a = \pi / (\sigma_x \cdot \sqrt{6})$

- N.B.
- 1) We should foresee when calculating X_d a safety factor γ_{Sd} in order to take account of the uncertainty in modelling actions, f.i. $\gamma_{Sd} = 1,05$.
 - 2) Knowing the fractile of X_k , figure 3 permits the calculation of β_k :
 fractile 2,27% $\rightarrow \beta_k = 2$
 5% $\rightarrow \beta_k = 1,645$
 50% $\rightarrow \beta_k = 0$
 80% $\rightarrow \beta_k = -0,8 \dots$ et $\Phi(-\beta_k) = 0,80$
 95 % $\rightarrow \beta_k = -1,645$ et $\Phi(-\beta_k) = 0,95$
 - 3) If we have a GUMBEL distribution we get for a fractile of X_k
 - of 80 % : $m_x = 0,822 \cdot X_k$, if $V_x = 0,3$ and $m_x = 0,735 \cdot X_k$, if $V_x = 0,5$;
 - of 95 % : $m_x = 0,641 \cdot X_k$ if $V_x = 0,3$ and $m_x = 0,517 \cdot X_k$ if $V_x = 0,5$.
 These results follow from equation (18) and from equations in table3.
 - 4) The BETA distribution permits to simulate well defined lower and upper limits. This allows to represent reality in a better way like concrete cracked or uncracked cross-sections.

Having defined for all variables X_i the parameters X_{ki} , m_{xi} and σ_{xi} as well as the best suitable distribution types, the program VaP permits to estimate

- for all variables the weighting factors α_{xi} such as

$$\sum_{i=1}^n (\alpha_{xi}^2) = 1$$

- the design values $X_{i,d}$ of all variables,
- the failure probability $p_f = \Phi(-\beta)$ connected to the physical aspect described by the limit state function, as well as the corresponding safety index β .

Note that the safety or reliability index β is also called index of HASOFER & LIND i.e. HL. Target values as well for p_f or β , proposed in tables C1 and C2 of EN1990 [15], may be taken from table 4.

Table 4. Target values for the reliability index β and the failure probability p_f .

Limit state	Life time ± 55 years		For 1year	
	β_{\min}	$p_{f \max}$	β_{\min}	$p_{f \max}$
Structural safety	3,8	$7,23 \cdot 10^{-5}$	4,7	$1,3 \cdot 10^{-6}$
Serviceability	1,5	$6,7 \cdot 10^{-2}$	3,0	$1,35 \cdot 10^{-3}$

2.3 Steel beam in the fire situation

" In this procedure the characteristic fire load $q_{f,k}$ [MJ/m²] is considered when establishing the limit state function, and the danger of fire activation as well as the influence of active fire fighting measures are taken into account when evaluating the probability of getting a fully fire engulfed compartment or a severe fire [7, 10] "

The analysis of the structural safety of a steel beam in the fire situation is of course much more complex. The limit state function regarding failure by bending may be written as follows:

$$F \equiv F_{fi} = M_{fi,R} - M_{fi,S} \geq 0 \quad (19)$$

and in general we would have

$$F = f[G; Q; R_{fi}; A_m/V; L; A_{fi}/A_{tot}; b; O; q_{floor}; K_1] \quad (20)$$

with

- G proper weight [kN/m]
- Q life load [kN/m]
- R_{fi} bending resistance of the beam in function of the temperature [kNm]
- A_m/V massivity, or section factor, of the beam [m⁻¹]
- L span of the beam [m]
- A_{fi} / A_{tot} ratio of the floor surface to the total surface surrounding the compartment [-]
- b thermal characteristic of compartment walls
 $b = \sqrt{\rho \cdot c \cdot \lambda}$ [J/m² sec^{1/2} K]
- O ventilation coefficient of the compartment [m^{1/2}]
- q_{floor} fire load related to the floor area [MJ/m²]
- κ_1 adaptation factor for non-uniform temperature in the cross-section [-]

This allows through the software VaP, to analyse in a rather general manner the influence of a fire on the stability of beams. The study called "INFLUENCE OF ACTIVE FIRE PROTECTION on the SAFETY LEVEL & its CONSEQUENCES on the DESIGN OF STRUCTURAL MEMBERS; by J.B. SCHLEICH, ETHZ, 01.09.98", is a quite convincing document [6].

In the frame of this Handbook 5, we will simplify the present example:

- by considering a particular steel profile and a well defined compartment, we eliminate the variables A_m/V , A_{fl}/A_{tot} , b et O ,
- we will keep the parameters G , Q , R_{fi} et q_{floor} as variables.

❖ Hence the limit state function is established in the following way on the basis of equation (19) and of figure 4:

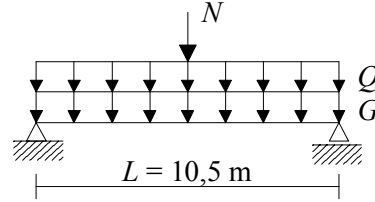


Figure 4. Statically determined steel beam loaded by the proper weight G of the concrete floor, the live load Q on the floor and a concentrated snow load N .

$$M_{fi, S} = (G + \psi_1 \cdot Q) L^2/8 + \psi_2 NL/4 \quad (21)$$

By taking Q as the main variable action, the accidental combination and the table of combination factors ψ from EN1990 [15] - see also Chapter I-6.2 - give for a building of category A or B, $\psi_1 = 0,5$ et $\psi_2 = 0$ hence

$$M_{fi, S} = (G + 0,5 Q) L^2/8 \quad (22)$$

According 4.2.3.3 (1), (3), (7) et (8) of prEN1993-1-2 [19] we will have

$$M_{fi, R} = (k_{y, \theta_{max}}) \cdot M_R / \kappa_1 \quad (23)$$

knowing that

- $k_{y, \theta_{max}}$ is the reduction coefficient of the yield point for the maximum temperature θ_{max} in steel and
- $\kappa_1 = 0,7$ according to prEN1993-1-2 [19], in case of a beam supporting a concrete floor and heated from below.

This leads to

$$M_{fi, R} = (k_{y, \theta_{max}}) R / 0,7 \quad (24)$$

The reduction coefficient of the yield point $k_{y, \theta_{max}}$ may be expressed in function of $\theta = \theta_{max}$ [°C] according to the following continuous algebraic function which simulates in a perfect way the values of $k_{y, \theta}$ given in table 3.1 of prEN1993-1-2 [19]:

$$k_{y, \theta} = 1,009 / (1 + e^{0,02556(\theta - 482)})^{0,2609} \quad (25)$$

❖ Let's consider the following dimensions for the compartment :

- $A_{floor} = 10 \times 20 = 200 \text{ m}^2$
- $H = 4 \text{ m}$, height of the compartment
- $A_{tot} = 2 \cdot 200 + 4 \cdot 60 = 640 \text{ m}^2$
- $h = 1,64 \text{ m}$, height of the openings
- $A_V = 50 \text{ m}^2$, surface of the openings,

which leads to

$$A_{fl} / A_{tot} = 0,3125$$

$$O = A_V \sqrt{h} / A_t = 0,10 \text{ m}^{1/2} \text{ and let's suppose}$$

$$b = 1\,500 \quad \text{J/m}^2 \text{ sec}^{1/2} \text{ K}$$

❖ By choosing the **unprotected profile IPE A 550**, supporting a slab we will get

$$A_m / V = 143 \text{ m}^{-1} \text{ (massivity for radiation on 3 sides)}.$$

These conditions allow to establish, on the basis of calculations done through the software OZONE and on the basis of 4.2.5.1 of prEN1993-1-2 [19] - see also Chapter I-5.2 - a relation between the fire load $q_{floor} = q_{f,k}$ and the maximum uniform temperature in the profile. This is illustrated by equation (26) and figure 5 [6].

$$\begin{aligned} \theta_{max}^{STEEL} &= \delta_{th} \cdot \theta^{AIR} \\ &= f(A_m/V ; O ; q_{f,k} \dots) \end{aligned} \quad (26)$$

with $\delta_{th} \leq 1$, for the rising part of the heating curve.

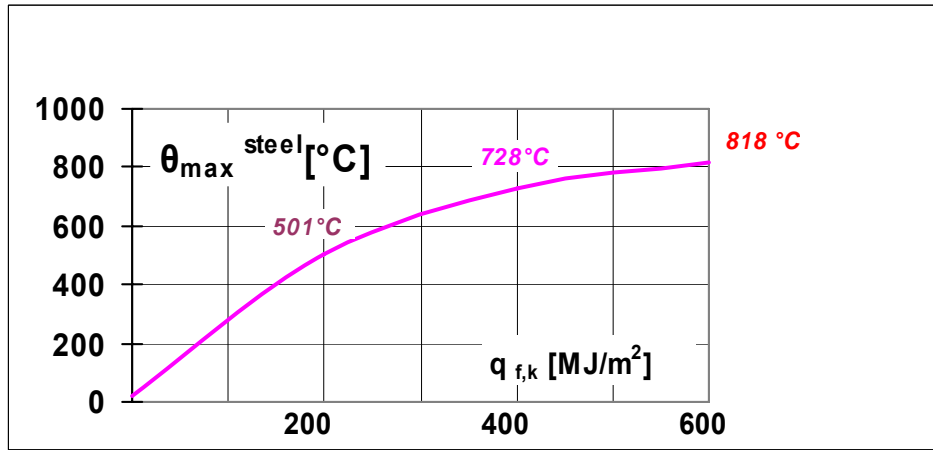


Figure 5. Maximum uniform temperature in the profile IPE A 550 in function of the fire load $q_{f,k}$ and for the given compartment..

We will have according to figure 5

$$\theta_{max}^{STEEL} = (39/16\,000\,000)q_{f,k}^3 - (371/80000)q_{f,k}^2 + (647/200)q_{f,k} + 20 \quad (27)$$

❖ **When considering the profile IPE A** with $f_y = 235 \text{ N/mm}^2$, $\gamma_{Mo} = 1$ and $W_{pl} = 2\,475 \text{ cm}^3$ as well as a bending resistance R with a LOGNORMAL distribution

$$R_k = 5\% = 23,5 \times 2\,475 = 58\,162 \text{ kNcm} = 581,6 \text{ kNm}$$

$$m_R = (e^{\beta_k \cdot V_R}) R_k \text{ avec } \beta_k = 1,645 \text{ et } V_R = 0,05 \text{ (see tables 2 and 3)}$$

$$m_R = (e^{1,645 \cdot 0,05}) 581,6$$

$$m_R = 631,5 \text{ kNm}$$

$$\sigma_R = m_R \cdot V_R = 31,6 \text{ kNm}$$

❖ The equations (19), (22), (24), (25) and (27) will lead to the following limit state function

$$F_{fi} = - (G + 0,5Q) L^2/8 + (R/0,7) \cdot [1,009 / [1 + e^{0,02556 ((39/16\,000\,000)q^3 - (371/80000)q^2 + (647/200)q - 462)}]]^{0,2609} \quad (28)$$

Note that the parameters of all the variables are given in table 5.

Table 5. Parameters of variables needed for the analysis of the limit state function (28).

Variable X	Type of distribution	X_k	m_x	σ_x	V_x	Units
G	N	15 50%	15	1,5	0,1	kN/m
Q	GL	10 95%	6,41	1,92	0,3	kN/m
R	LN	581,6 5%	631,5	31,6	0,05	kNm
L	D	10,5	10,5	/	/	m
q_{floor}	GL	200 80%	164,4	49,3	0,3	MJ/m ²
		250	205,5	61,7		
		300	246,6	74		
		400	329	99		
		500	411	123,3		

❖ Results from VaP calculations show that we will have a failure probability in bending of the beam in case of fire p_{ffi}

$$\begin{aligned}
 * p_{\text{ffi}} &= 0,0069 & \text{for } q_{f,k} &= 200 \text{ MJ/m}^2 \\
 ** p_{\text{ffi}} &= 0,702 & \text{for } q_{f,k} &= 500 \text{ MJ/m}^2.
 \end{aligned}$$

In order to understand the meaning of these values we should refer to the previously named study [6, 17] according to which

$$p_{f,55} = p_{\text{fi},55} \cdot p_{\text{ffi}} \leq 7,23 \cdot 10^{-5} \quad (29)$$

Whereas the probability of having a failure in case of fire p_{ffi} is given by the here presented "VaP" calculations, the probability $p_{\text{fi},55}$ of having a severe fire in a compartment during its life time (of 55 years) depends on the size of the compartment as well as on the type of occupancy, on the ability of OCCUPANTS and PUBLIC SAFETY SERVICES in stopping the fire before flash-over, but also on the existence and the quality of given active fire fighting measures like SPRINKLERS. These last factors might however only be quantified on the basis of a whole set of international statistical measurements, by the way collected in the study performed by Prof. M. Fontana [7, 10]. This gives for our calculation:

$$p_{\text{fi},55} = (p_{\text{fi},55}^{\text{IGNITION}}) \cdot (p_f^{\text{OC}} \cdot p_f^{\text{PS}} \cdot p_f^{\text{SP}}) \quad (30a)$$

For a compartment of a public or office building, the data base gives

$$\begin{aligned}
 p_{\text{fi},55}^{\text{IGNITION}} &= (10 \cdot 10^{-6} / \text{m}^2 \cdot \text{year}) (200 \text{ m}^2) (55 \text{ years}) \\
 &= 0,11
 \end{aligned}$$

$$p_f^{\text{OC}} = 0,40 \text{ the probability of failure of occupants in stopping the fire,}$$

$$p_f^{\text{PS}} = 0,05 \text{ à } \underline{0,10} \text{ the probability of failure of public safety services in stopping the fire,}$$

$p_f^{SP} = 0,02 * \alpha 0,05$ the probability of failure of sprinklers in stopping the fire, the value of 0,05 corresponding to sprinklers not in conformity with prescriptions.

Hence equations (29) and (30a) give the upper acceptable limit for p_{ffi}

$$p_{ffi} \leq (7,23 \cdot 10^{-5}) / p_{fi,55} = p_{ffi}^{lim} \quad (31)$$

Table 6. Acceptable limit for a failure in case of fire p_{ffi} .

Office buildings $A_n = 200 \text{ m}^2$	Assistance of occupants & intervention of public safety services	
	Without sprinklers	With sprinklers
$p_{fi,55}$	$4,40 \cdot 10^{-3}$	$8,8 \cdot 10^{-5}$
p_{ffi}^{lim}	0,0164	0,822

Table 6 finally permits, together with the results of the "VaP" calculations presented in table 7, to **find the limits of the fire load $q_{f,k}$ not to be exceeded in order to have no failure of the not protected steel beam**, in the case of the natural fire existing in this previously defined compartment.

Table 7. Acceptable limit for a failure in case of fire p_{ffi}^{lim} compared with p_{ffi} established by VaP.

Office buildings $A_n = 200 \text{ m}^2$		Assistance of occupants & intervention of public safety services	
		Without sprinklers	With sprinklers
p_{ffi}^{lim}		0,0164	0,822
NOT PROTECTED	$q_{f,k}$ [MJ/m ²]	p_{ffi} by VaP	
BEAM	/	/	/
IPEA550	200	0,0069	id.
	250	0,0382	id.
L = 10,5 m	300	0,115	0,115
$K_1 = 0,7$	400	0,402	0,402
	500	0,702	0,702

As a conclusion, according to table7, the not protected steel beam is sufficiently safe in case of fire :

- without sprinklers, if $q_{f,k} \leq 220 \text{ MJ/m}^2$
- with sprinklers*, if $q_{f,k} \leq 560 \text{ MJ/m}^2$.

N.B.: Let's also note the importance of the fire load among all variables, as the weighting factor α_q is systematically above 0,98 .

3 SEMI-PROBABILISTIC APPROACH

3.1 Calibration of the global factor related to the fire load.

This concerns the performance based procedure "LEVEL 1", where the probabilistic approach allows to use any target failure probability obtained through improved reliability considerations. This leads to a global factor γ_{qf} giving the design fire load according to

$$q_{f,d} = \gamma_{qf} \cdot q_{f,k} \quad [\text{MJ/m}^2] \quad (2)$$

The calibration of the global factor γ_{qf} is given hereafter for the target failure probability $p_{t,55}$ of $7,23 \cdot 10^{-5}$ for the building life.

This means that in case of fire

$$p_{f,55} (\text{probability of failure}) = p_{fi,55} (\text{probability of severe fire}) \cdot p_{ffi} (\text{failure probability in case of fire})$$

and hence

$$p_{f,55} = p_{fi,55} \cdot p_{ffi} \leq p_{t,55} (\text{target failure probability}) = 7,23 \cdot 10^{-5}. \quad (29)$$

This allows to extract the failure probability in case of fire as

$$p_{ffi} \leq (p_{t,55} / p_{fi,55}) = p_{fi,t} \quad (31)$$

which is the target failure probability in case of fire.

On the level of reliability indexes this means $\beta_{fi} \geq \beta_{fi,t}$.

❖ It is assumed that p_{ffi} follows the Gaussian normal distribution and hence the corresponding reliability index β_{fi} is given by the inverse of the cumulative normal distribution. Therefore in case of perfect design such as $p_{ffi} = p_{fi,t}$ we will get

$$\beta_{fi} = \beta_{fi,t} = -\Phi^{-1}(p_{fi,t}) = -\Phi^{-1}(7,23 \cdot 10^{-5} / p_{fi,55}) \quad (32)$$

This allows to establish a quite interesting relation between $p_{fi,55}$, $p_{fi,t}$, and $\beta_{fi,t} = \beta_{fi}$ as shown in figure 6.

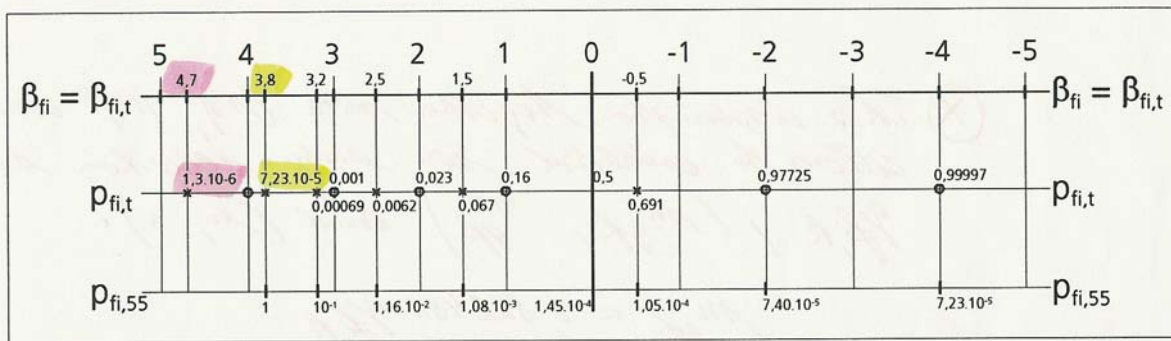


Figure 6. Connection between the reliability index β_{fi} , related to the probability of structural failure in case of fire p_{fi} , and the probability $p_{fi,55}$ of getting a fully fire engulfed compartment during the life time of the building.

In fact equation (32) shows that a relation is now established between
 ° the structural failure probability in case of fire p_{ffi} related to β_{fi}

- °° and the probability $p_{fi,55}$ of getting a fully fire engulfed compartment during the life time of the building, which depends on the compartment size, the type of occupancy and the active fire safety measures.

❖ Reliability calculations (see 2.9.2.3 of [11]) have shown that the weighing factor for the main action at room temperature is strongly reduced in case of fire and may therefore be considered as a secondary action, whereas the fire load becomes the main action.

This leads to a global factor γ_{qf} giving the design fire load according to

$$q_{f,d} = \gamma_{qf} \cdot q_{f,k} \quad [\text{MJ/m}^2] \quad (2)$$

Moreover these calculations have pointed out that the assumption of the weighing factor of (-0,7) for the main action has to be modified and that a value of (-0,9) should be chosen for α_{qf} ; see also page III -14 where however for the software VaP the sign of α_{qf} is inversed [9].

According to the literature, the data for fire loads fit well into a **Gumbel type I** distribution. Hence a variation coefficient V_{qf} of 0,3 and an 80 % fractile for the characteristic fire load $q_{f,k}$ have been chosen; see also table 2. Moreover a safety factor for the model uncertainty $\gamma_{sd}=1,05$ has been considered, when calculating the design fire load.

Using the relations given in table 3 the design fire load is calculated as:

$$q_{f,d} = \gamma_{sd} \{ u - a^{-1} \cdot \ln[-\ln\Phi(-\alpha_{qf}\beta_{fi})] \} \quad (33)$$

with

γ_{sd} model uncertainty factor taken as 1,05

$u = m_{qf} - 0,577216 / a$

$a = \pi / (\sigma_{qf} \cdot \sqrt{6})$

m_{qf} mean value of the fire load

σ_{qf} standard deviation of the fire load

Φ normal cumulative distribution function

α_{qf} weighing factor related to the fire load taken as (-0,9)

β_{fi} reliability index related to p_{fi} .

This gives at the end with $\sigma_{qf} = m_{qf} \cdot V_{qf}$

$$q_{f,d} = \gamma_{sd} m_{qf} \left\{ 1 - (V_{qf}(\sqrt{6})/\pi) (0,577216 + \ln[-\ln\Phi(0,9\beta_{fi})]) \right\} \quad (34)$$

Similarly follows the calculation of the characteristic value of the fire load

$$q_{f,k} = u - a^{-1} \cdot \ln[-\ln\Phi(-\beta_k)] \quad (35a)$$

This gives finally with $\Phi(-\beta_k) = 0,8$; see page III-9

$$q_{f,k} = m_{qf} \left\{ 1 - (V_{qf}(\sqrt{6})/\pi) (0,577216 + \ln[-\ln 0,8]) \right\} \quad (35b)$$

and the global factor γ_{qf} , taking V_{qf} as 0,3 and γ_{sd} as 1,05, is given by

$$\gamma_{qf} = q_{f,d} / q_{f,k} = 0,863605 \{ 1 - 0,233909 (0,577216 + \ln[-\ln\Phi(0,9\beta_{fi})]) \} \quad (36)$$

which brings us to the evolution of γ_{qf} as a function of β_{fi} indicated in figure 7.

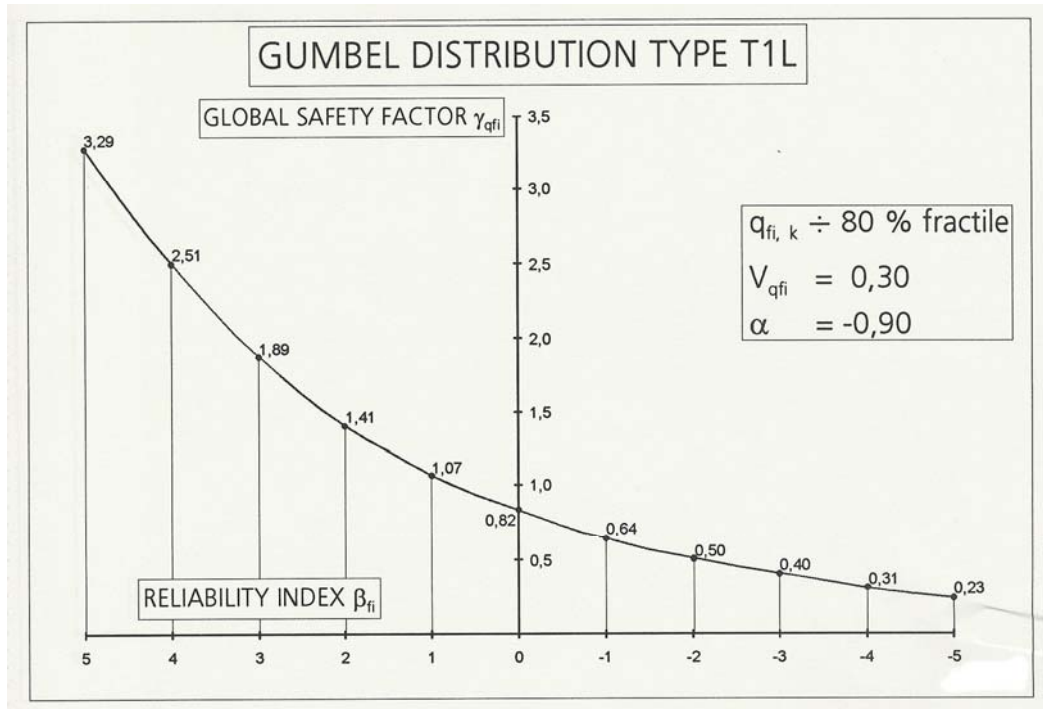


Figure 7. Evolution of γ_{qf} as a function of β_{fi} .

Figure 6 based on equation (32) together with figure 7 based on equation (36) allow to create the connection between the probability $p_{fi,55}$ of getting a fully fire engulfed compartment during the life time of the building - the compartment size, the type of occupancy and active fire safety measures included - and the global factor γ_{qf} affecting the characteristic value $q_{f,k}$ of the fire load.

Knowing the effect of the compartment size, the type of occupancy and the active fire fighting measures on the probability $p_{fi,55}$ of getting a fully fire engulfed compartment according to the research undertaken [6, 7, 10, 17] - see also pages III-12/13 - this global procedure "LEVEL 1" may be summarized by following tables 9 to 12, based on a probability $p_{fi,55}$ of getting, in an office building, a fully fire engulfed compartment of

$$\begin{aligned}
 p_{fi,55} &= (p_{fi,55}^{IGNITION}) \cdot (p_f^{OC} \cdot p_f^{PS}) \\
 &= (10 \cdot 10^{-6} / m^2 \cdot year) \cdot (55 \text{ years}) \cdot (0,40 \cdot 0,10) \\
 &= 2,2 \cdot 10^{-5} \text{ per } m^2 \text{ of compartment floor area.}
 \end{aligned} \tag{30b}$$

As indicated in table 8 an additional positive effect on the probability $p_{fi,55}$ of getting a fully fire engulfed compartment and due to the intervention of the fire brigade might be justified for the professional fire brigade arriving on site before 20 minutes after alarm.

This positive effect is however only to activate in tables 9 to 12 if the professional fire brigade is really fulfilling the requirement of arriving in due time to the fire site.

Table 8. Probability of failure of fire brigade p_f^{FB} in stopping the fire.

p_f^{FB} Type of firemen	Time between alarm and action of the firemen		
	$\leq 10'$	$10' < t \leq 20'$	$20' < t \leq 30'$
Professional	0,05	0,1	0,2
Not-professional	0,1	0,2	1

Tables 9 to 12 allow to determine progressively, for an office building, the parameters defined in equations (32) and (36) in function of the compartment area and the active fire safety measures i.e.

- ° the probability $p_{fi,55}$ of getting a fully fire engulfed compartment during the life time of the building,
- °° the target failure probability in case of fire, $(p_{t,55} / p_{fi,55}) = p_{fi,t}$,
- °°° the corresponding reliability index $\beta_{fi,t}$ equal to β_{fi} and
- °°°° the global factor γ_{qf} .

It has to be noted that the dark areas of these tables correspond to the domain for which the probability $p_{fi,55}$ of getting a fully fire engulfed compartment gets inferior to the general target failure probability of $7,23 \cdot 10^{-5}$, so that fire safety is always guaranteed and a special fire resistance design in general not required.

Chapter III - Calibration of reliability parameters

Pfi,55																	
Af _i [m2]		Sprinkler	Sprinkler	Sprinkler	Detect. by heat	Detect. By smoke	Work Firemen	Off Site Firemen	Off Site Firemen	Off Site Firemen	Off Site Firemen	Off Site Firemen	Off Site Firemen	Sprinkler	Sprinkler	Sprinkler	Sprinkler
		1Wat. Suply	2 Wat. Suply					Detect. by heat	Detect. By smoke	Detect. by heat	Detect. By smoke	Detect. by heat	Detect. By smoke	Off Site Firemen	Off Site Firemen	Off Site Firemen	Off Site Firemen
		0.02	0.02	0.02	0.25	0.0625	0.02	0.1	0.1	0.1	0.1	0.1	0.1	0.02	0.02	0.02	0.02
			0.5	0.25				0.25	0.0625	0.25	0.0625	0.25	0.0625	0.1	0.1	0.1	0.1
														0.25	0.0625	0.25	0.0625
																0.25	0.25
		0.02	0.01	0.005	0.25	0.0625	0.02	0.1	0.025	0.00625	0.00625	0.0015625	0.0005	0.000125	0.000125	0.00003125	
1	2.20E-05																
25	5.50E-04																
50	1.10E-03																
75	1.65E-03																
100	2.20E-03																
125	2.75E-03																
150	3.30E-03																
175	3.85E-03	7.70E-05															
200	4.40E-03	8.80E-05															
225	4.95E-03	9.90E-05															
250	5.50E-03	1.10E-04															
275	6.05E-03	1.21E-04															
300	6.60E-03	1.32E-04															
325	7.15E-03	1.43E-04															
350	7.70E-03	1.54E-04	7.70E-05														
375	8.25E-03	1.65E-04	8.25E-05														
400	8.80E-03	1.76E-04	8.80E-05														
425	9.35E-03	1.87E-04	9.35E-05														
450	9.90E-03	1.98E-04	9.90E-05														
475	1.05E-02	2.09E-04	1.05E-04														
500	1.10E-02	2.20E-04	1.10E-04														
525	1.16E-02	2.31E-04	1.16E-04														
550	1.21E-02	2.42E-04	1.21E-04														
575	1.27E-02	2.53E-04	1.27E-04														
600	1.32E-02	2.64E-04	1.32E-04														
625	1.38E-02	2.75E-04	1.38E-04														
650	1.43E-02	2.86E-04	1.43E-04														
675	1.49E-02	2.97E-04	1.49E-04	7.43E-05													
700	1.54E-02	3.08E-04	1.54E-04	7.70E-05													
725	1.60E-02	3.19E-04	1.60E-04	7.98E-05													
750	1.65E-02	3.30E-04	1.65E-04	8.25E-05													
775	1.71E-02	3.41E-04	1.71E-04	8.53E-05													
800	1.76E-02	3.52E-04	1.76E-04	8.80E-05													
825	1.82E-02	3.63E-04	1.82E-04	9.08E-05													
850	1.87E-02	3.74E-04	1.87E-04	9.35E-05													
875	1.93E-02	3.85E-04	1.93E-04	9.63E-05													
900	1.98E-02	3.96E-04	1.98E-04	9.90E-05													
925	2.04E-02	4.07E-04	2.04E-04	1.02E-04													
950	2.09E-02	4.18E-04	2.09E-04	1.05E-04													
975	2.15E-02	4.29E-04	2.15E-04	1.07E-04													
1000	2.20E-02	4.40E-04	2.20E-04	1.10E-04													
2000	4.40E-02	8.80E-04	4.40E-04	2.20E-04													
3000	6.60E-02	1.32E-03	6.60E-04	3.30E-04													
4000	8.80E-02	1.76E-03	8.80E-04	4.40E-04													
5000	1.10E-01	2.20E-03	1.10E-03	5.50E-04													
6000	1.32E-01	2.64E-03	1.32E-03	6.60E-04													
7000	1.54E-01	3.08E-03	1.54E-03	7.70E-04													
8000	1.76E-01	3.52E-03	1.76E-03	8.80E-04													
9000	1.98E-01	3.96E-03	1.98E-03	9.90E-04													
10000	2.20E-01	4.40E-03	2.20E-03	1.10E-03													

$$p_{fi,55} < 7,23 \cdot 10^{-5}$$

Table 9. Probability $p_{fi,55}$ of getting a fully fire engulfed compartment during the life time of the office building.

Chapter III - Calibration of reliability parameters

Pt/Pfi																	
Probability of failure of the Active measures	Afi [m2]	Sprinkler	Sprinkler 1Wat. Suply	Sprinkler 2 Wat. Suply	Detect. by heat	Detect. By smoke	Work Firemen	Off Site Firemen	Off Site Firemen Detect. by heat	Off Site Firemen Detect. By smoke	Off Site Firemen Detect. by heat Autom. Transm.	Off Site Firemen Detect. By smoke Autom. Transm.	Sprinkler Off Site Firemen Detect. by heat	Sprinkler Off Site Firemen Detect. By smoke	Sprinkler Off Site Firemen Detect. by heat Autom. Transm.	Sprinkler Off Site Firemen Detect. By smoke Autom. Transm.	
		0.02	0.02 0.5	0.02 0.25	0.25	0.0625	0.02	0.1	0.1 0.25	0.1 0.0625	0.1 0.25	0.1 0.0625	0.02 0.1 0.25	0.02 0.1 0.0625	0.02 0.1 0.25	0.02 0.1 0.0625	
→		0.02	0.01	0.005	0.25	0.0625	0.02	0.1	0.025	0.00625	0.00625	0.0015625	0.0005	0.000125	0.000125	0.00003125	
1																	
25	0.131455					0.525818182											
50	0.065727					0.262909091										0.657272727	
75	0.043818					0.175272727	0.701090909									0.438181818	
100	0.032864					0.131454545	0.525818182								0.328636364		
125	0.026291					0.105163636	0.420654545									0.262909091	
150	0.021909					0.087636364	0.350545455								0.219090909	0.876363636	
175	0.018779	0.93896104				0.075116883	0.300467532	0.938961039	0.187792208							0.751168831	
200	0.016432	0.82159091				0.065727273	0.262909091	0.821590909	0.164318182							0.657272727	
225	0.014606	0.73030303				0.058424242	0.23369697	0.73030303	0.146060606							0.584242424	
250	0.013145	0.65727273				0.052581818	0.210327273	0.657272727	0.131454545							0.525818182	
275	0.01195	0.59752066				0.047801653	0.191206612	0.597520661	0.119504132							0.478016529	
300	0.010955	0.54772727				0.043818182	0.175272727	0.547727273	0.109545455							0.438181818	
325	0.010112	0.50559441				0.040447552	0.16179021	0.505594406	0.101118881							0.404475524	
350	0.00939	0.46948052	0.938961039			0.037558442	0.150233766	0.469480519	0.093896104							0.375584416	
375	0.008764	0.43818182	0.876363636			0.035054545	0.140218182	0.438181818	0.087636364							0.350545455	
400	0.008216	0.41079545	0.821590909			0.032863636	0.131454545	0.410795455	0.082159091							0.328636364	
425	0.007733	0.38663102	0.773262032			0.030930481	0.123721925	0.386631016	0.077326203							0.309304813	
450	0.007303	0.36515152	0.73030303			0.029212121	0.116848485	0.365151515	0.073030303							0.292121212	
475	0.006919	0.34593301	0.691866029			0.027674641	0.110698565	0.345933014	0.069186603							0.276746411	
500	0.006573	0.32863636	0.657272727			0.026290909	0.105163636	0.328636364	0.065727273							0.262909091	
525	0.00626	0.31298701	0.625974026			0.025038961	0.100155844	0.312987013	0.062597403							0.25038961	
550	0.005975	0.29876033	0.597520661			0.023900826	0.095603306	0.298760331	0.059752066	0.239008264	0.956033058	0.956033058					
575	0.005715	0.28577075	0.571541502			0.02286166	0.09144664	0.285770751	0.05715415	0.228616601	0.914466403	0.914466403					
600	0.005477	0.27386364	0.547727273			0.021909091	0.087636364	0.273863636	0.054772727	0.219090909	0.876363636	0.876363636					
625	0.005258	0.26290909	0.525818182			0.021032727	0.084130909	0.262909091	0.052581818	0.210327273	0.841309091	0.841309091					
650	0.005056	0.2527972	0.505594406			0.020223776	0.080895105	0.252797203	0.050559441	0.202237762	0.808951049	0.808951049					
675	0.004869	0.24343434	0.486868687	0.973737374			0.019474747	0.07789899	0.243434343	0.048686869	0.194747475	0.778989899					
700	0.004695	0.23474026	0.469480519	0.938961039			0.018779221	0.075116883	0.23474026	0.046948052	0.187792208	0.751168831					
725	0.004533	0.22664577	0.453291536	0.906583072			0.018131661	0.072526646	0.226645768	0.045329154	0.181316614	0.725266458					
750	0.004382	0.21909091	0.438181818	0.876363636			0.017527273	0.070109091	0.219090909	0.043818182	0.175272727	0.701090909					
775	0.00424	0.21202346	0.424046921	0.848093842			0.016961877	0.067847507	0.21202346	0.042404692	0.169618768	0.678475073					
800	0.004108	0.20539773	0.410795455	0.821590909			0.016431818	0.065727273	0.205397727	0.041079545	0.164318182	0.657272727					
825	0.003983	0.19917355	0.398347107	0.796694215			0.015933884	0.063735537	0.199173554	0.039834711	0.159338843	0.637355372					
850	0.003866	0.19331551	0.386631016	0.773262032			0.015465241	0.061860963	0.193315508	0.038663102	0.154652406	0.618609626					
875	0.003756	0.18779221	0.375584416	0.751168831			0.015023377	0.060093506	0.187792208	0.037558442	0.150233766	0.600935065					
900	0.003652	0.18257576	0.365151515	0.73030303			0.014606061	0.058424242	0.182575758	0.036515152	0.146060606	0.584242424					
925	0.003553	0.17764128	0.355282555	0.710565111			0.014211302	0.056845209	0.177641278	0.035528256	0.142113022	0.568452088					
950	0.003459	0.17296651	0.345933014	0.691866029			0.013837321	0.055349822	0.172966507	0.034593301	0.138373206	0.553492823					
975	0.003371	0.16853147	0.337062937	0.674125874			0.013482517	0.05393007	0.168531469	0.033706294	0.134825175	0.539300699					
1000	0.003286	0.16431818	0.328636364	0.657272727			0.013145455	0.052581818	0.164318182	0.032863636	0.131454545	0.525818182					
2000	0.001643	0.08215909	0.164318182	0.328636364			0.006572727	0.026290909	0.082159091	0.016431818	0.065727273	0.262909091					
3000	0.001095	0.05477273	0.109545455	0.219090909			0.004381818	0.017527273	0.054772727	0.010954545	0.043818182	0.175272727					
4000	0.000822	0.04107955	0.082159091	0.164318182			0.003286364	0.013145455	0.041079545	0.008215909	0.032863636	0.131454545					
5000	0.000657	0.03286364	0.065727273	0.131454545			0.002629091	0.010516364	0.032863636	0.006572727	0.026290909	0.105163636					
6000	0.000548	0.02738636	0.054772727	0.109545455			0.002190909	0.008763636	0.027386364	0.005477273	0.021909091	0.087636364					
7000	0.000469	0.02347403	0.046948052	0.093896104			0.001877922	0.007511688	0.023474026	0.004694805	0.018779221	0.075116883	0.075116883	0.300467532	0.938961039		
8000	0.000411	0.02053977	0.041079545	0.082159091			0.001643182	0.006572727	0.020539773	0.004107955	0.016431818	0.065727273					
9000	0.000365	0.01825758	0.036515152	0.073030303			0.001460606	0.005842424	0.018257576	0.003651515	0.014606061	0.058424242					
10000	0.000329	0.01643182	0.032863636	0.065727273			0.001314545	0.005258182	0.016431818	0.003286364	0.013145455	0.052581818					

>

1

> 1

Table 10. The target failure probability in case of fire, $(p_{t,55} / p_{fi,55}) = p_{fi,t}$, for an office building.

Chapter III - Calibration of reliability parameters

BETA fi

Aft [m2]																															
	Sprinkler	Sprinkler 1Wat. Suply	Sprinkler 2 Wat. Suply	Detect. by heat	Detect. By smoke	Work Firemen	Off Site Firemen	Off Site Firemen Detect. by heat	Off Site Firemen Detect. By smoke	Off Site Firemen Detect. by heat Autom. Transm.	Off Site Firemen Detect. By smoke Autom. Transm.	Sprinkler Off Site Firemen Detect. by heat	Sprinkler Off Site Firemen Detect. By smoke	Sprinkler Off Site Firemen Detect. by heat Autom. Transm.	Sprinkler Off Site Firemen Detect. By smoke Autom. Transm.																
Probability of failure of the Active measures	0.02	0.02 0.5	0.02 0.25	0.25	0.0625	0.02	0.1	0.1 0.25	0.1 0.0625	0.1 0.25	0.1 0.0625	0.02 0.1 0.25	0.02 0.1 0.0625	0.02 0.1 0.25	0.02 0.1 0.0625																
→	0.02	0.01	0.005	0.25	0.0625	0.02	0.1	0.025	0.00625	0.00625	0.0015625	0.0005	0.000125	0.000125	0.00003125																
1	<div>< - 9</div>																														
25																	1.119541748			-0.064761826											
50																	1.508390764			0.634402495			-0.405031243								
75																	1.70799886			0.93353181	-0.52754067		0.155580576								
100																	1.840279096			1.119541748	-0.064761826		0.443681701								
125																	1.938339485			1.252666032	0.200219278		0.634402495								
150																	2.015825923			1.355454715	0.38384827		0.775267147	-1.156999102							
175																	2.079641347	-1.5461103		1.438706256	0.523056314	-1.54611034	0.886061449	-0.678172483							
200																	2.133745292	-0.9214449		1.508390764	0.634402495	-0.921444927	0.976864248	-0.405031243							
225																	2.180612076	-0.6137297		1.568139907	0.72672581	-0.61372973	1.053479659	-0.212758735							
250																	2.221887504	-0.4050312		1.62031962	0.805286196	-0.405031243	1.119541748	-0.064761826							
275																	2.258719697	-0.2469348		1.666553077	0.873458488	-0.246934808	1.177469249	0.055132307							
300																	2.291940256	-0.1199213		1.70799886	0.93353181	-0.119921346	1.228949051	0.155580576							
325																	2.322170138	-0.0140236		1.745515913	0.987126925	-0.014023555	1.275201976	0.241779468							
350																	2.349884827	0.07657577	-1.54611034	1.779750003	1.035431305	0.076575765	1.317138489	0.317098542							
375																	2.375456194	0.15558058	-1.1569991	1.811205217	1.079339605	0.155580576	1.355454715	0.38384827							
400																	2.399180376	0.22549925	-0.92144493	1.840279096	1.119541748	0.22549925	1.390694185	0.443681701							
425																	2.421296893	0.28811066	-0.74963272	1.867290993	1.15658036	0.288110661	1.423288959	0.497821833							
450																	2.442002126	0.34472246	-0.61372973	1.892501136	1.190889493	0.344722461	1.453587855	0.547198416							
475																	2.461459017	0.39632399	-0.50114661	1.91612425	1.222821484	0.396323994	1.481876324	0.592534354							
500	2.479804201	0.4436817	-0.40503124	1.938339485	1.252666032	0.443681701	1.508390764	0.634402495																							
525	2.497153345	0.48740122	-0.32120908	1.959297793	1.280664061	0.487401224	1.533329031	0.673264205																							
550	2.513605194	0.52796928	-0.24693481	1.979127501	1.307017961	0.527969275	1.556858298	0.709496329	-1.706398637	-1.706398637																					
575	2.529244702	0.56578271	-0.18030008	1.997938573	1.331899301	0.565782709	1.579121023	0.74341048	-1.368782753	-1.368782753																					
600	2.544145464	0.60116924	-0.11992135	2.015825923	1.355454715	0.601169236	1.600239536	0.775267147	-1.156999102	-1.156999102																					
625	2.55837164	0.63440249	-0.06476183	2.03287202	1.377810452	0.634402495	1.62031962	0.805286196	-0.999852658	-0.999852658																					
650	2.571979493	0.66571325	-0.01402355	2.049148947	1.399075947	0.665713246	1.639453338	0.83365482	-0.874037371	-0.874037371																					
675	2.585018625	0.69529781	0.032921267	2.064720065	1.419346644	0.695297809	1.657721276	0.860533638	-0.768786268	-0.768786268																					
700	2.597532976	0.72332454	0.076575765	2.079641347	1.438706256	0.72332454	1.675194359	0.886061449	-0.678172483	-0.678172483																					
725	2.609561656	0.74993885	0.117349536	2.093962478	1.457228589	0.749938848	1.691935317	0.910358969	-0.598558879	-0.598558879																					
750	2.621139617	0.77526715	0.155580576	2.107727751	1.474979028	0.775267147	1.70799886	0.93353181	-0.52754067	-0.52754067																					
775	2.632298218	0.79941999	0.19155111	2.120976814	1.492015757	0.799419994	1.7234378	0.955672863	-0.463438827	-0.463438827																					
800	2.643065702	0.82249461	0.22549925	2.133745292	1.508390764	0.822494607	1.738293615	0.976864248	-0.405031243	-0.405031243																					
825	2.653467588	0.84457691	0.257627745	2.146065308	1.524150683	0.844576906	1.752607392	0.997178889	-0.351398702	-0.351398702																					
850	2.663527013	0.86574318	0.288110661	2.157965924	1.539337494	0.865743178	1.766415281	1.016681829	-0.301831196	-0.301831196																					
875	2.67326501	0.88606145	0.317098542	2.169473512	1.553989115	0.886061449	1.779750003	1.035431305	-0.255768148	-0.255768148																					
900	2.682700763	0.90559262	0.344722461	2.180612076	1.568139907	0.905592622	1.792641269	1.053479659	-0.212758735	-0.212758735																					
925	2.691851808	0.92439143	0.371097235	2.191403523	1.581821096	0.92439143	1.805116133	1.070874097	-0.172434663	-0.172434663																					
950	2.700734218	0.94250722	0.396323994	2.201867899	1.595061139	0.942507224	1.817199295	1.08765733	-0.134490966	-0.134490966																					
975	2.709362763	0.95989466	0.420492271	2.212023591	1.60788604	0.959894657	1.828913367	1.10386812	-0.098672126	-0.098672126																					
1000	2.717751043	0.97686425	0.443681701	2.221887504	1.62031962	0.976864248	1.840279096	1.119541748	-0.064761826	-0.064761826																					
2000	2.939599489	1.39069418	0.976864248	0.443681701	2.479804201	1.938339485	1.390694185	2.133745292	1.508390764	0.634402495	0.634402495																				
3000	3.063053469	1.60023954	1.228949051	0.775267147	2.621139617	2.107727751	1.600239536	2.291940256	1.70799886	0.93353181	-0.52754067																				
4000	3.148130741	1.73829361	1.390694185	0.976864248	2.717751043	2.221887504	1.738293615	2.399180376	1.840279096	1.119541748	1.119541748	-0.064761826																			
5000	3.212785237	1.8402791	1.508390764	1.119541748	2.790776186	2.30739648	1.840279096	2.479804201	1.938339485	1.252666032	1.252666032	0.200219278																			
6000	3.264789498	1.92067473	1.600239536	1.228949051	2.849280847	2.375456194	1.920674731	2.544145464	2.015825923	1.355454715	1.355454715	0.38384827																			
7000	3.308204839	1.98676854	1.675194359	1.317138489	2.897971752	2.431815046	1.986768544	2.597532976	2.079641347	1.438706256	1.438706256	0.523056314	-1.54611034																		
8000	3.345416508	2.04272624	1.738293615	1.390694185	2.939599849	2.479804201	2.042726243	2.643065702	2.133745292	1.508390764	1.508390764	0.634402495	-0.921444927																		
9000	3.377942675	2.09114407	1.792641269	1.453587855	2.975909334	2.52152165	2.091144067	2.682700763	2.180612076	1.568139907	1.568139907	0.72672581	-0.61372973																		
10000	3.406808302	2.13374529	1.840279096	1.508390764	3.008074024	2.55837164	2.133745292	2.717751043	2.221887504	1.62031962	1.62031962	0.805286196	-0.405031243																		

Table 11. The evolution of the corresponding reliability index $\beta_{fi,t}$ equal to β_{fi} , for an office building.

Chapter III - Calibration of reliability parameters

GAMMA_{qf}

Alt [m2]	Sprinkler	Sprinkler 1Wat. Suply	Sprinkler 2 Wat. Suply	Detect. by heat	Detect. By smoke	Work Firemen	Off Site Firemen	Off Site Firemen Detect. by heat	Off Site Firemen Detect. By smoke	Off Site Firemen Detect. by heat Autom. Transm.	Off Site Firemen Detect. By smoke Autom. Transm.	Sprinkler Off Site Firemen Detect. by heat	Sprinkler Off Site Firemen Detect. By smoke	Sprinkler Off Site Firemen Detect. by heat Autom. Transm.	Sprinkler Off Site Firemen Detect. By smoke Autom. Transm.
0.02	0.02	0.02	0.02	0.25	0.0625	0.02	0.1	0.1	0.1	0.1	0.1	0.02	0.02	0.02	0.02
0.02	0.02	0.5	0.25					0.25	0.0625	0.25	0.0625	0.1	0.1	0.1	0.1
0.02	0.01	0.005		0.25	0.0625	0.02	0.1	0.025	0.00625	0.00625	0.0015625	0.0005	0.000125	0.000125	0.00003125
1															
25	1.104256				0.807637229										
50	1.230404				0.968473484					0.741444557					
75	1.301853				1.049543124	0.719247597				0.8544327					
100	1.35187				1.104255858	0.807637229				0.920877462					
125	1.390368				1.145588573	0.864323048				0.968473484					
150	1.421664				1.17880289	0.906556454				1.005632019	0.616866515				
175	1.448028	0.56188228			1.206562408	0.94031919	0.561882276			1.036124472	0.693039921				
200	1.470801	0.65305874			1.23040373	0.968473484	0.653058742			1.06198206	0.741444557				
225	1.490845	0.70410997			1.251294216	0.99262791	0.704109971			1.084427704	0.777968935				
250	1.508742	0.74144456			1.269882399	1.013781292	0.741444557			1.104255858	0.807637229				
275	1.524908	0.77133453			1.286624261	1.032598041	0.771334527			1.122012144	0.832690823				
300	1.539647	0.79642618			1.301852599	1.049543124	0.796426181			1.138087597	0.8544327				
325	1.553191	0.81812339			1.315817731	1.064954923	0.818123391			1.152772088	0.873660975				
350	1.565719	0.83727353	0.561882276		1.328712666	1.079087491	0.837273526			1.166286469	0.8909099				
375	1.577372	0.8544327	0.616866515		1.340689351	1.092136493	0.8544327			1.17880289	0.906556454				
400	1.588265	0.86998802	0.653058742		1.351869549	1.104255858	0.869988021			1.190458136	0.920877462				
425	1.59849	0.88422102	0.681004845		1.36235233	1.115568876	0.884221017			1.201362698	0.934082659				
450	1.608125	0.89734349	0.704109971		1.37221938	1.126175835	0.897343494			1.211607103	0.946335013				
475	1.617233	0.90951918	0.723961217		1.381538842	1.136159413	0.909519179			1.221266451	0.957763823				
500	1.62587	0.92087746	0.741444557		1.39036815	1.145588573	0.920877462			1.23040373	0.968473484				
525	1.634082	0.93152251	0.757112094		1.398756162	1.154521442	0.93152251			1.239072289	0.97854956				
550	1.641908	0.9415395	0.771334527		1.406744785	1.163007468	0.941539501			1.247317706	0.988063086	0.540789918	0.540789918		
575	1.649383	0.9509903	0.78437457		1.414370232	1.171089066	0.950990303			1.255179228	0.99707371	0.586244159	0.586244159		
600	1.656537	0.95996031	0.796426181		1.42166401	1.17880289	0.959960309			1.26269089	1.005632019	0.616866515	0.616866515		
625	1.663397	0.96847348	0.807637229		1.428653701	1.186180833	0.968473484			1.269882399	1.013781292	0.640748896	0.640748896		
650	1.669985	0.97658144	0.818123391		1.435363587	1.193250816	0.976581441			1.276779839	1.021558857	0.660634055	0.660634055		
675	1.676323	0.98432114	0.827977096	0.51165626	1.441815155	1.200037423	0.984321139			1.283406233	1.028997136	0.677821087	0.677821087		
700	1.682429	0.99172467	0.837273526	0.561882276	1.448027512	1.206562408	0.991724669			1.289782007	1.036124472	0.693039921	0.693039921		
725	1.688319	0.99882008	0.846074754	0.593145276	1.454017722	1.21284512	0.998820077			1.295925365	1.042965789	0.706746602	0.706746602		
750	1.694007	1.00563202	0.8544327	0.616866515	1.459801089	1.218902837	1.005632019			1.301852599	1.049543124	0.719247597	0.719247597		
775	1.699508	1.01218229	0.862391284	0.636349908	1.465391388	1.224751056	1.012182292			1.307578351	1.055876056	0.730760129	0.730760129		
800	1.704833	1.01849026	0.869988021	0.653058742	1.470801066	1.23040373	1.018490262			1.313115822	1.06198206	0.741444557	0.741444557		
825	1.709993	1.02457321	0.87725524	0.66778343	1.476041403	1.235873463	1.024573212			1.318476962	1.067876799	0.751423121	0.751423121		
850	1.714997	1.03044664	0.884221017	0.681004845	1.481122656	1.241171682	1.030446635			1.323672617	1.073574367	0.760791455	0.760791455		
875	1.719856	1.03612447	0.8909099	0.693039921	1.486054178	1.246308774	1.036124472			1.328712666	1.079087491	0.769625994	0.769625994		
900	1.724577	1.04161931	0.897343494	0.704109971	1.490844523	1.251294216	1.041619311			1.333606128	1.084427704	0.777968935	0.777968935		
925	1.729168	1.04694256	0.903540918	0.714376441	1.495501531	1.256136671	1.046942564			1.338361263	1.089605491	0.78593167	0.78593167		
950	1.733635	1.0521046	0.909519179	0.723961217	1.500032409	1.260844083	1.052104603			1.342985651	1.094630408	0.793497222	0.793497222		
975	1.737986	1.05711489	0.915293478	0.732958891	1.504443795	1.26542375	1.057114886			1.347486269	1.099511194	0.800722022	0.800722022		
1000	1.742226	1.06198206	0.920877462	0.741444557	1.508741815	1.269882399	1.06198206			1.351869549	1.104255858	0.807637229	0.807637229		
2000	1.858078	1.19045814	1.06198206	0.920877462	1.625870223	1.39036815	1.190458136			1.470801066	1.23040373	0.968473484	0.968473484		
3000	1.925681	1.26269089	1.138087597	1.005632019	1.694007253	1.459801089	1.26269089			1.539647096	1.301852599	1.049543124	1.049543124	0.719247597	
4000	1.973586	1.31311582	1.190458136	1.06198206	1.742225954	1.508741815	1.313115822			1.588265038	1.351869549	1.104255858	1.104255858	0.807637229	
5000	2.010715	1.35186955	1.23040373	1.104255858	1.779567727	1.546556355	1.351869549			1.625870223	1.39036815	1.145588573	1.145588573	0.864323048	
6000	2.041035	1.38334224	1.26269089	1.138087597	1.810044343	1.577372341	1.383342241			1.656537059	1.42166401	1.17880289	1.17880289	0.906556454	
7000	2.066659	1.40983668	1.289782007	1.166286469	1.835790532	1.603377085	1.409836684			1.682428888	1.448027512	1.206562408	1.206562408	0.94031919	0.561882276
8000	2.088847	1.43271178	1.313115822	1.190458136	1.858078299	1.625870223	1.432711777			1.704832824	1.470801066	1.23040373	1.23040373	0.968473484	0.653058742
9000	2.108413	1.45283669	1.333606128	1.211607103	1.877727014	1.645687171	1.452836694			1.72457705	1.490844523	1.251294216	1.251294216	0.99262791	0.704109971
10000	2.125911	1.47080107	1.351869549	1.23040373	1.895295543	1.663968816	1.470801066			1.742225954	1.508741815	1.269882399	1.269882399	1.013781292	0.741444557

< 0,019

Table 12. The global factor γ_{qf} leading to $q_{f,d} = \gamma_{qf} \cdot q_{f,k}$, for an office building.

3.2 Calibration of partial and differentiation factors related to the risk of fire activation and to the active fire safety measures.

This concerns the performance based procedure "LEVEL 2", where the design fire load is calculated by multiplying the characteristic fire load by the partial factors δ_{q1} , δ_{q2} and the differentiation factors δ_n based on the target failure probability of $7,23 \cdot 10^{-5}$ for the building life.

3.2.1 Danger of fire activation related to the size of the compartment.

The establishment of δ_{q1} , partial factor taking into account the fire activation risk due to the size of the compartment, is based on equation (30b) which gives **for an office building** the probability $p_{fi,55}$ of getting a fully fire engulfed compartment for the life time of 55 years and per m² of compartment

$$p_{fi,55} = 2,2 \cdot 10^{-5} \text{ per m}^2 \text{ of compartment floor area} \quad (30b)$$

According to equation (31) and for a compartment area of $A_{fi} = 25\text{m}^2$ we obtain

$$p_{ffi} \leq (p_{t,55} / p_{fi,55}) = (7,23 \cdot 10^{-5}) / (25 \cdot 2,2 \cdot 10^{-5}) = 0,131$$

Hence equation (32) gives $\beta_{fi} = 1,12$ and equation (36) leads to

$$\gamma_{qf} \equiv \delta_{q1} = 1,1$$

This whole procedure is used in table 13; for more refined results see the second column of table 12.

Table 13. Partial factor δ_{q1} taking into account the fire activation risk due to the size of the compartment.

$A_{fi} [\text{m}^2]$	$p_{fi,55}$	$p_{t,55} / p_{fi,55}$	β_{fi}	δ_{q1}
25	$5,5 \cdot 10^{-4}$	0,13145	1,12	1,10
100	$2,2 \cdot 10^{-3}$	0,03286	1,84	1,35
250	$5,5 \cdot 10^{-3}$	0,01315	2,22	1,51
1000	$2,2 \cdot 10^{-2}$	0,00328	2,72	1,74
2500	$5,5 \cdot 10^{-2}$	0,00131	3,01	1,90
5000	$11 \cdot 10^{-2}$	0,00066	3,21	2,01
7000	$15,4 \cdot 10^{-2}$	0,00047	3,31	2,07
10000	$22 \cdot 10^{-2}$	0,00033	3,41	2,13

3.2.2 Danger of fire activation related to the occupancy.

The previous calculation has been based on a probability $p_{fi,55}$ of getting a fully fire engulfed compartment for the life time of 55 years and per m² of compartment of **$2,2 \cdot 10^{-5}$** , corresponding to an office building. It is obvious that the risk is much higher for a fireworks industry and lower for an art gallery. In this way, buildings may be classified according to their inherent danger of fire activation. For instance, according to the experts composing the Advisory Committee in [7, 10, 17], the category 2 comprising hotels, schools or office buildings should present a danger of fire activation 10 times higher than the category 1

comprising museums, art galleries etc. and 10 times lower than the category 3 for machine works etc. This is illustrated in table 14.

Table 14. Probability $p_{fi,55}$ of getting a fully fire engulfed compartment depending on the occupancy.

Type of building Occupancy	Danger of fire activation	$p_{fi,55}$ in [$10^{-5}/m^2$]	$\frac{(p_{fi,55})^{CATi}}{(p_{fi,55})^{CAT2}}$
Museum, Art gallery CAT 1	Low	0,22	10^{-1}
Hotel, School, Office CAT 2	Normal	2,2	1
Machine Works CAT 3	High	22	10
Paint Workshop Chemistry Laboratory CAT 4	Very High	220	100
Paint Factory Fireworks Industry CAT 5	Ultra-High	2200	1000

We may calculate the γ_{qf} factor for the five building categories, given in table 14, and characterised by different dangers of fire activation or in other words by a different probability of getting a severe fire $p_{fi,55}$. It follows from the knowledge of $p_{fi,55}$ that by using again equations (32) and (36) the global factor γ_{qf} may be calculated for the different building occupancies and in function of the compartment area A_{fi} . This is shown in figure 8.

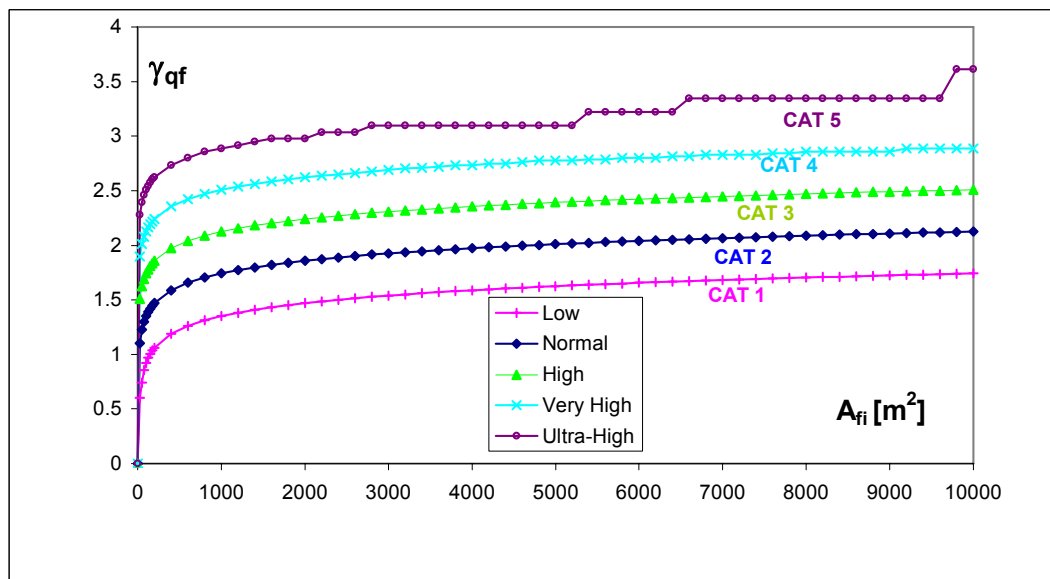


Figure 8. Global factor γ_{qf} for the different building categories 1 to 5 and as a function of the compartment area A_{fi} .

For each building category, it is possible to deduce an additional partial factor δ_{q2} , which is the ratio between the γ_{qf} of that building category given in figure 8 and the partial factor δ_{q1} given in table 13 such as

$$[\gamma_{qf}]^{\text{Figure 8}} = [\delta_{q1}]^{\text{Table 13}} \cdot [\delta_{q2}]^{\text{Figure 9}} \quad (37)$$

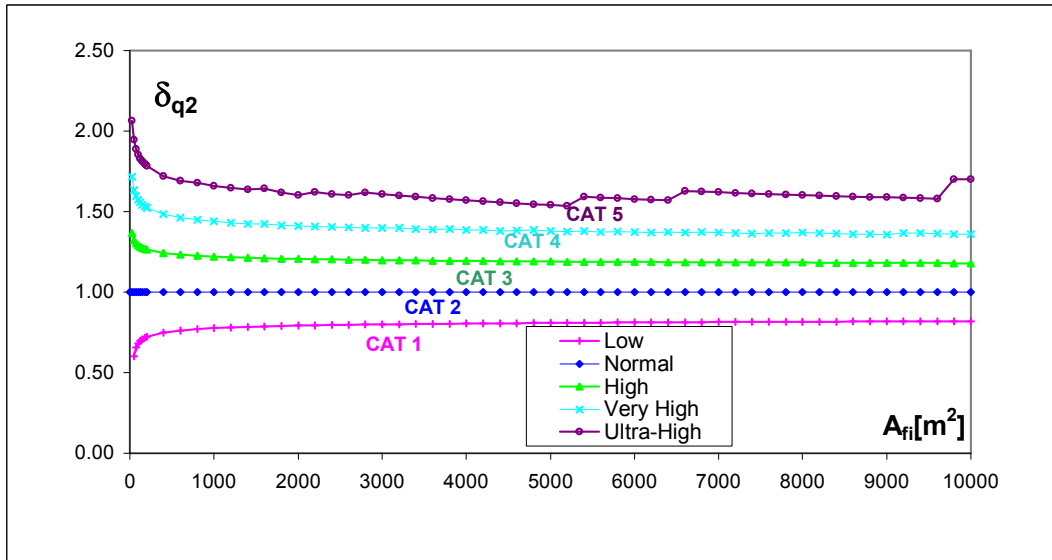


Figure 9. Partial factor δ_{q2} taking into account the fire activation risk due to the different building categories 1 to 5, as a function of the compartment area A_{fi} .

Figure 9 illustrates that the dependence of δ_{q2} in face of the different building categories is much more pronounced than its dependence in face of the compartment area A_{fi} . In fact as that last dependence is rather constant for a large part of the compartment area variation - see also table 15 - it is suggested also for practical reasons to consider δ_{q2} values for the fixed compartment area A_{fi} of 1000m². Of course the real area A_{fi} may always be considered, but this should then be done together for all differentiation factors δ_{ni} .

Table 15. Partial factor δ_{q2} for some compartment areas.

Partial factor δ_{q2}		Compartment area A_{fi} [m ²]			
Type of building					
Occupancy		100	200	1.000	10.000
Museum, Art gallery	CAT 1	0,68	0,72	0,78	0,82
Hotel, School, Office	CAT 2	1	1	1	1
Machine Works	CAT 3	1,29	1,26	1,22	1,18
Paint Workshop	CAT 4	1,57	1,52	1,44	1,36
Chemical Laboratory					
Paint Factory	CAT 5	1,85	1,78	1,66	1,70
Fireworks Industry					

3.2.3 Influence of active fire safety measures.

The influence of active fire fighting measures may be quantified in the same way. Each active measure reduces the probability that a starting fire is developing and turns to flash-over or a fully engulfed compartment. Therefore, the probability of getting a severe fire in case of active measures is equal to the probability $p_{fi,55}$ without active measure multiplied by the product of the different failure probabilities of active fire safety measures in extinguishing the fire as given hereafter

$$p_{fi,55} = [(p_{fi,55}^{\text{IGNITION}}) \cdot (p_f^{OC} \cdot p_f^{PS})] \cdot [\prod p_f^{\text{ACTIVE-MEASURE}}] \quad (30c)$$

According to the experts composing the Advisory Committee in [7, 10, 17], the failure probabilities of active fire safety measures in extinguishing the fire should be considered as given in table 16.

Table 16. Failure probabilities of active fire safety measures in extinguishing the fire.

Active fire safety measure	Failure probability of active fire safety measure in extinguishing the fire
Automatic water extinguishing system	0,02
Automatic water extinguishing system, with 1 independent water supply	0,01
Automatic water extinguishing system, with 2 independent water supplies	0,005
Automatic fire detection and alarm by heat	0,25
Automatic fire detection and alarm by smoke	0.0625
Automatic alarm transmission to fire brigade	0,25
Manual fire suppression by work fire brigade	0,02
Manual fire suppression by off site fire brigade	0,1 (*)

The positive effect of manual fire suppression through off site fire brigade is however only to activate in table 16 (*) if the professional fire brigade is really fulfilling the requirement of arriving in due time to the fire site according to table 8.

The differentiation factors δ_{ni} , related to the various active fire safety measures, may be established through the following relation:

Chapter III - Calibration of reliability parameters

$$[\delta_{ni}]^{\text{ACTIVE MEASURE}} = [\gamma_{qf}]^{\text{ACTIVE MEASURE}} / [\gamma_{qf}]^{\text{NO ACTIVE MEASURE}} \quad (38)$$

This is illustrated in the following example for a compartment area A_{fi} of 1000m² of an office building without and with a sprinkler system.

$$\begin{aligned} p_{fi,55} &= 2,2 \cdot 10^{-5} \text{ per m}^2 \text{ of compartment floor area, according to equation (30b)} \\ &= 2,2 \cdot 10^{-5} \cdot 1000 = 2,2 \cdot 10^{-2} \\ \beta_{fi} &= \Phi^{-1}(7,23 \cdot 10^{-5} / 2,2 \cdot 10^{-2}) = \Phi^{-1}(3,29 \cdot 10^{-3}) = 2,718, \text{ according to equation (32)} \\ [\gamma_{qf}]^{\text{NO ACTIVE MEASURE}} &= 0,863605 \{1 - 0,233909(0,577216 + \ln[-\ln\Phi(0,9 \cdot 2,718)])\} \\ &= 1,74, \text{ according to equation (36).} \end{aligned}$$

When a sprinkler system is considered with, according to table 16,

$$\begin{aligned} p_f^{SP} &= 0,02 \\ p_{fi,55} &= 2,2 \cdot 10^{-2} \cdot 0,02 = 4,4 \cdot 10^{-4} \\ \beta_{fi} &= \Phi^{-1}(7,23 \cdot 10^{-5} / 4,4 \cdot 10^{-4}) = \Phi^{-1}(1,643 \cdot 10^{-1}) = 0,977 \\ [\gamma_{qf}]^{\text{WITH SPRINKLER}} &= 0,863605 \{1 - 0,233909(0,577216 + \ln[-\ln\Phi(0,9 \cdot 0,977)])\}, \\ &= 1,062. \end{aligned}$$

The differentiation factor δ_{ni} for sprinklers follows as

$$\begin{aligned} [\delta_{ni}]^{\text{SPRINKLER}} &= [\gamma_{qf}]^{\text{WITH SPRINKLERS}} / [\gamma_{qf}]^{\text{NO ACTIVE MEASURE}} \\ &= 1,062 / 1,74 \\ &= 0,61. \end{aligned}$$

It is through the previous procedure that the differentiation factors δ_{ni} have been established for all active fire safety measures given in table 16 and for compartment areas varying up to 10000 m². This has been compiled in table 17.

According to table 17 the variation of the differentiation factors δ_{ni} is only significant for compartment areas smaller than 200 m². For larger areas these differentiation factors only slightly increase with enlarging compartment areas - see also table 18.

Therefore it is again suggested, also for practical reasons, to consider δ_{ni} values for the fixed compartment area A_{fi} of 1000m². Of course the real area A_{fi} may always be considered, but this should then be done together for all differentiation factors δ_{ni} and for the partial factor δ_{q2} .

It is obvious that, in all cases, the real area A_{fi} shall be considered when calculating the partial factor δ_{q1} following table 13.

Chapter III - Calibration of reliability parameters

DELTA n																
Probability of failure of the Active measures	Afi [m2]															
		Sprinkler	Sprinkler 1Wat. Suply	Sprinkler 2 Wat. Suply	Detect. by heat	Detect. By smoke	Work Firemen	Off Site Firemen	Off Site Firemen Detect. by heat	Off Site Firemen Detect. By smoke	Off Site Firemen Detect. by heat Autom. Transm.	Off Site Firemen Detect. By smoke Autom. Transm.	Sprinkler Off Site Firemen Detect. by heat	Sprinkler Off Site Firemen Detect. By smoke	Sprinkler Off Site Firemen Detect. by heat Autom. Transm.	Sprinkler Off Site Firemen Detect. By smoke Autom. Transm.
→		0.02	0.02	0.02	0.25	0.0625	0.02	0.1	0.1	0.1	0.1	0.1	0.1	0.02	0.02	0.02
			0.5	0.25					0.25	0.0625	0.25	0.25	0.02	0.1	0.1	0.1
													0.25	0.0625	0.25	0.0625
															0.25	0.25
		0.02	0.01	0.005	0.25	0.0625	0.02	0.1	0.025	0.00625	0.00625	0.0015625	0.0005	0.000125	0.000125	0.00003125
	1															
	25					0.731385959										
	50					0.787118456				0.602602657						
	75					0.806191979				0.656320616						
	100					0.816836106				0.597422459						
	125					0.823946213				0.621650494						
	150					0.829171226				0.637672789						
	175	0.3880329				0.8332455	0.649379368	0.388032874	0.715541979	0.478609637						
	200	0.4440157				0.836553466	0.658466673	0.444015685	0.722043303	0.504109342						
	225	0.4722893				0.839319055	0.665815848	0.472289337	0.727391547	0.521844446						
	250	0.4914324				0.841683041	0.671938221	0.491432364	0.731905119	0.535305127						
	275	0.5058238				0.843739141	0.677154481	0.505823768	0.735790232	0.546059842						
	300	0.5172784				0.845552596	0.681677721	0.517278396	0.739187311	0.554953601						
	325	0.5267371				0.847170478	0.685656037	0.526737076	0.742195866	0.562494157						
	350	0.5347534	0.35886532			0.848627766	0.689196115	0.534753359	0.744888723	0.569010063						
	375	0.541681	0.39107223			0.849951097	0.692377104	0.541681046	0.747320629	0.57472572						
	400	0.54776	0.41117743			0.851161183	0.695259186	0.547759977	0.749533678	0.579800877						
	425	0.5531601	0.42603003			0.85227442	0.697889082	0.553160102	0.751560866	0.584353063						
	450	0.5580061	0.43784533			0.85330399	0.700303718	0.5580061	0.75342849	0.588471096						
	475	0.562392	0.44765413			0.854260635	0.702532735	0.562392028	0.755157815	0.592223618						
	500	0.5663905	0.45602936			0.855153216	0.704600254	0.566390508	0.756766262	0.595664691						
	525	0.5700587	0.46332573			0.85598912	0.706526141	0.57005871	0.758268258	0.598837596						
	550	0.5734424	0.46977946			0.856774566	0.708326932	0.573442393	0.759675882	0.601777473			0.329366813	0.329366813		
	575	0.5765787	0.47555641			0.85751483	0.710016528	0.576578718	0.760999333	0.604513213			0.355432438	0.355432438		
	600	0.5794982	0.48077776			0.858214431	0.711606712	0.579498239	0.762247294	0.607068832			0.372383166	0.372383166		
	625	0.5822264	0.48553491			0.858877261	0.713107553	0.582226367	0.763427216	0.60946449			0.385205076	0.385205076		
	650	0.5847844	0.48989854			0.859506696	0.714527717	0.584784437	0.764545534	0.611717258			0.395592725	0.395592725		
	675	0.5871905	0.49392448	0.30522529		0.860105681	0.715874709	0.587190529	0.765607843	0.613841711			0.404349868	0.404349868		
	700	0.5894601	0.4976576	0.33397089		0.8606768	0.717155071	0.589460081	0.766619033	0.615850381			0.411928211	0.411928211		
	725	0.5916064	0.50113452	0.35132306		0.861222332	0.718374534	0.591606377	0.767583399	0.617754114			0.418609724	0.418609724		
	750	0.5936409	0.5043855	0.36414632		0.861744296	0.719538145	0.593640917	0.768504737	0.619562355			0.42458354	0.42458354		
	775	0.5955737	0.50743585	0.37443184		0.862244488	0.720650371	0.595573721	0.769386414	0.621283376			0.429983347	0.429983347		
	800	0.5974136	0.51030694	0.38306321		0.862724512	0.721715181	0.597413569	0.770231429	0.622924456			0.434907486	0.434907486		
	825	0.5991682	0.51301696	0.3905183		0.863185807	0.722736117	0.599168189	0.771042464	0.624492033			0.439430609	0.439430609		
	850	0.6008444	0.51558154	0.39708797		0.863629667	0.723716353	0.600844421	0.771821927	0.625991824			0.443610844	0.443610844		
	875	0.6024483	0.5180142	0.40296389		0.864057263	0.72465874	0.602448342	0.772571987	0.627428931			0.447494405	0.447494405		
	900	0.6039854	0.52032671	0.4082798		0.864469653	0.72565852	0.603985372	0.773294604	0.628807918			0.451118687	0.451118687		
	925	0.6054604	0.52252935	0.4131331		0.864867798	0.726440016	0.605460369	0.773991556	0.630132889			0.454514407	0.454514407		
	950	0.6068777	0.52463121	0.41759718		0.865252574	0.727283345	0.606877698	0.774664457	0.631407543			0.45770712	0.45770712		
	975	0.6082413	0.52664029	0.42172887		0.865624783	0.728097762	0.608241296	0.77531478	0.632635225			0.460718326	0.460718326		
	1000	0.6095547	0.52856374	0.42557313	0.865985156	0.72888502	0.609554724	0.77594387	0.633818969	0.463566294	0.463566294					
	2000	0.6406932	0.57154861	0.49560746	0.87502783	0.748282863	0.640693203	0.791571091	0.66219154	0.521223182	0.521223182					
	3000	0.6557115	0.59100535	0.52222158	0.879692703	0.758070169	0.655711455	0.799533953	0.676048009	0.545024483	0.545024483			0.373503042		
	4000	0.665345	0.60319538	0.5380976	0.882771609	0.764467711	0.665345023	0.804760875	0.684981218	0.559517391	0.559517391			0.409223163		
	5000	0.6723326	0.61192334	0.54918554	0.885042043	0.769157237	0.672332595	0.808602832	0.691479312	0.569741761	0.569741761			0.429858456		
	6000	0.6777651	0.61865224	0.55760317	0.886826697	0.772829632	0.67776507	0.811616188	0.696540725	0.577551526	0.577551526			0.444165067		
	7000	0.6821817	0.62409048	0.56433435	0.888289181	0.775830626	0.682181682	0.814081646	0.700661186	0.583822781	0.583822781			0.454994918	0.271879574	
	8000	0.6858864	0.62863185	0.56991157	0.889523361	0.778357696	0.685886378	0.816159698	0.704120977	0.589034844	0.589034844			0.463640197	0.312640757	
	9000	0.6890665	0.63251655	0.57465359	0.890587848	0.780533584	0.689066459	0.817950294	0.707093207	0.593476802	0.593476802			0.470793863	0.333952582	
	10000	0.6918451	0.63590129	0.5787654	0.891521582	0.782439533	0.691845078	0.819519702	0.709691897	0.597335634	0.597335634			0.476869111	0.348765567	

< 0,019

Table 17. The differentiation factors δ_{ni} , related to the various active fire safety measures, as a function of the compartment area A_{fi} .

Table 18. Differentiation factors δ_{ni} for some compartment areas following table 17.

Differentiation factors δ_{ni} for various Active Fire Safety Measures	Compartment area A_{fi} [m ²]			
	200	500	1.000	10.000
Automatic water extinguishing system	0,44	0,57	0,61	0,69
Automatic water extinguishing system, with 1 independent water supply	0	0,46	0,53	0,64
Automatic water extinguishing system, with 2 independent water supplies	0	0	0,43	0,58
Automatic fire detection and alarm by heat	0,84	0,86	0,87	0,89
Automatic fire detection and alarm by smoke	0,66	0,70	0,73	0,78
Automatic alarm transmission to fire brigade	0,84	0,86	0,87	0,89
Manual fire suppression by work fire brigade	0,44	0,57	0,61	0,69
Manual fire suppression by off site fire brigade	0,72	0,76	0,78	0,82

So it is suggested to choose the partial factor δ_{q2} and the differentiation factors δ_{ni} for a compartment area A_{fi} of 1000m², as this area dependency is not critical and the results appear to be on the safe side.

Of course the Level 1 approach leads to more economic conclusions, but **this Level 2 method has the enormous advantage to be userfriendly as all the partial and differentiation factors may be taken directly from Annex E of EN1991-1-2 [16].**

The design value of the fire load $q_{f,d}$ is finally defined as :

$$q_{f,d} = m \cdot \delta_{q1} \cdot \delta_{q2} \cdot \delta_n \cdot q_{f,k} \quad [\text{MJ/m}^2] \quad (3)$$

where

- m is the combustion factor,
- δ_{q1} is the partial factor taking into account the fire activation risk due to the size of the compartment (see tables 13 and 19),
- δ_{q2} is the partial factor taking into account the fire activation risk due to the type of occupancy (see tables 15 and 19),
- $\delta_n = \prod \delta_{ni}$ is the product of the differentiation factors δ_{ni} taking into account the different active fire fighting measures (sprinkler, detection, automatic alarm transmission, firemen ...). These active measures are generally imposed for life safety reason (see tables 18 and 20),
- $q_{f,k}$ is the characteristic fire load density per unit floor area [MJ/m²], which may be taken according to table 3 of Chapter I.

Table 19. Partial factors δ_{q1} function of the compartment size, and δ_{q2} function of the occupancy of the building.

Compartment floor area A_f [m ²]	Danger of Fire Activation		Type of building Occupancy
	δ_{q1}	δ_{q2}	
25	1,10	0,78	art gallery, museum, swimming pool
250	1,50	1,00	offices, residence, hotel, paper industry
2 500	1,90	1,22	manufactory for machinery & engines
5 000	2,00	1,44	chemical laboratory, painting workshop
10 000	2,13	1,66	manufactory of fireworks or paints

Table 20. Differentiation factors δ_{ni} , accounting for various active fire safety measures.

Official Document		δ_n Function of Active Fire Safety Measures										$\delta_n^{\min} = \delta_{n1} \dots \delta_{n10}$ $\delta_n^{\max} = \delta_{n4} \cdot \delta_{n7}$		
		Automatic Fire Suppression		Automatic Fire Detection			Manual Fire Suppression							
		Automatic Water Extinguish. System δ_{n1}	Independ. Water Supplies 0 1 2 δ_{n2}	Automatic Fire Detection & Alarm by Heat δ_{n3}	Automatic Alarm Transmission to Fire Brigade by Smoke δ_{n4}	δ_{n5}	Work Fire Brigade δ_{n6}	Off Site Fire Brigade δ_{n7}	Safe Access Routes δ_{n8}	Fire Fighting Devices δ_{n9}	Smoke Exhaust System δ_{n10}			
Title	Date of publication	SIA 81	1984	0,50 0,59	—	0,83 or 0,69		0,83	0,67 or 0,63 $\delta_{n6} \cdot \delta_{n7} = 0,53$		—	1,0 1,39*	0,85	0,13 0,43
ANPI	1988	0,58 ⊙	1,0 0,86 0,65	0,82	0,68	included in ⊙		0,50	0,68	—	1,0 1,36*	—	0,07 0,46	
DIN 18230-1	1987/98	0,60	—	0,90		—		0,60	—	—	—	—	0,32 0,90	
ENV 1991-2-2	1995	0,60	—	—	—	—		—	—	—	—	—	0,60	
EC1-1-2	2002	0,61	1,0 0,87 0,7	0,87 or 0,73		0,87		0,61 or 0,78		0,9 or 1 1,5*	1,0 1,5*	1,0 1,5*	0,15 0,57	

For the normal fire fighting measures, which should almost always be present, such as the safe access routes, fire fighting devices, and smoke exhaust systems in staircases, the δ_{ni} values of table 20 should be taken as 1,0. However, if these fire fighting measures have not been foreseen, the corresponding δ_{ni} value should be taken as 1,5. If staircases are put under overpressure in case of fire alarm, the factor δ_{n8} of table 20 may be taken as 0,9.

The preceding approach is based on the assumption that the requirements in the relevant European standards on sprinklers, detection, alarm and smoke exhaust systems are met. However local circumstances may influence the numbers given in table 20. Reference is made to the Background Document CEN/TC250/SC1/N300A [14] based on [17].

However apart from the fact that this procedure, summarized in equation (3) and tables 19 and 20, is clearly based on a sound and credible development, it also appears in table 20, that this method is in line with the previous sometimes only partial elaborations produced over the last 20 years.

REFERENCES

- [1] Schleich J.B.; Stahlbauarchitektur und Brandschutz. Oesterreichischer Stahlbautag, Linz, 1993 - Stahlbau-Rundschau 82/1994, S. 3 bis 16.
- [2] Schleich J.B.; Global fire safety concept, the ARBED office building. Nordic Steel Construction Conference 95, Malmö, June 19-21, 1995.
- [3] Schneider, J.; Introduction to safety and reliability of structures. Structural Engineering Documents, N°5, International Association for Bridge and Structural Engineering, IABSE, Zurich, 138 p., 1997.
- [4] Schleich J.B.; Concept Global de Sécurité Incendie pour les Bâtiments. Construction Métallique, Paris, N°1-1997, ISSN 0045-8198 p. 3 à 19.
- [5] Schleich J.B. ; Globales Brandsicherheitskonzept. Ernst & Sohn, Stahlbau 67, Heft 2, 1998, S. 81 bis 96.
- [6] Schleich J.B.; Influence of active fire protection on the safety level & its consequence on the design of structural members. « Abschlussarbeit Nachdiplomkurs Risiko & Sicherheit », ETHZ, Zuerich 1.09.1998.
- [7] Fontana M., Fetz C; Natural fire safety concept, Part 4 - Statistics. ECSC Research 7210-SA/522, 9.9.1998.
- [8] Kindmann R., Schweppe H., Schleich J.B., Cajot L.G.; Zum Sicherheitskonzept für den baulichen Brandschutz. Bauingenieur Bd. 73, Nr 10 - Oktober, 1998, S. 455 bis 461.
- [9] Schneider J.; VaP, Variables Processor. Institut für Baustatik und Konstruktion, ETHZ, Zürich, 15.2.1999.
- [10] Fontana M., Favre J.P., Fetz C.; A survey of 40000 building fires in Switzerland. Fire Safety Journal 32 (1999) p. 137-158.
- [11] Schleich J.B.; Conception & Exécution des Structures. Cours 2^{me} Construction, Faculté des Sciences Appliquées, Université de Liège, 1999, p. 2.9/17 à 35.
- [12] Schleich J.B.; Das globale Brandsicherheitskonzept. Deutscher Stahlbautag, Stuttgart, 19-21 Oktober 2000 - Bauen mit Stahl, Dokumentation 654, S.15 bis 31.
- [13] Schleich J.B.; Fire safe design of buildings. Seminar on EN1991- Actions on structures, Pisa, May 2001 - Proceedings by Department of Structural Engineering, Pisa University, p. 91 to 118.
- [14] CEN; Background Document CEN/TC250/SC1/N300A - Valorisation project on Natural Fire Safety Concept, 9.11.2001.
- [15] CEN; EN1990, Eurocode – Basis of Structural design . CEN Central Secretariat, Brussels, DAV 24.4.2002.
- [16] CEN; EN1991-1-2 , Eurocode 1 – Actions on structures , Part 1.2 – Actions on structures exposed to fire. CEN Central Secretariat, Brussels, DAV 20.11.2002.
- [17] Schleich J.B., Cajot L.G.; Natural fire safety concept. ECSC Research 7210-SA/522 etc., B-D-E-F-I-L-NL-UK & ECCS, 1994-98, Final Report EUR 20360EN, 2002.
- [18] Schleich J.B.; Actions on structures exposed to fire-EC1, Free choice between ISO-fire and Natural fire. International Symposium on Fire safety of Steel Structures ISFSSS 2003, Cologne, 11-12.9.2003.
- [19] CEN; prEN1993-1-2, Eurocode 3 – Design of steel structures, Part1.2 – General rules – Structural fire design. CEN Central Secretariat, Brussels, Stage 49 draft, June 2004.
- [20] Schleich J.B.; Global fire safety for buildings, the approach of the Eurocodes. Nordic Steel Construction Conference 2004, Copenhagen, 7-9 June 2004.

CHAPTER IV – LIFE SAFETY CONSIDERATIONS

Milan Holický¹ and Jean-Baptiste Schleich²

¹Klockner Institute, Czech Technical University in Prague, Czech Republic

² University of Technology Aachen, University of Liège

1 INTRODUCTION

1.1 Background documents

Safety in case of fire is one of the essential requirements imposed on construction works by Council Directive 89/106/EEC [2], new European documents [22, 24, 25] and International Standards [6, 9]. Experience and available data [3, 7, 8, 12] indicate, that depending on particular conditions and the applied fire safety systems, the probability of fire flashover may be expected within a broad range.

General information concerning reliability is available in the important international publications [1, 4, 10, 11, 14] which have been used as background materials for the estimations of risk including injuries to human life. In addition to the above mentioned materials, relevant findings described in various documents [5, 13, 15, 16, 17, 18, 19, 20, 23, 26] have influenced the analysis of Bayesian belief networks applied to the probability of fire flashover and to life safety.

1.2 General principles

Experience and available data indicate that the conditional probability of fire flashover, given fire starts, may be expected in a building within a broad range depending on the applied fire safety system. Similarly the probabilities of structural failure and of possible injuries, given fire is fully developed, considerably depend on the system of structural safety and the arrangement of escaping routes.

It appears that Bayesian causal, belief networks supplemented by appropriate input data may provide an effective tool to analyse the significance of various characteristics of fire safety systems to the resulting probability of flash over. Moreover Bayesian networks supplemented by decision nodes and a number of utility nodes (influence diagram) make it possible to estimate the expected total risk for both the buildings and their occupants.

The input data for influence diagrams consist of conditional probabilities concerning states of chance nodes and data describing possible consequences of unfavourable events including costs due to injuries. Present analysis clearly indicates that the expected total risk depends significantly on the size of the building and on the application of various fire safety measures including arrangements for the escaping routes of occupants.

2 BAYESIAN NETWORK APPLIED TO LIFE SAFETY

2.1 Introduction

Recent studies attempt to show that reliability methods applied commonly for the persistent design situation may be also applied for the accidental, fire design situation. Basic probabilistic concepts of fire safety analysis are developed using international documents. An acceptable probability of failure due to fire is derived from the total probability of failure due

to persistent and accidental design situation. Illustrative examples related to office areas are provided. The Bayesian causal, belief network is investigated and recommended as an approach for additional investigation of fire safety and risk assessment.

It appears that Bayesian belief networks provide an effective tool to find a more accurate estimate for the probability of fire flashover and to make estimations of risk including injuries to human life in a rational way. The network presented in this study was developed as a combination of previously investigated networks including those with active measures (sprinklers and fire brigade) developed by Holicky and Schleich [15, 16, 18, 19, 20, 23, 26]. The network consists of chance nodes (fire starts, detection, tampering, sprinklers, smoke detection, fire brigade, fire flashover, structural collapse and number of endangered persons), decision and utility nodes. All nodes are connected by arrows corresponding to causal links between relevant nodes.

2.2 Probabilistic concepts

Probabilistic approach to risk aims at consideration of all possible events that might lead to unfavourable effects [1,10]. These events are often caused by accidental actions as fire, impact, explosion and extreme climatic loads. In the following it is assumed that during the specified design period adequate situations H_i (based on common design situations and hazard scenarios) occur with the probability $P\{H_i\}$. If the failure (unfavourable consequence) of the structure F due to a particular situation H_i occurs with the conditional probability $P\{F|H_i\}$, then the total probability of failure p_F is given by the law of total probability as:

$$p_F = \sum P\{F|H_i\} \cdot P\{H_i\} \quad (1)$$

Equation (1) can be used to harmonise partial probabilities $P\{F|H_i\}$ $P\{H_i\}$ in order to comply with the design condition $p_F < p_t$, where p_t is a target (design) probability of failure. The target value p_t may be determined using probabilistic optimisation, however, up to now it is mostly based on past experience e.g. $7,23 \times 10^{-5}$ per 55 years [22].

Similarly as in previous studies by Holicky and Schleich [15, 16, 18, 19, 20, 23, 26] two basic design situations for a given structure are considered only:

- **H_1 normal (persistent and transient) design situation**, assumed to occur with the probability $P\{H_1\}=0,9$;
- **H_2 accidental design situation due to fire starting**, assumed to occur with the probability $P\{H_2\} = 0,1$ which corresponds to an office area of 250 m² [15,16];

The accidental design situation H_2 may lead to further two subsequent situations:

- **H_3 accidental design situation without fire flashover**, which is assumed to occur with the probability $P\{H_3|H_2\} = 0,934$;
- **H_4 accidental design situation with fire flashover**, which is assumed to occur with the probability $P\{H_4|H_2\} = 0,066$ and which corresponds to an ISO-fire.

The conditional probabilities $P\{H_3|H_2\}$ and $P\{H_4|H_2\}$ indicated above were obtained in previous studies for a structure without sprinklers; with sprinklers these probabilities are 0,998 and 0,002 respectively. Considering the above-defined situations it follows from general equation (1) that the total probability of failure p_F can be written as [11, 13, 14]:

$$p_F = P\{F|H_1\} P\{H_1\} + [P\{F|H_3\} P\{H_3|H_2\} + P\{F|H_4\} P\{H_4|H_2\}] P\{H_2\} \quad (2)$$

The conditional probabilities $P\{F|H_i\}$ entering equation (1) must be determined by a separate probabilistic analysis of the respective situations H_i .

2.3 Bayesian network

Bayesian network (influence diagram) used in the following analysis is shown in Figure 1. The network consists of seven chance nodes numbered 1, 2, 3, 4, 5, 12 and 14, four decision nodes 6, 7, 15 and 16, and six utility nodes 8, 9, 10, 11, 13 and 17. The utility nodes represent the costs of various fire safety measures (nodes 8, 10, 17), damage to the building (nodes 9, 11), and injuries (node 13).

All the nodes are interconnected by directional arrays indicating causal links between parent and children nodes. Note that all the utility nodes except the utility node 13 are directly dependent on the size of a building (node 15). The utility node 13, describing the cost of injury, is however affected by the size of the building through the number of endangered persons represented by the chance node 14.

The chance nodes 1, 2, 3, 4, 5, 12 and 14 represent alternative random variables having two or more states. The node 1-Situation describes occurrence of the design situations H_1 and H_2 . The chance node 2-Sprinklers describes functioning of sprinklers provided that the decision (node 6) is positive; the probability of active state of sprinklers given fire start is assumed to be very high 0,999. The chance node 3-Flashover has two states: the design situation H_3 , fire design situation without flashover, and H_4 , fire design situation with flashover corresponding to a fully developed fire.

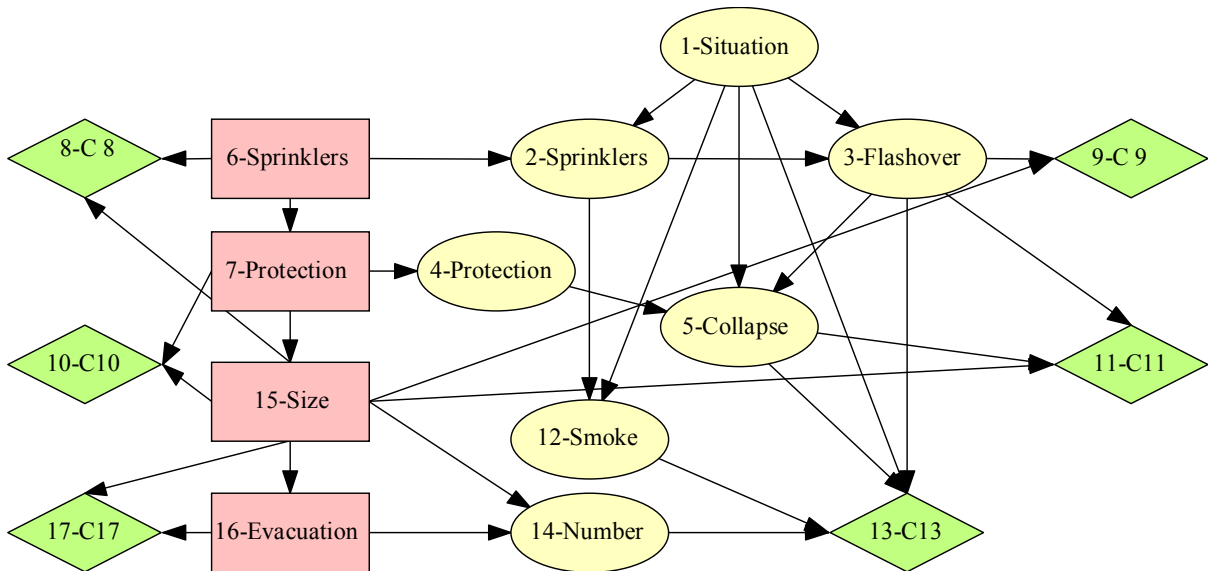


Figure 1. Bayesian network describing a structure under permanent i.e. normal and fire design situations [21].

If sprinklers are installed, the flashover in a compartment of 250 m² has the positive state with the conditional probability 0,002; if the sprinklers are not installed then $P\{H_4/H_2\} = 0,066$. It is assumed that with the probabilities equal to squares of the above values the fire will flash over the whole building, thus the values 0,000004 and 0,0044 are considered for the chance node 3. The chance node 4-Protection, introduced for formal computational reasons, has identical states as decision node 7-Protection. The chance node 5-Collapse represents structural failure of a steel beam that is described by the probability distribution given in Table 1 and developed in [18].

Table 1. Conditional probabilities of structural collapse (node 5 – Collapse).

1 – Situation	H1-Persistent		H2-ISO Fire			
3 – Flashover	No		Yes		No	
4 - Protection	Yes	No	Yes	No	Yes	No
5- Collapse yes	0,00000131		0,01	0,486	0,000000485	
5- Collapse no	0,99999869		0,99	0,514	0,999999515	

The chance node 12-Smoke describes the intensity of smoke due to fire. Table 2 shows the conditional probability distribution for the node 12-Smoke. Three states of the node 12 are considered here: no, light and heavy smoke. Judgement based mainly on past experience is used to assess the effect of sprinklers on the intensity of smoke, as indicated in Table 2.

Table 2. Conditional probabilities of smoke (node 12-Smoke).

1-Situation	H1-Persistent		H2-ISO Fire	
2-Sprinklers	Yes	No	Yes	No
12- Smoke no	1	1	0,95	0
12- Smoke light	0	0	0,05	0,05
12- Smoke heavy	0	0	0	0,95

Finally, the chance node 14-Number describes the number of endangered people that is dependent on the size of the building and on the evacuation system (decision nodes 15 and 16). The probability distribution describing the number of endangered persons (chance node 14) is indicated in Table 3 for the case when no special or no safe escaping routes are available, and in Table 4 for the case when special i.e. safe escaping routes are available.

Table 3. Probability distribution of the number of endangered persons (node14-Number) when no safe escaping routes are available (node16-Evacuation).

Number of endangered persons	Node 15-Size \equiv C11 [monetary units]			
	1000	10000	100000	1000000
0	0	0	0	0
1	0	0	0	0
10	0,1	0	0	0
100	0,8	0,3	0,2	0
1000	0,1	0,7	0,6	0,2
10000	0	0	0,2	0,8

Table 4. Probability distribution of the number of endangered persons (node14-Number) when safe escaping routes are available (node16-Evacuation).

Number of endangered persons	Node 15-Size $\equiv C_{11}$ [monetary units]			
	1000	10000	100000	1000000
0	0,99	0,9	0	0
1	0,01	0,1	1	0
10	0	0	0	1
100	0	0	0	0
1000	0	0	0	0
10000	0	0	0	0

In order to assess the consequences of possible decisions and various events it is further assumed that the cost due to structural collapse C_{11} , which is directly correlated to the size of the building (decision node 15), is considered within an hypothetical range from 10^3 to 10^6 monetary units. The maximum value 10^6 is included to investigate the overall trends in risk assessment, a realistic upper bound might however be 10^5 . The other costs due to installation of sprinklers C_8 , due to fire flash over C_9 , due to structural protection C_{10} , and the cost of providing safe escaping routes C_{17} are related to the cost C_{11} as indicated in Table 5.

Table 5. Cost of sprinklers C_8 , the cost due to fire flashover C_9 , the cost of protection C_{10} , and the cost of escaping routes C_{17} .

Cost of	Node 15-Size $\equiv C_{11}$ [monetary units]			
	1000	10000	100000	1000000
C_8 -Sprinklers	60	600	4000	6000
C_9 -Flashover	500	5000	50000	500000
C_{10} -Protection	60	600	4000	6000
C_{17} -Evacuation	10	100	1000	10000

It is assumed that the cost sprinklers C_8 is independent of the fact whether the protection is applied or not. The most difficult estimation concerns the cost due to injury C_{13} , which is indicated in Table 6 for one endangered person and was suggested for the first time in [19]. Taking into account available information it is assumed that the maximum value for one person is 40 units. This uttermost value is primarily derived from data provided by Roberts [5], that further refers to results obtained by the University of East Anglia in 1988. Similar data are also indicated in a recent study of Schneider [17].

Table 6. Cost C_{13} due to injury related to one person (node 13-Injuries), in case of fire.

5-Collapse	Yes						No					
12-Smoke	Non		Light		Heavy		Non		Light		Heavy	
3-Flashover	Y	N	Y	N	Y	N	Y	N	Y	N	Y	N
Cost C_{13}	4	0,8	8	4,8	40	36,8	3,2	0	7,2	4	39,2	36

The distribution of the cost C_{13} given states of parent nodes in case of fire (situation H2) has been derived assuming the maximum 40 units as an equivalent to fatality of one endangered person in the most severe case of structural collapse, heavy smoke and flashover. In case of normal situation H_1 , not indicated in Table 6, one half of the maximum injury cost (thus 20 units) has been assumed when collapse occurs under normal, i.e. persistent or transient situation.

2.4 Risk assessment

In general, the situations H_i may cause a number of events E_{ij} (including structural failure F) that will have economic consequences (e.g. excessive deformations, full development of the fire). It is assumed that adverse consequences of these events including injuries and fatalities can be normally expressed by the one-component quantities C_{ij} . If there is one-to-one mapping between the consequences C_{ij} and the events E_{ij} , then the total risk R related to the considered situations H_i is the sum

$$R = \sum C_{ij} P\{E_{ij}|H_i\} P\{H_i\} \quad (3)$$

In some cases it is necessary to describe the consequences of events E_{ij} by the quantity having more components, (for example by the cost, injuries or casualties). Furthermore, the dependence of consequences on relevant events may be more complicated than one-to-one mapping. An effective tool to estimate the total risk is the network shown in Figure 1, which is a simplified influence diagram described in detail in studies by Holicky & Schleich [15, 16], and which is being used in the program Hugin System [21].

Figure 2 shows the total risk R assuming that no safe escaping routes are provided, Figure 3 shows the total risk R assuming that safe escaping routes are provided. In both cases the total of 4 decisions are considered: 1 - sprinklers and protection, 2 - sprinklers but no protection, 3 - protection but no sprinklers, 4 - no sprinklers nor protection.

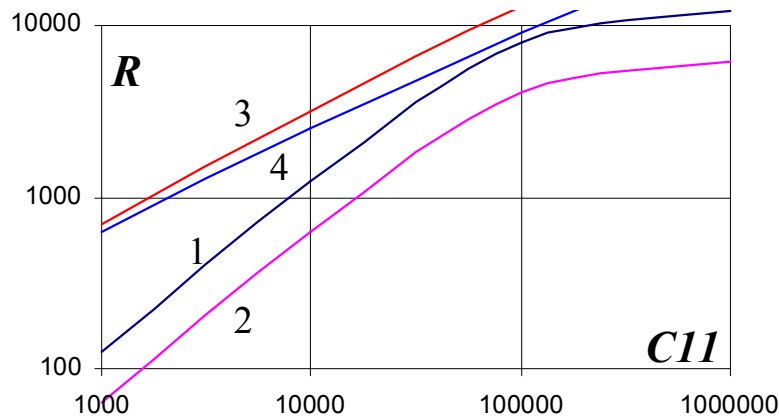


Figure 2. The total risk R when no safe escaping routes are provided, 1-sprinklers and protection, 2-sprinklers but no protection, 3-protection but no sprinklers, 4-no sprinklers nor protection.

Obviously the total risk in the first case (Figure 2 – no safe escape routes) is in general greater than in the second case (Figure 3 - safe escape routes are provided). It appears that when no safe escaping routes are provided then the lowest risk is very clearly achieved by decision 2 (sprinklers are installed but no protection).

In case when safe escape routes are provided then there is no need for sprinklers nor structural protection, so decision 4 leads to the lowest risk. However in that case the total failure probability, given by $p_F = 21,5 \cdot 10^{-5}$, is not acceptable! Hence decision 2 gives again the lowest risk; note that the differences between the total risks corresponding to the decisions 2 and 3 are negligible. Detailed results may be taken from table 7.

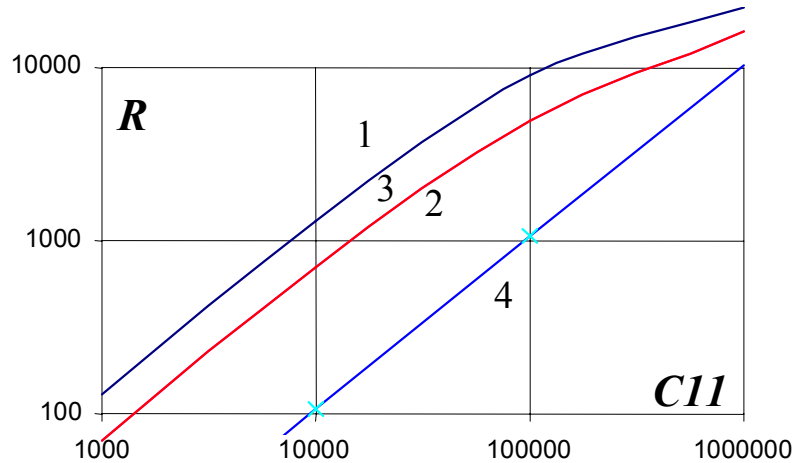


Figure 3. The total risk R when safe escaping routes are provided, 1-sprinklers and protection, 2-sprinklers but no protection, 3-protection but no sprinklers, 4-no sprinklers nor protection.

Figure 2 and 3 may be used to make adequate decisions depending on particular building conditions. However, it should be emphasised that the obtained results are valid for input data based on subjective assessments without considering particular conditions. The most significant input data include the cost data entering the utility nodes 8, 9, 10, 17, the cost C_{13} due to injuries and the distribution of the number of endangered people (node 14).

Table7. Probabilities of failure p_F and total risk R .

<i>Safe Escaping routes</i>		<i>Yes</i>				<i>No</i>		
6-Sprinklers	Yes		No		Yes		No	
7-Protection	Yes	No	Yes	No	Yes	No	Yes	No
Decision	1	2	3	4	1	2	3	4
$p_F \cdot 10^5$	0,12	0,16	0,56	21,5	0,12	0,16	0,56	21,5
15-Size $\equiv C_{11}$				<i>Risk</i>	<i>R</i>			
1000	130	70	70	10	124	64	683	623
10 000	1300	700	703	105	1217	617	3114	2517
100 000	9000	5000	5026	1046	8061	4061	13039	9060
1 000 000	22000	16002	16260	10469	12194	6194	34445	28656

A more detailed investigation may further concern the type of occupancy, which could have an influence on the expected risk. Obviously, when analysing a given building the network may have to be adjusted and new input data may be needed to make an appropriate

decision. In general all input data for utility nodes should be carefully related to the actual building conditions.

2.5 Conclusions

Probabilistic concepts provide effective operational methods for analysing structural reliability and life safety under various design situations including the normal and accidental design situation due to fire. Both structural safety and injuries may be taken into account.

Bayesian belief networks provide a logical, well-defined and effective tool to analyse the probability of fire flashover and probability of structural failure and injury. Different decisions concerning installation of sprinklers, application of structural protection and providing special escaping routes are considered. It appears that the target probability of structural failure $7,23 \times 10^{-5}$ (reliability index 3,8) is very likely to be exceeded if neither sprinklers nor structural protection are used in this case of an ISO-fire.

Bayesian networks supplemented by decision and utility nodes (influence diagram) enable to minimise the expected risk under normal and fire design situations. It appears that the most effective solution is to provide special i.e. safe escaping routes without sprinklers nor structural protection. However, in general it may not be an acceptable solution because of a high probability of structural failure. This results from the life saving function of escape routes (see tables 3 & 4), which however have no impact on structural stability.

When no safe escaping routes are provided then the decision 2, when only sprinklers without structural protection are used, is the most economic solution. Indeed **sprinklers play the role of live saving through smoke reduction** (see table 2), **but also decrease the structural failure probability by reducing the probability of flashover** according Schleich [25].

Further comprehensive studies focussed on the effects of various fire safety measures, on the probabilities of fire occurrence, on the types of standard and natural fires, and on flashover including economic assessment are needed.

REFERENCES

- [1] Ang A.H-S. & Tang W.H.; Probabilistic Concepts in Engineering Planning and Design Volume I - Basic principles, John Wiley, London, 409 p., 1975.
- [2] Council Directive (89/106/EEC), Official Journal of the European Communities, No 1. 40/13, Luxembourg, 1989.
- [3] CIB Report; Action on Structures - Fire, Publication 166, 1993.
- [4] Schleich J.B. et al.; International Iron and Steel Institute, Fire Engineering Design for Steel Structures, State of the Art, Brussels, ISBN 2-930069-00-7, 1993.
- [5] Roberts Lewis; The Public Perception of Risk, RSA Journal, pp 52-63., November 1995.
- [6] ISO 834; Fire Resistance - General Requirements, Zurich, 1995.
- [7] ECCS; Working Document No. 94, Background document to Eurocode 1, Brussels, 1996.
- [8] BSI; DD 240 - Fire Safety Engineering in Building, Part 1, Guide to the Application of Fire Safety Engineering Principles, London, 1997.
- [9] ISO 2394; General Principles on Reliability for Structures, Zurich, 1997.
- [10] Schneider, J.; Introduction to safety and reliability of structures. Structural Engineering Documents, N° 5, International Association for Bridge and Structural Engineering, IABSE, Zurich, 138 p., 1997.

- [11] Steward M.S. & Melchers R.E.; Probabilistic Risk Assessment of Engineering System, Chapman & Hall, London, 274 p., 1997.
- [12] DIN 18230-1; Baulicher Brandschutz im Industriebau, Teil 1 "Rechnerisch erforderliche Feuerwiderstandsdauer ", Berlin, 1998.
- [13] Ellingwood B.R.; Probability-Based Structural Design: Prospect for Acceptable Risk Bases, Proc. of Applic. of Statistics and Probability, Icasp 8, A.A. Balkema, Rotterdam, pp. 11-18, 1999.
- [14] Melchers R.E.; Structural Reliability Analysis and Prediction, John Wiley & Sons, Chichester, 437 p., 1999.
- [15] Holický M. & Schleich J.B.; Fire Safety Assessment using Bayesian Causal Network. Proc. of Foresight and Precaution Conf., ESREL 2000, Edinburgh, 15/17.5.00, A.A. Balkema, Rotterdam, pp. 1301-1306 , ISBN 90 5809 1422, 2000.
- [16] Holický M. & Schleich J.B.; Estimation of risk under fire design situation, Proc. of Risk Analysis 2000 Conf., Bologna, 11/13.10.00, WITpress, Southampton, Boston, pp. 63-72, ISBN 1-85312-830-9, 2000.
- [17] Schneider J.; Safety - A matter of Risk, Cost and Consensus, Structural Engineering International, No.4, pp. 266-269, November 2000.
- [18] Holický M. & Schleich J.B.; Modelling of a Structure under Permanent and Fire Design Situation, Proc. of Safety, Risk and Reliability - Trends in Engineering. International Conference, Malta, 21/23.3.01, A.A. Balkema, Rotterdam, pp. 789-794, ISBN 3-85748-120-4, 2001.
- [19] Holický M. & Schleich J.B.; Probabilistic risk analysis of a structure in normal and fire situation including life safety, Proc. of the International Conference ICOSAR 2001, Newport Beach, California, USA, 2001.
- [20] Schleich J.B.; Analyse probabiliste du risque pour les immeubles & leurs occupants, en cas d'incendie. 1st Albert Caquot International Conference "Modélisation et Simulation en Génie Civil: de la Pratique à la Théorie", PARIS, 3/5.10.2001, ISBN 2-85978-348-2, 2001.
- [21] Hugin System; Version 5.6 Light (free version), Hugin Expert A/S, Niels Jernes Vej 10, DK-9220 Aalborg , 2001.
- [22] CEN; EN1990, Eurocode – Basis of Structural design . CEN Central Secretariat, Brussels, DAV 24.4.2002.
- [23] Schleich J.B.; Fire risk assessment for steel buildings and occupants, EUROSTEEL 3. International Conference, Coimbra, Portugal, 19/20.9.2002.
- [24] CEN; EN1991-1-2 , Eurocode 1 – Actions on structures , Part 1.2 – Actions on structures exposed to fire. CEN Central Secretariat, Brussels, DAV 20.11.2002.
- [25] Schleich J.B., Cajot L.G.; Natural Fire Safety Concept. ECSC Research 7210-SA/522, etc., B-D-E-F-I-L-NL-UK&ECCS, 1994-98, Final Report EUR 20360EN, 2002.
- [26] Holický M.; Risk assessment of steel buildings and occupants under fire situation. ICASP 9, pp. 163- 168, Berkeley, 2003.

CHAPTER V - PROPERTIES OF MATERIALS

Jean-Baptiste Schleich¹

¹ University of Technology Aachen, University of Liège

1 INTRODUCTION

The objective of Handbook 5 is to describe a realistic and credible approach to the analysis of structural safety in case of fire. This of course leads us also to consider thermal and mechanical properties of materials depending on the material temperature obtained.

Temperature depending thermal and mechanical properties of concrete and steel have been published in a rather consistent manner through the " ECCS Model Code on Fire Engineering " in May 2001 [6]. Consequently these thermal and mechanical properties of concrete and steel have been more or less considered in the final drafts of the Fire Parts of Eurocode 2, Eurocode 3 and Eurocode 4 [9, 10, 11].

Nevertheless certain doubts subsist on the accuracy of thermal and mechanical properties of concrete. Indeed intense discussion took place the first half of 2002 on the new formulations proposed for the specific heat c_c , the thermal conductivity λ_c and the density ρ_c of concrete. Hence numerical simulations were done by the chairman of the project team for prEN1994-1-2 on a set of twelve different ISO-fire tests of composite structural beams and columns, performed between 1984 and 1991 in the Laboratories of Braunschweig and Gent Universities [1, 2, 7].

As a conclusion it was assumed that in prEN1992-1-2 the lower limit for the thermal conductivity λ_c of concrete is recommended, whereas in prEN1994-1-2 the upper limit for the thermal conductivity λ_c of concrete is recommended. This is of course an unsatisfactory situation as, for the same material, differences in the thermal conductivity λ_c of 47% are allowed at 20°C, and still of 23 % at 600°C .

Furthermore in prEN1992-1-2 different values, compared to [6], were adopted end 2001 for the strength reduction $k_{c,\theta}$ of concrete at 100°C and 200°C as well for the strain $\epsilon_{cu,\theta}$ corresponding to $f_{c,\theta}$ for the whole temperature field . Despite the strong opposition of the chairman of the project team for prEN1994-1-2 against this decision, as no scientific evidence for this modification was produced, this modification was maintained and is now published by CEN.

As a matter of fact, now beginning of May 2005, doubts are convincing certain experts that EN1992-1-2 should be amended by readopting the previous values for the strength reduction $k_{c,\theta}$ of concrete as well for the strain $\epsilon_{cu,\theta}$ corresponding to $f_{c,\theta}$. For that reason the mechanical properties of concrete given in this Chapter correspond to the " ECCS Model Code on Fire Engineering " from May 2001 [6].

Concerning mechanical properties of structural steel its maximum stress level in function of the temperature, strain hardening included, has been confirmed through numerical simulations of a set of 29 steel beams, uniformly heated and submitted to transient state bending tests [3 to 5].

2 THERMAL PROPERTIES OF CONCRETE

2.1 Normal weight concrete

The **thermal elongation** $\Delta l / l$ of normal weight concrete and siliceous concrete may be determined from the following:

$$\text{for } 20^{\circ}\text{C} \leq \theta_c \leq 700^{\circ}\text{C}: \quad \Delta l / l = -1,8 \cdot 10^{-4} + 9 \cdot 10^{-6} \theta_c + 2,3 \cdot 10^{-11} \theta_c^3 \quad (1)$$

$$\text{for } 700^{\circ}\text{C} < \theta_c \leq 1200^{\circ}\text{C}: \quad \Delta l / l = 14 \cdot 10^{-3}$$

where:

l is the length at 20°C of the concrete member

Δl is the temperature induced elongation of the concrete member

θ_c is the concrete temperature

For calcareous concrete, reference is made to 3.3.1(1) of EN1992-1-2.

The variation of the thermal elongation with temperature is illustrated in figure 1. In simple calculation models (see Chapter I-6.4) the relationship between thermal elongation and concrete temperature may be considered to be linear. In this case the elongation of concrete should be determined from:

$$\Delta l / l = 18 \cdot 10^{-6} (\theta_c - 20) \quad (2)$$

The **specific heat** c_c of normal weight dry, siliceous or calcareous concrete may be determined from:

$$c_{c,\theta} = 890 + 56,2 (\theta_c / 100) - 3,4 (\theta_c / 100)^2 \quad [\text{J/kg K}] \quad (3)$$

where θ_c is the concrete temperature [$^{\circ}\text{C}$].

The variation of the specific heat with temperature according to the previous equation is illustrated in figure 2. In simple calculation models the specific heat may be considered to be independent of the concrete temperature. In this case the following value should be taken:

$$c_c = 1000 \quad [\text{J/kg K}] \quad (4)$$

The moisture content of concrete should be taken equal to the equilibrium moisture content. If these data are not available, the moisture content should not exceed 4 % of the concrete weight. Where the moisture content is not considered on the level of the heat balance, equation (3) for the specific heat may be completed by a peak value c_c^* , shown in figure 2, situated between 100°C and 200°C . A moisture content of 10% may occur for hollow sections filled with concrete.

The **thermal conductivity** λ_c of normal weight concrete may be determined between the lower and upper limits given hereafter. The upper limit has been derived from tests of steel-concrete composite structural elements. The use of the upper limit is recommended.

The upper limit of thermal conductivity λ_c of normal weight concrete may be determined from:

$$\text{for } 20^{\circ}\text{C} \leq \theta_c \leq 1200^{\circ}\text{C}: \quad \lambda_c = 2 - 0,2451 (\theta_c / 100) + 0,0107 (\theta_c / 100)^2 \quad [\text{W/mK}] \quad (5a)$$

where θ_c is the concrete temperature.

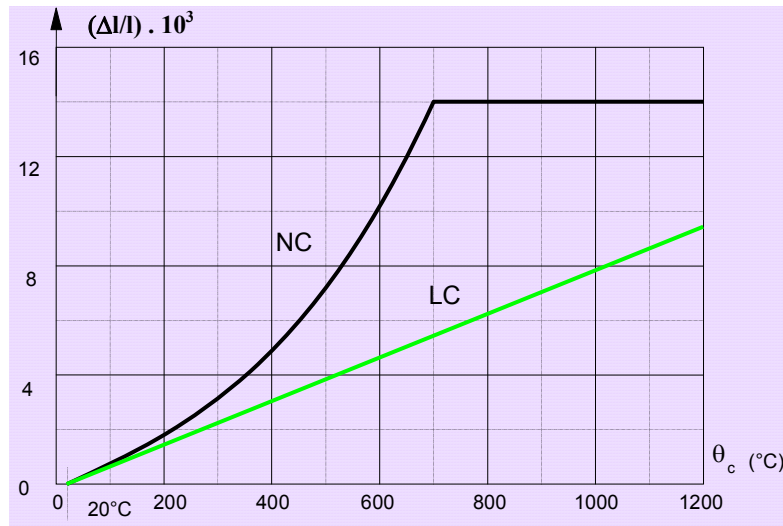


Figure 1. Thermal elongation of normal weight concrete (NC) and lightweight concrete (LC) as a function of the temperature.

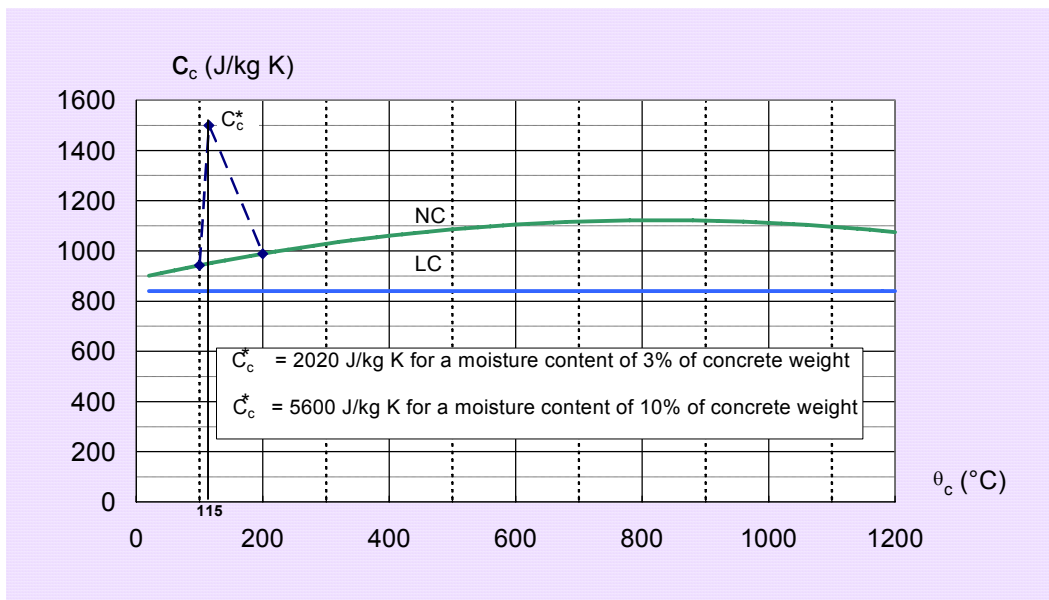


Figure 2. Specific heat of normal weight concrete (NC) and lightweight concrete (LC) as a function of the temperature.

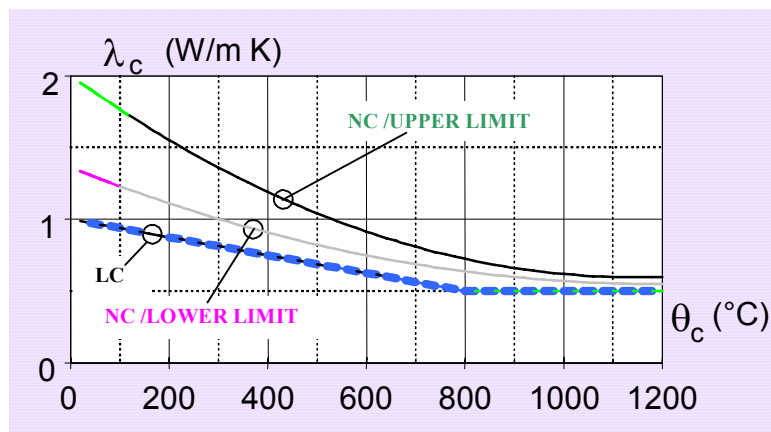


Figure 3. Thermal conductivity of normal weight concrete (NC) and lightweight concrete (LC) as a function of the temperature.

The lower limit of thermal conductivity λ_c of normal weight concrete may be determined from:

$$\text{for } 20^{\circ}\text{C} \leq \theta_c \leq 1200^{\circ}\text{C}: \lambda_c = 1,36 - 0,136 (\theta_c / 100) + 0,0057 (\theta_c / 100)^2 \quad [\text{W/mK}] \quad (5b)$$

where θ_c is the concrete temperature.

The variation of the thermal conductivity with temperature is illustrated in figure 3. In simple calculation models the thermal conductivity may be considered to be independent of the concrete temperature. In this case the following value should be taken:

$$\lambda_c = 1,30 \quad [\text{W/mK}] \quad (6)$$

2.2 Lightweight concrete

The thermal elongation $\Delta l / l$ of lightweight concrete may be determined from:

$$\Delta l / l = 8 \cdot 10^{-6} (\theta_c - 20) \quad (7)$$

with

l is the length at room temperature of the lightweight concrete member

Δl is the temperature induced elongation of the lightweight concrete member

θ_c is the lightweight concrete temperature [$^{\circ}\text{C}$].

The specific heat c_c of lightweight concrete may be considered to be independent of the concrete temperature:

$$c_c = 840 \quad [\text{J/kg K}] \quad (8)$$

The thermal conductivity λ_c of lightweight concrete may be determined from the following:

$$\text{for } 20^{\circ}\text{C} \leq \theta_c \leq 800^{\circ}\text{C}: \lambda_c = 1,0 - (\theta_c / 1600) \quad [\text{W/mK}] \quad (9)$$

$$\text{for } \theta_c > 800^{\circ}\text{C}: \lambda_c = 0,5 \quad [\text{W/mK}]$$

The variation with temperature of the thermal elongation, the specific heat and the thermal conductivity are illustrated in figures 1, 2 and 3. The moisture content of concrete should be taken equal to the equilibrium moisture content. If these data are not available, the moisture content should not exceed 5 % of the concrete weight.

2.3 Density

For static loads, the density of concrete ρ_c may be considered to be independent of the concrete temperature. For calculation of the thermal response, the variation of ρ_c in function of the temperature may be considered according to:

$$\rho_{c,\theta} = 2354 - 23,47 (\theta_c / 100) \quad [\text{kg/m}^3] \quad (10a)$$

For unreinforced normal weight concrete (NC) the following value may be taken:

$$\rho_{c,NC} = 2350 \quad [\text{kg/m}^3] \quad (10b)$$

The density of unreinforced lightweight concrete (LC), considered for structural fire design, shall be in the range of:

$$\rho_{c,LC} = 1600 \text{ to } 2000 \quad [\text{kg/m}^3] \quad (11)$$

3 THERMAL PROPERTIES OF STEEL

The **thermal elongation of steel** $\Delta l / l$ valid for all structural and reinforcing steel qualities, may be determined from the following:

$$\text{for } 20^{\circ}\text{C} < \theta_a \leq 750^{\circ}\text{C}: \Delta l / l = -2,416 \cdot 10^{-4} + 1,2 \cdot 10^{-5} \theta_a + 0,4 \cdot 10^{-8} \theta_a^2 \quad (12)$$

$$\text{for } 750^{\circ}\text{C} < \theta_a \leq 860^{\circ}\text{C}: \Delta l / l = 11 \cdot 10^{-3}$$

$$\text{for } 860^{\circ}\text{C} < \theta_a \leq 1200^{\circ}\text{C}: \Delta l / l = -6,2 \cdot 10^{-3} + 2 \cdot 10^{-5} \theta_a$$

where:

l is the length at 20°C of the steel member

Δl is the temperature induced elongation of the steel member

θ_a is the steel temperature.

The variation of the thermal elongation with temperature is illustrated in figure 4. In simple calculation models (see Chapter I-6.4) the relationship between thermal elongation and steel temperature may be considered to be linear. In this case the elongation of steel should be determined from:

$$\Delta l / l = 14 \cdot 10^{-6} (\theta_a - 20) \quad (13)$$

The **specific heat of steel** c_a valid for all structural and reinforcing steel qualities may be determined from the following:

$$\text{for } 20 \leq \theta_a \leq 600^{\circ}\text{C}: c_a = 425 + 7,73 \cdot 10^{-1} \theta_a - 1,69 \cdot 10^{-3} \theta_a^2 + 2,22 \cdot 10^{-6} \theta_a^3 \quad [\text{J/kgK}] \quad (14)$$

$$\text{for } 600 < \theta_a \leq 735^{\circ}\text{C}: c_a = 666 - \left(\frac{13002}{\theta_a - 738} \right) \quad [\text{J/kgK}]$$

$$\text{for } 735 < \theta_a \leq 900^{\circ}\text{C}: c_a = 545 + \left(\frac{17820}{\theta_a - 731} \right) \quad [\text{J/kgK}]$$

$$\text{for } 900 < \theta_a \leq 1200^{\circ}\text{C}: c_a = 650 \quad [\text{J/kgK}]$$

where θ_a is the steel temperature.

The temperature of 735°C is called "Curie-temperature" and corresponds to the magnetic phase transition. In this proposal the peak value is 5000 J/kgK . Phase Transition $\alpha \rightarrow \gamma$, at $\sim 900^{\circ}\text{C}$, leads to a discontinuity of c_a , which is not considered here.

The variation of the specific heat with temperature is illustrated in figure 5. In simple calculation models the specific heat may be considered to be independent of the steel temperature. In this case the following average value should be taken:

$$c_a = 600 \quad [\text{J/kgK}] \quad (15)$$

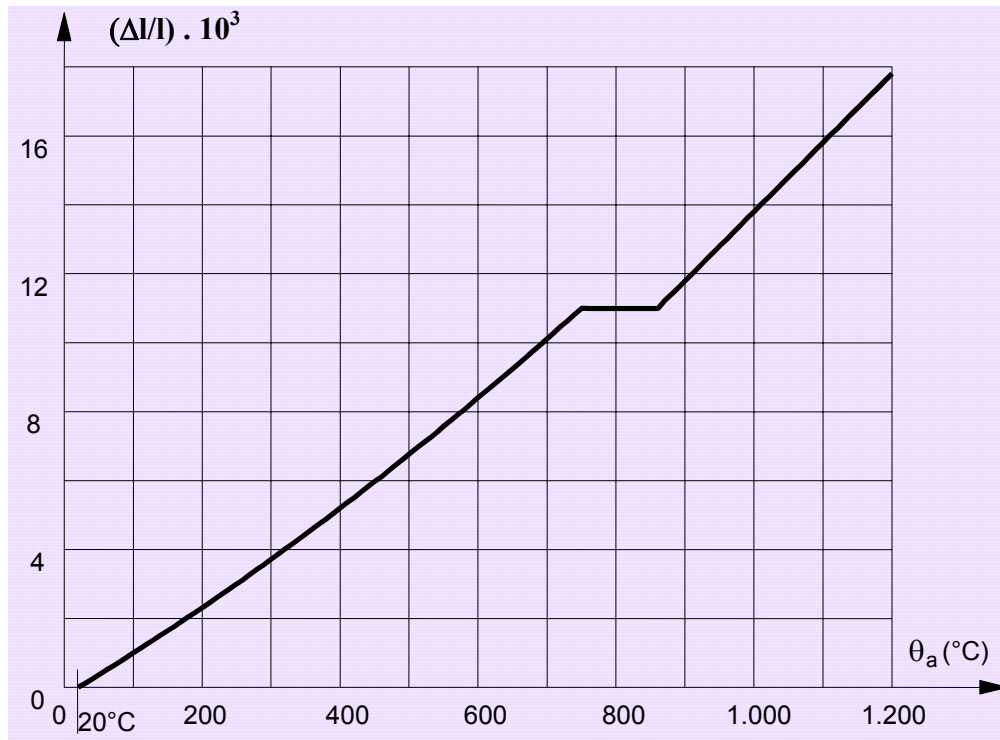


Figure 4. Thermal elongation of steel as a function of the temperature

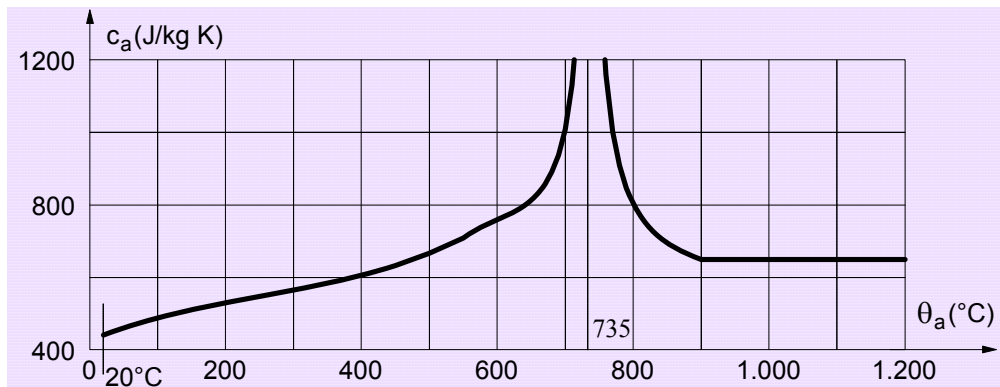


Figure 5. Specific heat of steel as a function of the temperature

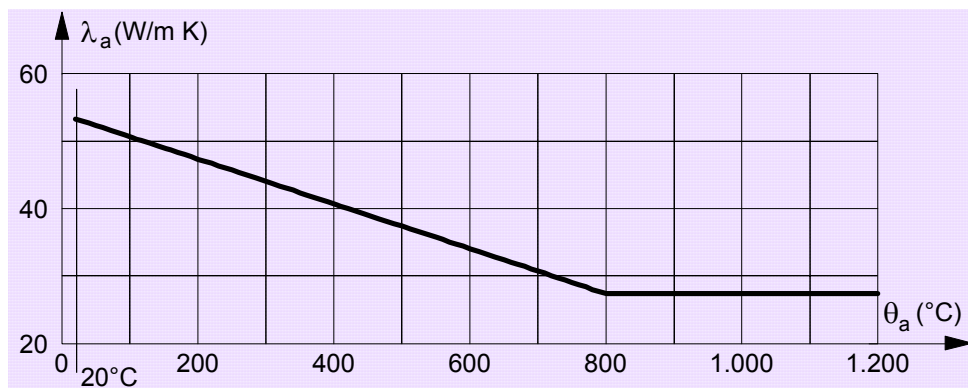


Figure 6. Thermal conductivity of steel as a function of the temperature

The **thermal conductivity of steel** λ_a valid for all structural and reinforcing steel qualities may be determined from the following:

$$\text{for } 20^{\circ}\text{C} \leq \theta_a \leq 800^{\circ}\text{C}: \quad \lambda_a = 54 - 3,33 \cdot 10^{-2} \theta_a \quad [\text{W/mK}] \quad (16)$$

$$\text{for } 800^{\circ}\text{C} < \theta_a \leq 1200^{\circ}\text{C}: \quad \lambda_a = 27,3 \quad [\text{W/mK}]$$

where θ_a is the steel temperature.

The variation of the thermal conductivity with temperature is illustrated in figure 6. In simple calculation models the thermal conductivity may be considered to be independent of the steel temperature. In this case the following average value should be taken:

$$\lambda_a = 45 \quad [\text{W/mK}] \quad (17)$$

4 MECHANICAL PROPERTIES OF CONCRETE

4.1 Strength and deformation properties of concrete

For heating rates between 2 and 50 K/min, the strength and deformation properties of concrete at elevated temperatures should be obtained from the stress-strain relationship given in figure 7. It is assumed that the heating rates normally fall within the specified limits.

The stress-strain relationships given in figure 7 are defined by two main parameters:

- the compressive strength $f_{c,\theta}$;
- the strain $\varepsilon_{cu,\theta}$ corresponding to $f_{c,\theta}$.

Table 1 gives for elevated concrete temperatures θ_c , the reduction factor $k_{c,\theta}$ to be applied to f_c in order to determine $f_{c,\theta}$ and the strain $\varepsilon_{cu,\theta}$. For intermediate values of the temperature, linear interpolation may be used.

Due to various ways of testing specimens, $\varepsilon_{cu,\theta}$ shows considerable scatter. Recommended values for $\varepsilon_{ce,\theta}$ defining the range of the descending branch may also be taken from table 1. For lightweight concrete (LC) the values of $\varepsilon_{cu,\theta}$, if needed, should be obtained from tests.

The parameters specified in table 1 hold for all siliceous concrete qualities. For calcareous concrete qualities the same parameters may be used. This is normally conservative. If a more precise information is needed, reference should be made to table 3.1 of EN 1992-1-2 [10].

In case of thermal actions corresponding to natural fire models according to 3.3 of EN 1991-1-2 [8], particularly when considering the decreasing temperature branch, the mathematical model for stress-strain relationships of concrete specified in figure 7 should be modified.

As concrete, which has cooled down after having been heated, does not recover its initial compressive strength, the proposal in paragraph 4.2 may be used in an advanced calculation model (see Chapter I-6.5).

Conservatively the tensile strength of concrete may be assumed to be zero. If tensile strength is taken into account in verifications carried out with an advanced calculation model, it should not exceed the values based on 3.2.2.2 of EN1992-1-2 [10].

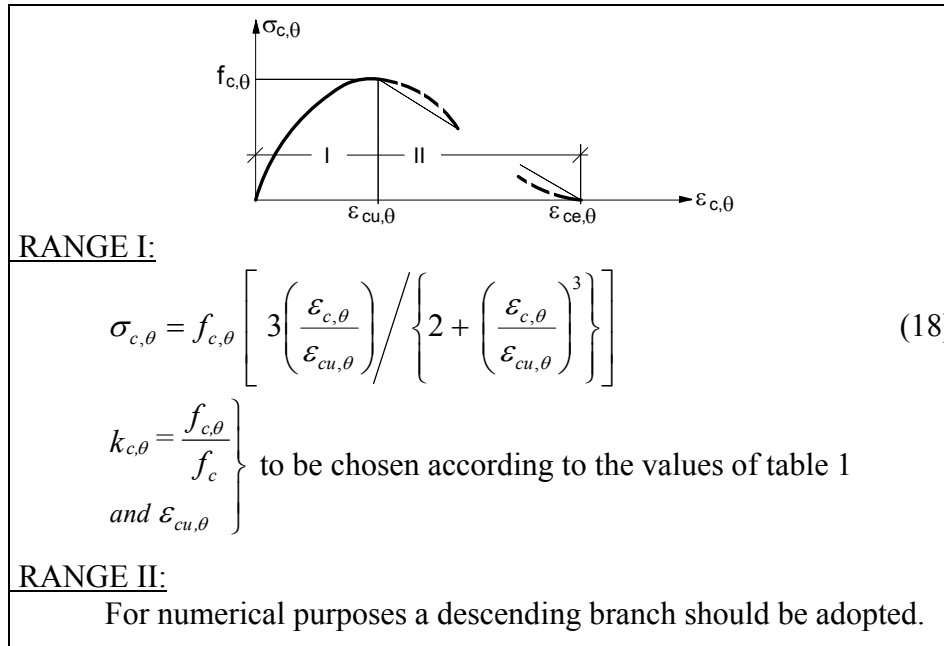


Figure 7. Mathematical model for stress-strain relationships of concrete under compression at elevated temperatures.

Table 1. Values for the parameters defining the stress-strain relationships of normal weight concrete (NC) and lightweight concrete (LC) at elevated temperatures.

Concrete Temperature θ_c [°C]	$k_{c,\theta} = f_{c,\theta} / f_{c,20^\circ\text{C}}$		$\varepsilon_{cu,\theta} \times 10^3$		$\varepsilon_{ce,\theta} \times 10^3$ recommended value for NC
	NC	LC	permitted range for NC	recommended value for NC	
20	1	1	2,5	2,5	20,0
100	0,95	1	2,5 : 4	3,5	22,5
200	0,90	1	3,0 : 5,5	4,5	25,0
300	0,85	1	4,0 : 7,0	6,0	27,5
400	0,75	0,88	4,5 : 10	7,5	30,0
500	0,60	0,76	5,5 : 15	9,5	32,5
600	0,45	0,64	6,5 : 25	12,5	35,0
700	0,30	0,52	7,5 : 25	14,0	37,5
800	0,15	0,40	8,5 : 25	14,5	40,0
900	0,08	0,28	10 : 25	15,0	42,5
1000	0,04	0,16	10 : 25	15,0	45,0
1100	0,01	0,04	10 : 25	15,0	47,5
1200	0	0	/	15,0	50,0

A graphical display of the stress-strain relationships for siliceous concrete is presented in figure 8 up to a maximum strain of $\varepsilon_{ce,\theta} = 4,5$ % for 1000°C. This presentation corresponds to the mathematical formulation of figure 7 and to the data of table 1.

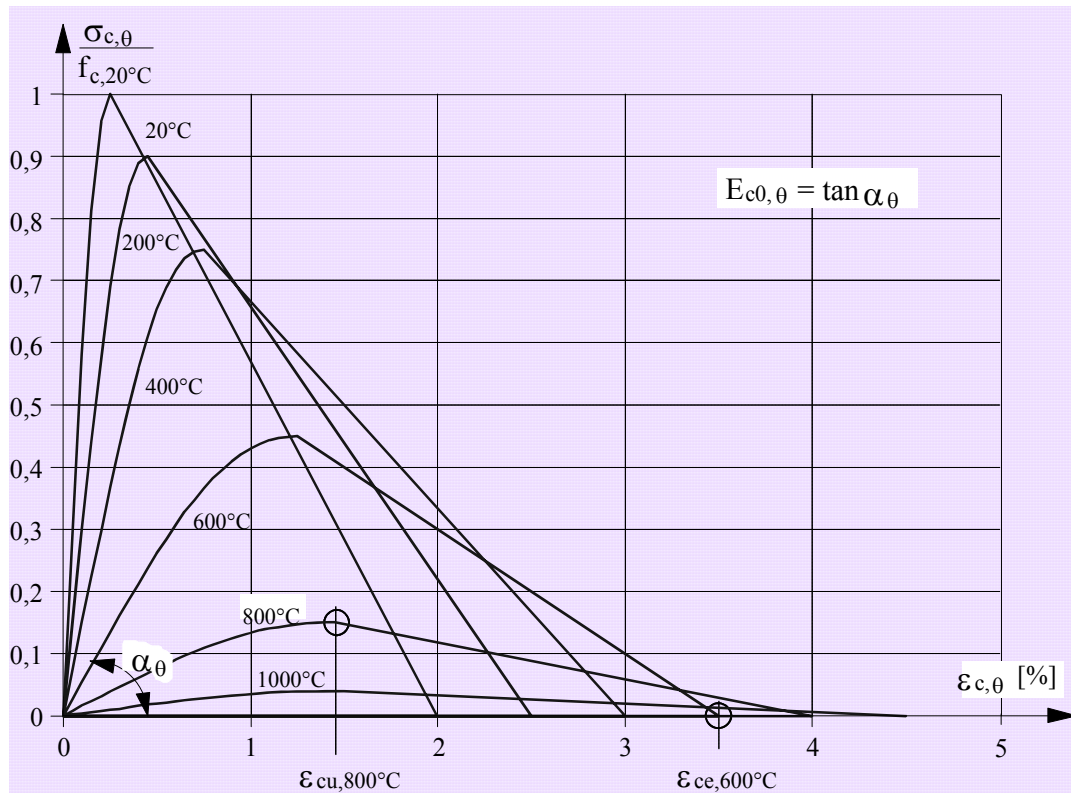


Figure 8. Graphical presentation of the stress-strain relationships for siliceous concrete with a linear descending branch, including the recommended values $\varepsilon_{cu,\theta}$ and $\varepsilon_{ce,\theta}$ of table 1.

The main parameters $f_{c,\theta}$ and $\varepsilon_{cu,\theta}$ of the stress-strain relationships at elevated temperatures, for siliceous normal concrete and for lightweight concrete, may be illustrated by figure 9. The compressive strength $f_{c,\theta}$ and the corresponding strain $\varepsilon_{cu,\theta}$ define completely range I of the material model together with the equations of figure 7.

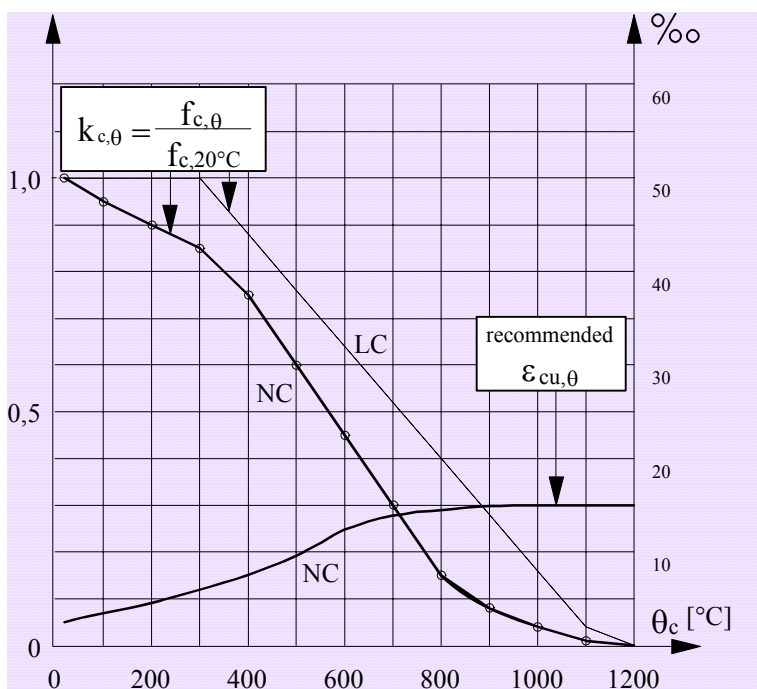


Figure 9. Parameters for stress-strain relationships at elevated temperatures of normal concrete (NC) and lightweight concrete (LC).

4.2 Concrete stress-strain relationships adapted to natural fires with a decreasing heating branch for use in advanced calculation models.

Following heating to a maximum temperature of θ_{max} , and subsequent cooling down to ambient temperature of 20°C, concrete does not recover its initial compressive strength f_c .

When considering the descending branch of the concrete heating curve (see figure 10), the value of $\varepsilon_{cu,\theta}$ and the value of the slope of the descending branch of the stress-strain relationship may both be maintained equal to the corresponding values for θ_{max} (see figure 11).

The residual compressive strength of concrete heated to a maximum temperature θ_{max} and having cooled down to the ambient temperature of 20°C, may be given as follows:

$$f_{c,\theta, 20^\circ C} = \varphi f_c \quad (19)$$

where for

$$\begin{aligned} 20^\circ C \leq \theta_{max} < 100^\circ C; & \quad \varphi = k_{c,\theta_{max}} \\ 100^\circ C \leq \theta_{max} < 300^\circ C; & \quad \varphi = 0,95 - [0,185 (\theta_{max} - 100)/200] \\ \theta_{max} \geq 300^\circ C; & \quad \varphi = 0,9 k_{c,\theta_{max}} \end{aligned}$$

The reduction factor $k_{c,\theta_{max}}$ is taken according to table 1.

During the cooling down of concrete with $\theta_{max} \geq \theta \geq 20^\circ C$, the corresponding compressive cylinder strength $f_{c,\theta}$ may be interpolated in a linear way between $f_{c,\theta_{max}}$ and $f_{c,\theta, 20^\circ C}$.

The above rules may be illustrated in figure 11 for a concrete grade C40/50 as follows:

$$\begin{aligned} \theta_1 = 200^\circ C; & \quad f_{c,\theta_1} = 0,9 \cdot 40 = 36 \text{ [N/mm}^2\text{]} \\ & \quad \varepsilon_{cu,\theta_1} = 0,45 \text{ [%]} \\ & \quad \varepsilon_{ce,\theta_1} = 2,5 \text{ [%]} \\ \theta_2 = 400^\circ C; & \quad f_{c,\theta_2} = 0,75 \cdot 40 = 30 \text{ [N/mm}^2\text{]} \\ & \quad \varepsilon_{cu,\theta_2} = 0,75 \text{ [%]} \\ & \quad \varepsilon_{ce,\theta_2} = 3,0 \text{ [%]} \end{aligned}$$

For a possible maximum concrete temperature of $\theta_{max} = 600^\circ C$:

$$\begin{aligned} f_{c,\theta_{max}} &= 0,45 \cdot 40 = 18 \text{ [N/mm}^2\text{]} \\ \varepsilon_{cu,\theta_{max}} &= 1,25 \text{ [%]} \\ \varepsilon_{ce,\theta_{max}} &= 3,5 \text{ [%]} \end{aligned}$$

For any lower temperature obtained during the subsequent cooling down phase as for $\theta_3 = 400^\circ C$ for instance:

$$\begin{aligned} f_{c,\theta, 20^\circ C} &= (0,9 k_{c,\theta_{max}}) f_c = 0,9 \cdot 0,45 \cdot 40 = 16,2 \text{ [N/mm}^2\text{]} \\ f_{c,\theta_3} &= f_{c,\theta_{max}} - [(f_{c,\theta_{max}} - f_{c,\theta, 20^\circ C})(\theta_{max} - \theta_3) / (\theta_{max} - 20)] = 17,4 \text{ [N/mm}^2\text{]} \\ \varepsilon_{cu,\theta_3} &= \varepsilon_{cu,\theta_{max}} = 1,25 \text{ [%]} \\ \varepsilon_{ce,\theta_3} &= \varepsilon_{cu,\theta_3} + [(\varepsilon_{ce,\theta_{max}} - \varepsilon_{cu,\theta_{max}}) f_{c,\theta_3} / f_{c,\theta_{max}}] = 3,4 \text{ [%]} \end{aligned}$$

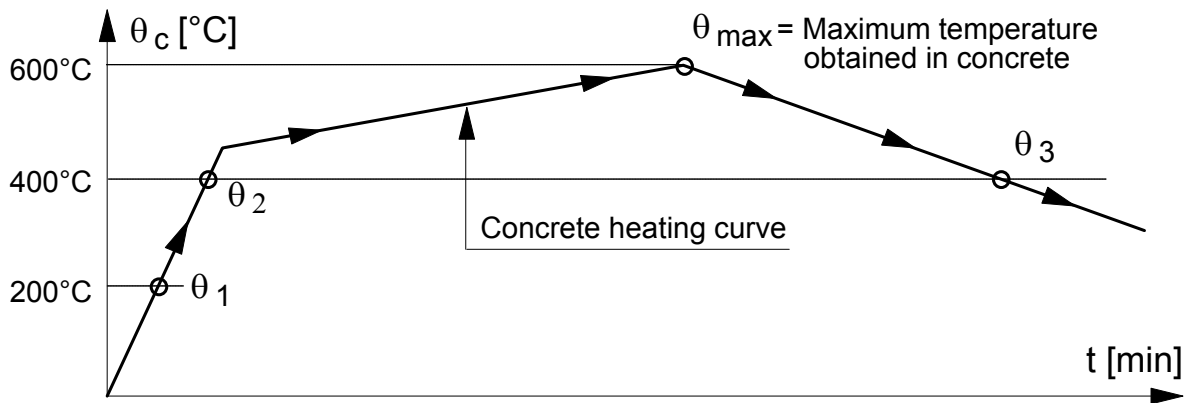


Figure 10. Example of concrete heating and cooling.

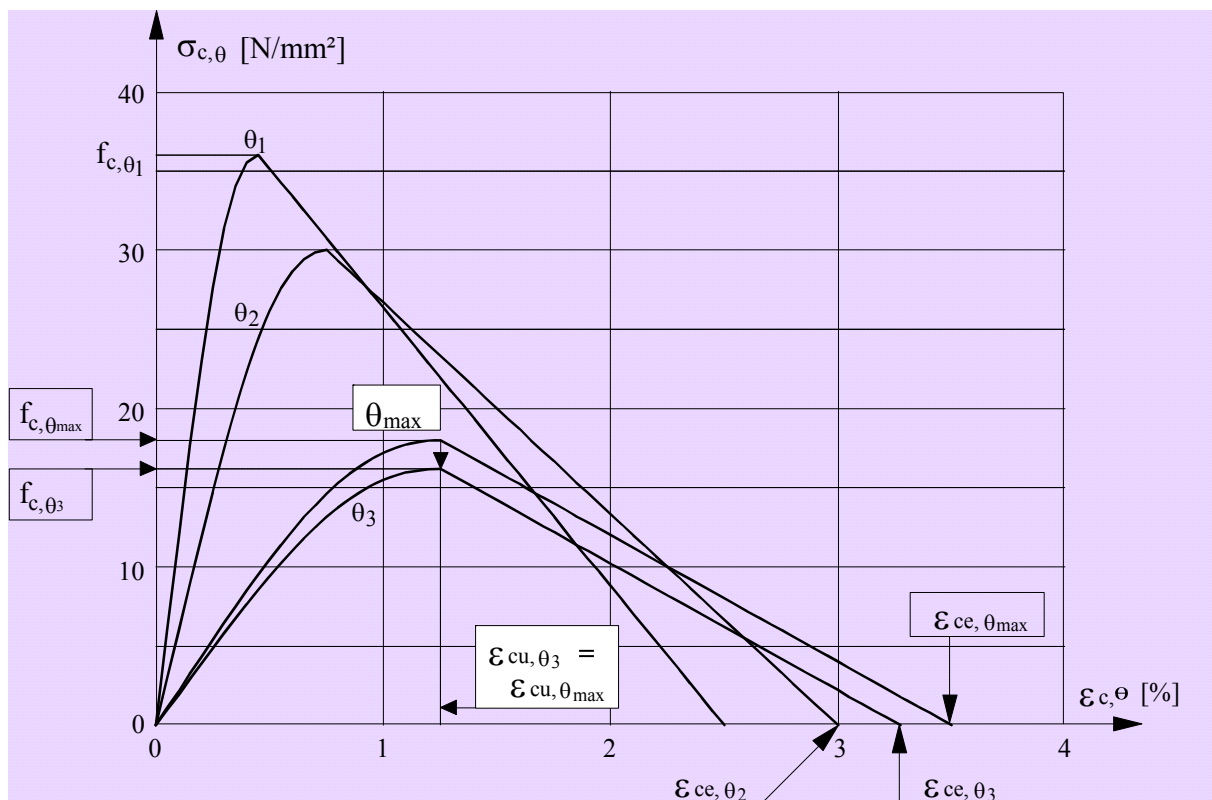


Figure 11. Stress-strain relationships of the concrete strength class C40/50, heated up to $\theta_1 = 200^\circ\text{C}$, $\theta_2 = 400^\circ\text{C}$, $\theta_{max} = 600^\circ\text{C}$ and cooled down to $\theta_3 = 400^\circ\text{C}$.

5 MECHANICAL PROPERTIES OF STEEL

5.1 Strength and deformation properties of structural steel

For heating rates between 2 and 50 K/min, the strength and deformation properties of structural steel at elevated temperatures should be obtained from the stress-strain relationship given in figure 12. It is assumed that the heating rates normally fall within the specified limits.

The stress-strain relationships given in figure 12 and table 2 are defined by three parameters:

- the slope of the linear elastic range $E_{a,\theta}$,
- the proportional limit $f_{ap,\theta}$,
- the maximum stress level or effective yield strenght $f_{ay,\theta}$.

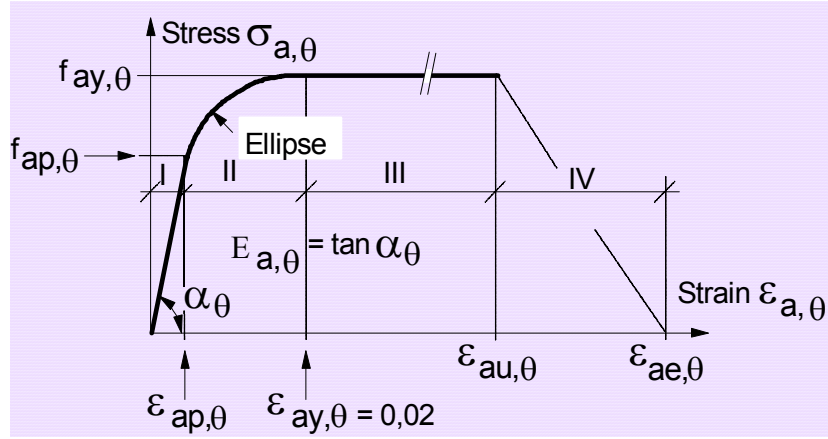


Figure 12. Mathematical model for stress-strain relationships of structural steel at elevated temperatures.

Table 2. Relation between the various parameters of the mathematical model of figure12.

Strain Range	Stress σ	Tangent modulus
I / elastic $\varepsilon \leq \varepsilon_{ap,\theta}$	$E_{a,\theta} \varepsilon_{a,\theta}$	$E_{a,\theta}$
II / transit elliptical $\varepsilon_{ap,\theta} \leq \varepsilon \leq \varepsilon_{ay,\theta}$	$(f_{ap,\theta} - c) + \frac{b}{a} \sqrt{a^2 - (\varepsilon_{ay,\theta} - \varepsilon_{a,\theta})^2} \quad (20)$ $a^2 = (\varepsilon_{ay,\theta} - \varepsilon_{ap,\theta})(\varepsilon_{ay,\theta} - \varepsilon_{ap,\theta} + c / E_{a,\theta})$ $b^2 = E_{a,\theta} (\varepsilon_{ay,\theta} - \varepsilon_{ap,\theta}) c + c^2$ $c = \frac{(f_{ay,\theta} - f_{ap,\theta})^2}{E_{a,\theta} (\varepsilon_{ay,\theta} - \varepsilon_{ap,\theta}) - 2(f_{ay,\theta} - f_{ap,\theta})}$	$\frac{b(\varepsilon_{ay,\theta} - \varepsilon_{a,\theta})}{a \sqrt{a^2 - (\varepsilon_{ay,\theta} - \varepsilon_{a,\theta})^2}}$
III / plastic $\varepsilon_{ay,\theta} \leq \varepsilon \leq \varepsilon_{au,\theta}$	$f_{ay,\theta}$	0

Table 3 gives for elevated steel temperatures θ_a , the reduction factors k_θ to be applied to the appropriate value E_a or f_{ay} in order to determine $E_{a,\theta}$ and $f_{ay,\theta}$. For intermediate values of the temperature, linear interpolation may be used.

Alternatively for temperatures below 400°C, the stress-strain relationships are extended by the strain hardening option given in table 3, provided local instability is prevented and the ratio $f_{au,\theta}/f_{ay}$ is limited to 1,25. The strain-hardening option is detailed hereafter.

The effect of strain hardening should only be accounted for if the analysis is based on advanced calculation models (see Chapter I-6.5). This is only allowed if it is proven that local failures (i.e. local buckling, shear failure, concrete spalling, etc) do not occur because of increased strains. Values for $\varepsilon_{au,\theta}$ and $\varepsilon_{ae,\theta}$ defining the range of the maximum stress branches and decreasing branches according to figure 12, may be taken from figure 14.

The formulation of stress-strain relationships has been derived from tensile tests. These relationships may also be applied for steel in compression.

In case of thermal actions corresponding to natural fire models according to 3.3 of EN 1991-1-2 [8], particularly when considering the decreasing temperature branch, the values specified in table 3 for the stress-strain relationships of structural steel may be used as a sufficiently precise approximation.

Table 3. Reduction factors k_θ for stress-strain relationships of structural steel at elevated temperatures, valid for steel grades S235 to S460.

Steel Temperature θ_a [°C]	$k_{E,\theta} = \frac{E_{a,\theta}}{E_a}$	$k_{p,\theta} = \frac{f_{ap,\theta}}{f_{ay}}$	$k_{y,\theta} = \frac{f_{ay,\theta}}{f_{ay}}$	$k_{u,\theta} = \frac{f_{au,\theta}}{f_{ay}}$
20	1,00	1,00	1,00	1,25
100	1,00	1,00	1,00	1,25
200	0,90	0,807	1,00	1,25
300	0,80	0,613	1,00	1,25
400	0,70	0,420	1,00	
500	0,60	0,360	0,78	
600	0,31	0,180	0,47	
700	0,13	0,075	0,23	
800	0,09	0,050	0,11	
900	0,0675	0,0375	0,06	
1000	0,0450	0,0250	0,04	
1100	0,0225	0,0125	0,02	
1200	0	0	0	

A graphical display of the stress-strain relationships for the steel grade S235 is presented in figure 13 up to a maximum strain of $\varepsilon_{ay,\theta} = 2\%$. This presentation corresponds to ranges I and II of figure 12 and to the tabulated data of table 3 without strain-hardening.

For steel grades S235, S275, S355, S420 and S460 the stress strain relationships may be evaluated up to a maximum strain of 2 % through the equations presented in table 2. For temperatures below 400°C, the alternative strain-hardening option mentioned in before may be used as follows.

A graphical display of the stress-strain relationships, strain-hardening included, is given in figure 14 where:

- for strains up to 2 %, figure 14 is in conformity with figure 12 (range I and II);
- for strains between 2 % and 4 %, a linear increasing branch is assumed (range IIIa);
- for strains between 4 % and 15 % (range IIIb) an horizontal plateau is considered with $\varepsilon_{au,\theta} = 15\%$;
- for strains between 15 % and 20 % a decreasing branch (range IV) is considered with $\varepsilon_{ae,\theta} = 20\%$.

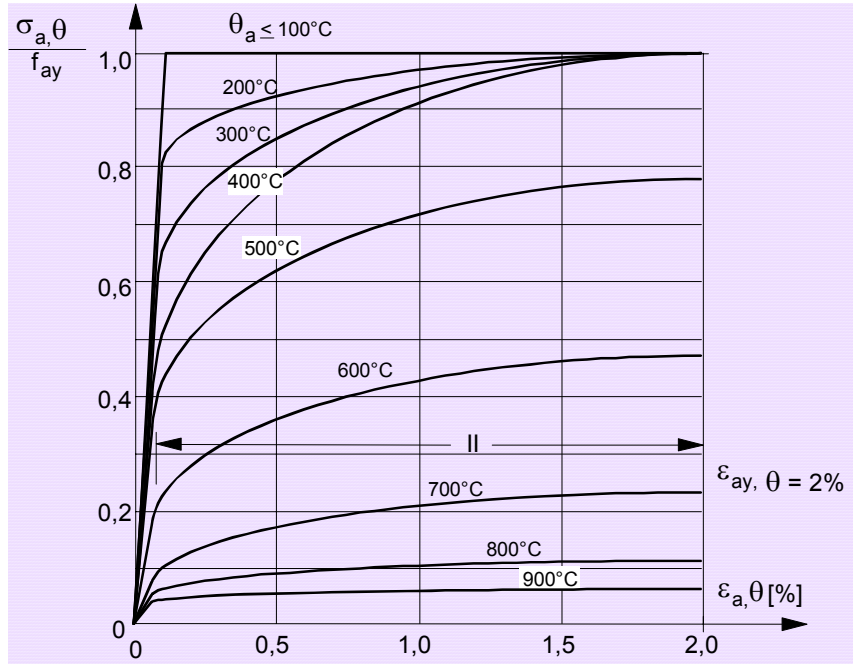


Figure 13. Graphical presentation of the stress-strain relationships for the steel grade S235 up to a strain of 2 %.

For strains $\varepsilon_{a,\theta}$ higher than 2 % the stress-strain relationships allowing for strain-hardening may be determined as follows:

$$2\% < \varepsilon_{a,\theta} < 4\% : \quad \sigma_{a,\theta} = \left[(f_{au,\theta} - f_{ay,\theta}) / 0,02 \right] \varepsilon_{a,\theta} - f_{au,\theta} + 2 f_{ay,\theta} \quad (21)$$

$$4\% \leq \varepsilon_{a,\theta} \leq 15\% : \quad \sigma_{a,\theta} = f_{au,\theta}$$

$$15\% < \varepsilon_{a,\theta} < 20\% : \quad \sigma_{a,\theta} = \left[1 - ((\varepsilon_{a,\theta} - 0,15) / 0,05) \right] f_{au,\theta}$$

$$\varepsilon_{a,\theta} \geq 20\% : \quad \sigma_{a,\theta} = 0$$

The tensile strength at elevated temperature $f_{au,\theta}$ allowing for strain-hardening (see figure 15), may be determined as follows:

$$\theta_a \leq 300^\circ\text{C} ; \quad f_{au,\theta} = 1,25 f_{ay} \quad (22)$$

$$300 < \theta_a \leq 400^\circ\text{C} ; \quad f_{au,\theta} = f_{ay} (2 - 0,0025 \theta_a)$$

$$\theta_a \geq 400^\circ\text{C} ; \quad f_{au,\theta} = f_{ay,\theta}$$

The main parameters $E_{a,\theta}$, $f_{ap,\theta}$, $f_{ay,\theta}$, and $f_{au,\theta}$ of the alternative strain-hardening option may be obtained from the reduction factors k_θ of figure 15.

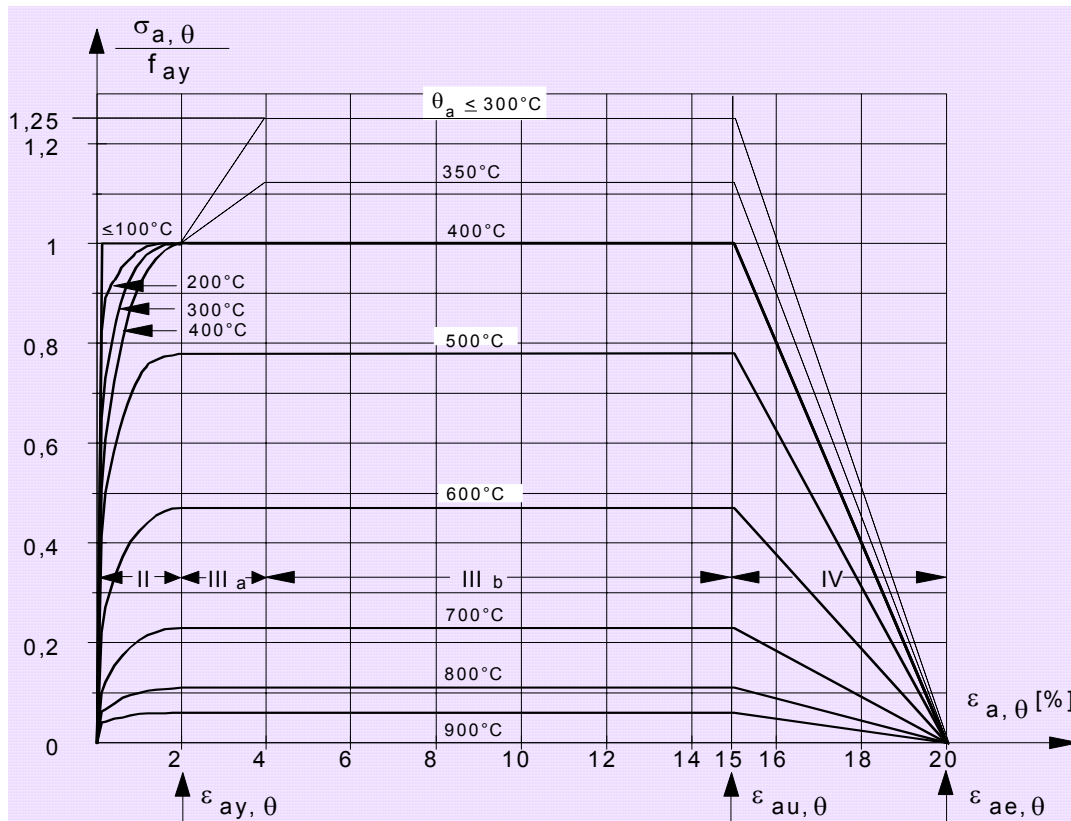


Figure 14. Graphical presentation of the stress-strain relationships of structural steel at elevated temperatures, strain-hardening included.

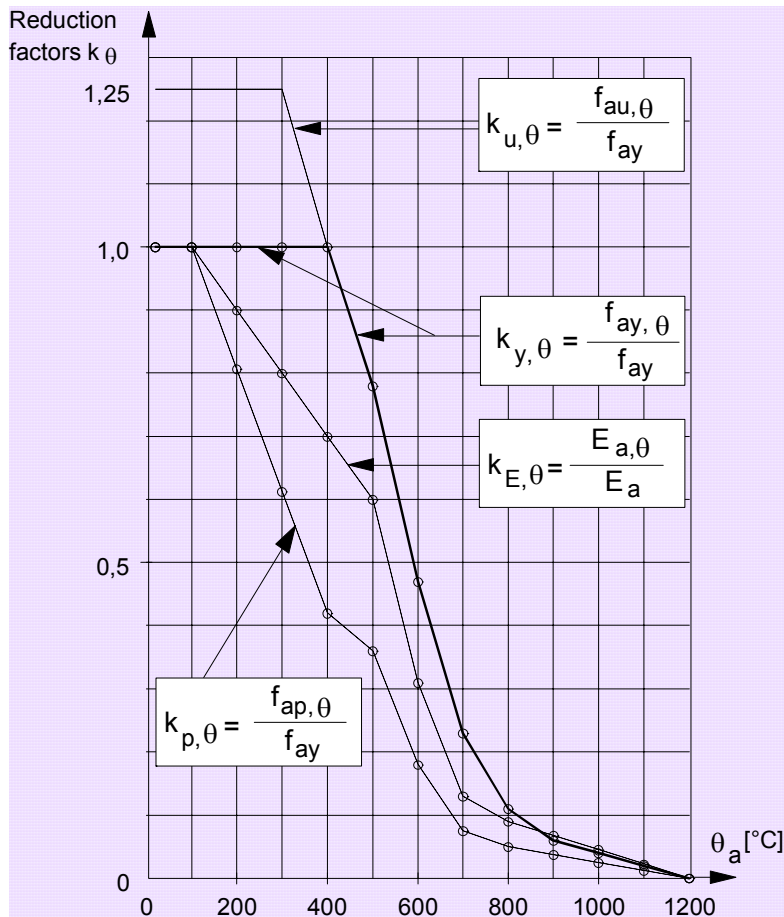


Figure 15.
Reduction factors k_{θ} for stress-strain relationships allowing for strain-hardening of structural steel at elevated temperatures (see table 3).

5.2 Strength and deformation properties of reinforcing steels

The strength and deformation properties of reinforcing steels at elevated temperatures may be obtained by the same mathematical model as that presented in 5.1. For hot rolled reinforcing steel the three main parameters given in table 3 may be used, except that the value of $k_{u,\theta}$ should not be greater than 1,1 and $\varepsilon_{au,\theta}$ limited by ~5% (see Annex C of EN1992-1-1).

The three main parameters for cold worked reinforcing steel are given in table 4. For prestressing steels see table 3.3N of EN1992-1-2 [10].

In case of thermal actions corresponding to natural fire models according to 3.3 of EN 1991-1-2 [8], particularly when considering the decreasing temperature branch, the values specified in table 3 for the stress-strain relationships of structural steel, may be used as a sufficiently precise approximation for hot rolled reinforcing steel.

Table 4. Reduction factors k_θ for stress-strain relationships of cold worked reinforcing steel.

Steel Temperature θ_s [°C]	$k_{E,\theta} = \frac{E_{s,\theta}}{E_s}$	$k_{p,\theta} = \frac{f_{sp,\theta}}{f_{sy}}$	$k_{y,\theta} = \frac{f_{sy,\theta}}{f_{sy}}$
20	1,00	1,00	1,00
100	1,00	0,96	1,00
200	0,87	0,92	1,00
300	0,72	0,81	1,00
400	0,56	0,63	0,94
500	0,40	0,44	0,67
600	0,24	0,26	0,40
700	0,08	0,08	0,12
800	0,06	0,06	0,11
900	0,05	0,05	0,08
1000	0,03	0,03	0,05
1100	0,02	0,02	0,03
1200	0	0	0

6 DETERMINATION OF MATERIAL PROPERTIES BY NUMERICAL SIMULATION OF REAL TESTS

6.1 Application to the thermal properties of concrete

Intense discussion took place the first half of 2002 on the new formulations proposed in April 2002 for the specific heat c_c and the thermal conductivity λ_c of concrete. As no scientific evidence for this modification was produced, we felt obliged to proceed to numerical simulations of previously performed real ISO-fire tests on composite beams and composite columns. Measured temperatures and failure times would be compared to the corresponding calculated temperatures and failure times for different formulations of thermal properties c_c and λ_c of concrete.

Finite Element calculations were undertaken on behalf of 12 completely different tests on composite structural beams & columns, performed between 1984 & 1991 in the laboratories of Braunschweig and Gent Universities [1, 2]. The position of the thermocouples which have been used for the comparison on the level of temperature in the various cross-sections is shown in figure 16.

In most cases thermocouples positioned on reinforcing bars, most important for the bending resistance of beams or the buckling resistance of columns, were considered. For columns 1.7 & 1.8 the point considered is on the outside of tees, still covered by 45 mm of concrete. For column 1.4 the thermocouple used is in the concrete bulk. It should be underlined that, for the analysis of failure times, of course the total differential temperature field in cross-sections, calculated every second, is used by the thermo-mechanical soft CEFICOSS (see Chapter I-6.5). This software, extensively used during ~ 15 research projects and for the design of ~ 300 buildings is accepted by engineering experts throughout Europe. This analysis has been done under the present author's personal leadership & responsibility, with the clear aim to present a scientific conclusion [7].

* The results obtained first half of May 2002, on these 12 single beam or single column test specimen, speak finally a clear language.

Figure 17 gives the three different formulations for λ_c , thermal conductivity, and c_c , specific heat of concrete with the rather important difference between the proposals of EC4-Part 10 from 1990 and ENV 1994-1-2 from 1995 on one side, & the proposal of prEN1992-1-2 from April 2002 on the other side.

Table 5 gives the measured and calculated temperatures, relevant for the tested specimen at the failure times, but also shows the ratios of temperature calculated to temperature measured for any test, as well as the mean & standard deviation in case of these 3 thermal proposals.

This shows, that at least from the temperature point of view & for the here tested structural elements, the proposal of prEN1992-1-2 from April 2002 is in a mean unsafe by ~20%.

The best result is obtained with the old thermal proposal of EC4- Part 10 from 1990, which in a mean fits with -0.5%.

Table 6 gives the measured and calculated failure times, for the tested specimen, but also shows the ratios of failure time calculated to failure time measured for any test, as well as the mean & standard deviation in case of these 3 thermal proposals.

Again, this time from the failure time point of view & for the here tested structural elements, **the proposal of prEN1992-1-2 from April 2002 is in a mean unsafe by ~20%**, with a standard deviation of 10,4%.

The best result is obtained with the old thermal proposal of EC4- Part 10 from 1990, which in a mean fits with -0.2%.

For beams B 2.11 to B 2.14 the failure criterion chosen is the deflection limit $L/30$.

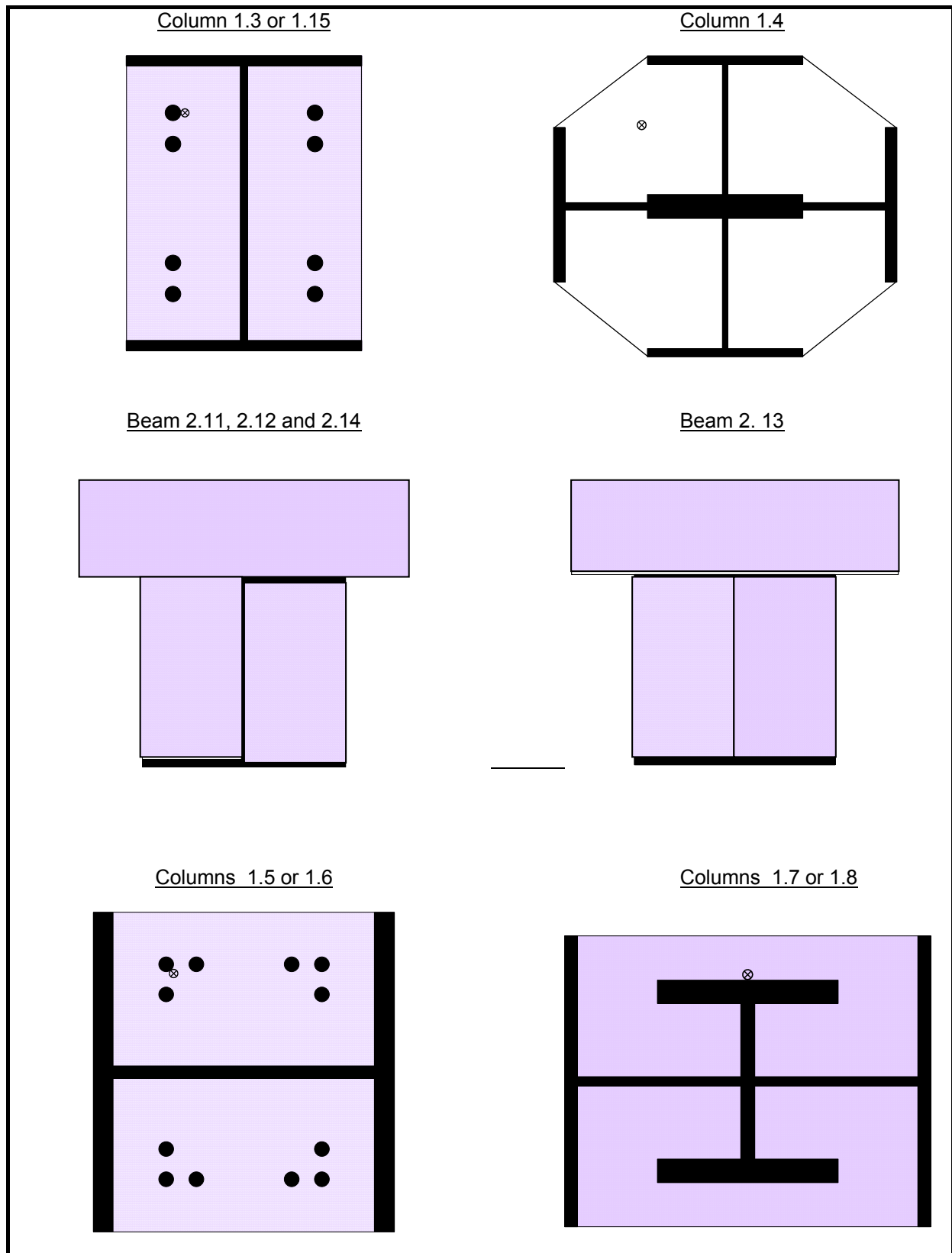


Figure 16. Relevant position of the thermocouples for temperature comparison ⊗.

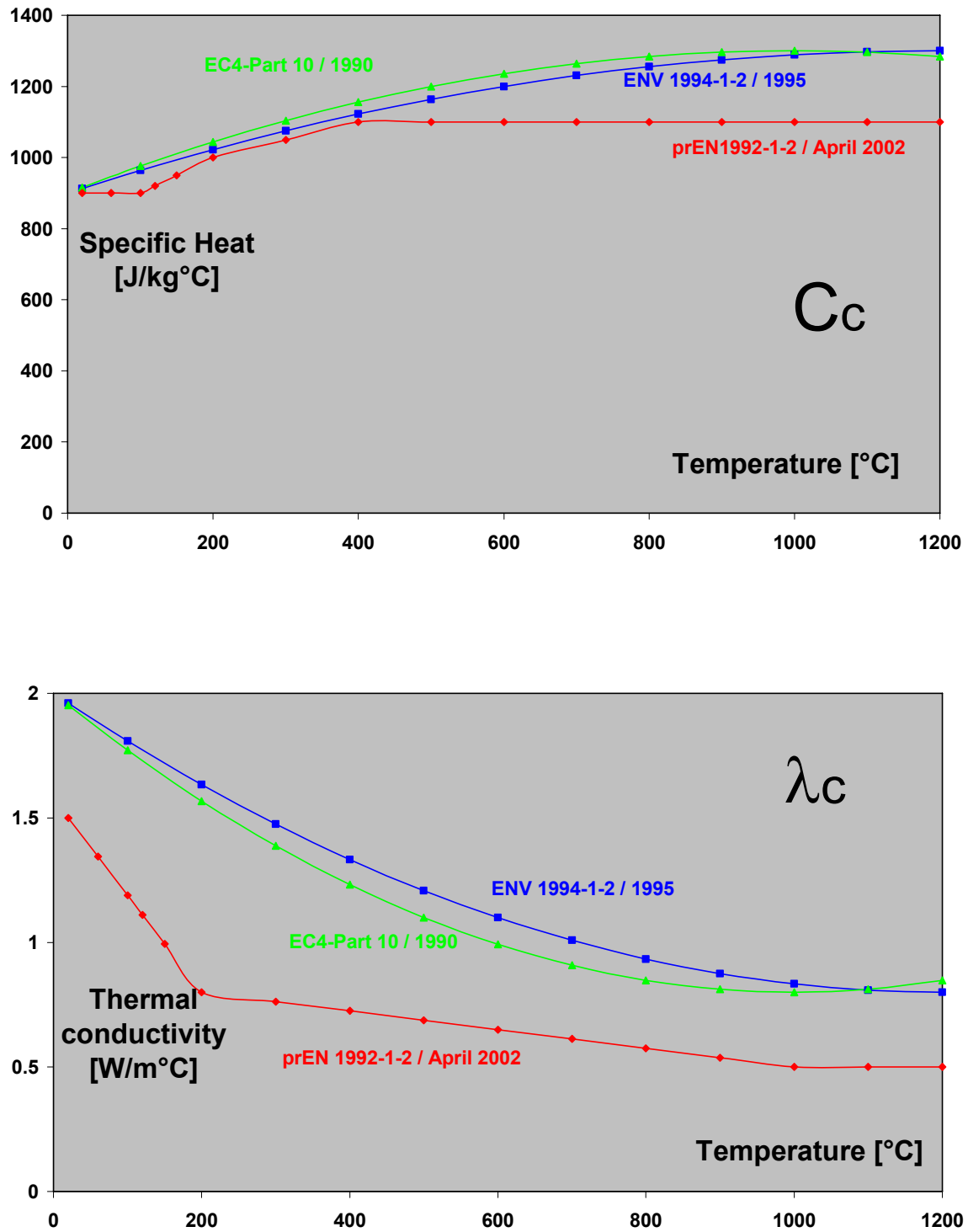


Figure 17. The three different formulations for λ_c , thermal conductivity, and c_c , specific heat of concrete with the rather important difference between the proposals of EC4-Part 10 from 1990 and ENV 1994-1-2 from 1995 on one side, & the proposal of prEN1992-1-2 from April 2002 on the other side.

Chapter V - Properties of materials

Test number	Measured Relevant T° [°C]	Calculated T° [°C] EC4-10/1990	$\frac{T^{\circ}_{\text{calculated}}}{T^{\circ}_{\text{measured}}}$	Calculated T° [°C] ENV/1995	$\frac{T^{\circ}_{\text{calculated}}}{T^{\circ}_{\text{measured}}}$	Calculated T° [°C] EC2-1-2/ May 2002	$\frac{T^{\circ}_{\text{calculated}}}{T^{\circ}_{\text{measured}}}$
C 1.3	490	495	1,0102	536	1,0939	415	0,8469
C 1.15	570	586	1,0281	626	1,0982	489	0,8579
C 1.4	450	458	1,0178	500	1,1111	363	0,8067
B 2.11	635	611	0,9622	654	1,0299	507	0,7984
B 2.12	740	723	0,9770	764	1,0324	617	0,8338
B 2.13	670	635	0,9478	677	1,0105	530	0,7911
B 2.14	375	391	1,0427	426	1,136	310	0,8267
C 1.5	435	418	0,9609	460	1,0575	309	0,7103
C 1.6	440	403	0,9159	445	1,0114	297	0,675
C 1.7	360	379	1,0528	412	1,1444	292	0,8111
C 1.8	345	358	1,0377	390	1,1304	274	0,7942
B T3	425	419	0,9859	458	1,0776	318	0,7482
mean			0,9949		1,0778		0,7917
standard deviation			0,0412		0,0467		0,0526

Test number	Measured Failure Time [min]	Calculated Failure Time [min] EC4-10/1990	$\frac{t_{\text{calculated failure}}}{t_{\text{measured failure}}}$	Calculated Failure Time [min] ENV/1995	$\frac{t_{\text{calculated failure}}}{t_{\text{measured failure}}}$	Calculated Failure Time [min] EC2-1-2/ May 2002	$\frac{t_{\text{calculated failure}}}{t_{\text{measured failure}}}$
C 1.3	116	121	1,0431	111	0,9569	143	1,2328
C 1.15	189	162	0,8571	148	0,7831	206	1,08
C 1.4	172	161	0,936	150	0,8721	172	1,0
B 2.11	171	181	1,0585	167	0,9766	208	1,2164
B 2.12	244	234	0,959	220	0,9016	267	1,0943
B 2.13	178	194	1,0899	177	0,9944	225	1,264
B 2.14	92	99	1,0761	92	1,0	118	1,2826
C 1.5	136	127	0,9338	117	0,8603	157	1,1544
C 1.6	120	124	1,0333	114	0,95	141	1,175
C 1.7	111	114	1,027	105	0,946	151	1,3604
C 1.8	157	138	0,879	126	0,8025	176	1,121
B T3	120	130	1,0833	118	0,9833	161	1,3417
mean			0,998		0,9189		1,1944
standard deviation			0,078		0,0712		0,1041

Tables 5 & 6. Measured and calculated temperatures, relevant for the tested specimen at the failure times, as well as measured and calculated failure times.

****** As a conclusion an improved set of formulations for λ_c the thermal conductivity, c_c the specific heat and also ρ_c the density of concrete in function of the temperature obtained in the concrete was developed in May-June 2002.

Of course recalculations, on the basis of numerical simulations, have been done again by the chairman of the project team for prEN1994-1-2 beginning of June 2002, similar to those explained before.

The first set of calculations was done with

* the specific heat $c_{c,\theta}$ according to 3.3.2(1) of prEN1992-1-2; the 4 corresponding equations give the red points in figure 18 which the present author has simulated by a 2nd order equation representing quite well the before mentioned 4 equations:

$$c_{c,\theta} = 890 + 56,2(\theta_c / 100) - 3,4 (\theta_c / 100)^2,$$

** the density $\rho_{c,\theta}$ according to 3.3.2(3) of prEN1992-1-2 given by 4 equations, was also simulated by a 2nd order equation as given on figure 18 and as follows:

$$\rho_{c,\theta} = 2365,5 - 33,62(\theta_c / 100) + 0,77(\theta_c / 100)^2,$$

*** after a certain number of test calculations, the **upper limit of the thermal conductivity**, given in figure 19, was found:

$$\lambda_{c,\theta} = 2 - 0,2451(\theta_c / 100) + 0,0107(\theta_c / 100)^2 \quad (5a)$$

With this set of formulations the correspondence between test and simulation results is perfect as recorded in tables 7 and 8. Note that figure 19 also contains

° $\lambda_{c,\theta}$ according to EC4- Part10 from 1990, which together with $c_{c,\theta}$ from 1990 and $\rho_{c,\theta} = \text{constant}$ gave the best correlation with test results (see also tables 5 and 6),

°° **lower limit for $\lambda_{c,\theta}$** from 3.3.3(2) of prEN1992-1-2 given by

$$\lambda_{c,\theta} = 1,36 - 0,136(\theta_c / 100) + 0,0057(\theta_c / 100)^2 \quad (5b)$$

The 2nd set of calculations was done with the same equations as before but

* $\rho_{c,\theta} = \text{constant} = 2350 \text{ kg/m}^3$,

** temperatures & fire resistance times were compared to the 12 tests as shown in tables 7 and 8. The fact to take a constant density leads to safe results, as in a mean the critical temperature is only decreased by 2% and the fire resistance time increased by 1 to 6 minutes.

The 3rd set of calculations was done with exactly all the parameters according to prEN1992-1-2 of June 2002, which means that the lower limit of $\lambda_{c,\theta}$ given in 3.3.3(2) was activated. This leads, according to tables 7 and 8, in a mean to a critical temperature decrease of ~10% and a fire resistance time increase of ~7%, compared to measured values. This is still unsafe but is an improvement compared to tables 5 and 6.

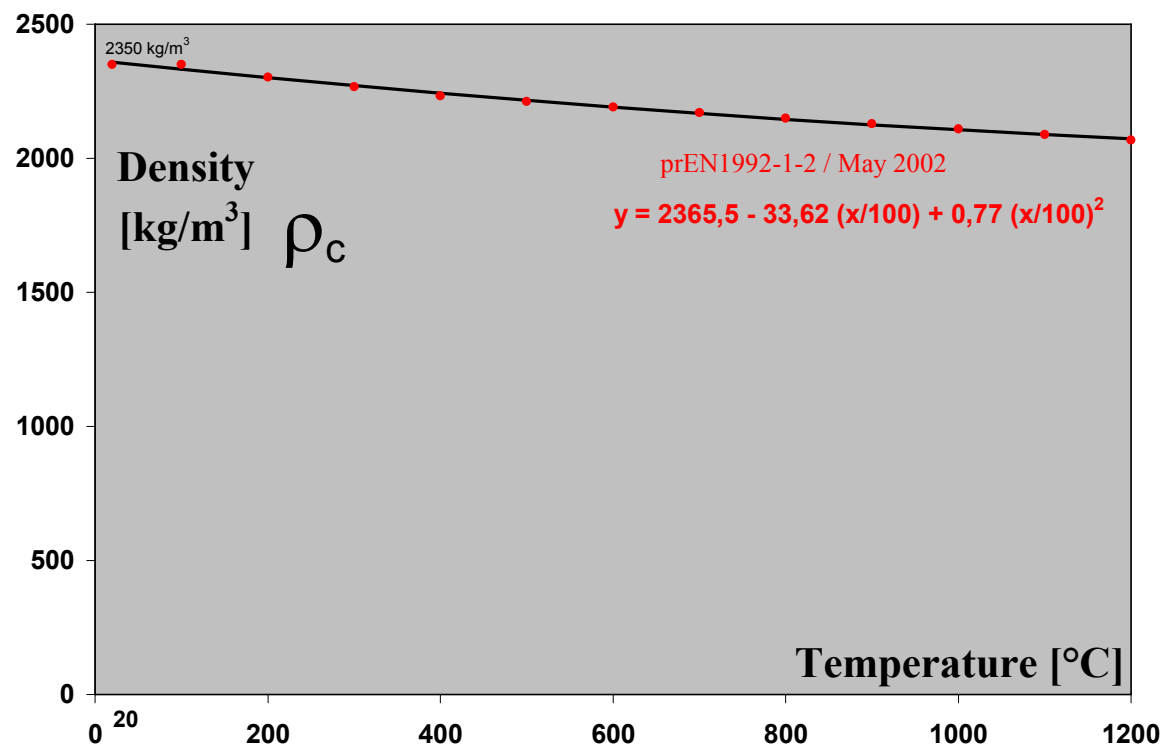
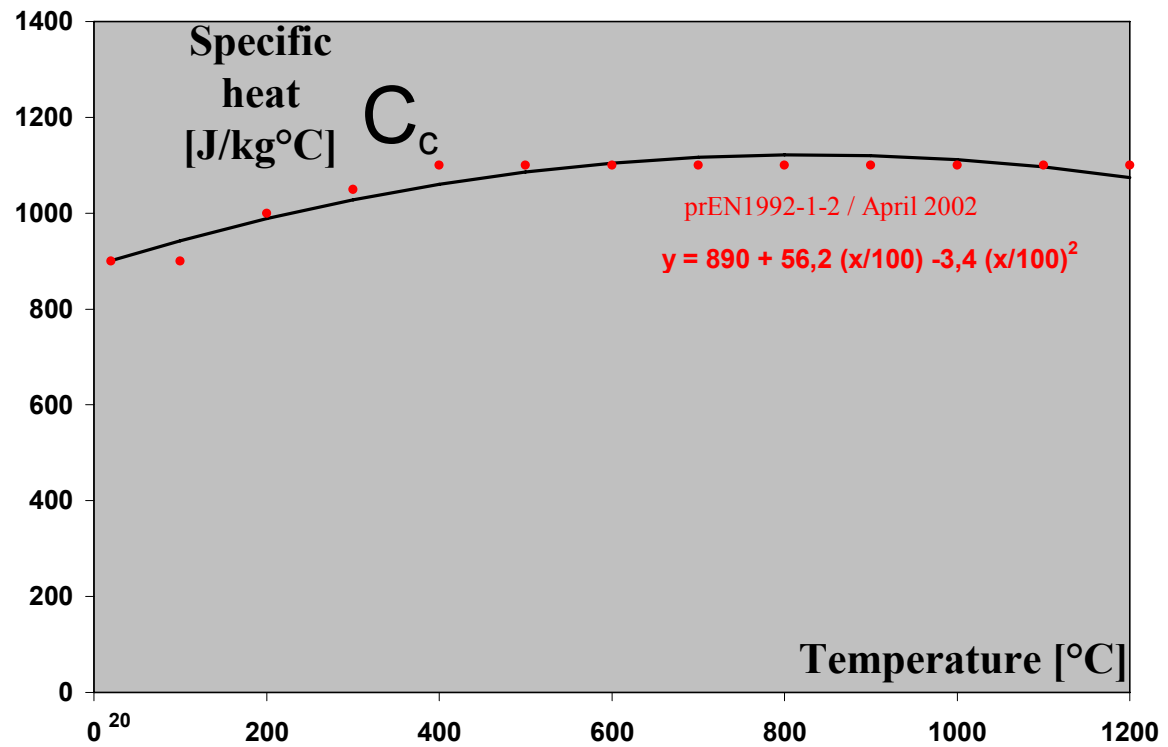


Figure 18. Specific heat proposed in April 2002 and density of concrete proposed in May 2002.

For ρ_c the density of concrete in function of the temperature the following is suggested:

- * 2nd order equation, in figure 18, is easier to handle than 4 linear equations,
- ** but figure 18 shows that this variation could also be represented by a simple line as given by equation (10a).
- *** according to the 2nd set of calculations (see tables 7 and 8), the fact to keep ρ_c the density of concrete constant as 2350 kg/m^3 has a rather small influence on failure times (increase of 1 to 6 minutes).
- **** furthermore according to 3.3.2(3) of prEN1992-1-2, $\rho_{c,\theta}$ decreases from 2350 kg/m^3 at 20°C to 2073 kg/m^3 at 1200°C , which corresponds to a density reduction of $\sim 12\%$ or 280 l/m^3 . However in practical tests, we have performed, this water content was normally 40 l/m^3 and only exceptionally reached 120 l/m^3 .

Hence equation in 3.3.2(3) of prEN1992-1-2 should be modified to give less weight reduction due to water loss, or which would be better, **forget about this temperature variation and take $\rho_{c,\theta} = \text{constant} = 2350 \text{ kg/m}^3$** .

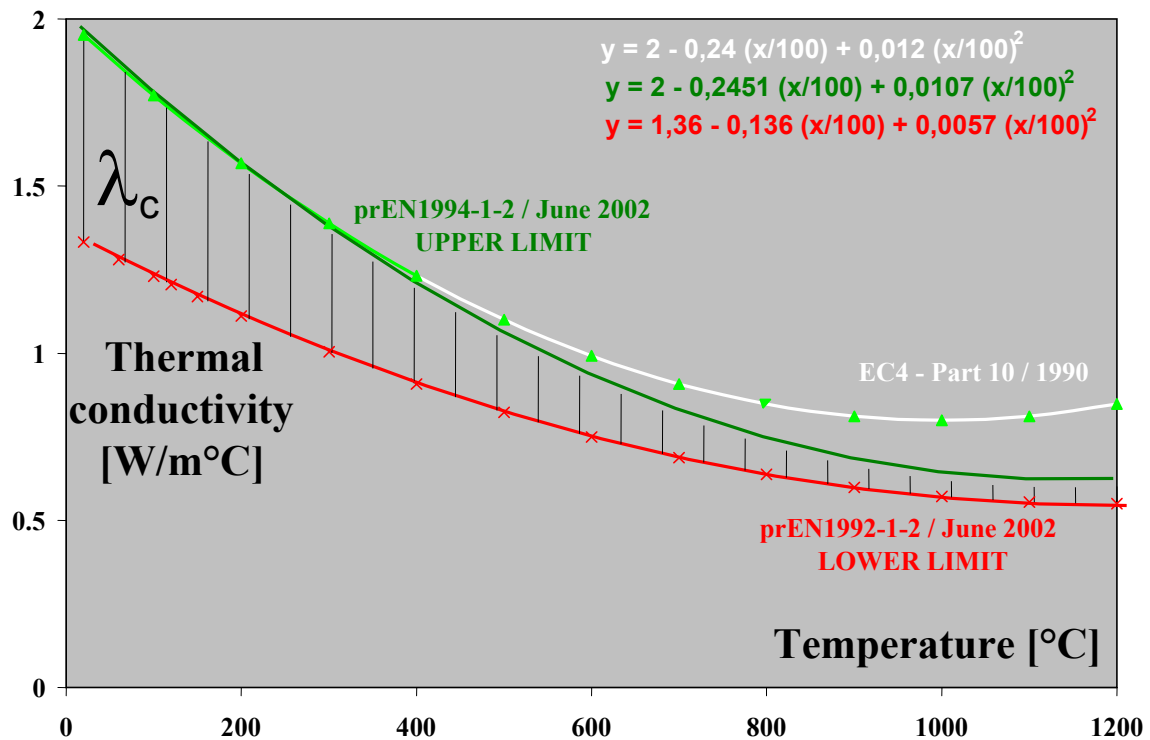


Figure 19. Upper and lower limits for the thermal conductivity of concrete as chosen in June 2002, compared to the formulation in 1990.

Chapter V - Properties of materials

	Measured Relevant T° [°C] at failure	Calculated T° EC4-1-2/ June 2002/ Upper Limit of λ_c	$\frac{T^{\circ}_{\text{calculated}}}{T^{\circ}_{\text{measured}}}$	Calculated T° EC4-1-2/ June 2002/ Upper Limit of $\lambda_c / \rho_c = C^t$	$\frac{T^{\circ}_{\text{calculated}}}{T^{\circ}_{\text{measured}}}$	Calculated T° EC2-1-2/ 06-06-2002/ Lower Limit of λ_c	$\frac{T^{\circ}_{\text{calculated}}}{T^{\circ}_{\text{measured}}}$
C 1.3	490	504	1,03	495	1,010	455	0,929
C 1.15	570	594	1,042	584	1,025	555	0,974
C 1.4	450	469	1,042	460	1,022	417	0,927
B 2.11	635	614	0,967	603	0,95	570	0,898
B 2.12	740	722	0,976	710	0,96	684	0,924
B 2.13	670	637	0,95	626	0,934	594	0,887
B 2.14	375	400	1,067	386	1,029	351	0,936
C 1.5	435	423	0,972	416	0,956	363	0,834
C 1.6	440	409	0,93	402	0,914	348	0,791
C 1.7	360	382	1,061	377	1,047	330	0,917
C 1.8	345	361	1,046	357	1,035	310	0,899
B T3	425	425	1,0	418	0,983	369	0,868
mean			1,007		0,989		0,899
standard deviation			0,045		0,043		0,047

Test number	Measured Failure Time [min]	Calculated Failure Time EC4-1-2/ June 2002/ Upper Limit of λ_c	$\frac{t_{\text{calculated failure}}}{t_{\text{measured failure}}}$	Calculated Failure Time EC4-1-2/ June 2002/ Upper Limit of $\lambda_c / \rho_c = C^t$	$\frac{t_{\text{calculated failure}}}{t_{\text{measured failure}}}$	Calculated Failure Time EC2-1-2/ 06-06-2002/ Lower Limit of λ_c	$\frac{t_{\text{calculated failure}}}{t_{\text{measured failure}}}$
C 1.3	116	118	1,017	121	1,043	130	1,121
C 1.15	189	161	0,852	165	0,873	175	0,926
C 1.4	172	156	0,907	160	0,93	162	0,942
B 2.11	171	179	1,047	183	1,07	187	1,094
B 2.12	244	232	0,951	238	0,975	242	0,992
B 2.13	178	192	1,079	196	1,101	202	1,135
B 2.14	92	97	1,054	98	1,065	106	1,152
C 1.5	136	126	0,926	129	0,948	137	1,007
C 1.6	120	123	1,025	125	1,042	130	1,083
C 1.7	111	115	1,036	117	1,054	132	1,189
C 1.8	157	138	0,879	140	0,892	155	0,987
B T3	120	129	1,075	131	1,092	143	1,192
mean			0,987		1,007		1,068
standard deviation			0,077		0,076		0,09

Tables 7 & 8. Measured temperatures and failure times compared to the corresponding calculated temperatures and failure times for the upper limit of the thermal conductivity with first and 2nd set of calculations, and for the lower limit of the thermal conductivity with 3rd set of calculations.

6.2 Application to the mechanical properties of steel

Mechanical properties of structural steels, as given in 3.2.1 and Annex A of prEN1994-1-2 [11], were developed among others by [4] on the basis of a set of 29 transient state bending tests performed on IPE 80 steel beams. These tests done by GST-KRUPP, "Gesellschaft für Systemtechnik mbH" during 1988 to 1989 [3], were published in [5].

These test specimen were based on the following yield point and tensile strength:

- 12 beams S1 to S12 with $f_{ay,20^{\circ}\text{C}} = 514 \text{ N/mm}^2$ and $f_{au,20^{\circ}\text{C}} = 663 \text{ N/mm}^2$,
- 10 beams N1 to N10 with $f_{ay,20^{\circ}\text{C}} = 346 \text{ N/mm}^2$ and $f_{au,20^{\circ}\text{C}} = 523 \text{ N/mm}^2$,
- 7 beams V1 to V7 with $f_{ay,20^{\circ}\text{C}} = 312 \text{ N/mm}^2$ and $f_{au,20^{\circ}\text{C}} = 504 \text{ N/mm}^2$.

* Tests contained 3 specimen tested under ambient temperature, and 26 specimen submitted to a uniform temperature field in the beams increasing linearly, by 3,2 to 3,5°C per minute, from 20°C to the critical temperature θ_{pl} corresponding to the formation of a plastic hinge at mid-span.

All specimen were loaded by a single force "F" at mid-span, which remained constant during the heating process, but was varying from test to test. Hence the following load level range was covered

$$1,38 \geq F / F_{pl,cold} \geq 0,05 \quad (23)$$

with $F_{pl,cold}$ the force applied at mid-span for which a plastic hinge forms under ambient temperature. This permitted to find the relation between $F / F_{pl,cold}$ and θ_{pl} .

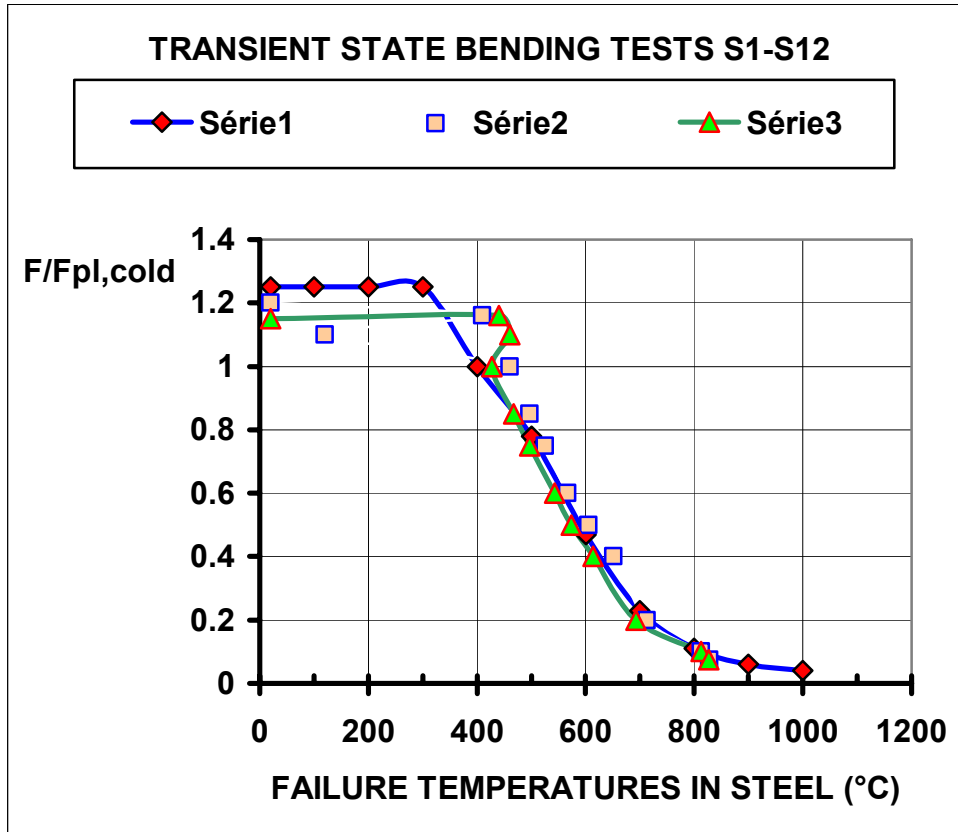


Figure 20. Measured (série 2) and calculated (série 3) failure temperatures for test-specimen S1 to S12 [3, 4, 5] compared to the corresponding temperatures of the reduction factors $k_{y,\theta}$ and $k_{u,\theta}$ of table 3 (série 1).

However it was necessary to find the correspondence between $(F / F_{pl,cold}) = X(\theta_{pl})$ and $(f_{ay,\theta} / f_{ay,20^\circ C}) = Y(\theta)$.

Knowing that under ambient temperature a plastic hinge gives $M_{pl} = W_{pl} \cdot f_{ay,20^\circ C}$ and for a mid-span loaded simple supported beam $M_{pl} = F_{pl,cold} \cdot (L/4)$ we obtain $f_{ay,20^\circ C} = F_{pl,cold} \cdot (L/4) / W_{pl}$

For high temperatures we have in a similar way:

$$M_{pl,\theta} = W_{pl} \cdot f_{ay,\theta}; \quad M_{pl,\theta} = F \cdot (L/4) \quad \text{and} \quad f_{ay,\theta} = F \cdot (L/4) / W_{pl}.$$

This gives

$$(f_{ay,\theta} / f_{ay,20^\circ C}) \equiv (F / F_{pl,cold}) \quad (24)$$

which means that the effective yield strength $f_{ay,\theta}$, function of the temperature, may be determined by these transient state bending tests. Furthermore as the load level $F / F_{pl,cold}$ was tested up to 1,38 even the maximum stress level of structural steel in function of the temperature - strain hardening included - may be covered (see figure 20). This development was in fact one important source for the choice of the reduction factors $k_{y,\theta}$ and $k_{u,\theta}$ given in Table 3.

In fact table 3 is essentially based on transient state bending test specimen based on the steel grade S460. However lower steel grades, with a higher ratio $(f_{au,20^\circ C} / f_{ay,20^\circ C})$, lead to larger reduction factors. This was not considered in table 3 valid for all steel grades S235 to S460; hence its use is on the safe side.

****** It has to be mentioned that all 29 tests have been simulated through the thermo-mechanical soft CEFICOSS which permitted to determine the critical temperature θ_{pl} corresponding to the formation of a plastic hinge at mid-span for the different load levels. One example is given in figure 21 for the load level $F / F_{pl,cold} = 1,0$.

This shows that for load level $F / F_{pl,cold} = 1,0$

- ° the test S1 gave $\theta_{pl} = 461^\circ C$
- °° the simulation gives $\theta_{pl} = 428^\circ C$
- °°° and table 3 gives $\theta_{pl} = 400^\circ C$.

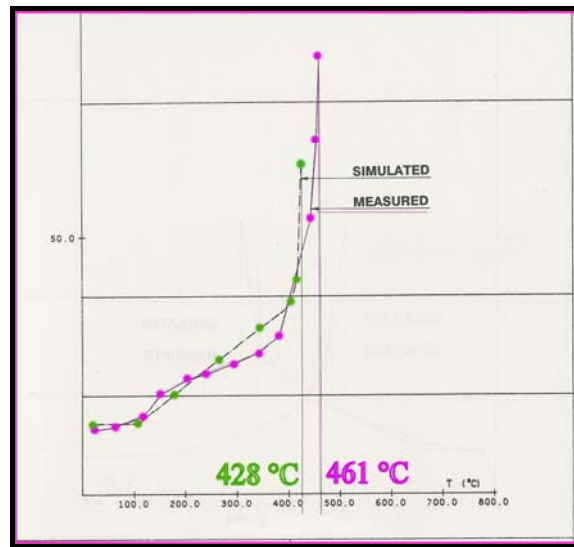


Figure 21. Measured and calculated deformation at mid-span in mm, in function of the steel temperature, for test S1 with the load level $F / F_{pl,cold} = 1,0$.

*** Another interesting aspect is the initial choice of a quadrolinear idealization of the stress-strain relationship of structural steel at elevated temperatures as presented in [5], and which might be considered as the forerunner of figure 14. Figures 22 and 23 show this quadrolinear idealization at 20°C and 400°C.

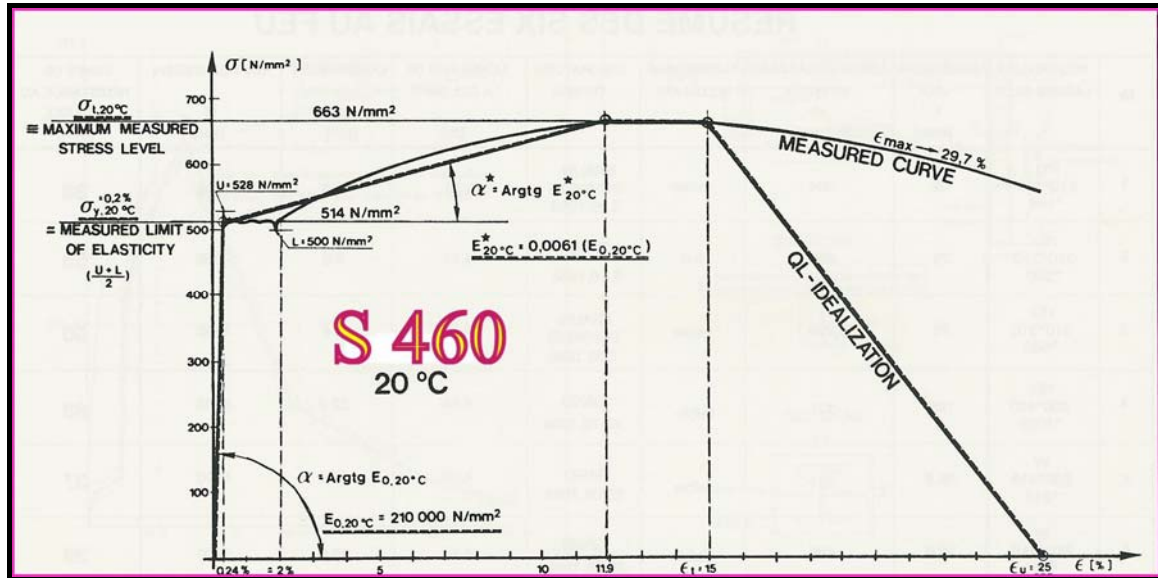


Figure 22. Stress-strain relationship of structural steel S460 under ambient temperature.

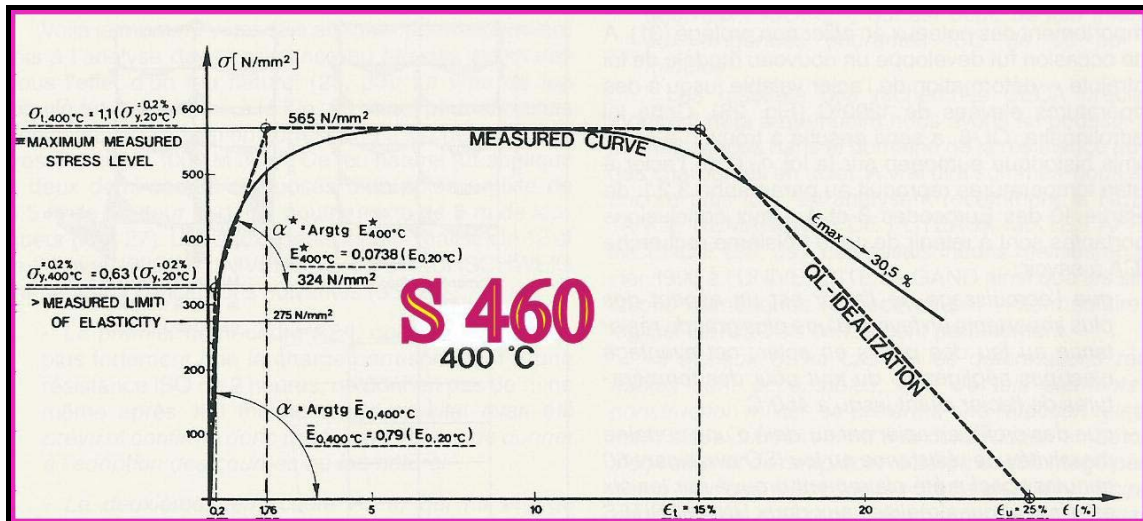


Figure 23. Stress-strain relationship of structural steel S460 at 400°C.

REFERENCES

- [1] Minne R., Vandeveld R., Odou M.; Fire test reports N° 5091 to 5099, Laboratorium voor Aanwending der Brandstoffen en Warmte-overdracht. Gent, University 1985.
- [2] Kordina K., Hass R.; Untersuchungsbericht N°85636, Amtliche Materialprüfanstalt für das Bauwesen. TU Braunschweig 1985.
- [3] GST-Krupp, Gesellschaft für Systemtechnik mbH. Traglastversuche an Trägern IPE 80 im kalten Zustand und unter Temperaturbelastung; Untersuchungsbericht U-Nr. 338/89, Essen, 21.11.1989.
- [4] Schleich J.B; Maximum stress level of structural steel in function of the temperature - strain hardening included - through numerical simulations of uniformly heated steel beams during transient state bending tests. Working documents, Luxembourg, 1988-1989.
- [5] Cajot L.G., Chantrain Ph., Mathieu J., Schleich J.B.; REFAO III, Practical design tools for unprotected steel columns submitted to ISO-fire / C.E.C. Research 7210-SA/505 1986/88. Final Report EUR 14348 EN, Luxembourg, 1993.
- [6] Schleich J.B., Kruppa J., Newman G., Twilt L.; ECCS Model Code on Fire Engineering ECCS Technical Note N° 111-First Edition, Brussels, May 2001.
- [7] Schleich J.B; Concrete material properties checked through numerical simulations of real ISO-fire resistance tests. Working documents, Luxembourg, May - June 2002.
- [8] CEN; EN1991-1-2 , Eurocode 1 – Actions on structures , Part 1.2 – Actions on structures exposed to fire. CEN Central Secretariat, Brussels, DAV 20.11.2002.
- [9] CEN; prEN1993-1-2, Eurocode 3 – Design of steel structures, Part1.2 – General rules – Structural fire design. CEN Central Secretariat, Brussels, Stage 49 draft, June 2004.
- [10] CEN; EN1992-1-2, Eurocode 2 – Design of concrete structures, Part1.2 – General rules – Structural fire design. CEN Central Secretariat, Brussels, December 2004.
- [11] CEN; prEN1994 -1-2, Eurocode 4 – Design of composite steel and concrete structures, Part1.2 – General rules – Structural fire design. CEN Central Secretariat, Brussels, Stage 49 draft, December 2004.

CHAPTER VI - EXAMPLE OF A REINFORCED CONCRETE STRUCTURE

Angel Arteaga¹, Luque Rodriguez² and Jean-Baptiste Schleich³

^{1,2} Institute of Construction Sciences 'E. Torroja', CSIC, Madrid

³ University of Technology Aachen, University of Liège

Summary

This chapter shows an example of the design of a reinforced concrete structure for the fire situation. It concentrates on the determination of temperatures inside concrete cross-sections and how the increase of those temperatures affects the strength of the structural elements. Some information is given on the loads and load effects at normal temperatures in order to determine the safety in case of fire. Examples of the calculation of concrete structures of buildings at normal temperatures are given in Handbook 3, Load Effects for Buildings.

1 INTRODUCTION

In the present example the behaviour of a reinforced concrete building structure is analysed for the fire situation according to the Eurocodes. The normal procedure for the verification of a structure, in this situation, is first to design the structure at normal temperature, then to verify it for the fire situation.

For the normal temperature design the following standards are mainly taken into account: for the safety criteria, the EN 1990, Basis of structural design [1]; for the loads and load effects to be considered the EN 1991-1-1, Actions on structures i.e. densities, self-weight and imposed loads for buildings [2]; for the determination of the structural strength of elements the EN 1992-1-1, Design of concrete structures, general rules and rules for buildings [3]. For the verification in the fire situation we will take account also of the EN 1991-1-2, Actions on structures exposed to fire [4] and of the EN 1992-1-2, Design of concrete structures, structural fire design [5].

In this example the part of the design corresponding to the normal temperature is skipped, as supposed having been done before, and only the details needed for the design in case of fire are given. Detailed design of concrete structures for buildings can be found in Handbook 3, Load Effects for Buildings.

2 DESIGN CONDITIONS

2.1 Building characteristics

The building considered has six storeys, each with 3 m height, used as offices plus a ground floor of 3,5 m height with retail shops. Hence the evacuation height of the building is 18,5 m. This building is located in the centre of Madrid. It is represented on figure 1.

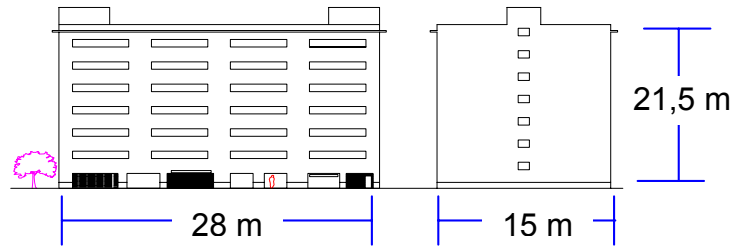


Figure 1. Building layout.

Every storey forms a fire compartment. The floor area of each compartment is $28 \times 15 = 420 \text{ m}^2$ and every compartment has four openings $5 \times 1,5 \text{ m}^2$ in each main façade.

2.2 Structural characteristics

The building structure is formed by four vertical and plane rectangular frames, at 5 m each, connected by tie beams and floors. Each frame forms four 7 m long bays and 6 storeys of 3,0 m height and the ground floor of 3,5 m height. The floor is formed by 200 mm thick hollow core slab covered by a 50 mm thick in situ concrete layer.

The reinforced concrete structure is composed of the concrete quality C 25/30 based on siliceous aggregates and reinforced by hot rolled bars S 235.

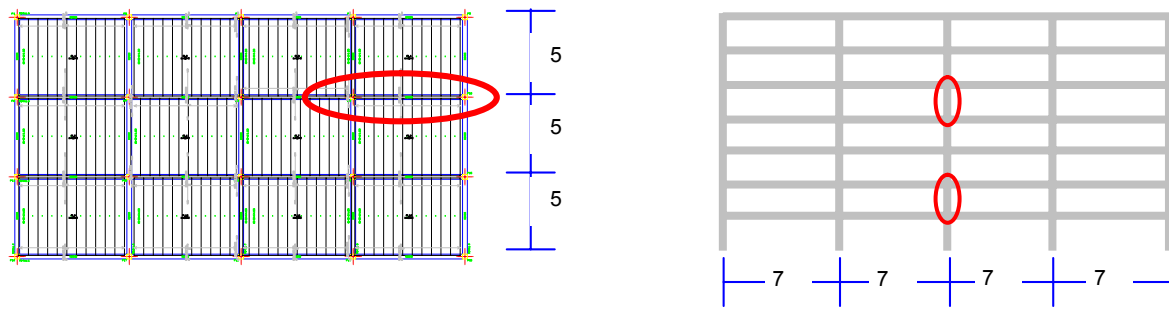


Figure 2. Frames and floors distributions

The self-weight of the floor, hollow core slab plus concrete layer, is $4,45 \text{ kN/m}^2$. The density of the concrete is taken as 25 kN/m^3 ([2]).

2.3 Definition of the Limit state equation

Due to the simplified procedures used in the reliability evaluation of the concrete structure in case of fire, a member analysis will be performed in this example. Hence examples referred to beams and columns will be shown, using tabulated data and simple calculation models as indicated in the figure to the Foreword of [4].

The Limit state equation will be defined in the strength domain, according to 2.5 of [4]. That is:

$$R_{fi,d,t} \geq E_{fi,d,t} \quad (1)$$

where :

- $R_{fi,d,t}$ is the design value of the resistance of the member in the fire situation at time t ;
- $E_{fi,d,t}$ is the design value of the relevant effect of actions in the fire situation at time t .

These two terms will be defined in the following paragraphs. In order to obtain the action effects we need to take account of two kinds of actions: the static loads derived from the normal use of the building and the thermal loads due to the fire situation. Thermal actions may be obtained from National requirements, from Eurocodes or through Fire engineering.

The resistance of the member may be obtained either by using tabulated data, which means we may obtain the minimum dimensions of the cross section, including the value for the concrete cover, that assure enough resistance to withstand a design fire defined in terms of the standard temperature-time curve and for a specified time. The resistance of the member may be also be obtained by using simple calculation models, that allow to obtain the resistance of the cross section taking account of the temperatures reached in the different parts of the section, at a specified time and for a heating by the standard fire.

2.4 Combination of actions

2.4.1 Permanent situation for normal temperature design

Due to the simple structure and characteristics of the building, only the permanent and imposed loads are considered in the design whereas wind, earthquake or other variable actions are not considered. Therefore, the equation 6.10 of [1] for permanent situations is limited to:

$$\sum_{j \geq 1} \gamma_{G,j} G_{k,j} + \gamma_{Q,1} Q_{k,1} ; \quad (2)$$

where

- $\gamma_{G,j}$ is the partial factor for permanent actions; recommended value 1,35
- $\gamma_{Q,1}$ is the partial factor for imposed loads; recommended value 1,50
- $G_{k,j}$ are the characteristic values of permanent loads and
- $Q_{k,1}$ is the characteristic value of imposed load.

The characteristic values of the loads are given in table 1.

Table 1. Characteristic values of loads

Load	Value	Characteristic value [kN/m]
Floor	4,45 x 5,0	22,25
Beams	0,3 x 0,6 x 25,0	4,50
Other permanent	1,00 x 5,0	5,00
Total permanent		$g_k = 31,75$
Offices	3,0 x 5,0 (Table 6.2 [2])	15,00
Movable partitions	0,8 x 5,0 (6.3.1.2 [2])	4,00
Total imposed loads		$q_k = 19,00$

The design is carried out on the basis of the values given in table 1. All the inner beams in every floor, but for the roof, have the same cross section 300mm x 600 mm and the lower reinforcement comprises 5 Φ 16mm steel bars and Φ 8 mm stirrups. The minimum cover is taken as 20 mm. This cover means a distance from the bottom of the beam to the axis of the bars of 36 mm, i.e. $(20 + 8 + 1/2 \cdot 16 = 36)$, and the same for the distance from the side of the beam to the axis of the corner bars. A quarter of this cross section is depicted in figure 3a.

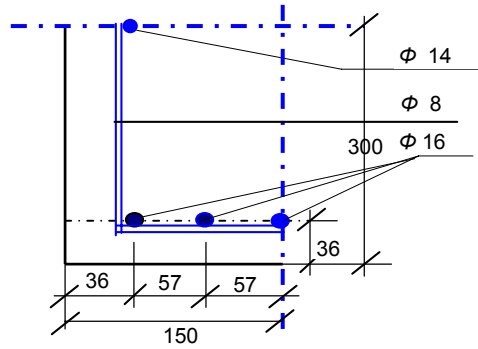


Figure 3a. Cross section of the beam

The cross sections of the columns vary as a function of their position and of the height considered. The worst cases will be studied i.e. the central column of the inner frames at the first and at the fourth floor. The cross sections obtained from the normal temperature design are shown in figure 3b, as given by the computer design program with dimensions in centimeters, but bar diameters in millimeters. With the same nominal cover of 20 mm than in beams, this leads to distances of the axis of the main rebar to the concrete border of 41 mm i.e. ($\approx 20 + 8 + 1/2 \cdot 25$) for the 400x400 cross-section and of 36 mm i.e. ($20 + 6 + 1/2 \cdot 20$) for the 300x300 cross-section. Table 2 contains the critical load effects under normal temperature for this central column at the first and at the fourth floor.

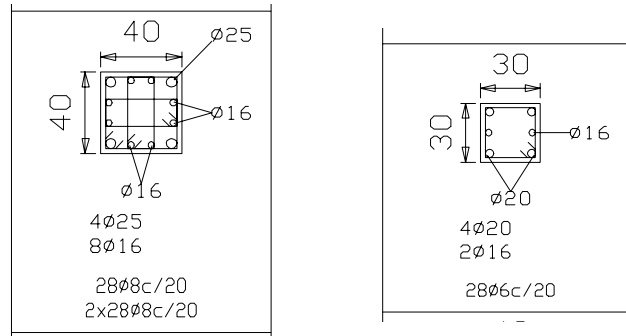


Figure 3b. Cross-section 400mm x 400 mm and 300mm x 300 mm of the column studied

Table 2. Load effects on the column at first and fourth floor

Column	Floor	Height m	Load	N kN	Mx kN m	My kN m	Q x kN	Qy kN	T kN m
P 7	4	12.50/14.65	permanent variable	740,6 433,7	-1,4 -0,9	-0,3 -0,8	-1,6 -0,9	-0,3 -0,7	-0,0 -0,0
	1	3.50/5.65	permanent variable	1 469,5 851,4	-2,3 -1,5	-0,5 -0,3	-1,5 -1,0	-0,5 -0,3	-0,0 -0,0

2.4.2 Accidental situation in the fire situation

The load combination for accidental situation is given in [1] as:

$$\sum_{j \geq 1} G_{k,j} + P + A_d + (\Psi_{1,1} \text{ or } \Psi_{2,1}) Q_{k,1} + \sum_{i > 1} \Psi_{2,i} Q_{k,i} ; \quad (3)$$

without defining the coefficient of combination to be applied, letting this task to the different parts of EN 1991 or to the National authorities. In [4] the value $\Psi_{2,1}$ is recommended and it will be used in this example. Given that no other variable loads than imposed ones are considered, the combination of actions finally will be:

$$\sum_{j \geq 1} G_{k,j} + A_d + \Psi_{2,1} Q_{k,1} \cdot \quad (4)$$

For the sake of simplification a reduction factor is defined in EN 1992-1-2 [5] indicating the relationship between the load effect for the fire situation (4) and the load effect for the normal temperature design (2):

$$\eta_{fi} = \frac{G_k + \Psi_{2,1} Q_{k,1}}{\gamma_G G_k + \gamma_{Q1} Q_{k,1}} = 0,53 \quad (5)$$

The value of $\Psi_{2,1}$ for offices is given as 0,3 in Annex A of [1].

3 DESIGN FIRE

In order to consider the design fire, we will consider in this example two different possibilities. First we will consider the Spanish National requirement for that type of occupation and building height and we will compare the results with those obtained with the use of the equivalent time of fire exposure given in the Annex F of [4].

3.1 National requirements

The Spanish Technical Building Code [6] gives the fire resistance requirements according to table 3 for the different occupancies and evacuation heights.

Table 3. Required fire resistance for structural elements

Occupancy	Building evacuation height h_e			
	Basement	<15 m	$15m \leq h_e < 28$ m	≥ 28 m
Dwelling (detached and semi-detached)	R 30	R 30	-	-
Dwelling (flats), School, Office	R 120	R 60	R 90	R 120
Shopping, Hospital	R 120 ⁽¹⁾	R 90	R 120	R 180
Parking	R 90			

⁽¹⁾NOTE : R180 for buildings with evacuation height ≥ 28 m

Therefore, in our case we have to guarantee an R90 fire resistance in the office floors of our structure.

3.2 Equivalent time of fire exposure

The equivalent time of standard fire exposure is given in Annex F of EN1991-1-2. This time represents the time needed, for a fire following the standard temperature-time curve defined in 3.2.1 [4], to produce the same temperature effect in the element than the real fire.

In the case of concrete elements submitted to bending it corresponds to the time when the lower tension reinforcement reaches the same temperature during the standard fire than the maximum temperature obtained in the reinforcement for the real fire.

To obtain this value we need to take account of the parameters that affect a real fire. This comprises the fire load, the amount of ventilation and the thermal properties of the enclosure surfaces of the compartment. The corresponding formula is:

$$t_{e,d} = (q_{f,d} \cdot k_b \cdot w_f) k_c \quad (6)$$

The parameters of this formula correspond to:

- $q_{f,d}$ the design value of the fire load,
- k_b the conversion factor depending on the thermal properties of the enclosure,
- w_f the ventilation factor,
- k_c the correction factor function of the material composing structural cross-sections (concrete or steel protected or not).

The procedure for obtaining the design fire load is indicated in Annex E [4]. Table 4 shows the values obtained in a spreadsheet for this example.

Table 4. Calculation of the equivalent time of standard fire exposure

Equivalent time of fire exposure						
$t_{e,d} = (q_{f,d} \cdot k_b \cdot w_f) k_c$						
Design fire load density, $q_{f,d} =$	625	MJ/m ²				
			$k_c =$	1 for concrete or protected steel		
$k_b =$	0,07			13,7*0 for unprotected steel		
For small compartments $A_f < 100\text{m}^2$				Floor area, A_f	420	m ²
				vertical openings, A_v	60	m ²
$O_{1/2}$	3,835			horizontal openings, A_h	0	m ²
$A_f \cdot$	420			Height of the compartment, H	2,8	m
$1./A_t$	0,000925					
				$\alpha_v = A_v/A_f =$	0,143	
$w_f = O_{1/2} A_f / A_t =$		1,49		$\alpha_h = A_h / A_f =$	0	
				$b_v = 12,5(1 + 10 \cdot \alpha_v - \alpha_v^2) > 10,0$	30,12	
				$w_f = (6,0/H)^{0,3} [0,62 + 90(0,4 - \alpha_v)^4 / (1 + b_v \cdot \alpha_h)]$	1,273	
$t_{e,d} =$	65	min		$t_{e,d} =$	56	min
Not applicable						
For concrete and protected steel				For concrete and protected steel		

As an illustration of the background of this equivalent time of fire exposure, the standard fire curve and the parametric curve, obtained according to Annex A of EN1991-1-2 for the fire parameters used in this example, are represented in figure 4. From the figure it can be seen that the parametric fire is more “violent” than the standard fire at the beginning of the fire. It reaches high temperatures in a few minutes, but it decays very quickly due to the large ventilation of the compartment permitting to consume rather quickly all the fire loads. The equivalent time of standard fire exposure does not correspond to the maximum temperature in the parametric curve neither to any determined point in these curves, as it is determined by the heating up of reinforcement bars.

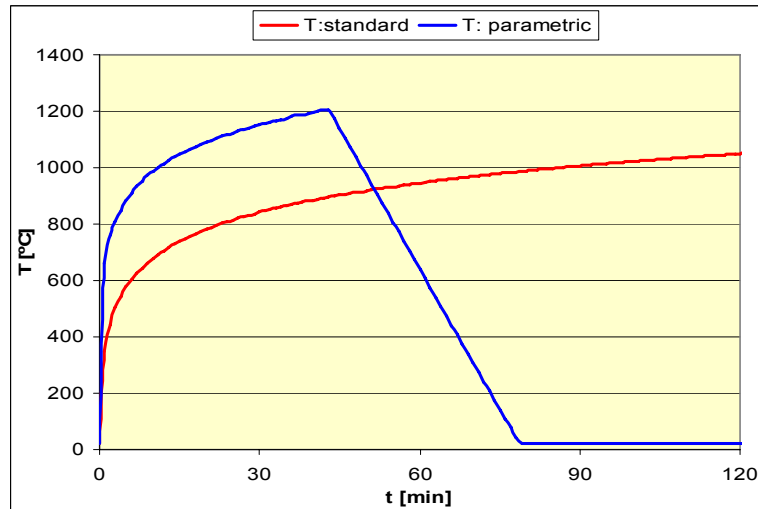


Figure 4. Standard and parametric fire curves

4 FIRE RESISTANCE DESIGN

4.1 Tabulated data design

The simplest way that EN1992-1-2 [5] provides for the verification of the fire resistance is the Tabulated data approach. This permits, for the required fire resistance time according to the standard fire curve i.e. 30, 60, 90, 120, 180 or 240 minutes, to give the minimum dimensions of the cross-section and the minimum distance of the axis of the rebars to the border of the section. This verification is on the safe side and it is not needed to take account of indirect actions or other effects.

4.1.1 Beams

The tabulated data are valid for beams exposed to fire on three sides following 5.6.1 of EN 1992-1-2. In the case of rectangular beams the application is straightforward.

The table 5.6 of EN 1992-1-2 gives for continuous beams and a required fire resistance of R 90 the following minimum dimensions. The beam width b_{min} should be 250 mm and the concrete cover from the side or bottom of the beam to the axis of the rebar a should be 25 mm. The side cover a_{sd} has to be increased by 10 mm for the corner bar in beams with one layer reinforcement, according to 5.6.1 (8) of EN1992-1-2.

These minimum dimensions are satisfied by the normal temperature design described in figure 3a. No modification of the geometry of the beams is needed for the fire resistance design.

4.1.2 Columns

For columns two methods are provided. The method A of 5.3.2 in EN1992-1-2 may be applied if:

- $l_{0,fi} < 3m$. In this case the columns are quite short as $l_{0,fi} = 0,5 \times 3 = 1,5m$.
- first order eccentricity $e = M_{0Ed,fi} / N_{0Ed,fi} < e_{max} = 0,15 h = 0,045m$ for the small column of figure 3b. From the values given in table 2 we get $e \approx 0,002m < 0,045m$.
- the amount of reinforcement $A_s < 0,04 A_c = 3600 \text{ mm}^2$ for the small column of figure 3b. From the same figure we know the reinforcements foreseen by 4 Φ 20mm and 2 Φ 16mm which gives $A_s = 1658 \text{ mm}^2 < 3600 \text{ mm}^2$.

Therefore method A will be applied. Table 5.2a of EN1992-1-2 gives the following minimum dimensions for R 90 and for $\mu_{fi} = 0,5 \sim \eta_{fi}$ of equation (5):

- for the column width $b_{min} = 300 \text{ mm}$ and the axis distance to concrete border of rebars 45mm, or 400 mm and 38 mm respectively,
- this minimum cover is not satisfied for the column of 300mm x 300mm which has an axis distance for rebars of only 36 mm.

If however we consider the resistance R60 given by the equivalent time of fire exposure of 56 minutes according to table 4, instead of R 90, the minimum cover for this column would be 31 mm as obtained from table 5.2a of EN1992-1-2. So if the natural fire described under 3.2 is considered, the normal temperature design would entirely satisfy the fire resistance requirement.

4.2 Temperature analysis

In order to apply the simple calculation models given in 4.2.1 of EN1991-1-2 [5] the temperature in the cross section of beams and columns has to be determined. In Annex A, Temperature Profiles, of EN1991-1-2 the isotherms are given for different dimensions of concrete cross-sections and different specified times under standard heating conditions. Thanks to these isotherms it is possible to define the maximum temperatures reached in any point of the cross-section for the required fire duration. We will use for the beams the isotherms of a cross section of 300mmx600mm, and for the columns the isotherms of cross sections of 300mmx300 mm and 400mmx400 mm. This is being done for R90 and R60 min, this last fire class corresponding approximately to the equivalent time of fire exposure of 56 minutes.

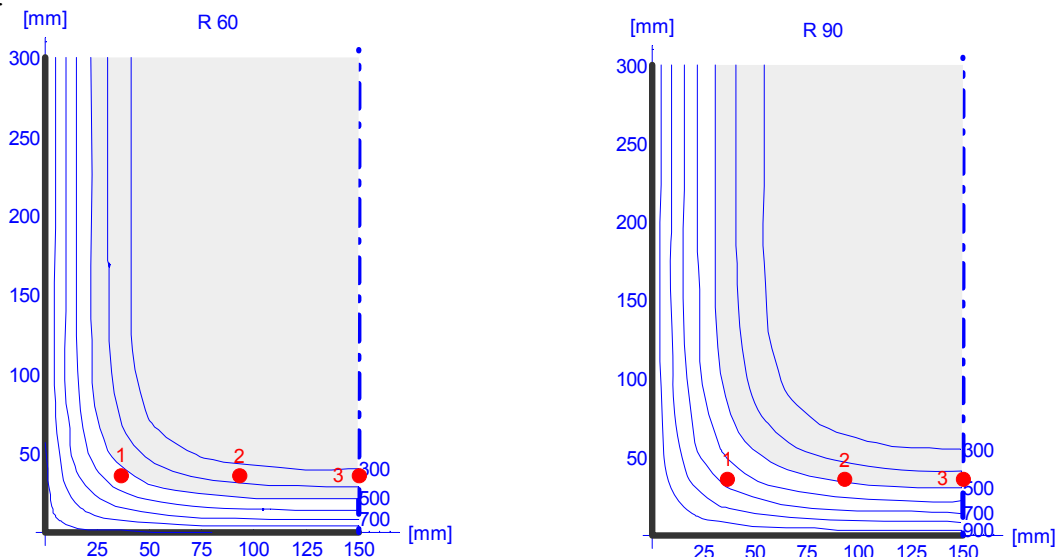


Figure 5. Isotherms of the beam cross-section 300mmx600mm for 60 and 90 minutes.

The 60 and 90 minutes isotherms following heating of the cross-sections by the standard temperature-time curve are represented in the figures 5 to 7. The position of the reinforcing steel bars are represented but the diameter of the rebar is not at scale. Furthermore the areas corresponding to temperatures below 500°C are highlighted.

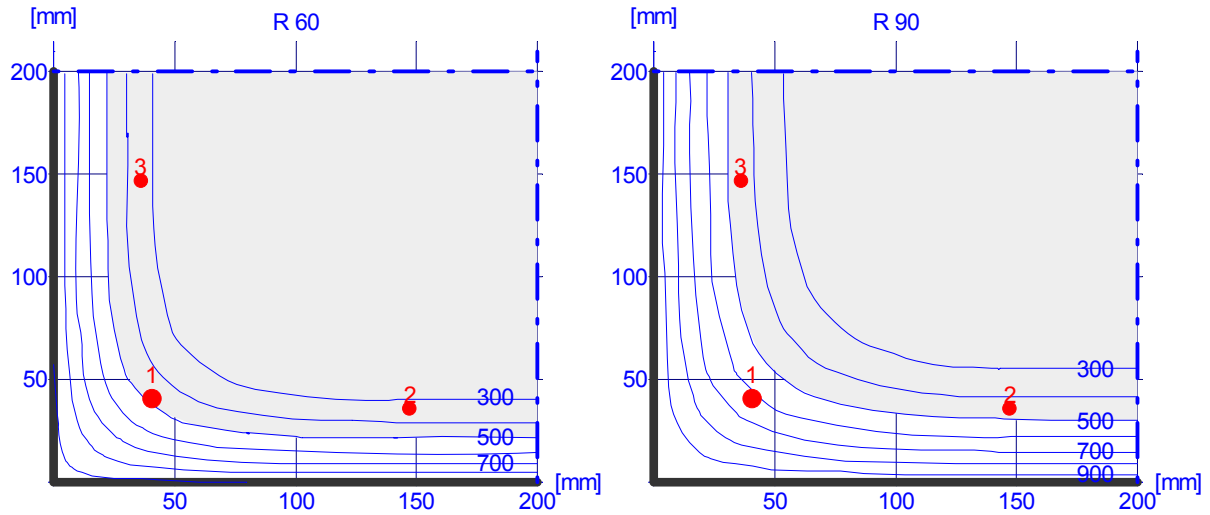


Figure 6. Isotherms of the column cross-section 400mm x 400mm for 60 and 90 minutes.

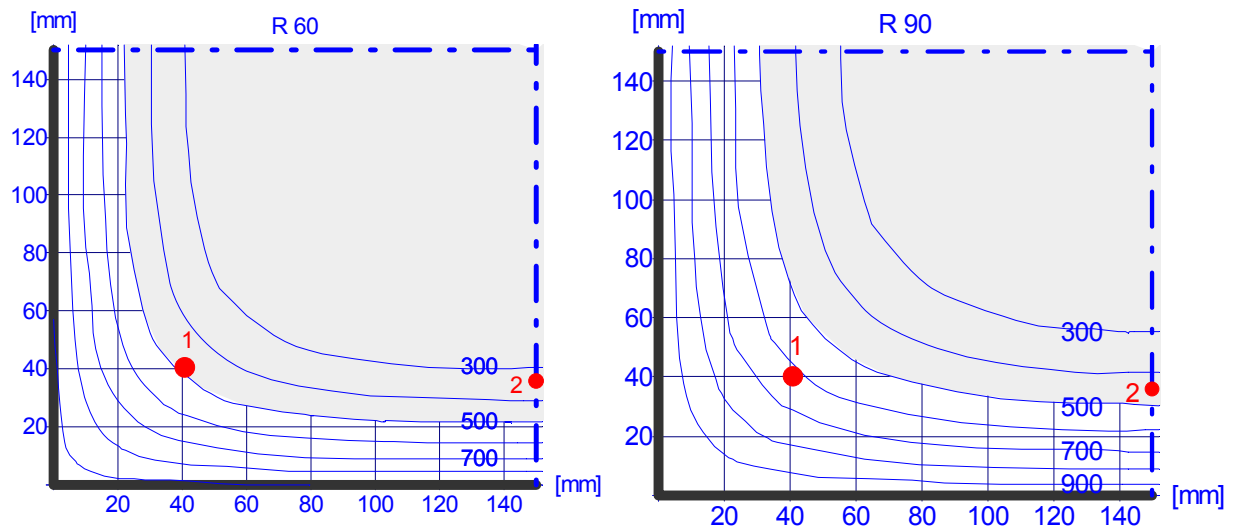


Figure 7. Isotherms of the column cross-section 300mm x 300mm for 60 and 90 minutes.

4.3 Cross-section resistance

Once the temperature in the concrete and in the reinforcing bars having been assessed, the simple calculation models given in 4.2.1 of EN1992-1-2 [5] will be used to determine the load bearing capacity of beams and columns in the fire situation.

4.3.1 Beams

As a simplification we consider that the positive bending moment resistance of the beams is limited only by the tension stress limit of the reinforcing steel (see 6.1 [3]), assuming that the concrete top flange is not enough affected by the fire to influence this resistance.

Therefore the positive bending moment resistance of the beams may be approximately obtained according to Annex E of EN1992-1-2 [5], taking into account that in the fire situation the partial material factor $\gamma_{s,fi}$ may be taken equal to unity:

$$M_{Rd(\theta)} = \sum k_{si(\theta)} (f_{ski} \cdot A_{si} \cdot d_i) \quad (7)$$

Where:

$M_{Rd(\theta)}$ is the design resistance to positive bending of the element in the fire situation,

$k_{si(\theta)}$ is the reduction factor of the characteristic yield strength of the steel rebar i at the temperature θ ,

f_{ski} is the characteristic yield strength of the rebar i at normal temperature,

A_{si} is the nominal section of the rebar i ,

d_i is the effective static depth of the rebar i .

The reduction factor for steel, $k_{si(\theta)}$, depending on the temperature is given in table 3.2a of [5] and is represented for Class N hot rolled steel in figure 8. From this figure the values of $k_{si(\theta)}$ may be obtained for the different reinforcing bars.

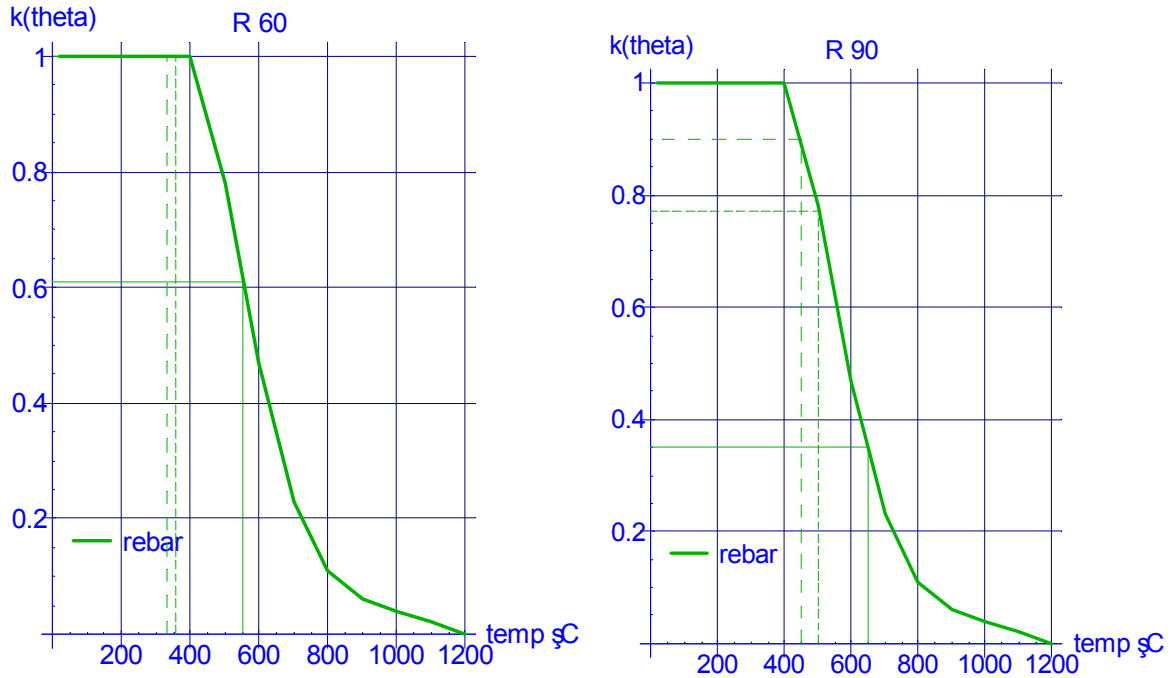


Figure 8. Coefficients $k_{s(\theta)}$ for the rebars of the beam according to the temperatures given in figure 5 for the standard heating.

The values of $k_{si(\theta)}$ are as follows

- for 60 minutes $k_{s1}(\theta) = 0,61$; $k_{s2}(\theta) = 1,0$ and $k_{s3}(\theta) = 1,0$
- and for 90 minutes $k_{s1}(\theta) = 0,35$; $k_{s2}(\theta) = 0,77$ and $k_{s3}(\theta) = 0,9$.

From these values the resulting moments obtained are $M_{Rd(60 \text{ min})} = 239 \text{ kNm}$ equal to 84,4 % of M_{Rd0} and $M_{Rd(90 \text{ min})} = 172 \text{ kNm}$ equal to 60,8 % of M_{Rd0} . $M_{Rd0} = 283 \text{ kNm}$ is obtained with the same procedure but with the partial material factor γ_s equal to 1,15.

Given that the action effect to be considered in the fire situation is 53 % of M_{Ed0} (see equation (5)) the solution chosen for the beams is acceptable.

4.3.2 Columns

In the case of columns we have of course to take account of the strength of the concrete at elevated temperatures. The simple model of the 500°C isotherm as defined in Annex B.1 of EN1991-1-2 will be used [5]. It considers the yield strength of the reinforcing bars taking account of the temperature obtained in steel for the specified time. For the concrete it is admitted, as a simplification, that for concrete temperatures lower than 500°C the strength and modulus of elasticity are not affected, but that the concrete above that temperature does not contribute any more to the load bearing capacity of the column.

Given the symmetry of the frames and the very low slenderness of the columns, the maximum compression load of the columns may be approximately obtained by the design resistance to axial compression of the column cross-section, taking into account that in the fire situation the partial material factor $\gamma_{s,fi}$ and $\gamma_{c,fi}$ may be taken equal to unity :

$$N_{Rd(\theta)} = f_{ck} \cdot A_{c500} + \sum k_{si(\theta)} (f_{ski} \cdot A_{si}) \quad (8)$$

where

- $N_{Rd(\theta)}$ is the design resistance to axial compression of the column cross-section,
- f_{ck} is the characteristic strength of the concrete at normal temperature,
- A_{c500} is the concrete area below 500°C,
- $k_{si(\theta)}$ is the reduction factors of the characteristic yield strength of the steel reinforcement i at the temperature θ ,
- f_{ski} is the characteristic yield strength of the rebar i at normal temperature,
- A_{si} is the nominal section of the reinforcement i .

The values of the coefficients $k_{s(\theta)}$, $k_{c(\theta)}$ are given in figures 9 and 10.

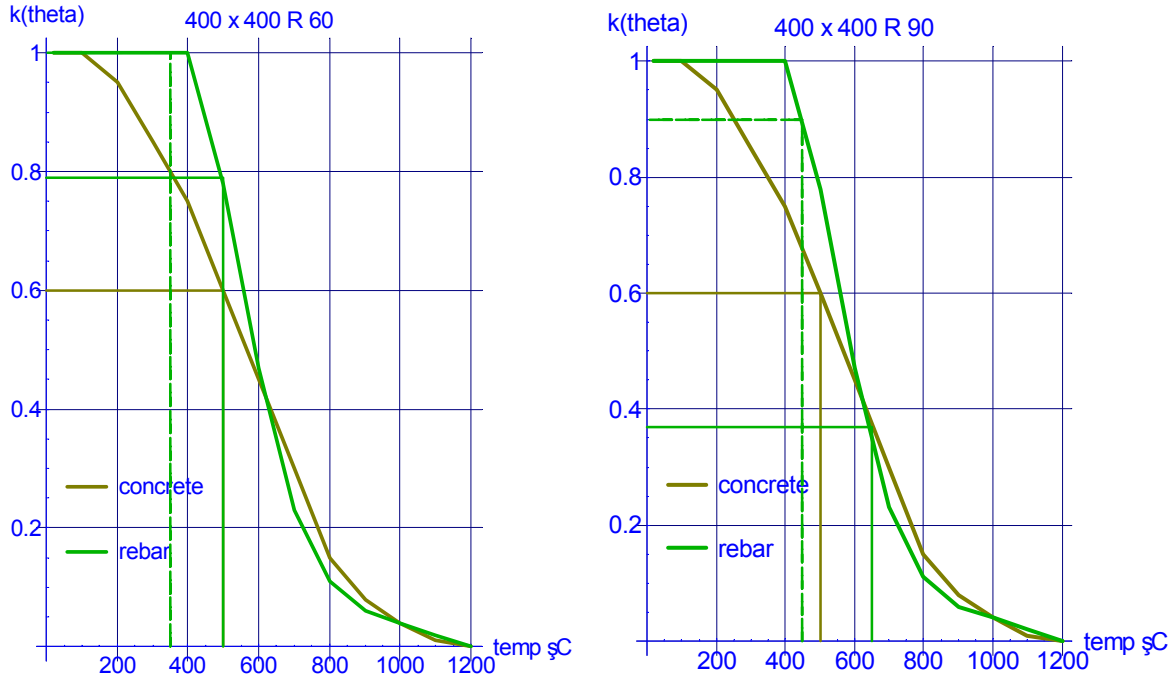


Figure 9. Coefficients $k_{s(\theta)}$ for the rebars of the column 400mmx400mm on 1st floor according to the temperatures given in figure 6 for the standard heating.

The values of $k_{si}(\theta)$ for the 400 mm x 400 mm column are as follows:

- for 60 minutes $k_{s1}(\theta) = 0,79$ and $k_{s2}(\theta) = k_{s3}(\theta) = 1,0$
- and for 90 minutes $k_{s1}(\theta) = 0,37$; $k_{s2}(\theta) = k_{s3}(\theta) = 0,9$.

From these values the resulting axial compression resistance of the column cross-section on the 1st floor is $N_{Rd(60 \text{ min})} = 3\,632 \text{ kN}$ equal to 75,1 % of N_{Rd0} and $N_{Rd(90 \text{ min})} = 3\,071 \text{ kN}$ equal to 63,5% of N_{Rd0} . $N_{Rd0} = 4836 \text{ kN}$ is obtained with the same procedure but with the partial material factor γ_s equal to 1,15 and γ_c equal to 1,5.

Given that the action effect to be considered in the fire situation is only 53 % of N_{Ed0} (see equation (5)) the solution chosen for the column 400mmx400mm is acceptable.

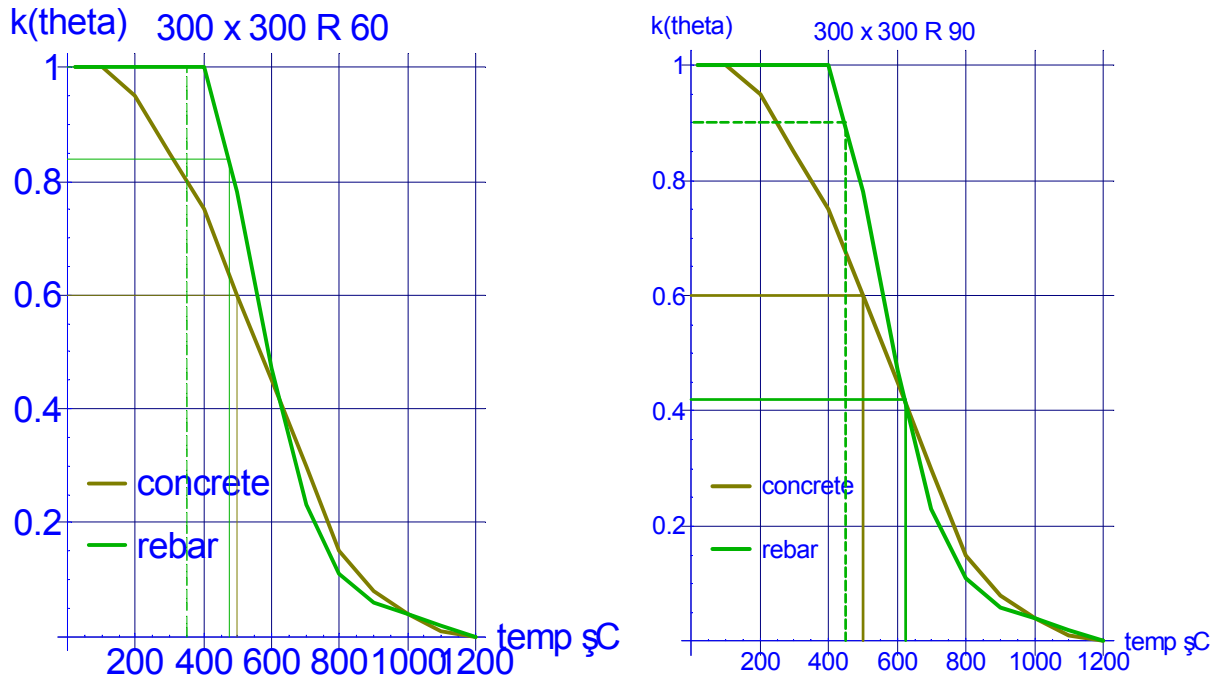


Figure 10. Coefficients $k_{si}(\theta)$ for the rebars of the column 300mmx300mm on 4th floor according to the temperatures given in figure 7 for the standard heating.

The values of $k_{si}(\theta)$ for the 300 mm x 300 mm column are as follows:

- for 60 minutes $k_{s1}(\theta) = 0,84$ and $k_{s2}(\theta) = 1$,
- and for 90 minutes $k_{s1}(\theta) = 0,42$ $k_{s2}(\theta) = 0,9$.

From these values the resulting axial compression resistance of the column cross-section on the 4th floor is $N_{Rd(60 \text{ min})} = 1\,905 \text{ kN}$ equal to 72,2 % of N_{Rd0} and $N_{Rd(90 \text{ min})} = 1\,531 \text{ kN}$ equal to 58,0 % of N_{Rd0} . $N_{Rd0} = 2638 \text{ kN}$ is obtained with the same procedure but with the partial material factor γ_s equal to 1,15 and γ_c equal to 1,5.

Given that the action effect to be considered in the fire situation is only 53 % of N_{Ed0} (see equation (5)) the solution chosen for the column 300mmx300mm is acceptable.

However it should not be forgotten that it is the very low slenderness of the columns, which allows to accept that the design resistance to axial compression of the columns may be approximately obtained by the design resistance to axial compression of the column cross-section.

4.4 Conclusions

The equivalent time of standard fire exposure allows to take into account the variables that affect the conditions of real fires in a simple straight way. This value may be significantly lower than that required by the National Authorities, as in the case presented it decreases from 90 to 60 minutes. But this procedure is not always reducing the required standard fire exposure time; in the case of concrete structures both values may be similar, or even the equivalent time be larger than that required by the National Authorities.

The tabulated data approach is very easy to use, but sometimes is too conservative. In our example it indicates the concrete cover in the column 300mmx300mm of the 4th floor as inadequate.

Simple calculation models are easy to use and they lead to less conservative results.

The difference between the design resistance obtained considering 60 instead of 90 minutes standard fire exposure is quite relevant in all the cases. It is worth to take advantage of the reduction of time of exposure by considering the time equivalence or even real fires.

It could be of interest to get results established by more refined methods as shown in Chapter I/6.5 of this Handbook 5. However in this case the calculation may not be done anymore by hand, as a computer and adequate computer programs will be needed.

REFERENCES

- [1] CEN; EN1990, Eurocode – Basis of Structural design. CEN Central Secretariat, Brussels, DAV 24.4.2002.
- [2] CEN; EN 1991-1-1, Eurocode 1 - Actions on structures, Part 1.1 - General actions-Densities, self-weight, imposed loads for buildings. CEN Central Secretariat, Brussels, DAV May 2002.
- [3] CEN; EN 1992-1-1, Eurocode 2 - Design of concrete structures, Part 1.1 - General rules and rules for buildings. CEN Central Secretariat, Brussels, 2004.
- [4] CEN; EN1991-1-2, Eurocode 1 – Actions on structures , Part 1.2 – Actions on structures exposed to fire. CEN Central Secretariat, Brussels, DAV 20.11.2002.
- [5] CEN; EN1992-1-2, Eurocode 2 – Design of concrete structures, Part1.2 – General rules – Structural fire design. CEN Central Secretariat, Brussels, December 2004.
- [6] Spanish Technical Building Code. Madrid 2005 (in Spanish).

CHAPTER VII - EXAMPLES OF STEEL AND COMPOSITE STRUCTURES

Jean-Baptiste Schleich¹

¹ University of Technology Aachen, University of Liège

1 INTRODUCTION

It is obvious that, for each structural system up to the required fire resistance time, the relationship $R_{fi,d,t} \geq E_{fi,d,t}$ shall be fulfilled, where at time t , $R_{fi,d,t}$ is the design load bearing resistance in the fire situation of the structural system considered and $E_{fi,d,t}$ is the design effect of actions on the same structural system in the fire situation, determined in general from the accidental combination rule for actions according to section 4.3 of EN1991-1-2 [12] and to equation (6.11b) of section 6.4.3.3 of EN1990 [11].

Advanced calculation models, which are more difficult in use but provide more realistic calculation results than the calculation models given by tabulated data or simple calculations models - see Chapter I-6 - permit to determine and understand the overall behaviour of a structure in the fire situation. Indeed this allows to explain, based on practical examples on beams and columns, the following important physical aspects.

* It may be noted first, that the increase of the flexural stiffness of a structural member will largely contribute in the fire situation to either an improvement of the fire resistance time either an enhancement of the load bearing resistance [6]. If longitudinal expansion of the structural member is not prevented, this quite interesting result may be obtained f.i. by the composite action between the concrete slab and the corresponding steel beam, by the effect produced from a continuous and no more simply supported steel beam or by the reinforcing bars of the slab which are continuing over intermediate supports.

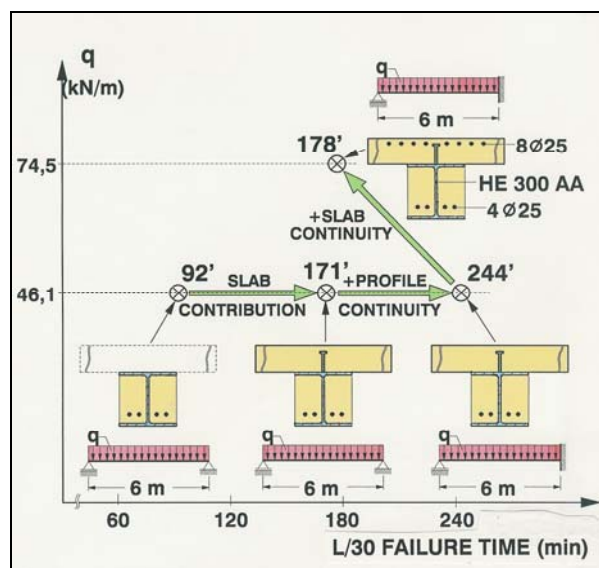


Figure 1. Improvement of the fire resistance time and enhancement of the load bearing resistance, by composite action or by continuity effects [2].

This behaviour is illustrated in figure 1, where the fire resistance times measured during ISO-fire tests performed in 1985 [2] are given for the deflection criterion $L/30$. These test results clearly demonstrate that:

- by adding the composite action of the slab to that of the underlying beam, the fire resistance time is growing from 92' to 171';
- by foreseeing moreover the continuity of the beam at least at one support, a fire resistance time of 244' is measured;
- by adding at that same support continuous reinforcing bars in the slab, and by increasing the total supported linear load by 62 %, the fire resistance time measured is nevertheless still 178'.

** **Static continuity** of structural beams so far helps to increase the fire resistance compared to simply supported beams. This favourable effect also appears when considering columns as being continuous, and if the fire remains confined to one level thanks to a convenient horizontal compartmentation of the building .

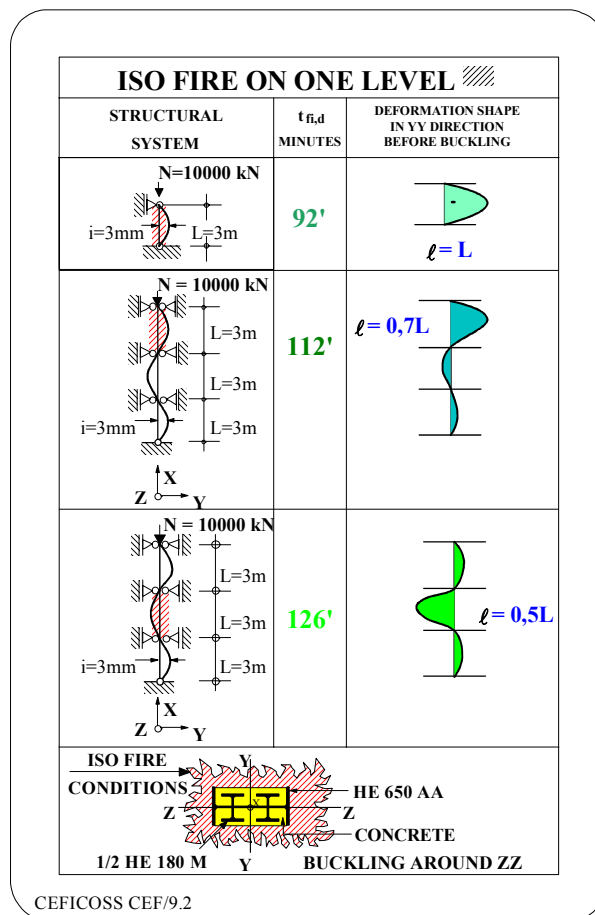


Figure 2. Improvement of the ISO-fire resistance time when considering columns as being continuous.

This behaviour is documented in figure 2, where - for the same cross-section of the column but for various structural systems - the calculated fire resistance times $t_{fi,d}$ are given for the buckling failure criterion. These calculation results [5] demonstrate that:

- the column, supposed to be hinged at its both ends on the level under fire, has an ISO fire resistance of 92';

- the column, considered as continuous and submitted to a fire at its highest level, has an ISO fire resistance of 112'. By the way this result corresponds at the heated level to an equivalent buckling length l of 0,7 times the system length L ;
- if the fire breaks out at an intermediate level of that same continuous column, its fire resistance would even be increased to 126'. At the heated level this corresponds to an equivalent buckling length l of 0,5 times the system length L .

*** Some other quite important physical aspects have also to be considered like the fact that any cross-section heated by the surrounding gas during the heating phase of a natural fire, will become hotter than the fire during the cooling down phase of that natural fire. This is shown in figure 3 where it also appears, that a highly differential internal temperature field is generated inside the cross-section, giving way to a strong inner stress field [4]. These thermal stresses, either in tension or compression, have to be considered if we want to enable all the components of a cross-section to work compositely together during a natural fire. Shear forces between the different components have to be transmitted and may be, that shear studs welded on steel parts are required in order to guarantee shear connection with concrete parts. This requirement may be fulfilled by foreseeing a full shear connection for the normal temperature design.

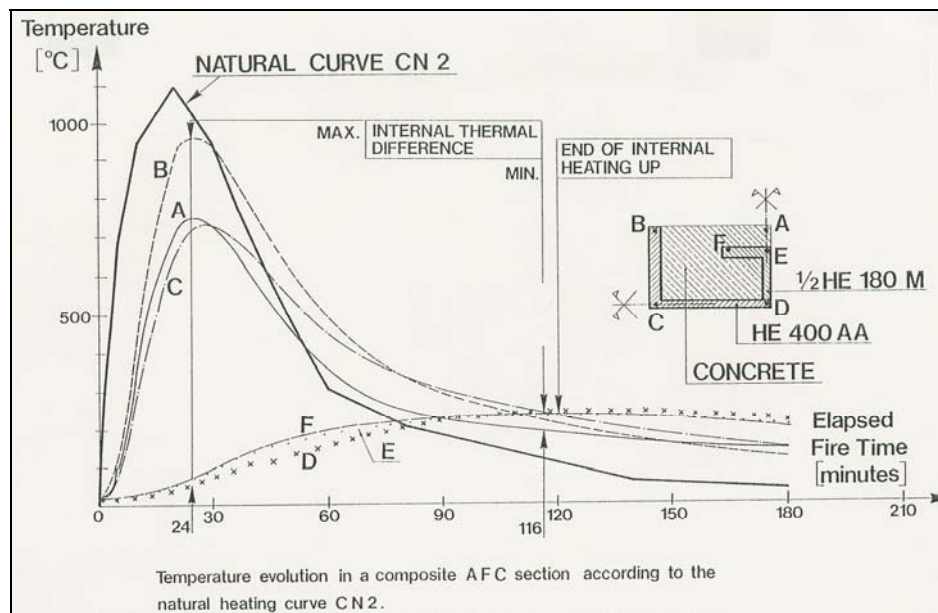


Figure 3. Temperature evolution in a composite cross-section heated by the natural fire curve CN2.

**** Another important aspect concerns the behaviour of beam to column connections, which during the heating up of a beam may be submitted to negative bending moments thus increasing the flexural stiffness of the beam, but which later on during the cooling process may be subject to positive bending!

This means that the lower part of the connection is finally submitted to high tension forces, which might lead to very dangerous tension failures of bolts during the cooling down phase of the fire. This happened during the demonstration tests in Vernon (see figure 4 and [10]), where an unprotected steel structure was submitted to the fire created by three cars. Whereas the structure behaved quite well during the whole fire duration, as foreseen by previous developments [8], there was bolt failure by tension at the end of the cooling down phase of the fire.

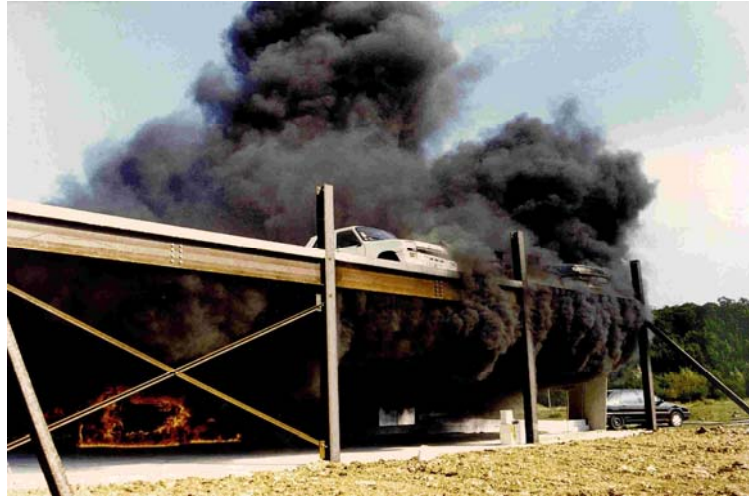


Figure 4. Car park fire tests in Vernon-France [10].

However the structure was not endangered as the bolted connection was composed of an end plate welded to the beam, which in turn was bolted to the steel column. Despite the loss of 3 to 4 bolts in the lower part of the connection, bolts placed in the upper part of the end plate and even inside the concrete slab were still able to support the shear forces.

During that fire the maximum air temperature on top of the burning cars reached 800°C as given in figure 5, which led to a maximum heating up of the lower flange of the profile IPE 600 of 650°C. The deflection of the beam at mid span is shown in figure 6 with a maximum of 150 mm at 20 to 25 minutes, which corresponds to $\approx 1/100$ of the span of 16m.

Nevertheless figure 6 also reveals, through the positive deflection after 75 minutes, that positive bending now exists at intermediate supports leading to bolt tension failure.

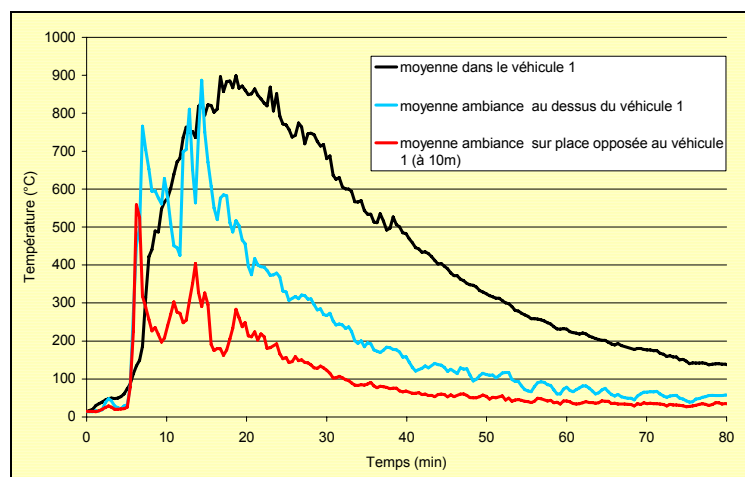


Figure 5. Heating inside the car —, on top of it —, alongside the car —.

The lesson to learn from this is two-fold:

- * the fire resistance under natural fires shall be performed with the complete cooling down curve, in order to make sure that load redistributions are fully considered, like bending moment inversion, but also that second order effects are taken into consideration which might lead to column buckling even at a later stage;

** concerning beam to column connections it is suggested to chose end plates so to take profit of continuity effects through the formation of negative bending. However these end plates shall be prolonged into the concrete slab, so to be able to place here some bolts well protected against heat and situated at the same time at the upper part of the connection not submitted to tension during the cooling phase. In the lower part of the connection only bolts with lower diameter, if any, shall be placed so that tension during the cooling is limited and does not damage the flanges of the steel column.

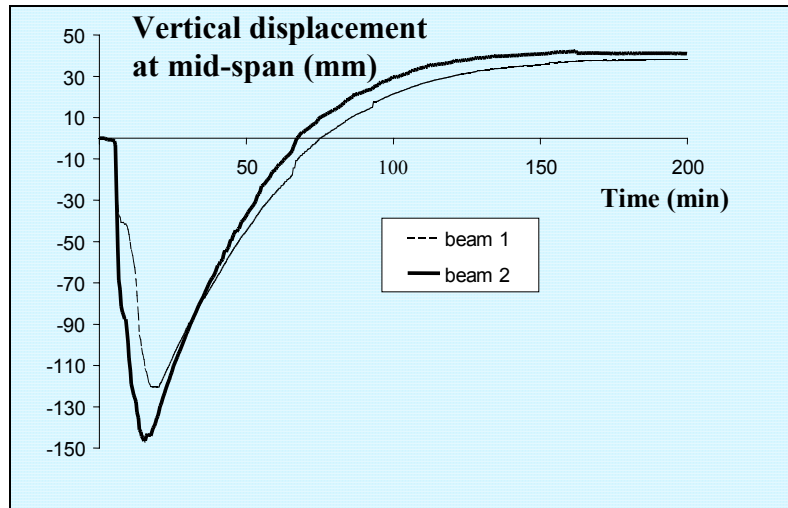


Figure 6. Deflection of the beam during heating and subsequent cooling.

2 ISOLATED STRUCTURAL ELEMENTS

2.1 Heating according to the standard fire

2.1.1 Design of a not protected steel column

❖ The proposed example consists first in calculating the uniform critical temperature of the following element;

- Section HE 220 A
- radius of gyration $i_z = 5,51$ cm
- sectional area $A = 64,34$ cm²
- Buckling axis weak
- Length $L = 3,30$ m
- Yield point $f_y = 355$ N/mm²
- Fire design axial load given by $N_{fi,Sd} = 150$ kN

Preliminary calculations refer to the classification of the cross section and to the non-dimensional slenderness:

$$\varepsilon = \sqrt{\frac{235}{f_y}} = 0,814$$

This permits to classify the cross section for normal temperature design according to sheets 1 and 2 of table 5.2 of prEN1993-1-2 [14] as follows:

$$(c/t)_{web} = 152 / 7 = 21,7 = 26,7\varepsilon \rightarrow \text{class 1}$$

$$(c/t)_{flange} = 88,5 / 11 = 8,04 = 9,88\varepsilon \rightarrow \text{class 2}$$

$$\bar{\lambda}_{(20^\circ\text{C})} = \frac{\lambda}{\lambda_{E(20^\circ\text{C})}} = \frac{L/i_z}{93,91\varepsilon} = \frac{330/5,51}{93,91 \cdot 0,814} = 0,784$$

For the fire situation the classification of the cross section is based on

$$\varepsilon = 0,85 \sqrt{\frac{235}{f_y}} = 0,692 \text{ according to equation (37) of Chapter I-6.4.2 which leads to:}$$

$$(c/t)_{\text{web}} = 152/7 = 21,7 = 31,3 \varepsilon \rightarrow \text{class 1}$$

$$(c/t)_{\text{flange}} = 88,5/11 = 8,04 = 11,6 \varepsilon \rightarrow \text{class 3.}$$

This allows to use equations (39), (40) and (41) of **Chapter I-6.4.2** in order to estimate the uniform critical temperature:

$$N_{b,fi,Rd} = \chi_{fi} (A k_{y,\theta} f_y) / \gamma_{M,fi} \quad (39)$$

which gives according to 2.3 of prEN1993-1-2 [14], $\gamma_{M,fi} = 1,0$, and (39) leads to

$$k_{y,\theta}^{\max} = [N_{b,fi,Rd} / (\chi_{fi} A f_y)]^{\max}.$$

According to equation (41) of Chapter I-6.4.2 the non-dimensional slenderness $\bar{\lambda}_\theta$ for the steel temperature θ , is given by

$$\bar{\lambda}_\theta = \bar{\lambda} [k_{y,\theta} / k_{E,\theta}]^{0,5} \quad (41)$$

which according to table 3 of Chapter V, suggests to make a first calculation on the basis of a mean value for $[k_{y,\theta} / k_{E,\theta}]^{0,5}$ i.e.

$$\bar{\lambda}_\theta = 1,20 \cdot \bar{\lambda} = 1,20 \cdot 0,784 = 0,941$$

The calculation is continued as shown hereafter:

$$\varphi_\theta = 0,5(1 + \alpha \cdot \bar{\lambda}_\theta + \bar{\lambda}_\theta^2)$$

$$\varphi_\theta = 0,5(1 + 0,65 \cdot 0,814 \cdot 0,941 + 0,941^2) = 1,191$$

Equation (40) of Chapter I-6.4.2 gives

$$\chi_{fi} = \frac{1}{\varphi_\theta + \sqrt{\varphi_\theta^2 - \bar{\lambda}_\theta^2}} \quad (40)$$

$$\chi_{fi} = 1 / (1,191 + (1,191^2 - 0,941^2)^{0,5}) = 0,520 \text{ and hence we get}$$

$$k_{y,\theta}^{\max} = 150000 / (0,520 \cdot 6434 \cdot 355) = 0,126.$$

From the values of table 3 and figure 15 of Chapter V-5.1 we obtain by linear interpolation the critical temperature $\theta_{cr} = 787^\circ\text{C}$ as a first approximation.

This allows to check equation (39) by the same table 3 which gives for $\theta = 787^\circ\text{C}$ $k_{E,\theta} = 0,095$ and the relative slenderness is calculated as

$$\bar{\lambda}_\theta = \bar{\lambda} [k_{y,\theta} / k_{E,\theta}]^{0,5}$$

$$= 0,784 [0,126 / 0,095]^{0,5} = 0,902$$

$$\varphi_\theta = 0,5(1 + 0,65 \cdot 0,814 \cdot 0,902 + 0,902^2) = 1,145$$

$$\chi_{fi} = 1 / (1,145 + (1,145^2 - 0,902^2)^{0,5}) = 0,540 \text{ and hence}$$

$$\begin{aligned}
 N_{b,fi,Rd} &= \chi_{fi} (A k_{y,0} f_y) / \gamma_{M,fi} \\
 &= 0,540 \cdot 6434 \cdot 0,126 \cdot 355 / 1,0 \\
 &= 155408 \text{ N} \geq N_{fi,Sd} = 150000 \text{ N}.
 \end{aligned}$$

This result is sufficiently precise from a practical point of view, and further iteration is not needed. For information the theoretical critical temperature θ_{cr} equals 791 °C.

❖ The **fire resistance of the same column, heated all around by the ISO-fire** should be checked following equation (46) and **figure 35 of Chapter I-6.4.2**.

$$\mu_0 = E_{fi,d} / R_{fi,d,0} \quad (46)$$

$$E_{fi,d} = N_{fi,Sd} = 150 \text{ kN}$$

$$R_{fi,d,0} = N_{b,fi,Rd, t=0} \text{ calculated according to EN1993-1-1 with } \gamma_M = 1,0 \text{ i.e.}$$

$$N_{b,Rd} = \chi (A f_y) / \gamma_{M1} \text{ with}$$

$$\bar{\lambda} = 0,784; \alpha = 0,49 \text{ imperfection factor for buckling curve c of table 6.2 / EN1993-1-1}$$

$$\varphi = 0,5[1 + \alpha(\bar{\lambda} - 0,2) + \bar{\lambda}^2] = 0,950$$

$$\chi = \frac{1}{\varphi + \sqrt{\varphi^2 - \bar{\lambda}^2}} = 0,673$$

$$N_{b,Rd} = 0,673 \cdot 6434 \cdot 355 / 1,0 = 1537179 \text{ N} \rightarrow \mu_0 = 150000 / 1537179 = 0,097$$

This gives for a section factor of $A_m/V = 195 \text{ m}^{-1}$, for an adaptation factor κ of 1,2 and using figure 35 of Chapter I-6.4.2 an ISO-fire resistance of ~ 28 minutes.

2.1.2 Analysis of temperatures in a composite beam with insulated steel section.

Figure 7 gives the size of a composite beam with a steel section protected by 15 respectively 25 mm of sprayed material.

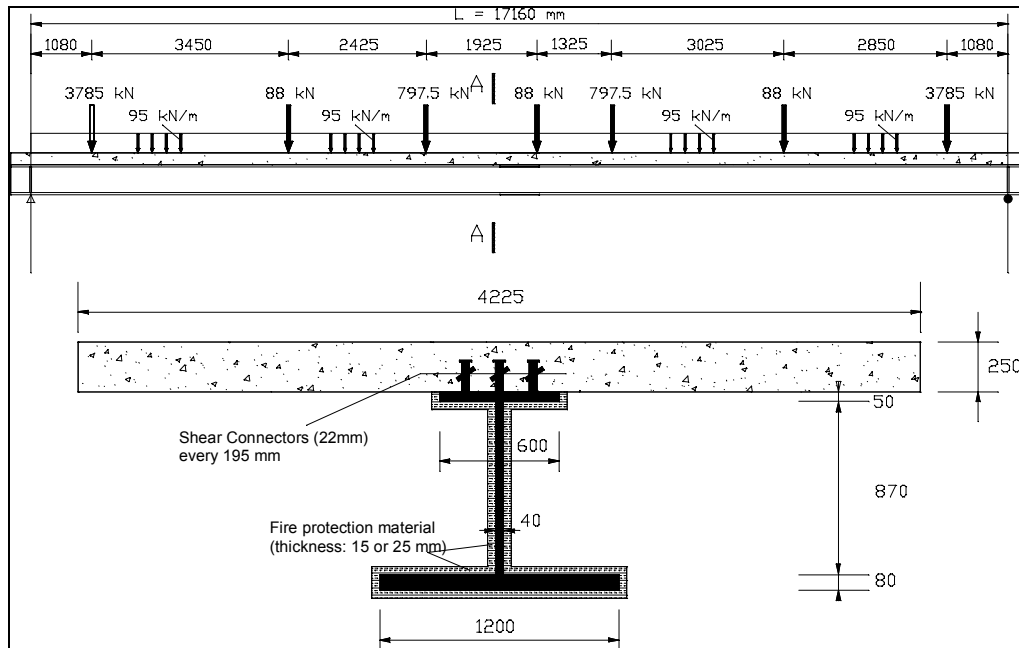


Figure 7. Composite beam of 17,16 m span composed of an insulated steel section with a height of 1m.

Using a finite element model and taking into account the thermal characteristics of steel and concrete given in Chapter V, as well as the relevant thermal characteristic of the insulation material, the temperature may be calculated in any part of the cross section when this beam is heated from below by the ISO-fire. The temperatures of the 2 flanges, of the web and within the concrete slab are given in figure 8.

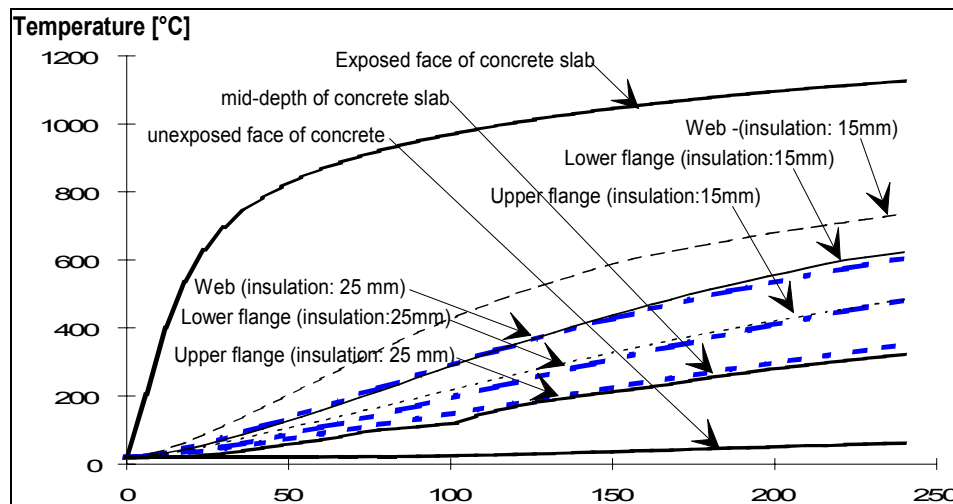


Figure 8. Temperature evolution within the various parts of the composite beam.

2.1.3 Design of a composite beam comprising a steel beam with partial concrete encasement.

The proposed example consists in establishing the fire resistance time for the element given in figure 9. Results are based on the simple calculation model given in **Annex F of prEN1994-1-2** [16] and on the corresponding software "AFCB-Version 12.12.2000".

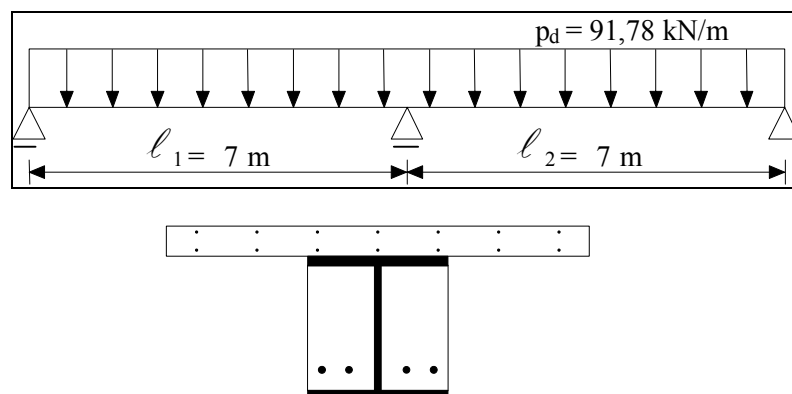


Figure 9. Cross section and geometric conditions of composite beam heated from below by the ISO-fire.

PROFILE

Profile name		HE 300 A
Height	[mm]	290
Width	[mm]	300
Web thickness	[mm]	8.50
Flange thickness	[mm]	14
Radius	[mm]	27

Width b^* of the concrete part	[mm]	300
<u>REINFORCING BARS</u>		
Number of bars in 1st row		4
Diameter of the bars in the 1st row		20 mm
Distance of the bars in the 1st row to the lower flange		30 mm
Distance of the bars in the 1st row to the concrete border		60 mm
<u>CONCRETE SLAB</u>		
Effective width of the concrete slab $\equiv 2(l_0/8) = 2(0,8 l_1/8)$		1400 mm
Thickness of the concrete slab		170 mm
Upper mesh section in the concrete slab		12 cm ² /m
Distance of the upper mesh section to the upper border of the concrete slab		35.00 mm
Lower mesh section in the concrete slab		12.00 cm ² /m
Distance of the lower mesh section to the lower border of the concrete slab		55.00 mm
<u>MATERIAL CLASSES</u>		
Yield point of the steel profile		355.00 N/mm ²
Yield point of the reinforcing bars		500.00 N/mm ²
Yield point of the meshes in the concrete slab		500.00 N/mm ²
Cylindric compressive strength of the concrete between the profile		30.00 N/mm ²
Cylindric compressive strength of the concrete of the slab		30.00 N/mm ²

DESIGN POSITIVE BENDING MOMENT RESISTANCE AND POSITION OF PLASTIC NEUTRAL AXIS $M^{+}_{fi,Rd}$

R0	Mpl	=	1025 kNm	XO	=	17.1 cm
R30	Mpl	=	1024 kNm	XO	=	13.7 cm
R60	Mpl	=	611 kNm	XO	=	9.2 cm
R90	Mpl	=	472 kNm	XO	=	7.3 cm
R120	Mpl	=	410 kNm	XO	=	6.5 cm
R180	Mpl	=	319 kNm	XO	=	5.1 cm

DESIGN NEGATIVE BENDING MOMENT RESISTANCE AND POSITION OF PLASTIC NEUTRAL AXIS $M^{-}_{fi,Rd}$

The beam is continuous without interruption on the support, and the reinforcement between the flanges is taken into account to calculate the design negative moment resistance.

R0	Mpl	=	-728 kNm	XO	=	36.7 cm
R30	Mpl	=	-415 kNm	XO	=	18.1 cm
R60	Mpl	=	-340 kNm	XO	=	17.9 cm
R90	Mpl	=	-256 kNm	XO	=	17.7 cm
R120	Mpl	=	-202 kNm	XO	=	17.5 cm
R180	Mpl	=	-150 kNm	XO	=	17.3 cm

DESIGN EQUIVALENT BENDING MOMENT RESISTANCE FOR CONTINUOUS

BEAMS $M^{equ}_{fi,Rd} \sim M^{+}_{fi,Rd} + 0,5 \cdot |M^{-}_{fi,Rd}|$

R0	Mfail	=	1389 kNm
R30	Mfail	=	1231 kNm
R60	Mfail	=	781 kNm
R90	Mfail	=	600 kNm
R120	Mfail	=	511 kNm
R180	Mfail	=	394 kNm

DESIGN SHEAR RESISTANCE FOR CONTINUOUS BEAMS (see (2) of 4.3.4.3.4 and (6) and (7) of F.2 of prEN1994-1-2)

R0	Shear resistance	= 456 kN	> (5/8)·(91,78·7) = 401kN
R30	Shear resistance	= 412 kN	
R60	Shear resistance	= 391 kN	
R90	Shear resistance	= 347 kN	
R120	Shear resistance	= 281 kN	~ (5/8)·(64,25·7) = 281kN
R180	Shear resistance	= 211 kN	

Table 1. Checking the bending moment resistance.

FIRE CLASS	DESIGN EQUIVALENT MOMENT RESISTANCE M^{equ} [kNm]	Applied design MOMENT $M_{fi,Sd}$ $p \cdot l^2 / 8$ [kNm]	Design load
R0	1389	563	$p_d = 91,78$ kN/m
R30	1231	393	} $p_{fi,d} = 64,25$ kN/m
R60	781	393	
R90	600	393	
R120	511	393	
R180	394	393	

Note that $p_{fi,d}$ is calculated in case of a building of category E according 2.4.2(3) of prEN1994-1-2 [16] :

$$p_{fi,d} = 0.7 \cdot p_d$$

with $p_d = 1,35 g + 1,50 q$ according table A1.2(B) of EN1990 [11], $\rightarrow \sim 92$ kN/m.

It is normally beneficial to calculate $p_{fi,d}$ on the basis of the "Combination rule for accidental design situations" according to table A1.1 of EN1990 i.e.

$$\rightarrow \text{for a building of CATEGORY E : } p_{fi,d} = 1,0 g + 0,9 q$$

$$\rightarrow \text{for a building of CATEGORY A \& B : } p_{fi,d} = 1,0 g + 0,5 q$$

This example shows that fire resistance depends on the type of criterion i.e.

\rightarrow fire class R180 is guaranteed for the bending moment resistance but

\rightarrow fire class R120 is only given for the shear resistance, hence the beam is to be classified R120.

2.2 Heating according to natural fires

2.2.1 Underground car-park, Auchan Phase II (1999-2000)

The conclusions of pages VII-4/5 concerning the consideration of the complete cooling down curve and how to conceive the beam to column connections, influenced the way the Kirchberg City Centre structure evolved between 1994 and 1999 in Luxembourg. In fact this entire major complex, covering an effective floor area of 185 000 m², was erected between 1994 and 1997. It has a composite framework with the required ISO R90 resistance but with the addition of active fire safety measures, in particular the installation of sprinklers .

Meanwhile, when the Auchan Phase II underground car-park was built from 1999 to 2000, it was à priori recognised by the local authority that the safety conferred by the active fire-prevention methods may be considered when analysing the stability of the load-bearing structure and that a realistic type of fire, from cars burning, may be taken into account. The car-park, in the extreme northwest of the Kirchberg City Centre complex, is built on 5 under-



Figure 10. Underground car-park with 5 levels and a total area of 15000m².



Figure 11. Visible unprotected steel structure, profile IPE550 for beams, designed for natural fire.

ground levels and covers 15 000 m² (see figure 10). The 16,8 m long floor beams are fully visible and no thermal insulation was applied to provide fireproofing (see figure 11).

However, great care has been taken in introducing a complete set of active fire safety measures:

- this is why there are smoke detectors that automatically boost the forced evacuation of smoke up to 45000 m³ per hour on the floor under fire,
- the fire doors will be activated automatically, restricting any heat and smoke to one level,
- the most important measure, however, is a high-density sprinkler system that will put out any fire as soon as it starts.

Unfortunately the **German Approval Authority did not accept to consider the positive effect of smoke detectors, forced smoke evacuation and sprinklers** arguing that these safety measures are foreseen for the safety of people and not for the safety of the structural elements.

Hence the calculation had to be based strictly on the natural heating resulting from burning cars and this led to the rate of heat release RHR given in figure 12. This corresponds to the **fire of 3 cars**, each with a maximum RHR of 4,5 MW, with ignition shifted by 10 minutes from car to car. This fire scenario was a requirement from the German Approval Authority.

Of course continuity effects could be activated, which was practically done by end plates welded to the beams and supported by bearing blocks welded to the columns. Furthermore a longitudinal reinforcement of 24 bars of diameter 12mm - in case of the profile IPE550 - was to be put into the concrete slab in the area of intermediate supports over a total length of 8m.

As a conclusion it may be said, that the beam analysed, on behalf of the software "CEFICOSS" [3], with the complete heating curve, cooling included up to 120 minutes, is never endangered as shown in figure 13. Indeed at that time the MPV-value gets stabilized; the low value of 0,25 is due to a definitive damage of the fire exposed concrete of the slab, which has to be repaired after this fire situation.

During the heating the maximum deflection reaches 27 cm, whereas a permanent deflection of ≈ 17 cm remains at the end of the fire, which corresponds to $\approx 1/100$ of the span of 16,8m. Figure 14 also demonstrates that this deformation gets stabilized at 90 minutes, which seems absolutely normal as, according to figure 12, the heat input has stopped at 75 minutes.

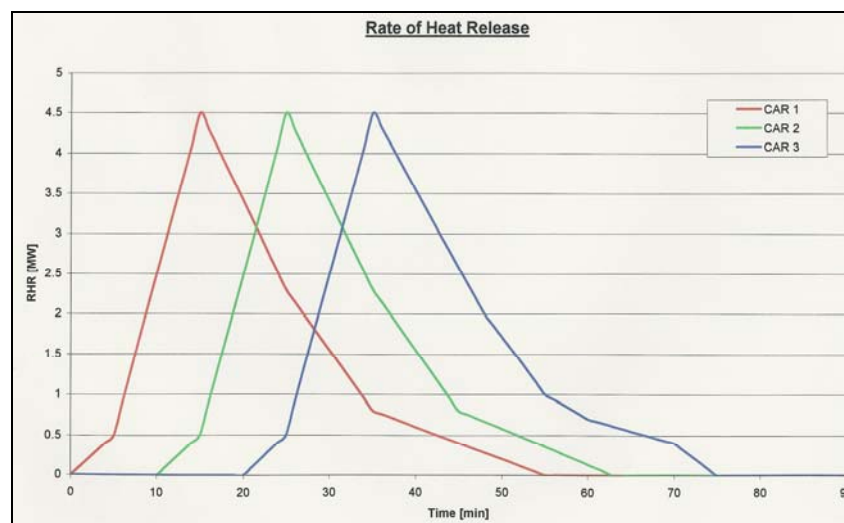


Figure 12. Rate of Heat Release from the 3 cars starting to burn at 0', 10' and 20'.

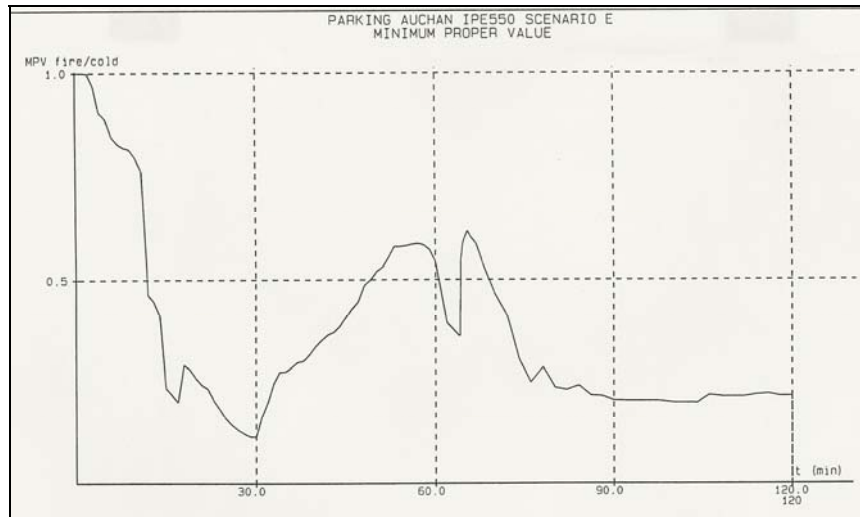


Figure 13. Minimum Proper Value of the composite beams of 16,8m span.

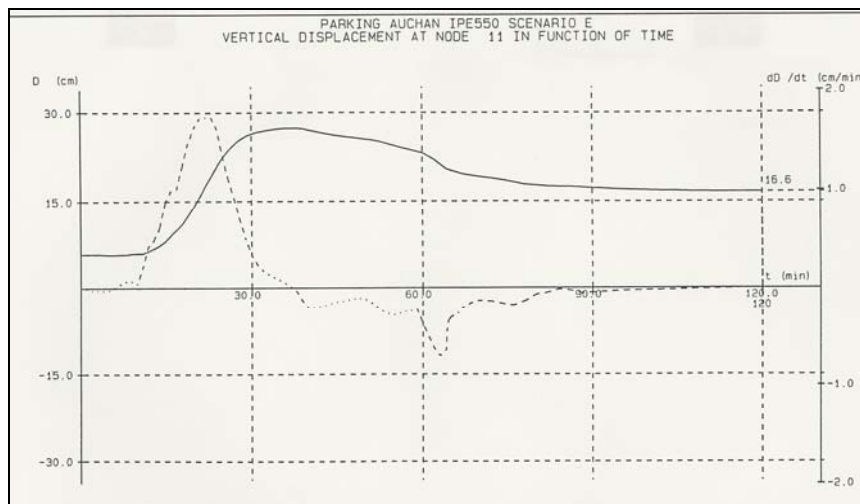


Figure 14. Deflection evolution in function of time calculated by the software "CEFICOSS".

2.2.2 Steel column in underground car-park

The project for this new complex comprises 5 underground car-park levels with the following safety measures:

- * smoke detection connected to the acoustic alarm and activating the following three steps,
- ** forced mechanical smoke evacuation in the level under fire with $18\text{m}^3 / \text{h} \cdot \text{m}^2$,
- *** automatic closure of fire doors restricting heat and smoke to one level,
- **** transmission of alarm to the fire brigade,
- ***** furthermore sprinklers are foreseen on all levels.

For the fire resistance design of columns these active measures had not to be activated. However the **fire was admitted to be limited to 1 car burning**, so considering that fire transmission to a second car was prevented by the effect of sprinklers [9].

Thermal data

Heat was released according to figure 15 with a peak of 8,3 MW at 25 minutes and a total energy release of 6,8 GJ.

Forced mechanical smoke evacuation on 1 level with

$$(18\text{m}^3 / \text{h} \cdot \text{m}^2) \cdot 1500\text{m}^2 = 27000\text{m}^3 / \text{h} \rightarrow \rightarrow \mathbf{7,5 \text{ m}^3 / \text{sec}}$$

Geometrical data

The size of one level is given by 2,3m height · 36m width · 42m depth.

Fire doors in normal service conditions have an opening of $5 \cdot 2,2 = 11\text{m}^2$.

The horizontal distance between the fire source and the column axis is given by $\delta_h = 1,2\text{m}$ which is quite small.

Statical data

The axial load on one typical column to be considered for the fire situation is obtained from

$$N_{d,\text{fire}} = G_k + \psi_1 \cdot Q_k = 8400 + 0,5 \cdot 3600 = \mathbf{10200\text{kN}}$$

The profil HD400x347 is chosen, with a massivity factor A_m/V of 53m^{-1} and with a buckling length in case of fire of

$$l = 0,7 \cdot 2,6 = 1,82\text{m}.$$

The analysis of this problem is detailed on the following pages VII-14 to VII-17 on behalf of the software OZONE [13] and the HASEMI approach following Annex C of EN1991-1-2 [12]. According to that study the unprotected steel column **HD 400 x 347 is not failing by this car burning, the fire source being supposed at $\delta_h = 1,2\text{m}$ from the axis of the column.....**

Only if that distance δ_h equals 0, which means that the car has hit the column, which corresponds rather to a terror act, the column may be endangered.

OZone V 2.2.2 Report

Prof. JB SCHLEICH / PROJET CJ / 1 CAR FORCED VENTILATION I+O

File Name: H:\NATURAL FIRE DESIGN\OZONE 2.2.2\APPLICATIONS\CJUD1CFV C.ozn
Created: 07/07/2005 at 13:52:56

ANALYSIS STRATEGY

Selected strategy:	Combination 2Zones - 1 Zone Model
Transition criteria from 2 Zones to 1 Zone	
Upper Layer Temperature	$\geq 500^\circ\text{C}$
Combustible in Upper Layer + U.L. Temperature	\geq Combustible Ignition Temperature = 300°C
Interface Height	≤ 0.2 Compartment Height
Fire Area	≥ 0.25 Floor Area

PARAMETERS

Openings

Radiation Through Closed Openings: 0.8
Bernoulli Coefficient: 0.7

Physical Characteristics of Compartment

Initial Temperature: 293 K
Initial Pressure: 100000 Pa

Parameters of Wall Material

Convection Coefficient at the Hot Surface: $25 \text{ W/m}^2\text{K}$
Convection Coefficient at the Cold Surface: $9 \text{ W/m}^2\text{K}$

Calculation Parameters

End of Calculation: 7200 sec
Time Step for Printing Results: 60 sec
Maximum Time Step for Calculation: 10 sec

**Air Entrained Model:
COMPARTMENT**

Mc Caffrey

Form of Compartment:	Rectangular Floor	
Height:	2.3	m
Depth:	42	m
Width:	36	m
Roof Type:	Flat Roof	

DEFINITION OF ENCLOSURE BOUNDARIES

Floor

Material (from inside to outside)	Thickness [cm]	Unit Mass [kg/m ³]	Conductivity [W/mK]	Specific Heat [J/kgK]
Normal weight Concrete [EN1994-1-2]	20	2300	1.6	1000

Ceiling

Material (from inside to outside)	Thickness [cm]	Unit Mass [kg/m ³]	Conductivity [W/mK]	Specific Heat [J/kgK]
Normal weight Concrete [EN1994-1-2]	20	2300	1.6	1000

Wall 1

Material (from inside to outside)	Thickness [cm]	Unit Mass [kg/m ³]	Conductivity [W/mK]	Specific Heat [J/kgK]
Normal weight Concrete [EN1994-1-2]	15	2300	1.6	1000

Openings

Sill Height [m]	Soffit Height [m]	Width [m]	Variation	Adiabatic
0	0	0	Constant	no

Wall 2

Material (from inside to outside)	Thickness [cm]	Unit Mass [kg/m ³]	Conductivity [W/mK]	Specific Heat [J/kgK]
Normal weight Concrete [EN1994-1-2]	15	2300	1.6	1000

Wall 3

Material (from inside to outside)	Thickness [cm]	Unit Mass [kg/m ³]	Conductivity [W/mK]	Specific Heat [J/kgK]
Normal weight Concrete [EN1994-1-2]	15	2300	1.6	1000

Openings/ 10% OF FIRE DOOR 5m· 2,2m

Sill Height [m]	Soffit Height [m]	Width [m]	Variation	Adiabatic
0	2.2	0.5	Constant	no

Wall 4

Material (from inside to outside)	Thickness [cm]	Unit Mass [kg/m ³]	Conductivity [W/mK]	Specific Heat [J/kgK]
Normal weight Concrete [EN1994-1-2]	15	2300	1.6	1000

Smoke Extractors

Height [m]	Diameter [m]	Volume [m ³ /sec]	In/Out
2	2	7.5	out
1	2	7.5	in

FIRE

Fire Curve:	User Defined Fire / 1 car burning with 6,8GJ	
Maximum Fire Area:	12	m ²
Fire Elevation:	0.3	m
Fuel Height:	0.5	m

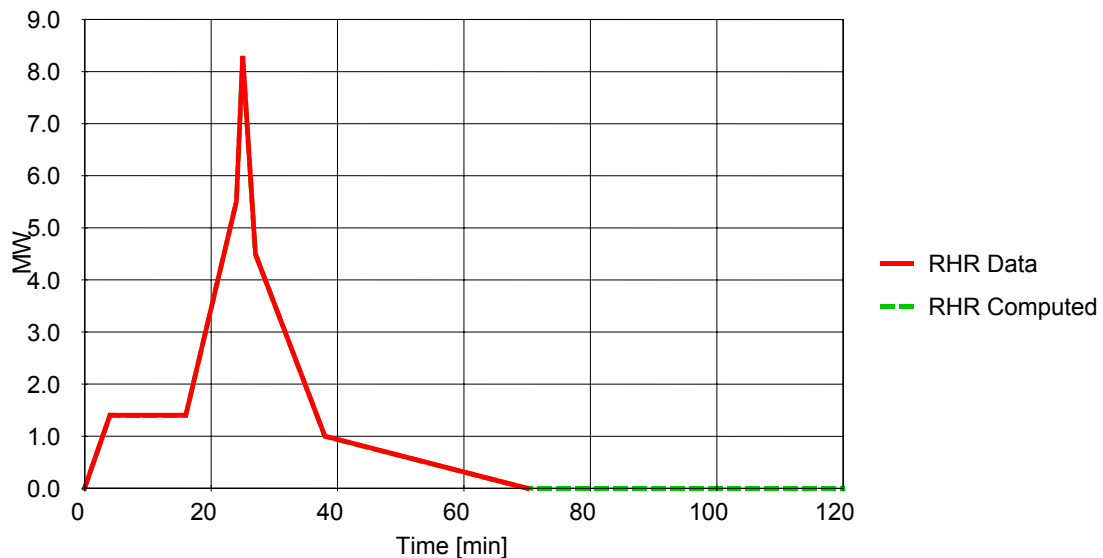
Point	Time [sec]	RHR [MW]	mf [kg/sec]	Fire Area [m ²]
1	0	0	0	0
2	240	1.4	0.1	2.024
3	960	1.4	0.1	2.024
4	1440	5.5	0.393	7.952
5	1500	8.3	0.593	12
6	1620	4.5	0.321	6.506
7	2280	1	0.071	1.446

8	4200	0	0	0
Combustion Heat of Fuel:		17.5	MJ/kg	
Combustion Efficiency Factor:		0.8		

RESULTS

Fire Area: The maximum fire area (12.00m²) is lower than 25% of the floor area (1512.00m²).
The fire load is localised.

Rate of Heat Release



Analysis Name: PROJET CJ / 1 CAR FORCED VENTILATION I+O

Figure 15. RHR Data and Computed; Peak: 8.30 MW at 25.00 min with total available energy of 6,8 GJ

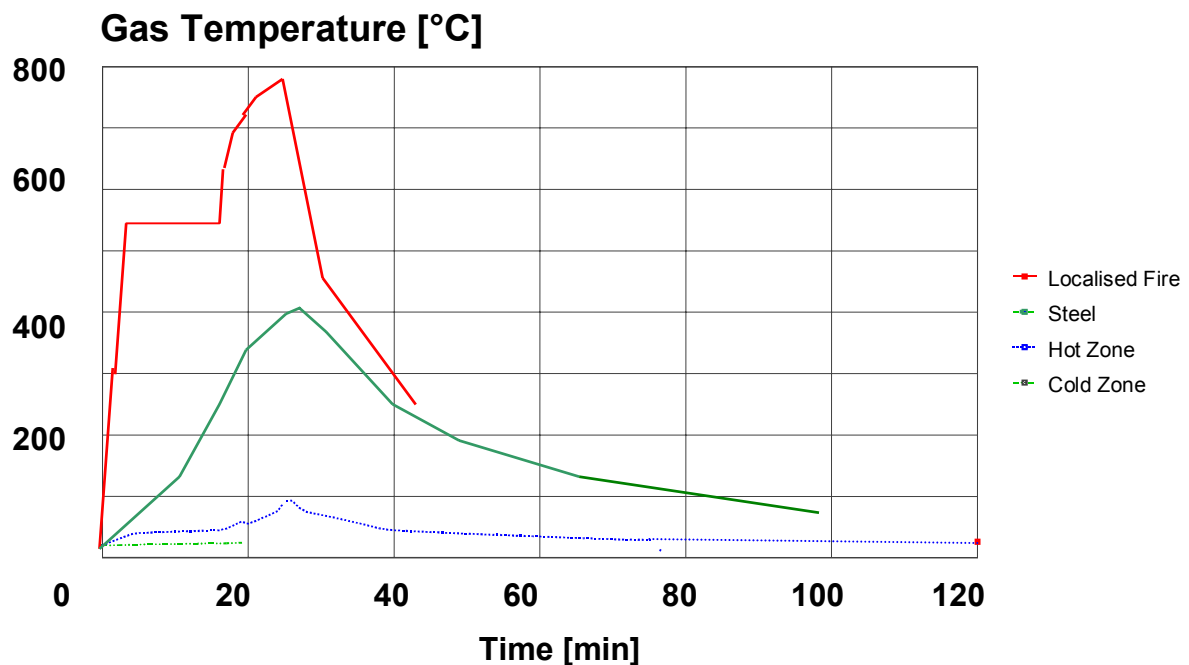


Figure 16. Temperatures on top of localised fire at 1,2m from axis of fire source, peak 780°C at 26'; Steel temperatures, peak 410 °C at 26' and Hot Zone temperatures, peak 93 °C at 26'.

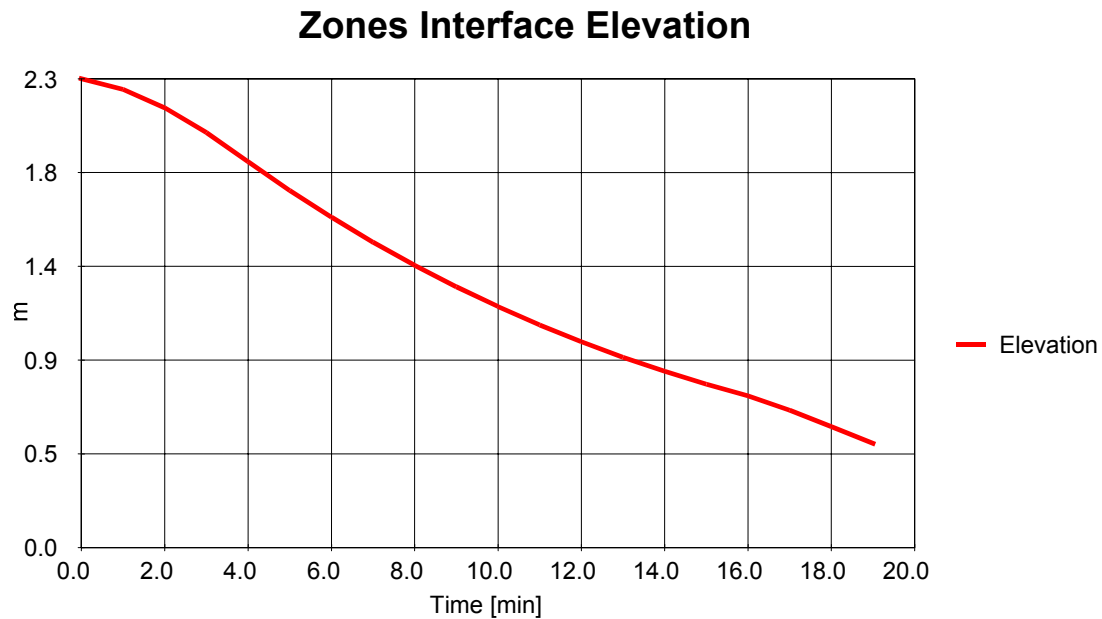


Figure 17. Zones Interface Elevation; smoke free lower zone 0,5m at 19'.

COLUMN STEEL PROFILE

Unprotected Section

Catalog Profile: **HD 400 x 347** with $A_m / V = 53\text{m}^{-1}$
 Exposed to Fire on: 4 sides

HEATING

Profile heated by: Maximum Between Hot Zone and Localised Fire Temperature
 Convection coefficient: $25 \text{ W/m}^2\text{K}$
 Relative emissivity: 0.5

Horizontal Distance Between Fire Axis and Profile: 1.2 m

FIRE RESISTANCE

Element Submitted to Compression
 Nominal Steel Grade: S 355
 Design effect of actions in fire situation

$N_{fi, d} = 10200 \text{ kN}$

Fire Design Buckling Length
 Buckling Length About Major Axis (y - y): 182 cm
 Buckling Length About Minor Axis (z - z): 182 cm

RESULTS

Critical Temperature: $467^\circ\text{C} > 410^\circ\text{C}$
Fire Resistance: UNLIMITED

3 FRAME ANALYSIS FOR NATURAL FIRES

3.1 School Campus ‘Geesseknäppchen’ in Luxembourg

3.1.1 Temperature field calculation

The temperature field calculations have been done using the software OZONE [13]. The data necessary to perform the temperature calculation, in the auditorium on the 5th and last floor of the school, have been defined by describing the compartment divided into the different walls, floor and ceiling with their respective components. Furthermore the Rate of Heat Release curve has been fixed by considering the occupancy of the compartment and the possible speed of the fire growth.

Figure 18 shows the result of the temperature calculation in the air of the compartment. This temperature curve will be used to verify the mechanical behaviour of the structure in case of fire. In this example the truss-like structure, shown in figure 19, is composed of **unprotected tubular steel sections** with a section factor of 141m^{-1} .

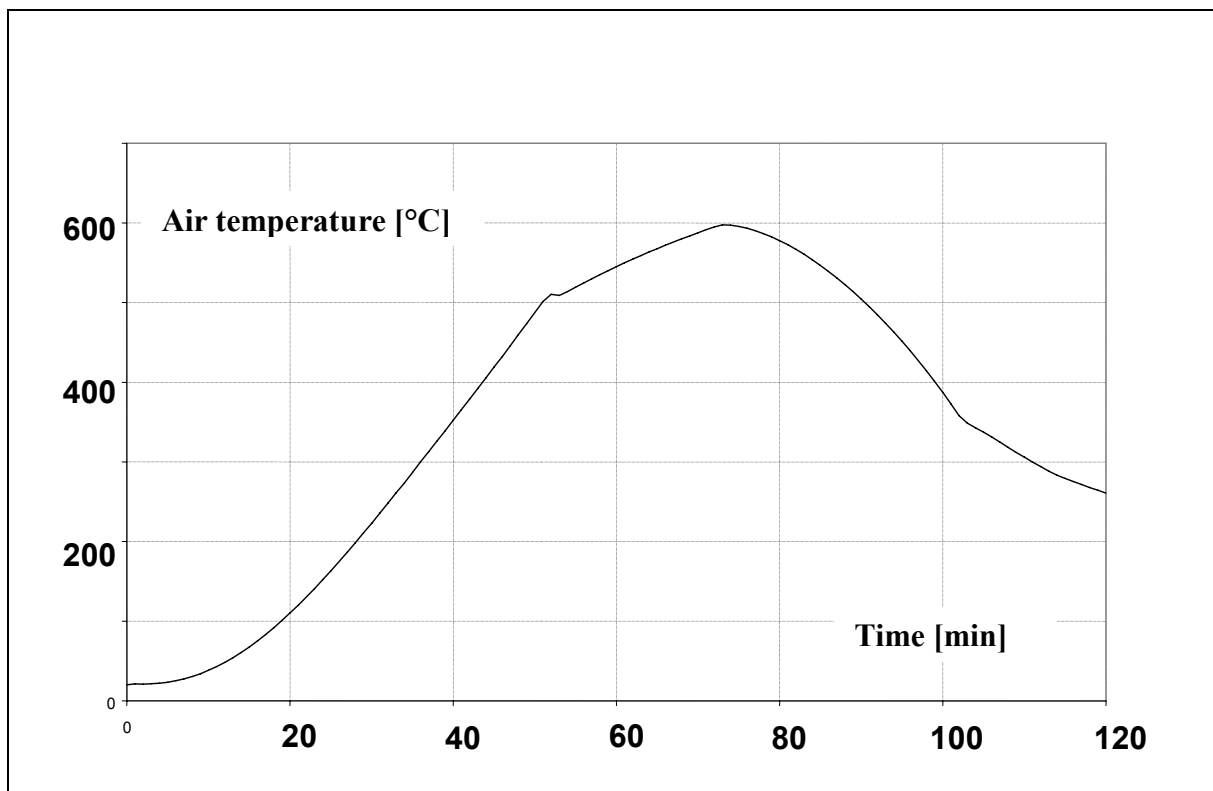


Figure 18. Temperature evolution in the auditorium.

3.1.2 Mechanical behaviour of the structure

The mechanical behaviour of the structure in case of fire has been verified using the software CEFICOSS [3]. The data necessary to perform the CEFICOSS calculation are given in figures 19 and 20.

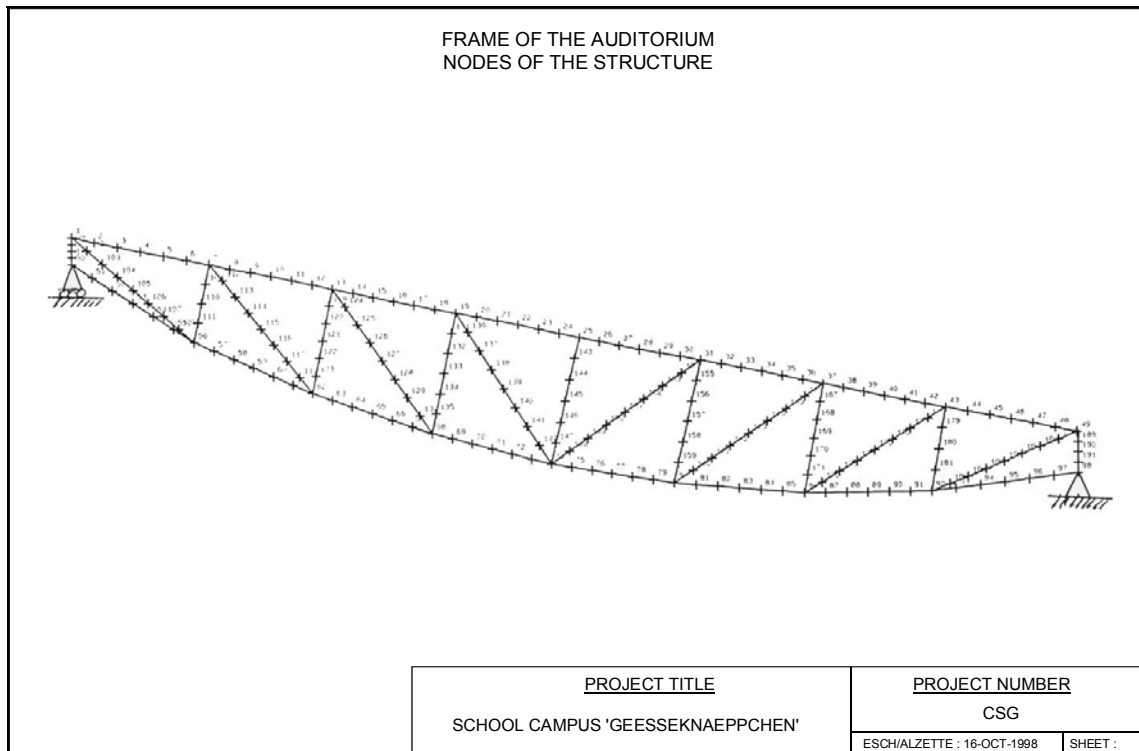


Figure 19. Roof truss with nodes of finite elements.

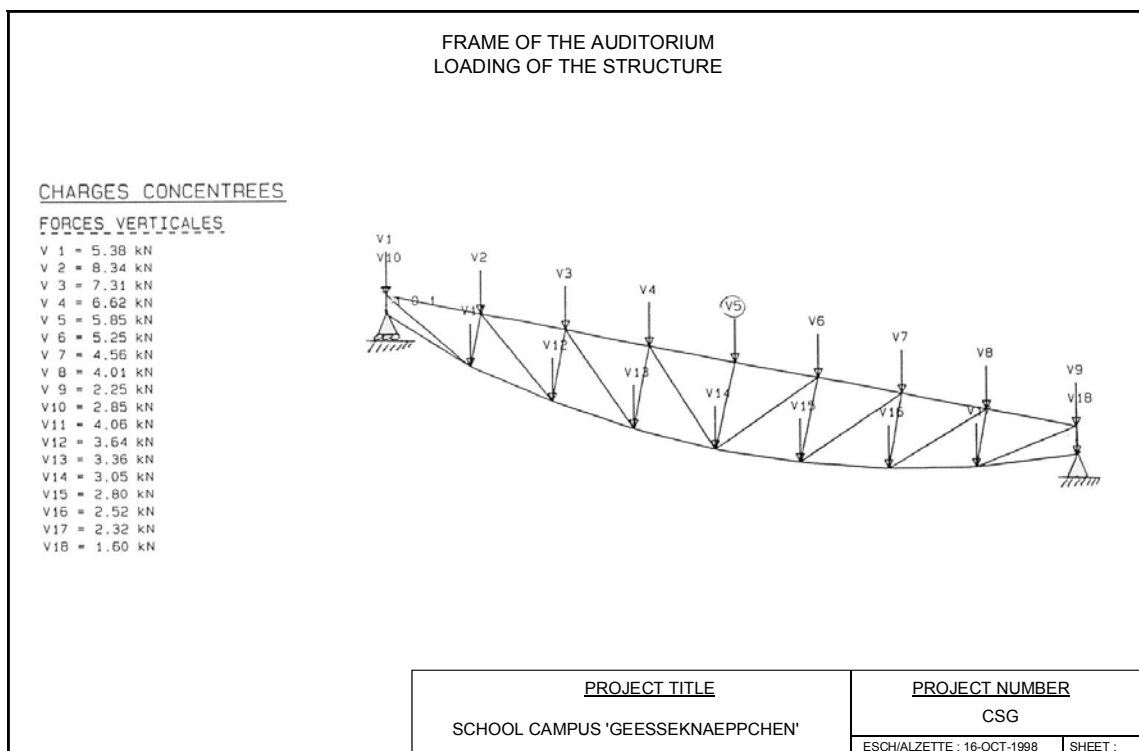


Figure 20. Loading of one roof truss.

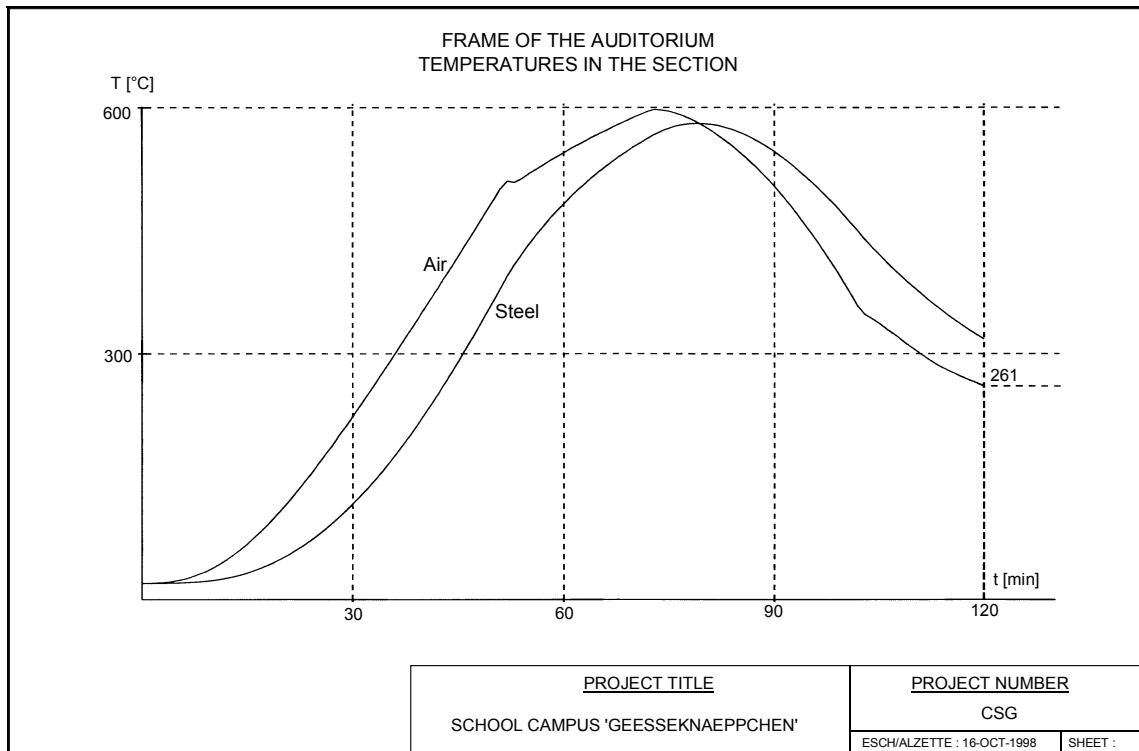


Figure 21. Temperatures in the unprotected tubular steel sections.

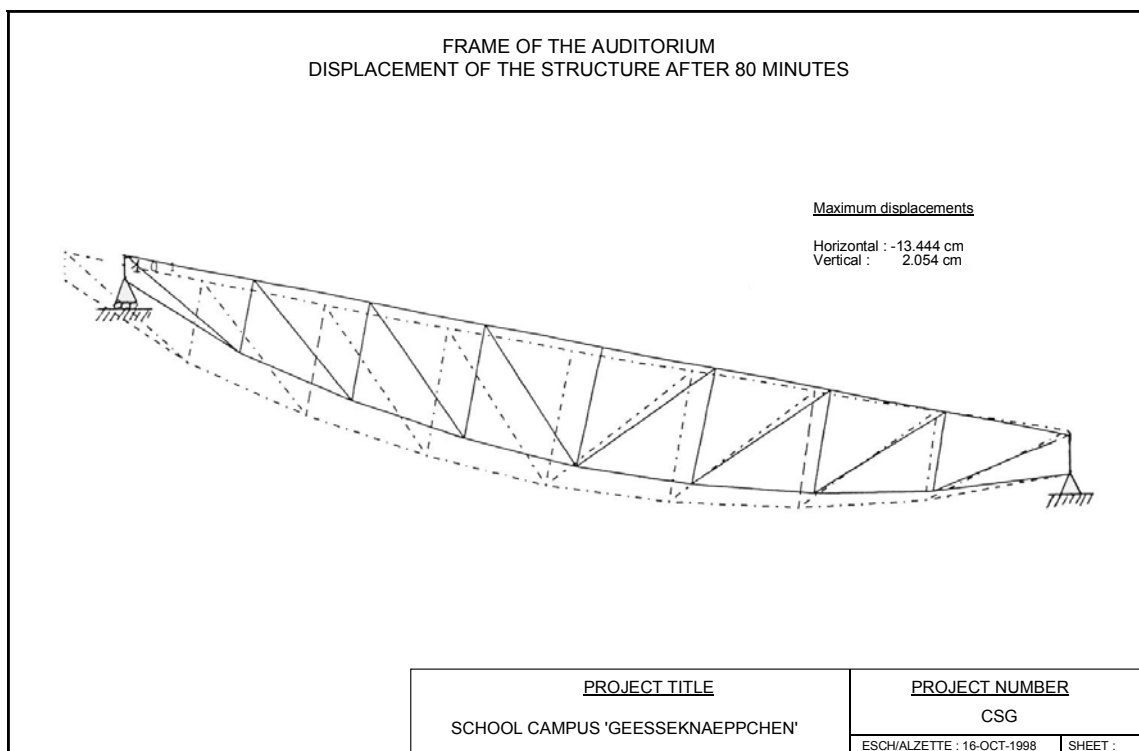


Figure 22. Displacement of the structure after 80 minutes of natural fire.

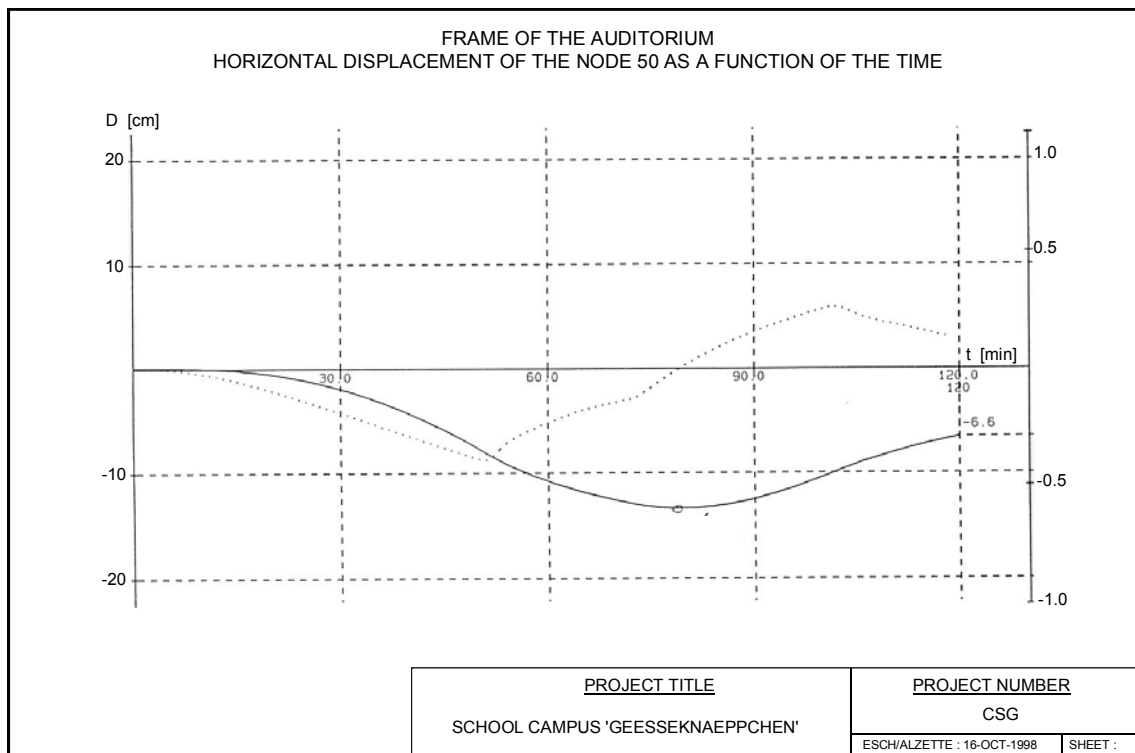


Figure 23. Horizontal displacement of the left part of the truss in function of time.

As demonstrated in figures 21 to 23 the roof truss composed of tubular steel sections is not endangered by the natural heating of figure 18, and this steel truss may remain visible and not protected. However it should be positionned in such a way that expansion at the upper left support is not restrained.

3.2 Frame with composite columns and composite beams

Thanks to the advanced numerical models, described in Chapter I-6.5, it is possible to simulate and understand the redistribution of forces inside a structure under the influence of any natural fire.

For instance, in the case of the structure of a car park subjected to the **fire of cars**, the structural deformations and the bending moment distribution at room temperature are illustrated in figures 24 and 25. The here given structure consists of composite columns composed of the steel profile HE 280A with partial concrete encasement and of beams composed of the steel profile IPE600 acting compositely with a concrete slab of 150mm thickness.

This numerical simulation finally proves that there is no danger of failure of the structure in this fire situation. How is it possible that a steel structure heated by approximately air temperatures of 800°C, leading to steel temperatures of about 650°C, is still able to bear the loads? The answer is that the fire remains localized and that the beams are continuous and composite.

Indeed as shown on figures 26 and 27 very high temperatures affect only the first five meters, directly heated by the burning car, of the continuous beam. That beam remains rather cool in its not directly heated part, so that at the central support a rather high negative bending moment may be activated as illustrated in figure 27.

During the fire we assist to a load redistribution as shown by the new static system indicated in figure 28. Finally we could completely forget the steel beam for the first five

meters, where the 150mm thick concrete slab is sufficient to bear the loads. This concrete slab is supported at the left end by the column and at the right end by the cantilever part of the continuous composite beam.

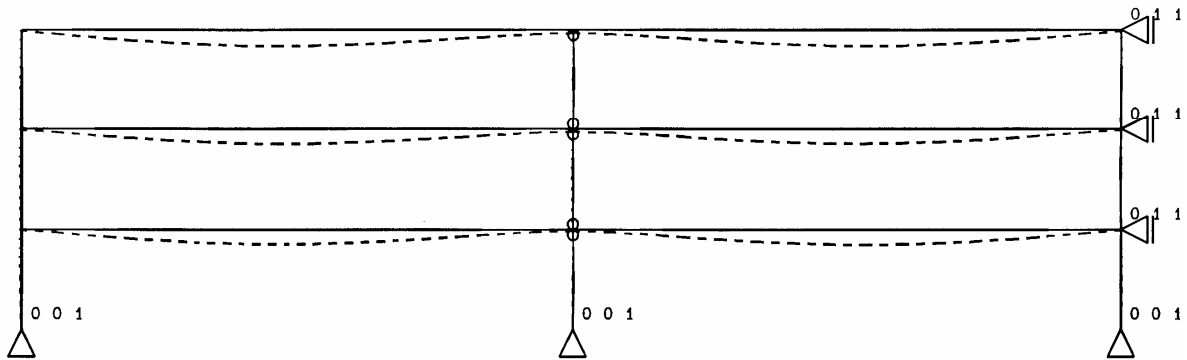


Figure 24. Displacement of the structure at room temperature.

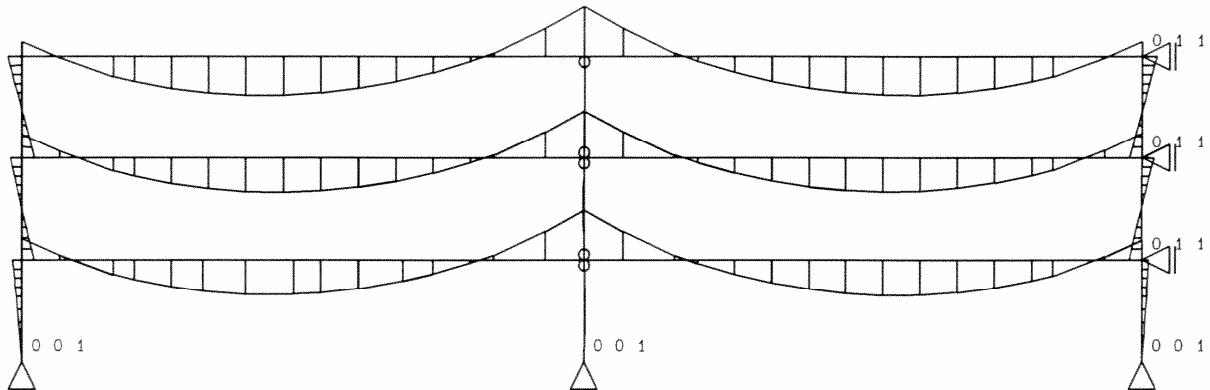


Figure 25. Bending moment distribution at room temperature.

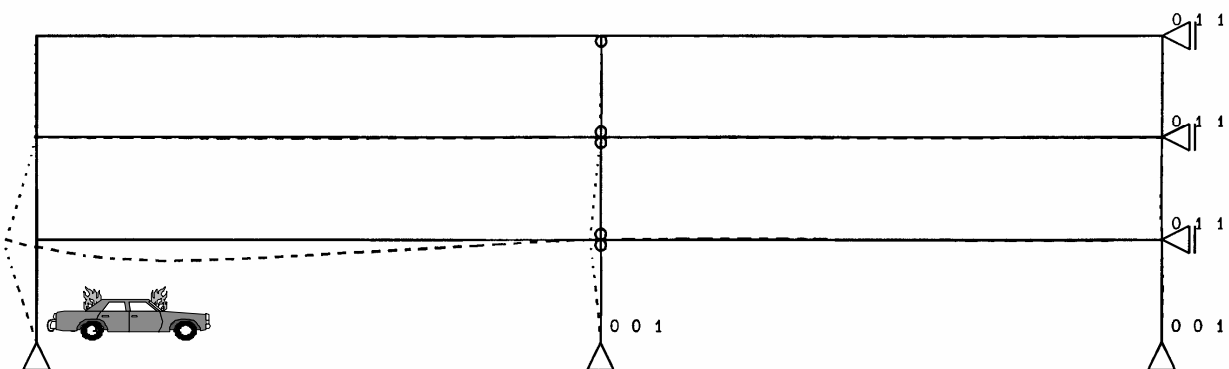


Figure 26. Displacement of the structure after 26 minutes of a car fire.

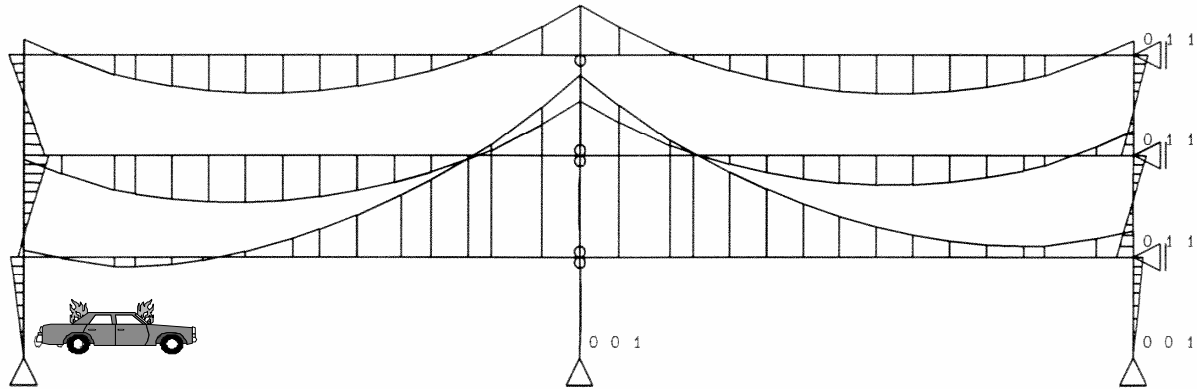


Figure 27. Bending moment distribution after 26 minutes of a car fire.

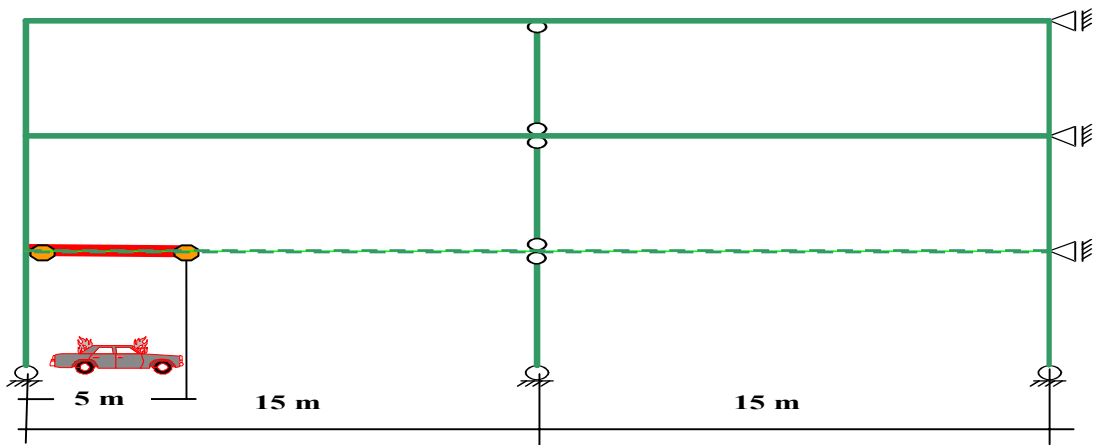


Figure 28. New static system due to partial plastification of the unprotected steel beam IPE600 on top of burning car.

4 APPLICATION OF THE SEMI-PROBABILISTIC APPROACH

4.1 Essentials

Before showing how to take full advantage of the Global Fire Safety Concept it is useful to recall the essentials of **Chapter III-3** concerning the **semi-probabilistic approach** as follows.

The probability of getting a fully fire engulfed compartment during life time is given by

$$p_{fi,55} = (p_{fi,55}^{IGNITION}) \cdot (p_f^{OC} \cdot p_f^{PS}) \cdot (p_f^{ACTIVE-MEASURE}) \quad (30c)$$

The failure probability in case of fire is expressed as

$$p_{ffi} \leq (p_{t,55} / p_{fi,55}) = p_{fi,t}, \text{ which is the target failure probability in case of fire} \quad (31)$$

This allows to create the connection between the probability $p_{fi,55}$ of getting a fully fire engulfed compartment during the life time of the building - the compartment size,

the type of occupancy and active fire fighting measures included - and the global factor γ_{qf} affecting the characteristic value $q_{f,k}$ of the fire load. This is illustrated in figures 6 and 7 of Chapter III-3.

The design fire load is obtained for the Level 1 approach by

$$q_{f,d} = \gamma_{qf} \cdot q_{f,k} \text{ [MJ/m}^2\text{]} \quad (2)$$

A simplification of the previous approach is given by the Level 2 approach, where the design fire load is obtained from

$$q_{f,d} = (m \cdot \delta_{q1} \cdot \delta_{q2} \cdot \prod \delta_{ni}) \cdot q_{f,k} \text{ [MJ/m}^2\text{]} \quad (3)$$

This Level 2 method has the enormous advantage to be userfriendly as all the partial factors δ_{q1} , δ_{q2} and differentiation factors δ_{ni} may be taken either directly from Annex E of EN1991-1-2 [12] either from tables 19 and 20 of Chapter III-3 of this Handbook.

4.2 Comparison between deterministic and semi-probabilistic approach

Using the Global Fire Safety Concept in its semi-probabilistic form does not automatically lead to a reduction of structural fire resistance. This concept is in fact above all allowing to adjust structural requirements to realistic and logical levels.

Of course, depending on the real safety situation, requirements may either become less or more severe than those imposed by conventional and deterministic regulations. This is illustrated by the following two different occupancies of on one side a 5 level Hotel and on the other side a school comprising a library [15].

4.2.1 Case study: Hotel - 5 levels

For this hotel, with 60 rooms and 2 beds per room, French regulations require for the structure an ISO-R60 fire resistance [1]. For this building

- no sprinklers are foreseen,
- smoke detection is only installed in corridors,
- in case of alarm smoke evacuation is activated in corridors.

The analysis of this situation requires the knowledge of following data:

- room size \rightarrow depth 6,25m \cdot width 4m \cdot height 3m $\rightarrow A_f = 25 \text{ m}^2$
- window size $\rightarrow 2\text{m} \cdot 2\text{m}$ with a window sill of 1m
- glass breaking during fire $\rightarrow 5\%$ at 20°C , 25% at 300°C , 100% at 500°C
- column length $\rightarrow 3,2\text{m}$
- for type and thickness of floor, ceiling and walls see pages VII-25 and VII-26.

Contrary to French regulations **we require that smoke detection is also installed in sleeping rooms; furthermore it is assumed that fire brigade arrives on site in less than 30 minutes after alarm.**

Hence in order to use equation (3) we need

$$\delta_{q1} = 0,1688 \ln A_f + 0,5752 = 1,118 \sim 1,12$$

$$\delta_{q2} = 1,0$$

$$\prod \delta_{ni} = \delta_{n4} \cdot \delta_{n7} = 0,73 \cdot 0,78 = 0,57$$

$$q_{f,k} = 377 \text{ MJ/m}^2 \text{ according to table 3 of Chapter I and}$$

$$\begin{aligned} q_{f,d} &= m \cdot \delta_{q1} \cdot \delta_{q2} \cdot \prod \delta_{ni} \cdot q_{f,k} \\ &= (0,8 \cdot 1,12 \cdot 1,0 \cdot 0,57) \cdot 377 = 192 \text{ MJ/m}^2. \end{aligned}$$

This permits to analyse the situation through the Software **Ozone** [13] showing on page VII- 28 that the column could be composed of a steel section HE 160A, quality S355, and protected by a sprayed layer of 6mm vermiculite-cement.

It has to be noted that the maximum air temperature of 926°C is obtained at 20 minutes and that the greatest steel temperature of 614°C is reached at 25 minutes. As this remains inferior to the critical column buckling temperature of 649°C, calculated inside Ozone on the basis of **prEN1993-1-2** [14], it may be assumed that the column will not fail.

OZone V 2.2.2 Report

Analysis Name: **Prof JB SCHLEICH**
 File Name: E:\FIRE-ENGINE\OZONE 2.2.2\MONTPELLIER-1A-DFC+P2.ozn
 Created: 06/09/04 at 11:03:26

ANALYSIS STRATEGY

Selected strategy: Combination 2Zones - 1 Zone Model
 Transition criteria from 2 Zones to 1 Zone
 Upper Layer Temperature $\geq 500^{\circ}\text{C}$
 Combustible in Upper Layer + U.L. Temperature \geq Combustible Ignition Temperature = 300 °C
 Interface Height ≤ 0.2 Compartment Height
 Fire Area ≥ 0.25 Floor Area

PARAMETERS

Openings

Radiation Through Closed Openings: 0.8
 Bernoulli Coefficient: 0.7

Physical Characteristics of Compartment

Initial Temperature: 293 K
 Initial Pressure: 100000 Pa

Parameters of Wall Material

Convection Coefficient at the Hot Surface: 25 W/m²K
 Convection Coefficient at the Cold Surface: 9 W/m²K

Calculation Parameters

End of Calculation: 7200 sec
 Time Step for Printing Results: 60 sec
 Maximum Time Step for Calculation: 10 sec

Air Entrained Model: Mc Caffrey

Temperature Dependent Openings

Temperature [°C]	Stepwise Variation % of Total Openings [%]
20	5
300	25
500	100

COMPARTMENT

Form of Compartment: Rectangular Floor
 Height: 3 m
 Depth: 4 m
 Length: 6.25 m
 Roof Type: Flat Roof

DEFINITION OF ENCLOSURE BOUNDARIES

Floor

Chapter VII - Examples of steel and composite structures

Material (from inside to outside)	Thickness [cm]	Unit Mass [kg/m³]	Conductivity [W/mK]	Specific Heat [J/kgK]		
Heavy Wood	1	720	0.2	1880		
Normal weight Concrete [EN1994-1-2]	15	2300	1.6	1000		
Gypsum board [EN12524]	1	900	0.25	1000		
Ceiling						
Material (from inside to outside)	Thickness [cm]	Unit Mass [kg/m³]	Conductivity [W/mK]	Specific Heat [J/kgK]		
Gypsum board [EN12524]	1	900	0.25	1000		
Normal weight Concrete [EN1994-1-2]	15	2300	1.6	1000		
Heavy Wood	1	720	0.2	1880		
Wall 1						
Material (from inside to outside)	Thickness [cm]	Unit Mass [kg/m³]	Conductivity [W/mK]	Specific Heat [J/kgK]		
GLASS	1	2500	1	720		
Openings / 4m²						
Sill Height [m]	Soffit Height [m]	Width [m]	Variation	Adiabatic		
1	3	2	Stepwise	no		
Wall 2						
Material (from inside to outside)	Thickness [cm]	Unit Mass [kg/m³]	Conductivity [W/mK]	Specific Heat [J/kgK]		
Normal Bricks	15	1600	0.7	840		
Wall 3						
Material (from inside to outside)	Thickness [cm]	Unit Mass [kg/m³]	Conductivity [W/mK]	Specific Heat [J/kgK]		
Normal Bricks	14	1600	0.7	840		
Wall 4						
Material (from inside to outside)	Thickness [cm]	Unit Mass [kg/m³]	Conductivity [W/mK]	Specific Heat [J/kgK]		
Normal Bricks	15	1600	0.7	840		
FIRE						
Fire Curve:	NFSC Design Fire					
Maximum Fire Area:	25	m²				
Fire Elevation:	0.2	m				
Fuel Height:	0.2	m				
Occupancy	Fire Growth Rate	RHRf	Fire Load qf,k	Danger of Fire		
		[kW/m²]	[MJ/m²]	Activation		
Hotel (room)	Medium	250	377	1		
Active Measures						
Description			Active	Value		
Automatic Water Extinguishing System			No	γn,1 = 1		
Independent Water Supplies			No	γn,2 = 1		
Automatic Fire Detection by Heat			No			
Automatic Fire Detection by Smoke			Yes	γn,4 = 0.73		
Automatic Alarm Transmission to Fire Brigade			No	γn,5 = 1		
Work Fire Brigade			No			
Off Site Fire Brigade			Yes	γn,7 = 0.78		
Safe Access Routes			Yes	γn, 8 = 1		
Staircases Under Overpressure in Fire Alarm			No			
Fire Fighting Devices			Yes	γn, 9 = 1		
Smoke Exhaust System			Yes	γn, 10 = 1		
Fire Risk Area:		25	m²	γq, 1= 1.12		
Danger of Fire Activation:				γq, 2= 1		
qf, d=		192.3	MJ/m²			
Combustion Heat of Fuel:	17.5	MJ/kg				
Combustion Efficiency Factor:	0.8					
Combustion Model:	Extended fire duration					

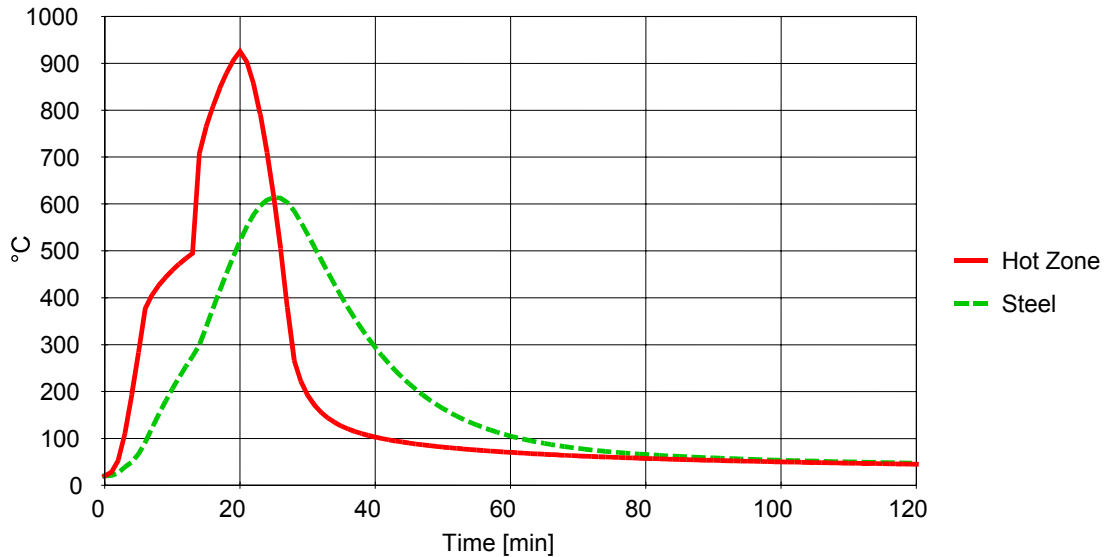
RESULTS

Fire Area: The maximum fire area (25.00m²) is greater than 25% of the floor area (25.00m²). **The fire load is uniformly distributed.**

Switch to one zone: Lower layer Height < 20.0% ocompartment height at time [s] 130.00

Fully engulfed fire: Temperature of zone in contact with fuel >300.0°C at time [s] 312.65

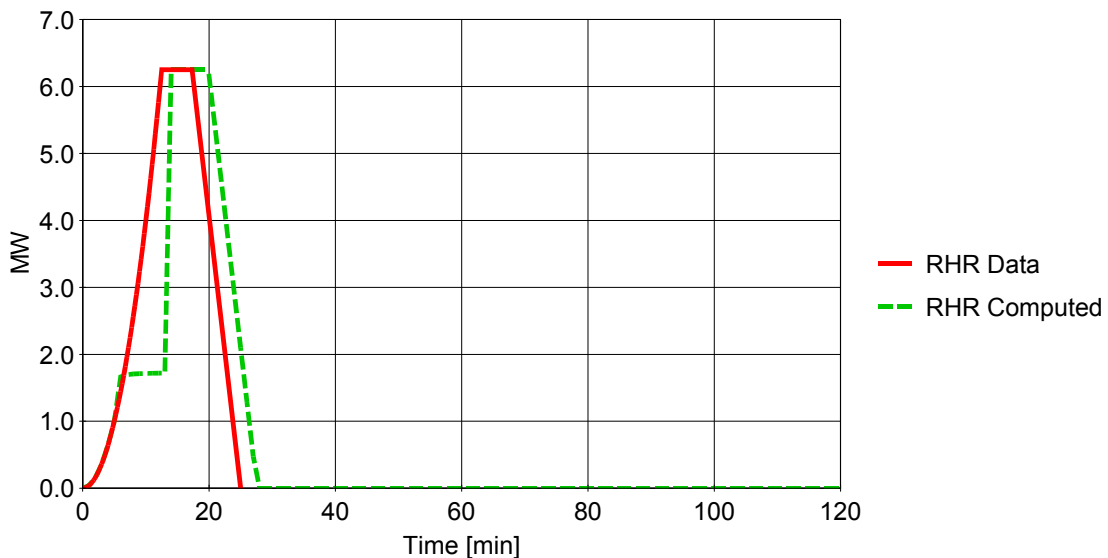
Gas & Steel Temperatures



Analysis Name: Prof JB SCHLEICH

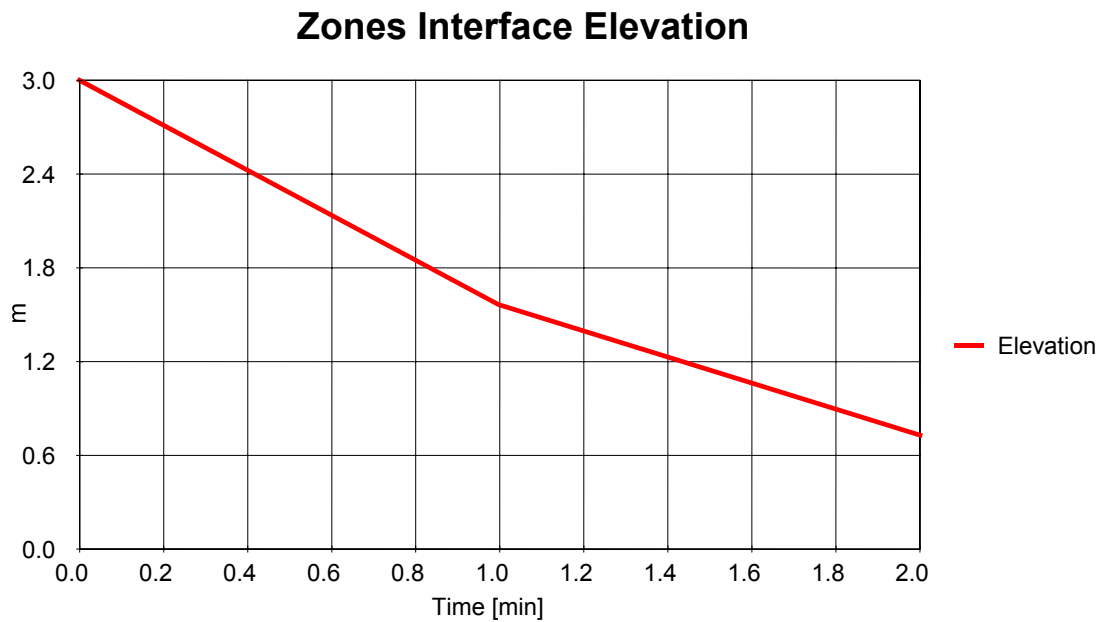
**Figure 29. Hot Zone and Steel Temperatures; Peak gas 926 °C at 20 min;
Peak steel temperatures 614°C at 25 min**

Rate of Heat Release



Analysis Name: Prof JB SCHLEICH

**Figure 30. RHR Data and Computed;
Available energy =192,3 MJ/m² x 25m² = 4807MJ
Peak 6.25 MW at 12.5 min**



Analysis Name: Prof JB SCHLEICH

Figure 31. Zones Interface Elevation; free smoke zone $h = 0.72$ m at 2.00 min.

STEEL PROFILE

Protected Section		
Catalog Profile:	HE 160 A	
Exposed to Fire on:	4 sides	
Contour Encasement		
Protection Material:	From Catalog	
Protection Thickness:	6 mm	
Material Name:	Spray Vermiculit - Cement	
Unit Mass	Specific Heat	Thermal Conductivity
[kg/m ³]	[J/kgK]	[W/mK]
800	1100	0.2

HEATING

Profile heated by:	Maximum Between Hot Zone and Localised Fire Temperature
Convection coefficient:	25 W/m ² K
Relative emissivity:	0.5

FIRE RESISTANCE

Element Submitted to Compression	
Nominal Steel Grade:	S 355
Design effect of actions in fire situation	
$N_{fi,Sd} = 300$ kN	
Fire Design Buckling Length	
Buckling Length About Major Axis (y - y):	160 cm
Buckling Length About Minor Axis (z - z):	160 cm

RESULTS

Critical Temperature:	649 °C > STEEL TEMPERATURE 614°C
Fire Resistance:	No failure

However in order to eliminate any doubt about second order effects, buckling stability was also checked through the **advanced calculation model CEFICOSS** [3]. **No buckling finally occurs**, the **largest horizontal deformation being 3,7mm at 26 minutes when the steel profile has also the highest temperatures** according to the figures 32 and 33. By the way at 26 minutes also occurs the minimum MPV level .

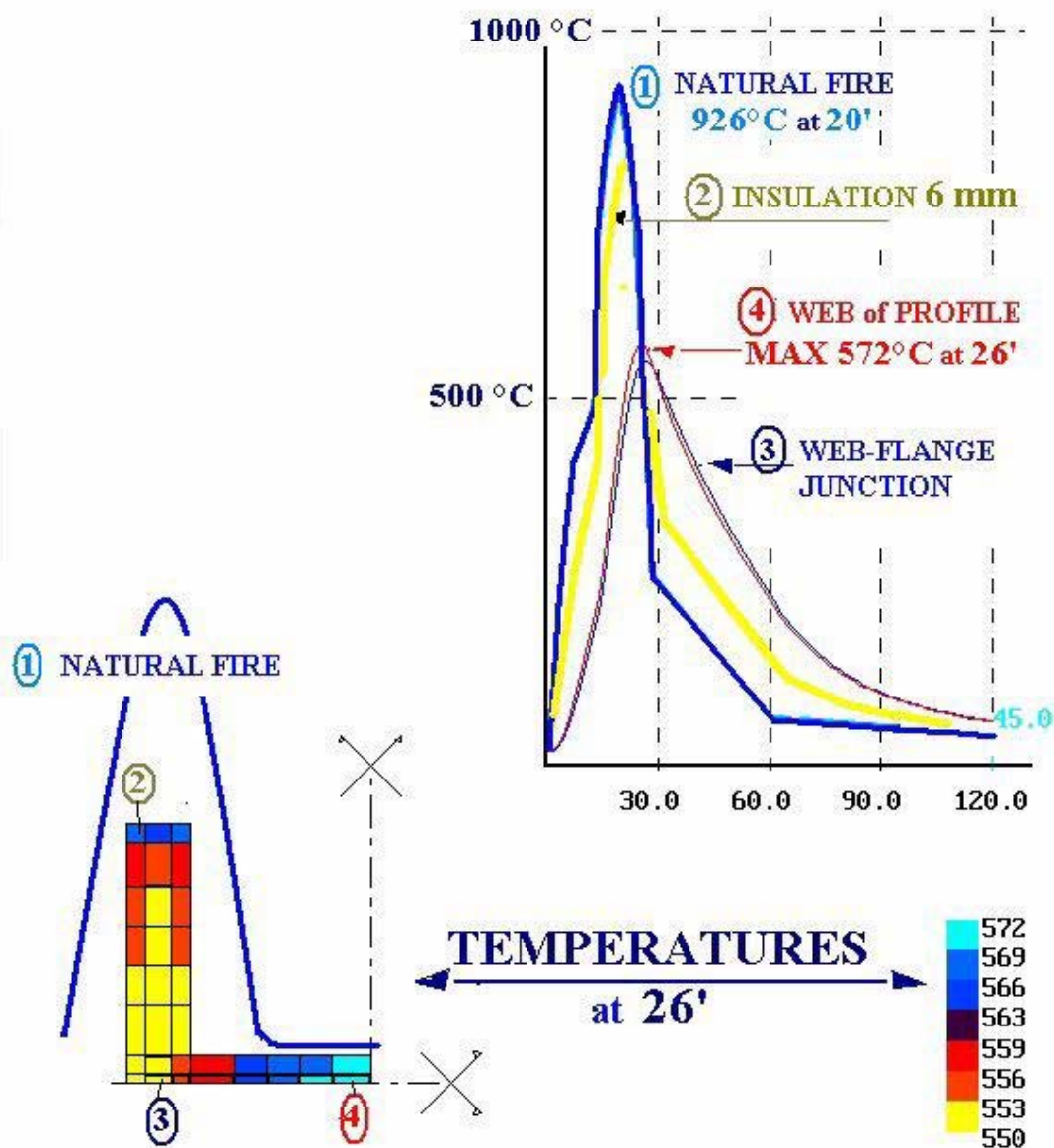


Figure 32. Temperatures in the insulated steel section HE 160A in function of time established by "CEFICOSS" for the natural fire given in figure 29.

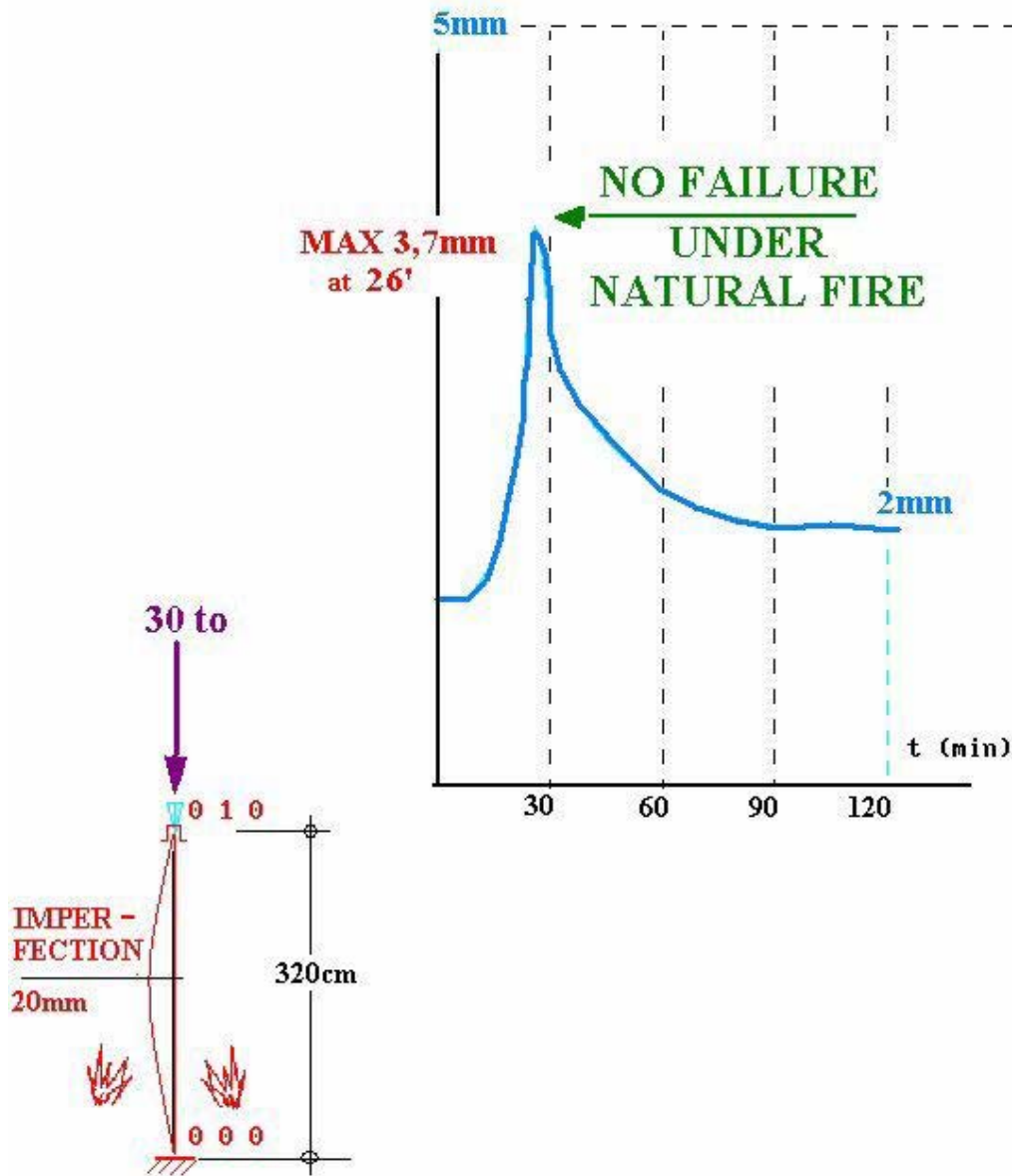


Figure 33. Horizontal deformation in function of time, at mid-height of the column composed of the insulated steel section HE 160A, for the natural fire.

The present steel section HE 160A, loaded with an axial load of $N_{fi,Sd} = 300$ kN and protected by 6mm of vermiculite-cement, is well designed for this natural fire as buckling indicated at 26 minutes in figure33 is clearly stopped. This is due to gas temperatures which, with a maximum of 926°C at 20 minutes, drop to ~ 572°C at 26 minutes and from now on cool down the steel section. That section has been heated to maximum temperatures of 572°C in the web and 559°C at the flange edge (see figure 32).

The same configuration submitted to the ISO-fire leads, according to figures 34 and 35, to the column buckling at 26 minutes when the steel section is heated up to 625°C. This means that the column designed for the natural fire, according to pages VII -24 to VII-26, corresponds to an ISO-R30 fire resistance.

The conclusion is that for this type of building, **Hotel - 5 levels**, the use of the **Global Fire Safety Concept** leads to a **practical reduction of the fire resistance requirement from R60 to R30**. However it has to be highlighted that this also leads to an improvement of the safety of people, as **we require that smoke detection is also installed in sleeping rooms**. Indeed figure 31 indicates that smoke has gone down to bed level at 2.00 minutes after fire has started in that room. **In fact it is totally irresponsible not to install smoke detection in hotel rooms.**

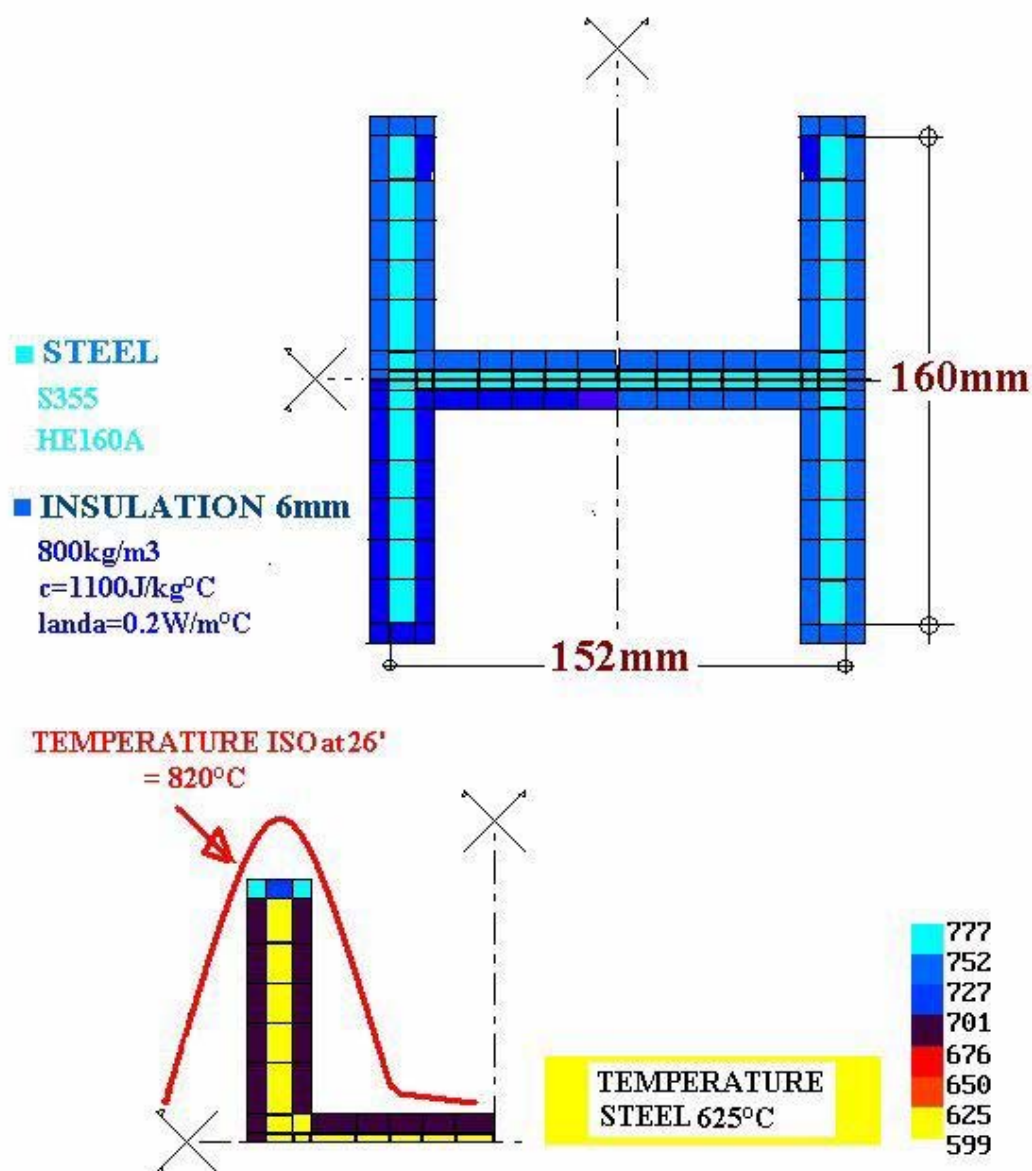


Figure 34. Temperatures at 26 minutes in the insulated steel section HE 160A, established by "CEFICOSS" for the ISO heating.

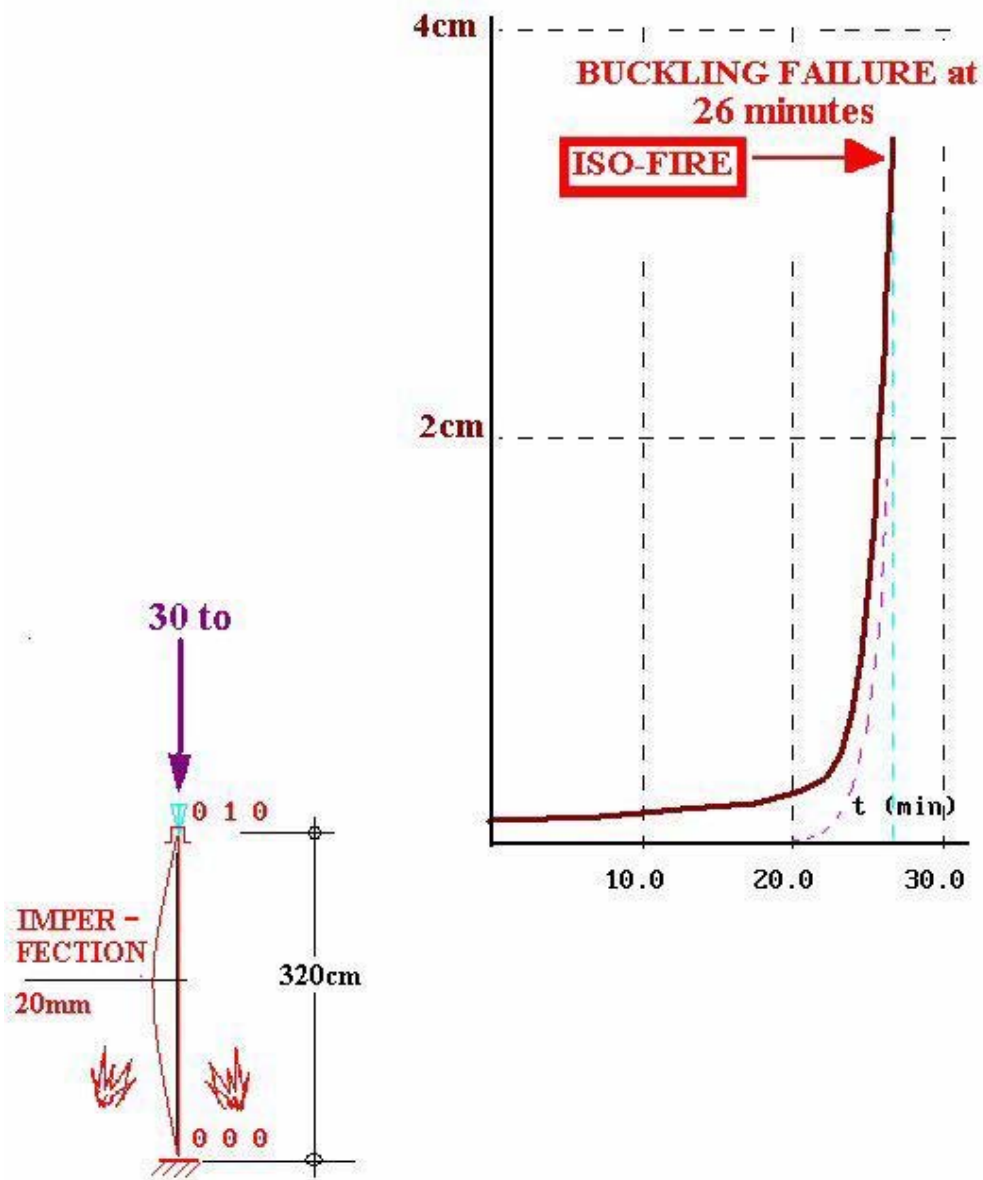


Figure 35. Horizontal deformation in function of time, at mid-height of the column composed of the insulated steel section HE 160A, for the ISO-heating.

4.2.2 Case study: School-3 levels with library on ground level

For this school, foreseen for 750 students, French regulations require for the structure an ISO-R30 fire resistance [1]. For this building

- no sprinklers are foreseen,
- smoke detection is nowhere installed,
- there is no smoke evacuation.

The analysis of this situation requires the knowledge of following data:

- room size of library → depth 6,25m · width 40,2m · height 3m → $A_f = 251 \text{ m}^2$
- window size → 40,2m · 2m with a window sill of 1m
- glass breaking during fire → 5% at 20°C, 25% at 300°C, 100% at 500°C
- column length → 3,2m
- type and thickness of floor, ceiling and walls is described on pages VII-34 and VII-35.

Contrary to French regulations **we require that smoke detection is installed in the library and that smoke evacuation is operating in that room;** furthermore it is assumed **that fire brigade arrives on site in less than 30 minutes after alarm.**

Hence in order to use equation (3) we need

$$\delta_{q1} = 0,1688 \ln A_f + 0,5752 = 1,507 \sim 1,51$$

$$\delta_{q2} = 1,0$$

$$\prod \delta_{ni} = \delta_{n4} \cdot \delta_{n7} = 0,73 \cdot 0,78 = 0,57$$

$$q_{f,k} = 1824 \text{ MJ/m}^2 \text{ according to table 3 of Chapter I and}$$

$$q_{f,d} = m \cdot \delta_{q1} \cdot \delta_{q2} \cdot \prod \delta_{ni} \cdot q_{f,k} \\ = (0,8 \cdot 1,51 \cdot 1,0 \cdot 0,57) \cdot 1824 = 1255 \text{ MJ/m}^2.$$

This permits to analyse the situation through the Software Ozone [13] showing on page VII-38 that the column could be composed of a steel section HE 160A, quality S355, and protected by a hollow encasement of 16mm fibre-cement boards.

It has to be noted that the maximum air temperature of 1306°C is obtained at 36 minutes and that the greatest steel temperature of 642°C is reached at 55 minutes (see figures 36 and 38). As this remains inferior to the critical column buckling temperature of 649°C, calculated inside Ozone on the basis of **prEN1993-1-2** [14], it may be assumed that the column will not fail.

The same configuration submitted to the ISO-fire leads to a column buckling at 73 minutes when using the Nomogram of ECCS (see [7] and figure 35 of Chapter I). This means that the column designed for the natural fire, according to pages VII-33 to VII -35, should correspond to an ISO-R90 fire resistance.

The conclusion is that for this type of building, **School-3 levels with library on ground level,** the use of the Global Fire Safety Concept leads to a shifting of the fire resistance requirement from R30 to R90. This seems to be absolutely logical as the real fire occurring in the library, with a quite high fire load, gives way to much higher temperatures as those produced by an ISO-fire (see figure 36).

However it has to be highlighted that this also leads to an improvement of the safety of the students, as **we require that smoke detection and smoke evacuation is installed in the library. Furthermore the library shall form an R90 compartment.**

Provided escape staircases remain free of any smoke, thus allowing safe evacuation of all students, the other structural elements relative to normal class-rooms may only fulfil R30 requirements.

OZone V 2.2.2 Report

Analysis Name: **Prof JB SCHLEICH**
 File Name: E:\FIRE-ENGINE\OZONE 2.2.2\MONTPELLIER-2-DFPDES.ozn
 Created: 31/08/04 at 23:24:13

ANALYSIS STRATEGY

Selected strategy: Combination 2Zones - 1 Zone Model
 Transition criteria from 2 Zones to 1 Zone
 Upper Layer Temperature $\geq 500^{\circ}\text{C}$
 Combustible in Upper Layer + U.L. Temperature \geq Combustible Ignition Temperature = 300°C
 Interface Height ≤ 0.2 Compartment Height
 Fire Area ≥ 0.25 Floor Area

PARAMETERS

Openings
 Radiation Through Closed Openings: 0.8
 Bernoulli Coefficient: 0.7
Physical Characteristics of Compartment
 Initial Temperature: 293 K
 Initial Pressure: 100000 Pa
Parameters of Wall Material
 Convection Coefficient at the Hot Surface: $25 \text{ W/m}^2\text{K}$
 Convection Coefficient at the Cold Surface: $9 \text{ W/m}^2\text{K}$
Calculation Parameters
 End of Calculation: 7200 sec
 Time Step for Printing Results: 60 sec
 Maximum Time Step for Calculation: 10 sec
Air Entrained Model: Mc Caffrey

Temperature Dependent Openings

Temperature [$^{\circ}\text{C}$]	Stepwise Variation % of Total Openings [%]
20	5
300	25
500	100

COMPARTMENT

Form of Compartment: Rectangular Floor
Height: 3 m
Depth: 6.25 m
Length: 40.2 m
 Roof Type: Flat Roof

DEFINITION OF ENCLOSURE BOUNDARIES

Floor

Material (from inside to outside)	Thickness [cm]	Unit Mass [kg/m^3]	Conductivity [W/mK]	Specific Heat [J/kgK]
Heavy Wood	1	720	0.2	1880
Normal weight Concrete [EN1994-1-2]	15	2300	1.6	1000
Gypsum board [EN12524]	1	900	0.25	1000

Ceiling

Material (from inside to outside)	Thickness [cm]	Unit Mass [kg/m^3]	Conductivity [W/mK]	Specific Heat [J/kgK]
Gypsum board [EN12524]	1	900	0.25	1000
Normal weight Concrete [EN1994-1-2]	15	2300	1.6	1000
Heavy Wood	1	720	0.2	1880

Wall 1

Material (from inside to outside)	Thickness [cm]	Unit Mass [kg/m^3]	Conductivity [W/mK]	Specific Heat [J/kgK]
Normal Bricks	15	1600	0.7	840

Chapter VII - Examples of steel and composite structures

Wall 2

Material (from inside to outside)	Thickness [cm]	Unit Mass [kg/m ³]	Conductivity [W/mK]	Specific Heat [J/kgK]
GLASS	1	2500	1	720

Openings / 80m²

Sill Height [m]	Soffit Height [m]	Width [m]	Variation	Adiabatic
1	3	40.2	Stepwise	no

Wall 3

Material (from inside to outside)	Thickness [cm]	Unit Mass [kg/m ³]	Conductivity [W/mK]	Specific Heat [J/kgK]
Normal Bricks	15	1600	0.7	840

Wall 4

Material (from inside to outside)	Thickness [cm]	Unit Mass [kg/m ³]	Conductivity [W/mK]	Specific Heat [J/kgK]
Normal Bricks	14	1600	0.7	840

FIRE

Fire Curve:	NFSC Design Fire	
Maximum Fire Area:	251	m ²
Fire Elevation:	0.2	m
Fuel Height:	0.2	m

Occupancy	Fire Growth Rate	RHRf	Fire Load qf,k [kw/m ²]	Danger of Fire [MJ/m ²]	Activation
Library	Fast	500	1824	1	

Active Measures

Description	Active	Value
Automatic Water Extinguishing System	No	$\gamma_{n,1} = 1$
Independent Water Supplies	No	$\gamma_{n,2} = 1$
Automatic Fire Detection by Heat	No	
Automatic Fire Detection by Smoke	Yes	$\gamma_{n,4} = 0.73$
Automatic Alarm Transmission to Fire Brigade	No	$\gamma_{n,5} = 1$
Work Fire Brigade	No	
Off Site Fire Brigade	Yes	$\gamma_{n,7} = 0.78$
Safe Access Routes	Yes	$\gamma_{n,8} = 1$
Staircases Under Overpressure in Fire Alarm	No	
Fire Fighting Devices	Yes	$\gamma_{n,9} = 1$
Smoke Exhaust System	Yes	$\gamma_{n,10} = 1$

Fire Risk Area: 251 m² **$\gamma_{q,1} = 1.51$**

Danger of Fire Activation: $\gamma_{q,2} = 1$

$q_{f,d} = 1254.6$ MJ/m²

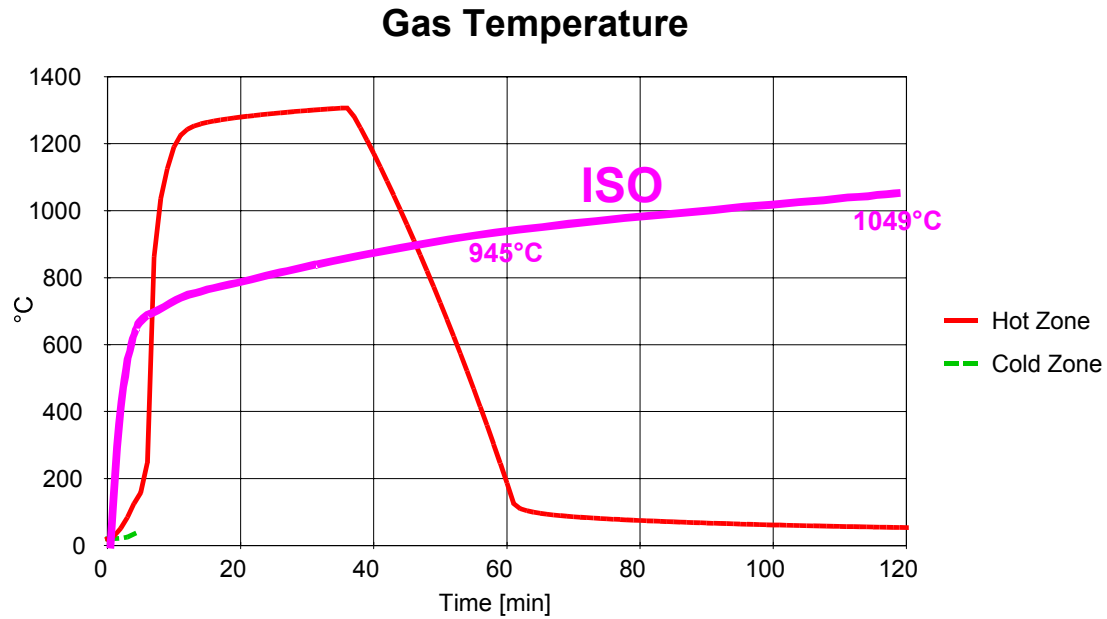
Combustion Heat of Fuel:	17.5	MJ/kg
Combustion Efficiency Factor:	0.8	
Combustion Model:	Extended fire duration	

RESULTS

Fire Area: The maximum fire area (251.00m²) is greater than 25% of the floor area (251.25m²). The fire load is uniformly distributed.

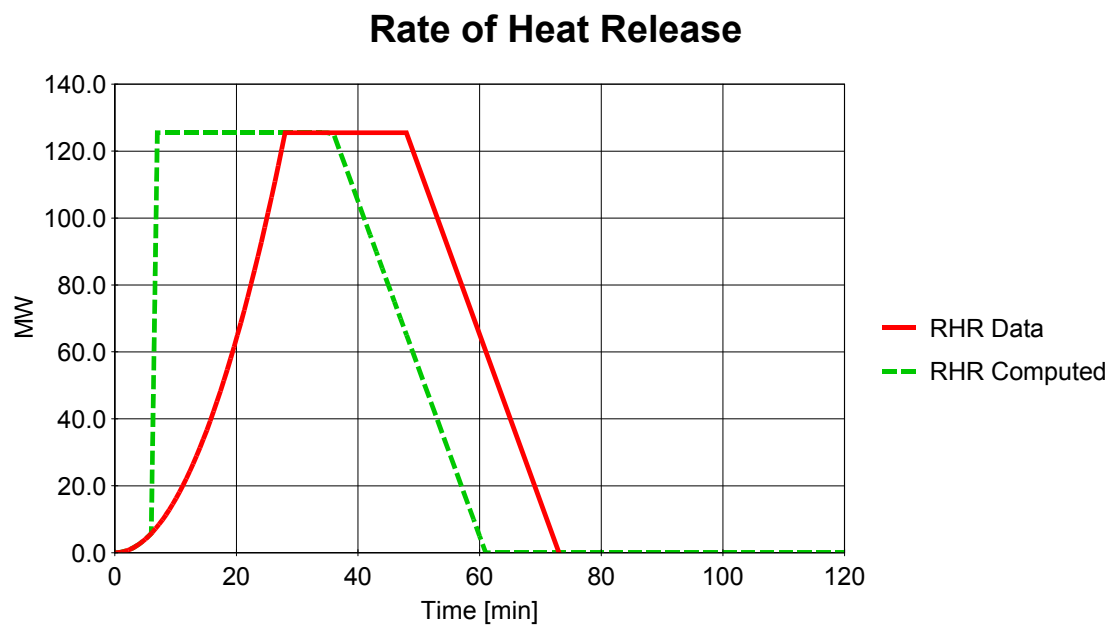
Switch to one zone: Lower layer Height < 20.0% ocompartment height at time [s] 293.38

Fully engulfed fire: Temperature of zone in contact with fuel >300.0°C at time [s] 408.07



Analysis Name: Prof JB SCHLEICH

Figure 36. Hot Zone Temperature with Peak of 1306 °C at 36 min

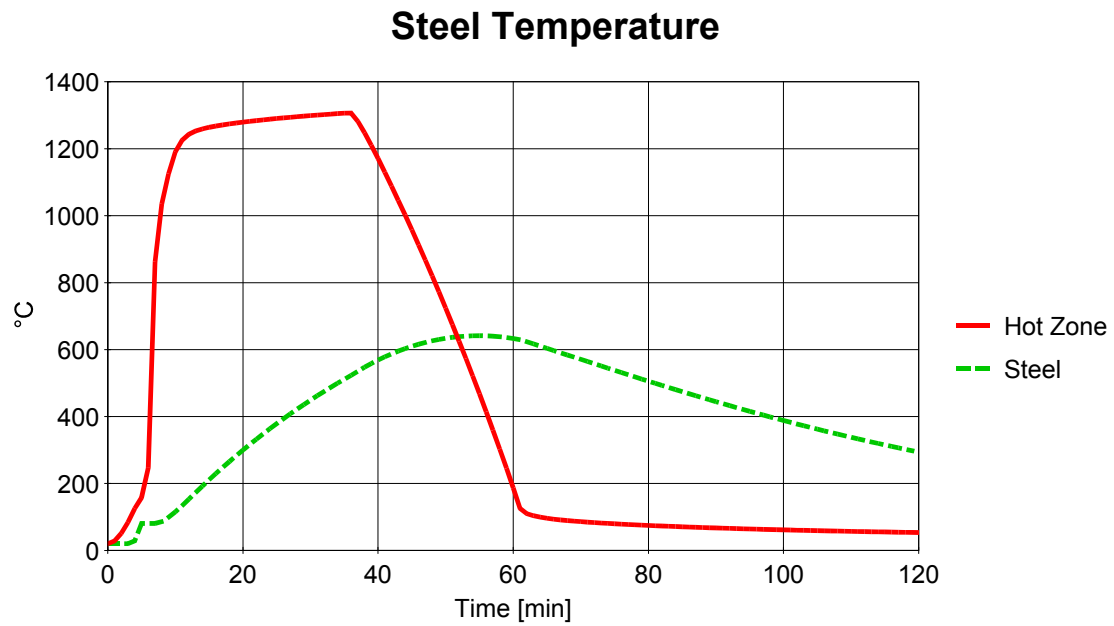


Analysis Name: Prof JB SCHLEICH

Peak: 125.50 MW

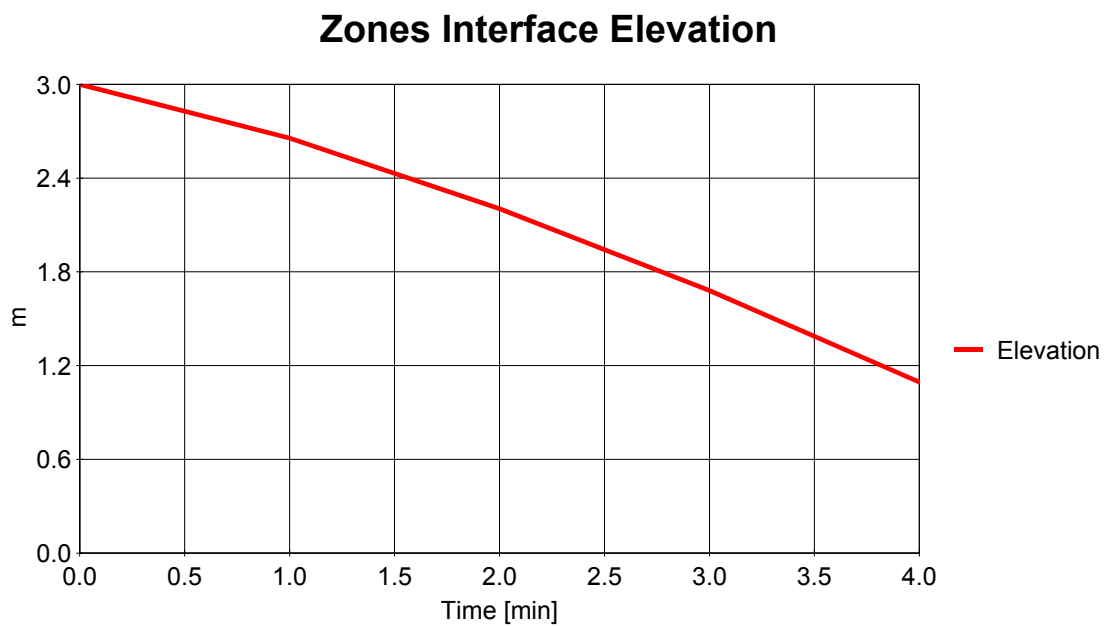
At: 28.0 min

**Figure 37. RHR Data and Computed;
Available energy = $1255 \text{ MJ/m}^2 \times 251 \text{ m}^2 = 315 \text{ GJ}$
Peak 126 MW at ~7 minutes**



Analysis Name: Prof JB SCHLEICH

**Figure 38. Hot Zone and Steel Temperature;
Peak steel temperature 642 °C at 55 min**



Analysis Name: Prof JB SCHLEICH

Figure 39. Zones Interface Elevation; free smoke zone $h = 1,08$ m at 4 min.

STEEL PROFILE

Protected Section		
Catalog Profile:	HE 160 A	
Exposed to Fire on:	4 sides	
Hollow Encasement		
Protection Material:	From Catalog	
Protection Thickness:	16 mm	
Material Name:	Board Fiber Cement	
Unit Mass	Specific Heat	Thermal Conductivity
[kg/m³]	[J/kgK]	[W/mK]
800	1200	0.15

HEATING

Profile heated by:	Maximum Between Hot Zone and Localised Fire Temperature
Convection coefficient:	25 W/m ² K
Relative emissivity:	0.5
Horizontal Distance Between Fire Axis and Profile:	0 m

FIRE RESISTANCE

Element Submitted to Compression	
Nominal Steel Grade:	S 355
Design effect of actions in fire situation	
N_{fi, d} = 300 kN	
Fire Design Buckling Length = 0,5L	
Buckling Length About Major Axis (y - y):	160 cm
Buckling Length About Minor Axis (z - z):	160 cm

RESULTS

Critical Temperature:	649 °C > STEEL TEMPERATURE 642°C
Fire Resistance:	NO FAILURE

4.3 Global fire safety concept applied to "Banque Populaire" /

Luxembourg_(2001-2003) / Arch. *Tatiana FABECK*

The architectural conception of this building is based on the intersection of two prismatic volumes enveloped by a double-glass façade (see figure 43). The steel structure (see figure 42) with its columns and composite cellular beams not protected by any insulation, contributes to the architectural expression.

In fact the beams "ACB-H600 – S460" with a maximum length of 16,8 m, are finally masked by the false ceiling with no special fire resistance requirement. However the columns, HD400 x 237 to 187, remain absolutely visible for a free office height of 3,1 m (see figure 44). This quite amazing result is due to the **implementation of the full set of active fire fighting measures as presented in Annex E of EN1991-1-2 [12]**, which means

- ❖ the building is completely sprinklered and a water-reservoir of 20 m³ has been foreseen,
- ❖ overall smoke detection is implemented and automatic alarm transmission to the fire brigade has been installed,
- ❖ in case of fire alarm smoke exhaust is activated in the compartment under fire, whereas air conditioning and any ventilation is completely stopped,
- ❖ furthermore staircases are put under overpressure in case of fire alarm.

Some constructive requirements were however imposed i.e

- ❖ full shear connection between steel beams and the corresponding concrete floor,
- ❖ web holes foreseen in ACB-beams prohibited in the neighbourhood of the connection to columns,
- ❖ horizontal stability of the building taken over by the concrete core.

This steel building comprises six office levels with a total surface of 6400 m², as well as three underground car-park levels.

For the fire safety analysis the following steps had to be done.

Characteristic fire load density in office buildings (80% fractile):	$q_{f,k} = 511 \text{ MJ/m}^2$
Maximum rate of heat release	$RHR_f = 250 \text{ kW/m}^2$
Fire growth rate - medium	300 sec
Combustion factor	$m = 0,8$
Danger of fire activation related to the compartment	$\delta_{q1} = 1,95^{1)}$
Danger of fire activation related to the occupancy	$\delta_{q2} = 1,0$

¹⁾ As the danger exists of fire progressing through the façade into the next level, the surface considered for estimating δ_{q1} is increased. **For compartment N°4**, comprising ground level and first floor, this surface is $1200 + 1016 + 1200 = 3416 \text{ m}^2$; this gives according to figure 40, $\delta_{q1} = 1,95$.

Active fire safety measures:

Sprinklers:	yes	$\delta_{n1} = 0,61$
Independent water-reservoir of 20 m ³ :	yes	$\delta_{n2} = 0,87$
Automatic fire detection:	yes by smoke	$\delta_{n4} = 0,73$
Automatic alarm transmission to the fire brigade:	yes	$\delta_{n5} = 0,87$
Professional fire brigade:	yes	$\delta_{n7} = 0,78$
Safe access ways:	yes	$\delta_{n8} = 0,9^{2)}$

Fire fighting devices:

yes

$$\delta_{n9} = 1,0^{(3)}$$

Smoke evacuation:

yes

$$\delta_{n10} = 1,0^{(4)}$$

$$\prod \delta_{ni} = 0,237$$

²⁾ staircases are put under overpressure in case of fire alarm,

³⁾ for every compartment we need sufficient fire-extinguishers and fire-hoses,

⁴⁾ in case of fire alarm smoke exhaust is activated in the compartment under fire with 20000 m³/hour.

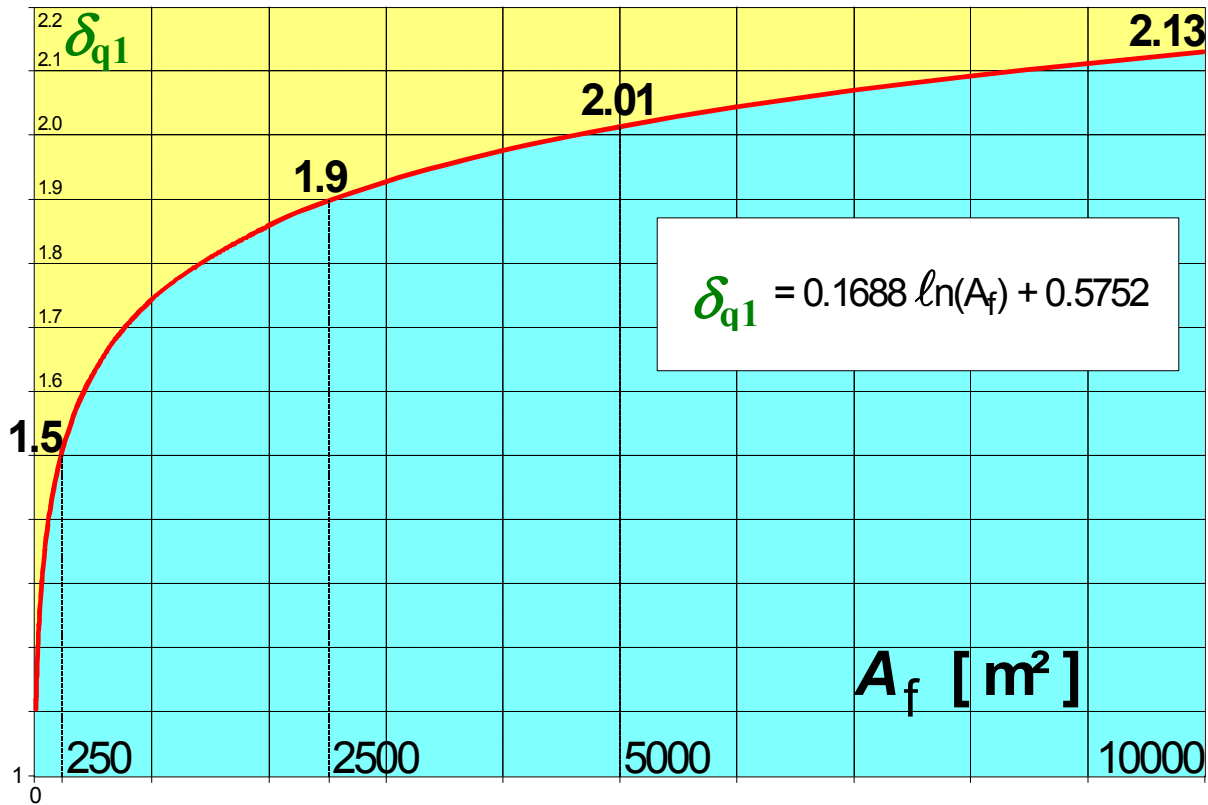


Figure 40. Partial factor δ_{q1} , taking into account the fire activation risk due to the size of the compartment A_f , is represented by the above indicated equation which gives values quite similar to table E.1, Annex E of EN1991-1-2 [12].

Design fire load:

For compartment N°4, comprising ground level and first floor, and considered as one compartment, the characteristic fire load may be estimated for the ground floor of 1200 m² as

$$q_{f,k} = 511 \text{ MJ/m}^2 (1200 \text{ m}^2 + 1016 \text{ m}^2) / 1200 \text{ m}^2 = 944 \text{ MJ/m}^2$$

$$\begin{aligned} q_{f,d} &= (m \cdot \delta_{q1} \cdot \delta_{q2} \cdot \prod \delta_{ni}) \cdot q_{f,k} \quad [\text{MJ/m}^2] \\ &= (0,8 \cdot 1,95 \cdot 1,0 \cdot 0,237) \cdot 944 \\ &= 349 \text{ MJ/m}^2 \end{aligned}$$

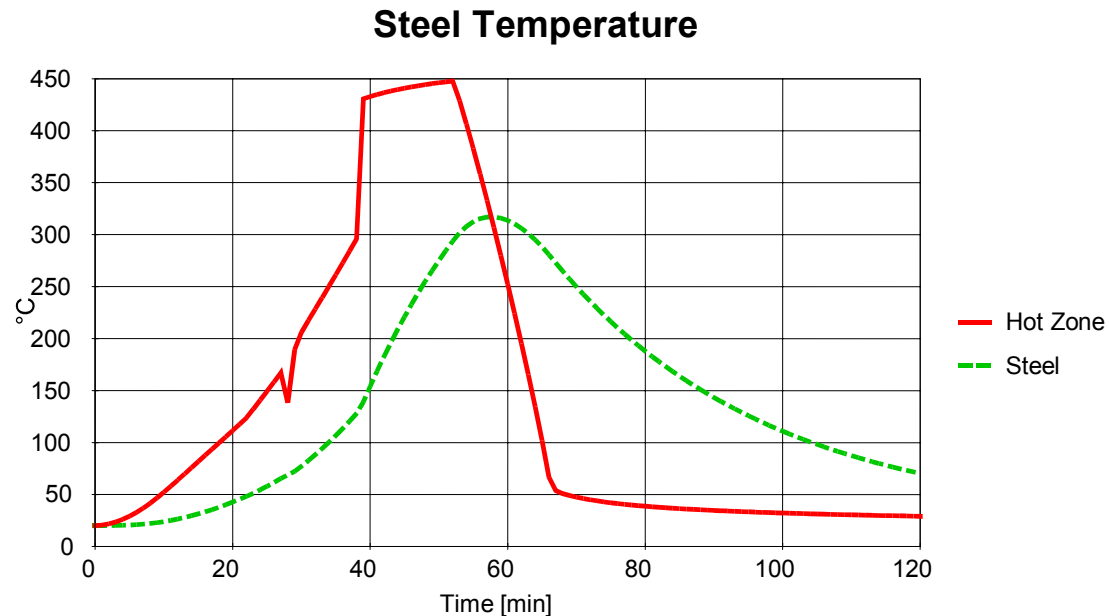
Ventilation conditions during fire

For compartment N°4, comprising ground level and first floor, we have:

- outer façade glass surface of 1230m²,
- inner façade glass surface of 199m²,

- height of compartment 9,05m,
- glass breaking during fire → 5% at 20°C, 25% at 400°C, 50% at 500°C
- smoke exhaust with 20000 m³/hour.

All these conditions lead to the following results of gas temperature evolution and temperatures in structural steel columns HD400 x 187 to 237 given in figure 41.



Analysis Name: BANQUE POPULAIRE/COMPARTMENT N°4/ Prof JB SCHLEICH

Figure 41. Hot Zone and Steel Temperature: Peak gas 448 °C at 52 min, peak steel HD400X237, 317°C at 58 minutes.

As a conclusion, this steel structure may be kept unprotected provided the full set of active fire fighting measures is really implemented as indicated on pages VII-39 and VII-40 and of course maintained in time.

Furthermore the following live saving measures are to be implemented:

- ❖ sufficient safe escape ways,
- ❖ escape signs to place in relevant areas,
- ❖ in case of alarm elevators move to the ground floor, where they are definitively blocked.



Figure 42. "Banque Populaire" with steel frame and concrete floors completely erected in June 2002.



Figure 43. "Banque Populaire" with double-glass façade.



Figure 44. "Banque Populaire" with entrance hall and visible, unprotected steel columns in July 2003.

4.4 Global fire safety concept applied to "Chambre de Commerce" / Luxembourg(2000-2003) / Arch.Claude VASCONI

In this building complex, with a total occupancy area of 52000 m² (see figure 45) including underground parking levels, the relevant authorities imposed the ISO fire resistance requirement of R90 for all underground structural elements. This was encountered by performing on those levels composite columns and composite beams.

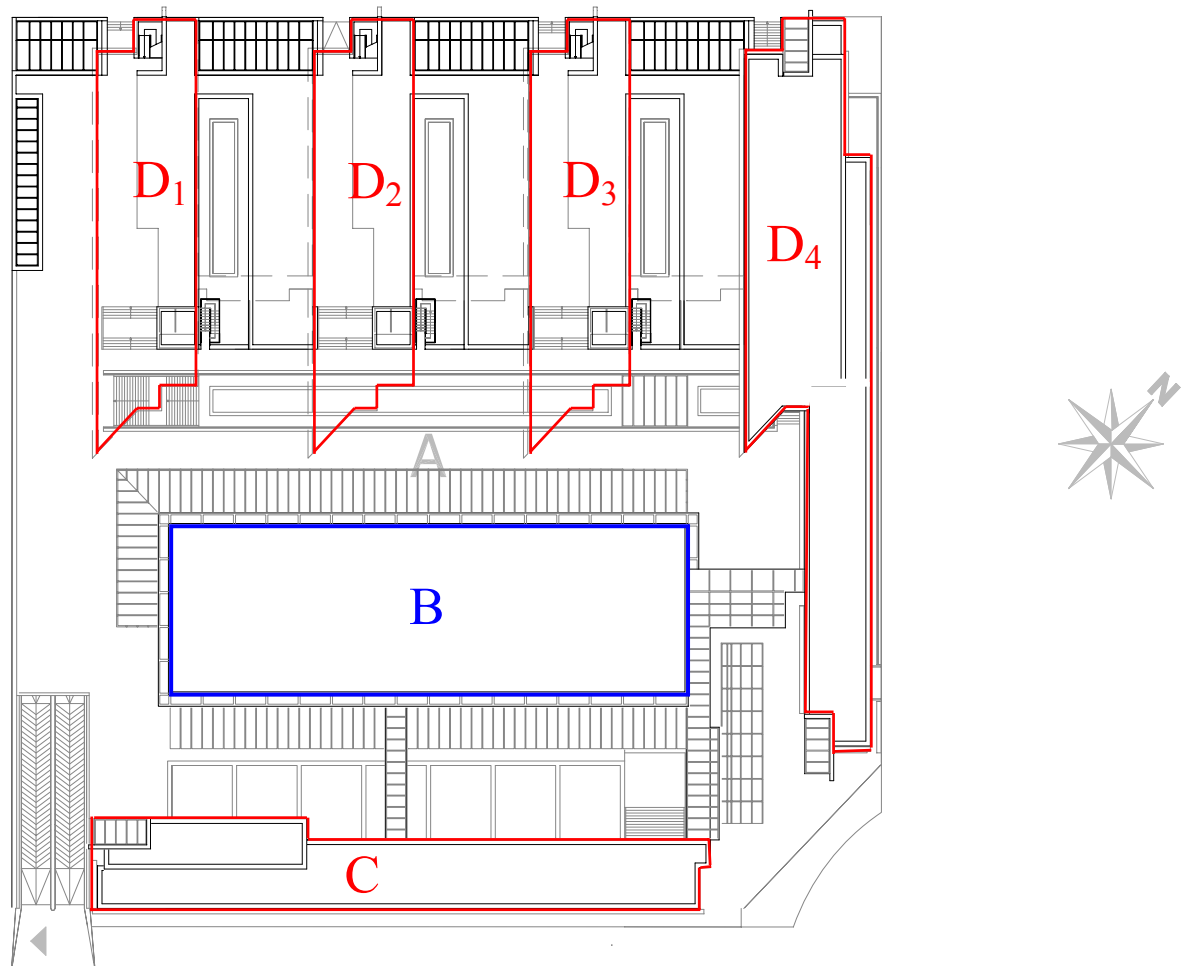


Figure 45. Whole complex with existing and refurbished building B, and new parts C and D₁ to D₄.

However the structure situated on the ground level and on the upper 5 floors could be designed according to natural fire models.

In fact the use of natural fire models corresponds to the new European CEN standard EN1991-1-2 which, as an alternative to the ISO-fire, permits the use of natural fire models. That standard [12], dealing with actions on structures exposed to fire, contains in Annex E all numerical values allowing to determine the design fire load, and gives in Annex D the rules required to be fulfilled by any software programme in order to calculate the real heating evolution.

In the specific situation of this building safety aspects were addressed by implementing the full set of active fire fighting measures:

- ❖ the danger of fire activation has been limited on one side by the limitation of the size of compartments to a maximum of 750 m², and on the other side by the choice of a clear occupancy of offices respectively of education areas...
- ❖ automatic fire suppression is given through an automatic water extinguishing system of sprinkler heads installed all over the building, underground levels included; sprinkler redundancy is guaranteed among others by independent water supply
- ❖ automatic fire detection is obtained by installation of smoke detectors all over the building, and by automatic alarm transmission to the professional fire brigade of the town of Luxembourg.....
- ❖ manual fire suppression is favoured through the short time of maximum 15 minutes needed by the fire brigade to reach the CCI building, through the existing and excellent safe access routes as well as staircases put under overpressure in case of fire alarm, through the numerous fire fighting devices existing all over the building, and through the smoke exhaust in staircases...
- ❖ furthermore life safety is ensured by the numerous existing and extremely redundant safe escape ways.

Lateral stability is essentially guaranteed - except in building C shown in figure 49 - through the concrete cores of staircases and elevator shafts, and of course through the diaphragm action of the composite floors. Hence composite beams essentially transmit gravity loads to the steel columns, which in turn are mainly loaded by axial loads and locally induced bending moments.

These columns have been fabricated and erected as continuous elements, consisting of rolled sections varying from HE260M at column bottom to HE260A at column top, and reinforced by lateral steel plates so to form a box section. Furthermore longitudinal stiffening steel ribs have been welded to that cross section, so to confer to those columns an appealingly structured outside aspect. This is clearly shown on figures 46 and 48.

Composite beams are normally composed of the rolled section HE280B reinforced by a steel bottom plate. They are encased in the concrete of the slabs, except for the lower flange which remains visible; for spans longer or equal to 10m these beams are sustained by massive tension rods with a diameter of 50mm as shown on figure 47.

The natural design fire curve has been calculated using the Software OZONE developed by the University of Liège and considering the safety aspects addressed previously [13]. The most critical fire scenario leads to air temperatures of approximately 500°C, which in turn provoke maximum steel temperatures of approximately 350°C; this is indicated in figure 50.

The influence of these temperatures has been checked through the **thermo-mechanical computer code "CEFICOSS"**, which clearly indicates that, under those natural heating, no failure, nor any critical deformation will occur.



Figure 46. "Chambre de Commerce" with visible, unprotected steel columns supporting the composite beams.



Figure 47. "Chambre de Commerce" with composite beams sustained by visible, unprotected massive tension rods.



Figure 48. "Chambre de Commerce" with visible, unprotected steel columns on ground level.



Figure 49. Building C with lateral steel bracing.

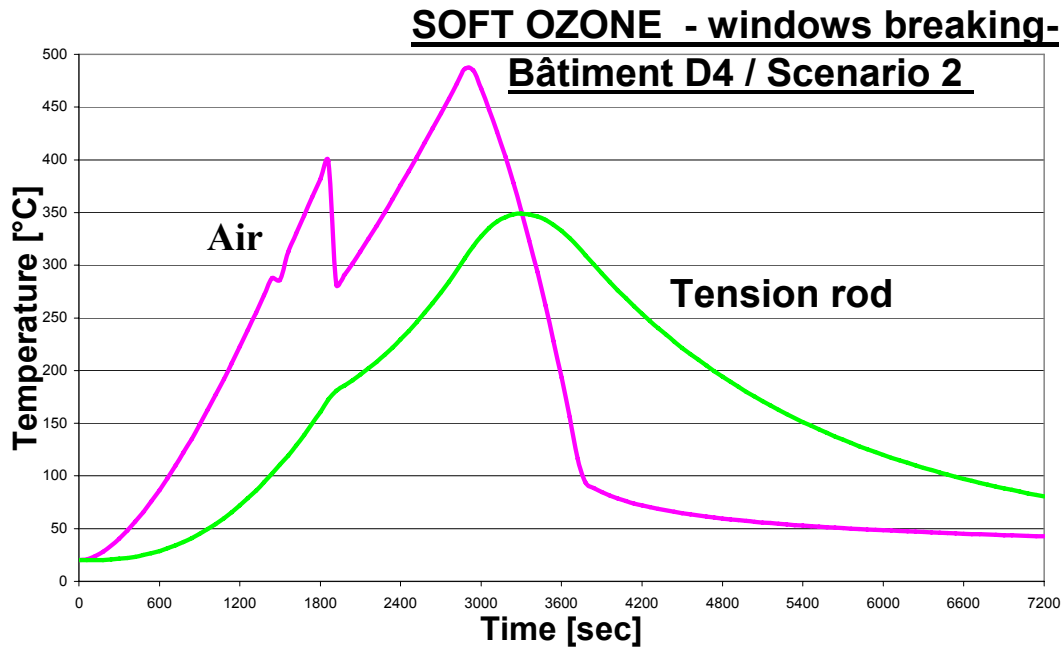


Figure 50. Natural fire evolution in a compartment of 750m² assuming windows breaking of 20% at 400°C; the corresponding temperature in the tension rod with $A_m/V = 80\text{m}^{-1}$ is limited to 350°C.

Applying active fire fighting measures such as fire detection, alarm, automatic alarm transmission to fire-fighters, smoke exhaust systems, and sprinklers, provide protection to people so that safety of people is ensured in an optimal way. The structure itself will automatically also benefit from those measures, which in fact primarily aim to save occupants. Hence the passive protection by insulation, needed in former times to guarantee the stability of the structure in case of fire, is strongly diminished and the budget dedicated to fire safety is being used in a perfectly efficient way.

Finally the whole steel structure of the "Chambre de Commerce" building, as described before, is in fact best protected by the active fire safety measures. Consequently steel columns and the lower visible parts of the composite beams need not be covered by any insulation nor by any intumescent coatings.

Hence structural steel is essentially visible and is permitted to fully exhibit its true filigrane feature.

REFERENCES

[1] Arrêté du 25 juin 1980, portant approbation des dispositions générales du règlement de sécurité contre les risques d'incendie et de panique dans les établissements recevant du public. Ministère de l'Intérieur de la République Française, Journal Officiel - N.C. du 14 août 1980.

[2] Minne R., Vandeveld R., Odou M.; Fire test reports N° 5091 to 5099, Laboratorium voor Aanwending der Brandstoffen en Warmte-overdracht. Gent, University 1985.

[3] Schleich J.B.; CEFICOSS, a computer program for the fire engineering of steel structures / International Conference on mathematical models for metals and materials applications, Sutton Coldfield, 12-14.10.1987. Institut of Metals, London, 1987.CEN;

[4] Schleich J.B.; Numerische Simulation: Zukunftsorientierte Vorgehensweise zur Feuersicherheitsbeurteilung von Stahlbauten / Springer Verlag. Bauingenieur 63, S. 17-26, 1988.

[5] Schleich, J.B.: Brandschutzkonzepte aus Europäischer Sicht; Deutscher Stahlbautag, Berlin, Okt. 1992. DTSV, Stahlbau-Verlagsgesellschaft mbH, Köln, Sept. 1992, ISBN 3-923726-39-2.

[6] Schleich, J.B.: Stahlbauarchitektur und Brandschutz; Oesterreichischer Stahlbautag, Linz, November 1993. Stahlbau Rundschau, Wien, April 1994.

[7] ECCS-TC3; Fire resistance of steel structures-Nomogram, Technical Note N° 89. Brussels, 1995.

[8] Schleich J.B., Cajot L.G.; Natural fires in closed car parks. ECSC Research 7210-SA/518 etc., B-E-F-L-NL, 1993-96, Final report EUR 18867 EN, 1997.

[9] Borgs i.A.; Untersuchungen zur Veränderung der Rauchschichtgrenzen im Fall eines Brandes von bis zu 3 PKW's innerhalb eines Geschosses der Tiefgaragenerweiterung bei Variation der Entrauchungsleistung auf der Grundlage eines computerunterstützten Simulationsprogramms für Raumbrände. Brandschutztechnische Stellungnahme, Paul Corall Dipl.-Ing., 24.10.2000.

[10] Schleich J.B.; Comportement au feu des parcs à voitures en superstructure / Essais de démonstration du 26.9.2000 et 25.10.2000 au Centre de Prévention et Protection à Vernon-France. Rapport Interne, novembre 2000.

[11] CEN; EN1990, Eurocode – Basis of Structural design . CEN Central Secretariat, Brussels, DAV 24.4.2002.

[12] EN1991-1-2 , Eurocode 1 – Actions on structures , Part 1.2 – Actions on structures exposed to fire. CEN Central Secretariat, Brussels, DAV 20.11.2002..

[13] Cadorin J.F.; Compartment Fire Models for Structural Engineering. Thèse de doctorat, Université de Liège, 17.6.2003.

[14] CEN; prEN1993-1-2, Eurocode 3 – Design of steel structures, Part1.2 – General rules – Structural fire design. CEN Central Secretariat, Brussels, Stage 49 draft, June 2004.

[15] Schleich J.B.; La stabilité au feu des bâtiments: une nouvelle approche par le feu naturel. 111^e Congrès de la F.N.S.P.de France, Montpellier, 16.9.2004.

[16] CEN; prEN1994 -1-2, Eurocode 4 – Design of composite steel and concrete structures, Part1.2 – General rules – Structural fire design. CEN Central Secretariat, Brussels, Stage 49 draft, December 2004.

CHAPTER VIII - CASE STUDIES OF REAL FIRES

Jean-Baptiste Schleich¹

¹ University of Technology Aachen, University of Liège

1 INTRODUCTION

At first it is convenient to have a look at some historical calamities, leading to great losses in the past either in lives either in property, buildings or cultural values.

1.1 The Great Lisbon Fire - 1.11.1755

In the morning of November 1, 1755, a large earthquake struck Lisbon - a great city legendary for its wealth, prosperity and sophistication. It was Sunday and the religious holiday of All Saints. Most of Lisbon's population of 250,000 were praying in six magnificent cathedrals, including the great Basilica de Sao Vincente de Fora. Within minutes, this great thriving city-port of Lisbon, capital of Portugal and of the vast Portuguese empire and seat of learning in Europe, was **reduced to rubble by the two major shocks of this great earthquake and the waves of the subsequent catastrophic tsunami. A huge fire completed the destruction of the great city** [1].

The quake's rocking ground motions weakened and cracked Lisbon's buildings which collapsed into the city's narrow streets below, crashing the panicked survivors seeking escape. People ran to the edge of the city and into the fields. Others sought refuge on the banks of the Tagus river, only to perish shortly thereafter by the waves of a huge tsunami.

The destruction caused by the earthquake was beyond description. Lisbon's great cathedrals, Basilica de Santa Maria, Sao Vincente de Fora, Sao Paulo, Santa Catarina, the Misericordia - all full of worshipers - collapsed, killing thousands. Lisbon's whole quay and the marble-built Cais De Pedra along the Tagus disappeared into the river, burying with it hundreds of people who had sought refuge.

The Lisbon earthquake caused considerable damage not only in Portugal but in Spain - particularly in Madrid and Seville. The shock waves were felt throughout Europe and North Africa, over an area of about 1,300,000 square miles. In Europe, ground motions were felt in Spain, France, Italy, Switzerland, Germany, and as far away as the Duchy of Luxembourg and Sweden. Unusual phenomena were observed at great distances. For example in Italy an ongoing volcanic eruption of Vesuvius stopped abruptly.

Precursory phenomena also had been widely observed prior to the great earthquake. For example in Spain, there had been reports of falling water levels. Turbid waters and a decrease in water flow in springs and fountains had been reported in both Portugal and Spain.

In North Africa the quake caused heavy loss of life in towns of Algeria and Morocco - more than 400 miles south of Lisbon. The town of Algiers was completely destroyed. Tangiers suffered great loss of lives and extensive damage. The earthquake was particularly destructive in Morocco, where approximately 10,000 people lost their lives. Archival records document that the coastal towns of Rabat, Larache, Asilah, and Agadir (named Santa Cruz while under Portuguese rule) suffered much damage. Even the interior cities of Fez, Meknes and Marrakesh were similarly damaged. In Meknes, numerous casualties occurred. Churches, mosques and many other buildings collapsed.

For most coastal regions of Portugal, the destructive effects of the resulting tsunami were more disastrous than those of the earthquake. The first three of the tsunami waves were particularly destructive along the west and south coasts of Portugal.

At the mouth of the Tagus river estuary and upstream, there was an initial recession of the water which left exposed large stretches of the river bottom. Shortly afterwards, the first of the tsunami waves arrived. It swamped Bugie Tower and caused extensive damage to the western part of Lisbon, the area between Junqueria and Alcantara. The same wave continued upstream spreading destruction and demolishing the Cais de Pedra at Terreiro do Paco and part of the nearby custom house. The maximum wave height at this location was estimated to be about 6 meters. Boats which were overcrowded with quake survivors seeking refuge, capsized and sank. There were two more large waves. It is estimated that the largest tsunami run up in the Tagus estuary was about 20 meters.

At the coastal town of Cascais, about 30 km west of Lisbon, large stretches of the sea floor were initially exposed, then the arriving tsunami waves demolished several boats. At Peniche, a coastal town about 80 km north of Lisbon, many people were killed by the tsunami. In Setubal, another coastal town 30 km south of Lisbon, the water reached the first floor of buildings.

The tsunami destruction was particularly severe in the province of Algarve, in southern Portugal, where almost all the coastal towns and villages were severely damaged, except Faro, which was protected by sandy banks. In some coastal regions of Algarve, the maximum tsunami wave run up was 30 meters. According to reports, the waves demolished coastal fortresses and razed houses to the ground. In Lagos, the waves reached the top of the city walls.

Whatever the earthquake shocks and the tsunami waves spared from destruction, a great fire - which started soon thereafter - finished.

Within minutes the fire spread and turned Lisbon into a raging inferno. Unable to run, hundreds of patients in the Hospital Real burned to death. Remaining survivors ran to the hills and the fields outside the city.

Fanned by steady northeast winds, the great fire burned out of control through the ruins of the city for more than 3 days. It swept everything in its path and destroyed houses, churches and palaces. Lisbon's magnificent museums, and its magnificent libraries - housing priceless documents and papers dealing with the great history of Portugal's great past - burned to the ground. Archives and other precious documents were completely destroyed. Works of art, tapestries, books, manuscripts, including the invaluable records of the India Company were destroyed. Also burned was the king's palace and its 70,000-volumes library. Over two hundred fine, priceless paintings, including paintings by Titan, Rubens, and Coreggio, were burned in the palace of the Marques de Lourcal.

Death Toll and Destruction from Earthquake, Tsunami and Fire may be summarized as follows. The earthquake destroyed Lisbon and other major cities in Portugal. More than 18,000 buildings, representing about 85% of the total were completely demolished. In the first two minutes of the earthquake, about 30,000 people lost their lives. **The total death toll in Lisbon, a city of 230,000, was estimated to be about 90,000. Another 10,000 people were killed in Morocco.**

1.2 The Great Boston Fire - 20.3.1760

".....After a grievous fire in 1676, the town decided to invest in a new hand-operated water pump imported from London. The device was a simple wooden box with handles that could be carried to fires. There it was filled with water by a bucket brigade, and when pumped, it shot a stream of water out a flexible hose. To operate the "hand tub fire engine," Boston named 12 men, who would be paid for responding to fires and using the new machine. With this resolution, passed Jan. 27, 1678, Boston became the first town in the nation to have paid fire fighters. As the town added more machines and more "engineers" to operate them, they decided that these firefighters should be trained "under the same discipline as soldiers," and **by 1720 Boston had the beginnings of a modern fire department with 10 fire wards, six machines, and 20 paid firefighters** [7].

Volunteers also played a major role in fighting Boston's fires. Responding to a fire had always been a civic duty of all men in Boston. When the cry of "fire" or the pealing of church bells signaled that flames had been spotted, every household was required to send a man with a leather bucket to help fight the fire. In September of 1718, Boston organized the "Boston Fire Society," the nation's first mutual aid organization. Members pledged to fight fires at each others homes, rescue their property, and guard against looting.

The "engine companies" with their hand-pumped "fire engine" were joined by volunteers and members of the Boston Fire Society to combat the blaze that broke out in Boston in the early morning of March 20, 1760. But the wind-whipped blaze spread quickly to businesses and homes around the central market area. The flames, described by one observer as "a perfect torrent of fire," consumed shops and homes along King and Congress streets and continued its march of destruction straight down to wharves, where it consumed ten ships docked at Long Wharf. One resident, looking out his window at 4 am, "beheld a blaze big enough to terrify any Heart of common Resolution, considering such valuable combustibles fed it." For ten hours the fire raged. Hundred of residents fled and "scarce knew where to take Refuge from the devouring flames; Numbers who were confined to Beds of Sickness and Pain, as well as the Aged and Infant... were removed from House to House....."

David Perry, a sailor from Nova Scotia, was in Boston at the time of the fire and recorded in his journal: "[W]e were billeted out at the house of a widow, named Mosely; and while we were here the town took fire in the night. It originated in a tavern... at about midnight, the wind in the north-west and pretty high; and in spite of all we could do with the engines, it spread a great way down King's Street, and went across and laid all that part of the town in ashes, down to Fort Hill. We attended through the whole, and assisted in carrying water to the engines"

Though **no life was lost**, the fire consumed about 350 homes, shops, and warehouses. The loss of property made it the worst fire to date in American colonies. Boston, staggering under the financial ruin of the fire, begged the King and Parliament in London for assistance; though their fellow colonies took up charitable collections for the city, the British government failed to respond. Some claim that the resentment felt by Bostonians for the Crown's indifference to their plight in March of 1760 sowed the first seeds of rebellion.

Boston's fires did not end with independence. Major blazes continued to plague the city.....".

1.3 The Great Chicago Fire - 8.10.1871

Despite a well known legend that the Great Chicago Fire was started by a cow kicking over a lantern in the barn owned by Mrs. O'Leary on DeKoven Street, historians now believe it was begun by Daniel "Pegleg" Sullivan, who first reported the fire [2].



Figure 1. Artist's rendering of the fire, Chicago 8.10.1871, by John R Chapin. Public domain, originally printed in Harper's Weekly.

The prevailing opinion today is that the Great Chicago Fire did start in Kate O'Leary's barn around 9:00 p.m. on October 8, 1871, but that she was not the cause of it. Mrs. O'Leary was the perfect scapegoat, she was a woman, an immigrant and Catholic, all making for a combination which did not fare well in the political climate of Chicago at that time. In 1997 the Chicago City Council formally investigated the fire and absolved Mrs. O'Leary of any guilt. It was surmised that Daniel Sullivan had committed the crime when trying to steal milk from her barn for a batch of "whisky punch."

The fire was reported and neighbors hurried to protect the O'Leary's house from the blaze. High winds from the southwest caused the fire to ignite neighboring houses and move towards the center of Chicago. Between superheated winds and throwing out flaming brands, the fire crossed the Chicago River by midnight. The fire spread so quickly because of plank sidewalks, high winds and the Chicago River itself starting on fire from the massive amounts of pollution in the greasy river.

When the fire was extinguished two days later, the smoldering remains were too hot for a survey of the damage to be completed for a couple of days. Eventually, it was determined that the fire destroyed a patch 6 km long and averaging 1 km wide, more than 2000 acres. This area included more than 73 miles (120 km) of roads, 120 miles (190 km) of sidewalk, 2000 lamp-posts, 17000 buildings, and \$200 million in property, about a third of the city's valuation. After the fire, 125 bodies were recovered. Final estimates of fatalities were in the range of 200-300 persons, low for such a large fire, for many had been able to escape ahead of the flames. However **100000 out of 300000 inhabitants were left homeless.**

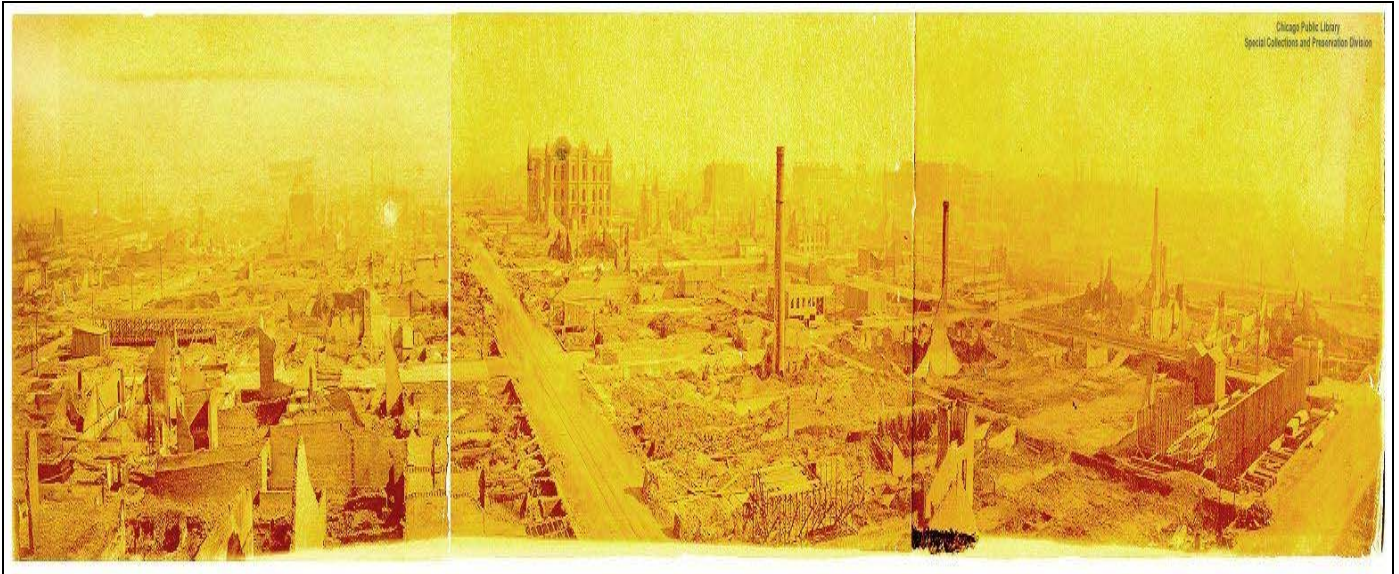


Figure 2. Panoramic view looking east along Randolph Street toward the shell of the Court House and City Hall. The nearest cross street is Franklin, while the street at the extreme right corner is Market (now Wacker). Reconstruction is just beginning: a contractor's shack is in the middle ground, and several larger temporary store structures are under construction.

2 RECENT CONFLAGRATIONS

2.1 Great fire, Chiado: Historical Centre of Lisbon - 28.8.1987

2.1.1 Characterization of the situation

Eighteen different buildings were involved in the Chiado fire. Most of them had been built to be used for commerce, as offices and dwellings and one of them as a monastery. Except for the monastery, which was being used as a commercial store at the time of the fire, all the other buildings were mainly serving for commerce, as offices and there were also some dwellings. Among them were the shopping stores “Armazéns do Chiado”, operating in the former monastery “Convento do Espirito Santo da Pedreira” built in the late years of the 16th century, the shopping store “Jerónimo Martins”, founded in 1792, the pastry shop “Pastelaria Ferrari”, founded in 1827 and the jewellery “Casa Batalha”, founded in 1635 [6].

Most of the buildings had load bearing masonry walls, wooden floors, wooden roof structure, plastered wooden partition walls, and wooden stairs. Some of them had an interior steel structure, including cast iron columns, or reinforced concrete elements.

Along the years **partition or even load bearing walls had been removed** to obtain open spaces, more adequate to the commercial use, without alternative fire safety measures, thus **facilitating the potential fire spread**. Load bearing walls were replaced in some cases by steel beams, without adequate fire protection. For administration or commercial purposes, unauthorized unprotected communication openings had been made by the owner or user in the fire walls separating two or more adjacent buildings, thus drastically changing the fire safety of those buildings.

The buildings were occupied mainly during the shopping hours. Only a few residents of the upper floors of some of the buildings slept there at night.

The fire load density inside the building “Grandella”, where the fire started, was very high. The fire load was estimated as 670×103 kg of wood, which means a total available energy of $1,21 \cdot 10^6$ MJ, and included easily ignitable items such as textiles, paper, plastics and camping gas bottles.



Figure 3. Historical Centre of Lisbon, 200m x150m burning down.

There was **no automatic detection system and the night watcher failed to detect the fire in due time**. There was **also no first attack fire equipment, no portable extinguishers, and no fixed automatic suppression system**. After receiving the alert, the fire brigade took only a few minutes to arrive to the quarters, but the alert had been given too late after the fire had started.

In the Building "Grandella", due to the various communication openings like unprotected wooden stairs, mechanical stairs and elevators between all the 8 storeys of the building and due to the easily ignitable character of the fire load, the fire and the fire effluents could propagate very quickly to all the floors. All the other affected buildings had unprotected vertical communication openings and wooden floors, which contributed to the quick fire spread inside.

2.1.2 The fire development

The fire developed during the night. **Only one resident and one fireman lost their lives**. One resident died from a fall when he was being helped to escape from his building. One of the two seriously burned firemen did not survive his injuries and 73 other people were reported as having suffered injuries. Had it been however during shopping hours and the number of casualties could have been much greater, as a consequence of the quick fire development and the inexistence of adequately protected evacuation paths and smoke extraction systems.

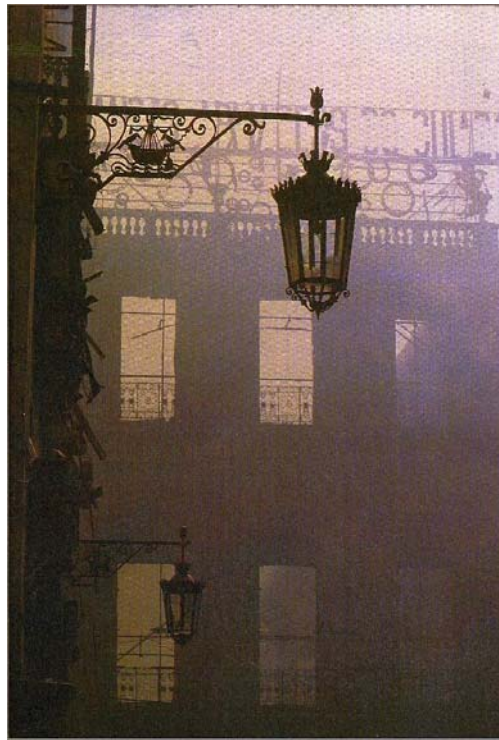


Figure 4. What remains after the fire.

At the time of the fire, renovation works were underway in the 3rd floor of the building "Grandella" and the plaster protection of the wooden ceiling had been totally removed. Although the causes of the fire were never exactly clarified, arson or welding work were pointed out as possible causes at that time. This brings to evidence the need to implement and enforce regulations to be applied at construction sites, including renovation works in existing buildings. This should of course especially be followed, when the fire protection of Cultural Heritage is the objective, either the protection of an historically

classified building or the fire protection of its contents with particular historical or artistic value.

The severity of the fire caused the complete destruction of several buildings or parts of them. Most of the main load bearing walls in these buildings were very thick (over 1 m) masonry walls, that withstand well the action of heat. Many of them however collapsed or had to be demolished immediately after the fire as a consequence of heavy damage caused by the thermal elongations of the horizontal construction elements. Original ancient 78 rpm music records made by “Valentim de Carvalho” as well as the old archives were lost in the fire, with a value difficult to estimate.

The direct damage to the buildings was estimated as 80 million Euros. The damage to the business in that area is difficult to quantify. Some firms moved to other zones in Lisbon, while some others stopped their activity. 5.7 million Euros was the amount paid to the workers of the shops and offices affected by the fire that lost their jobs. Twelve years were needed to rebuild and normalize the activity in the affected area.

2.1.3 The reconstruction and lessons learnt

The fire occurred in the old city centre, one of the appreciated shopping areas of Lisbon, where some of the oldest and most famous shops were located. The fact that so many buildings were involved and the fear that the area would lose its character after rebuilding produced a great social impact and heavy discussions in the media. The socio economic consequences of the fire developed over the 12 year-period of the reconstruction, with the loss of jobs for the workers of the directly affected commerce and offices, and the negative consequences of the rebuilding activity on the commerce in the nearby unaffected buildings.

The complex decision process after the fire was the main cause for the delayed reconstruction period. The heavy public pressure to **rebuild respecting as much as possible the original architecture** restrained the impetus to increase the volume of construction, and the final outcome resulted in a renewed zone, that locals and foreigners visit now with renewed pleasure.

The main reasons why the initial fire became a conflagration are listed up hereafter:

- 1) Human negligence and unqualified workmanship;
- 2) Lack of adequate fire safety regulations for construction sites and lack of corresponding enforcing measures;
- 3) **Inefficient, late fire detection;**
- 4) Easy ignitable and large quantities of fire load;
- 5) **Lack of horizontal and vertical fire compartments in the building**, leading to great heat radiation rates simultaneously through all the large openings in the façade of the building of fire origin to the facing buildings;
- 6) Very short distance between facing openings in a shaft common to the building of fire origin and a neighbouring one;
- 7) Combustible materials used in advertising elements placed outside the facades and in the windows;
- 8) Lack of horizontal and vertical fire compartments in the additional buildings involved in the fire;
- 9) The existence of illegal unauthorized communication openings between different adjacent buildings;
- 10) The existence of illegal combustible constructions, stored goods and waste in inner yards common to several buildings.

These shortcomings were seriously considered for the reconstruction.

2.2 Great fire, Duesseldorf Airport- 11.4.1996

2.2.1 Situation on active measures

The "Düsseldorf International Airport" built between 1971 and 1995 had a passenger capacity of 40000 persons per day, and contained more or less 2200 persons at the time the fire broke out (see figure 5) . In spite of existing fire safety requirements, certain important and live saving measures were clearly missing [3]:

- * no proper evacuation concept of smoke had been developed; by the way evacuation of smoke was not automatic,
- ** as a consequence escape routes could be filled with smoke,
- *** no heat neither smoke detectors were foreseen inside large false ceiling heights,
- **** sprinklers existed only locally in restaurants and duty free shops,
- ***** elevators could be activated even after fire alarm and be directed to the level under fire or filled with smoke,
- ***** polystyrol insulation plates were largely used in spite of their strong smoke production once ignited.

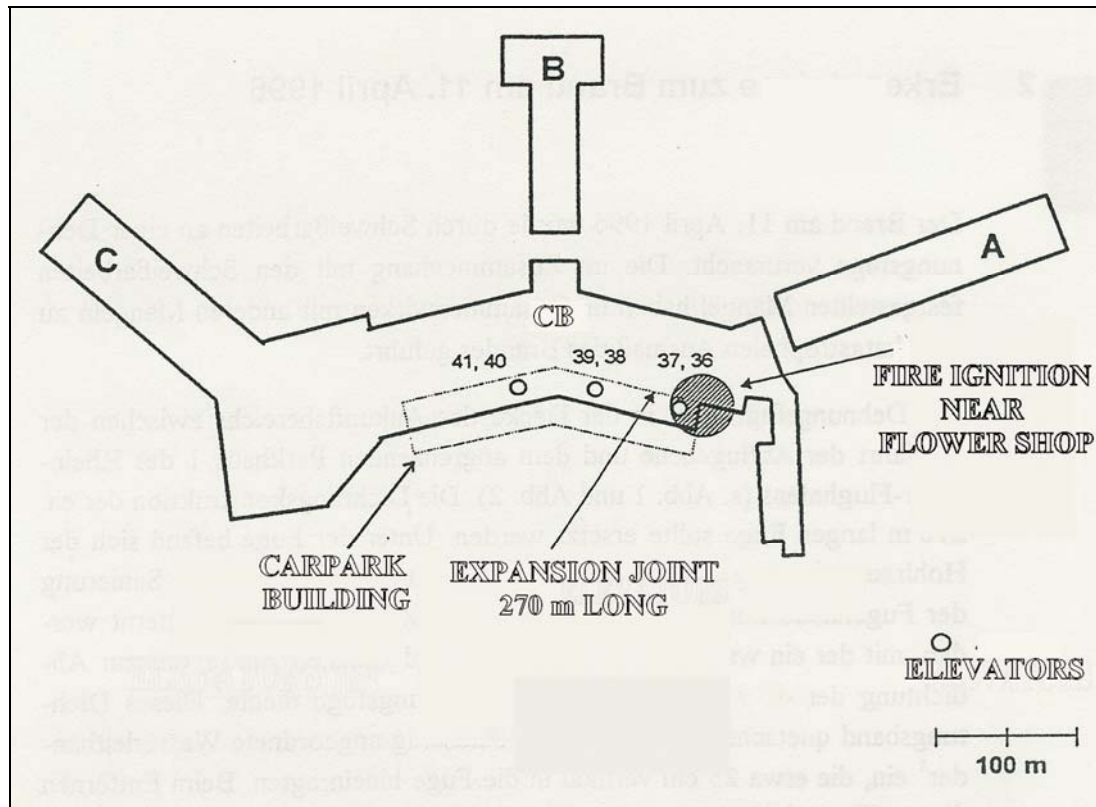


Figure 5. Horizontal view of the arrival level with central building CB and the three terminals A, B and C.

2.2.2 Fire activation and fatal issues

Fire was ignited when proceeding to welding operations at the 270m long expansion joint existing between the concrete floor for departure passengers and the car park building. Welding sparks fell down through the expansion joint and ignited first the water collecting rubber sheets, which in turn put the fire on polystyrol insulation plates situated, below that concrete floor, in the false ceiling with a height of 1m.

Having however foreseen no heat neither smoke detectors inside this large false ceiling, the fire was discovered only when a large part of that false ceiling fell down, which in turn let the fire break out to an area of 6000m² but above all accelerated the distribution of smoke to the level of arrivals and to that of departures.

Following time marks may be noted:

- 15h31: first fire alarm from a taxi driver to the Airport Fire Brigade.....
- 15h47: portion of false ceiling of arrival level falls down and the fire breaks out.....
- 15h58: public fire brigade is called.....
- 16h04: call for help from inside the **Air France Lounge** (see figure 6); indeed **smoke had completely surrounded and filled that lounge and blocked both escape ways**, and consequently leading to eight fatalities due to CO inhalation.....

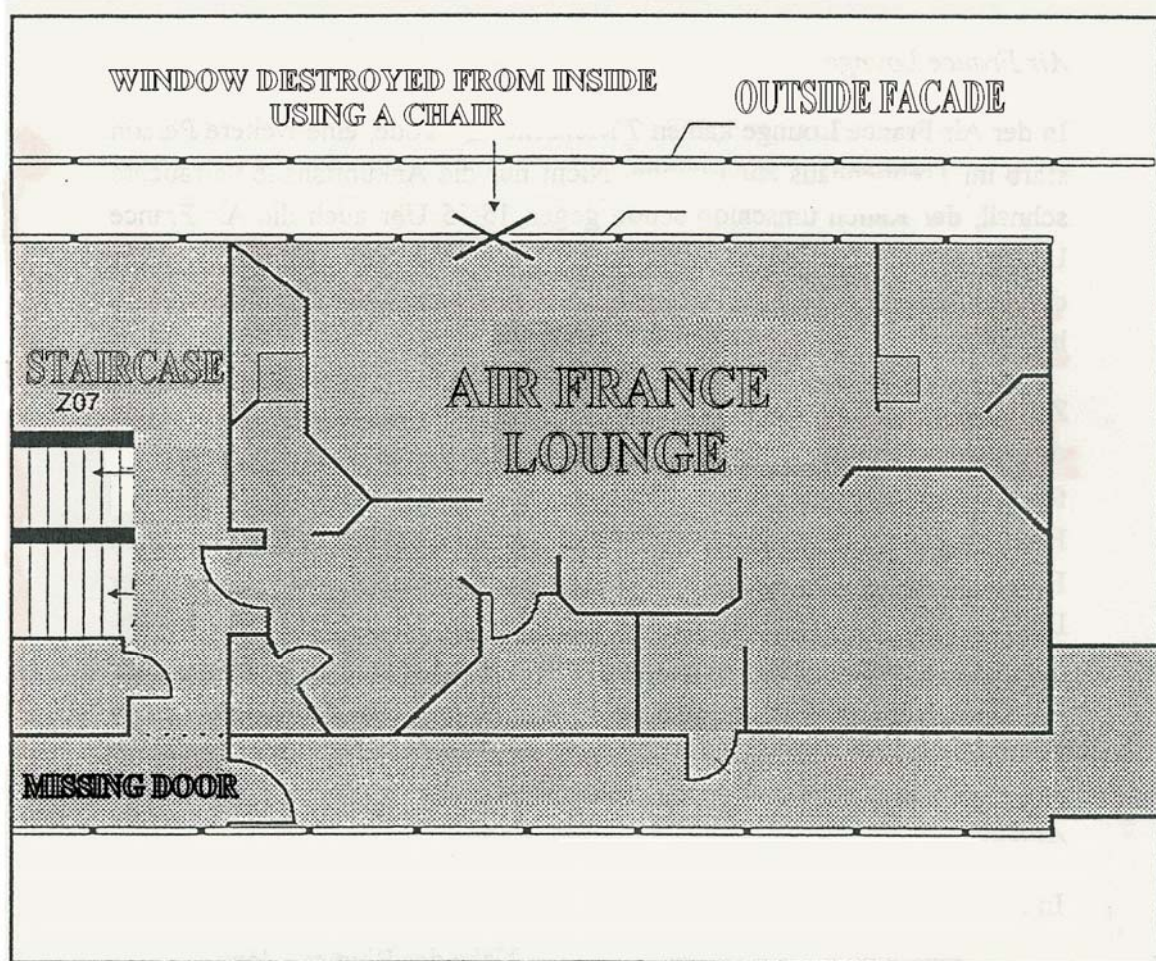


Figure 6. Air France Lounge endangered by smoke coming from the lower levels.

- 16h05: call for help from inside **two elevators having stopped on the level under fire and filled with smoke**. Due to smoke particles in the air entering into the cabins, doors didn't close anymore and seven persons were trapped, which led to seven fatalities due to CO inhalation.....

In fact these last persons could have been saved if they would have been informed on the existence of stair cases nearby the elevators; hence it is **vital to foresee the escape signs also near the floor level as smoke is always filling up first the upper part of any volume..**

- 16h25: the Tower is evacuated and all flight movements are stopped.....
- 16h28: all available fire brigades are called
-
-
- 19h20: the Fire is under controll.....**but finally 17 persons will have lost their lives in this building designed according to the ISO requirement R120.**

2.2.3 Recommendations

Following recommendations were issued for the future, correcting the previously enumerated shortcomings and being fully in line with our Natural Fire Safety concept.

- * Sprinklers shall be installed not only in restaurants and duty free shops, i.e. in areas where persons might be endangered right at the beginning of a fire, but also in underground areas foreseen for technics and material stocks, or in all areas with high fire loads. A separate Sprinkler Station is to be installed, including a water reservoir, according the "VdS" requirements.
- ** **Smoke detectors shall be installed in all areas**, of course false ceilings included, and their indication shall be continuously received at the Central Fire alarm station.
- *** Combustible construction materials are prohibited in false ceilings.
- **** **Escape staircases shall be kept by all means smoke free**, either by assuring fresh air circulation either by foreseeing overpressure in case of alarm.
- ***** All closed areas not directly connected to an outer façade should possess a second escape way leading to outside.
- ***** **A clear compartmentation between the different levels** shall be foreseen from the point of view of smoke evacuation.
- ***** Doors through compartmentation walls, opened in the normal situation, shall close on behalf of smoke detectors.
- ***** In case of alarm all elevators are automatically directed to one of the lower floors, which are smoke free according to the corresponding smoke detectors, and remain ultimately blocked at this level.

2.3 Great fire, Göteborg Disco - 30.10.1998

The Göteborg disco fire on October 30, 1998 has been investigated by SP, Swedish National Testing and Research Institute, under the leadership of Dr. Ulf Wickström [5]. The fire started in a stairwell adjacent to the disco hall. Four suspects have confessed that they were at place when the fire was ignited. As the trial proceeded a picture of the fire appeared that agrees very well with the results of the investigation by SP. The investigation contained two main parts: physical modelling on a scale of 1:4 and fire testing of various internal items and materials. The main finding, of vital importance to the police, was the precise time and position of the fire origin in the stairwell. From the modelling it also became clear that the flooring in the disco hall was decisive for the fire development.

2.3.1 The fire

At 23:42 h the door to the stairwell opened and smoke poured into the over-crowded disco. **Soon after 63 young people died and many more were injured.** About 400 were in the room although it was only approved for 150. The only way out was through the entrance door, which was soon blocked by the many young people desperately trying to get out. The width of the entrance door was only 82 cm.

The disco was on the upper floor of an old industrial two story building. At each end was a stairwell, according to figure 7. **In one stairwell approximately 40 chairs were stored on the middle landing.** These were normally placed in the disco room which was the assembly room of the Macedonian club of Göteborg.

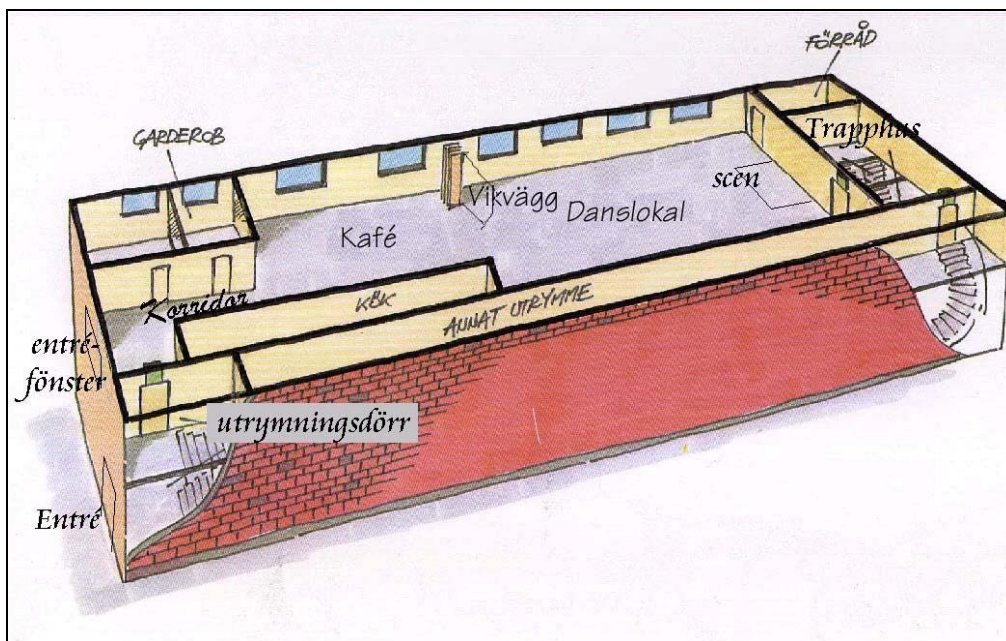


Figure 7. Disco with two stairwells, one of which was blocked.

2.3.2 The SP investigation

SP was engaged by the police soon after the fire. At this stage it was then already clear that the fire had started in one stairwell, the escape route. A long corridor leading to the outside was adjoining to the stairwell at the ground floor. The lower steel door of the stairwell was damaged from the inside. The outside had just some discolouring on the lower part.

Further, no smoke stains at all were observed in the adjoining corridor. It was also known from witness statements that the fire had developed very quickly after the upper door

was opened at 23.42 h. After that a severe fire had developed in the discothèque and after only 15 minutes flames shot out from the windows and ignited a roof 3 meters away, see figure 8.

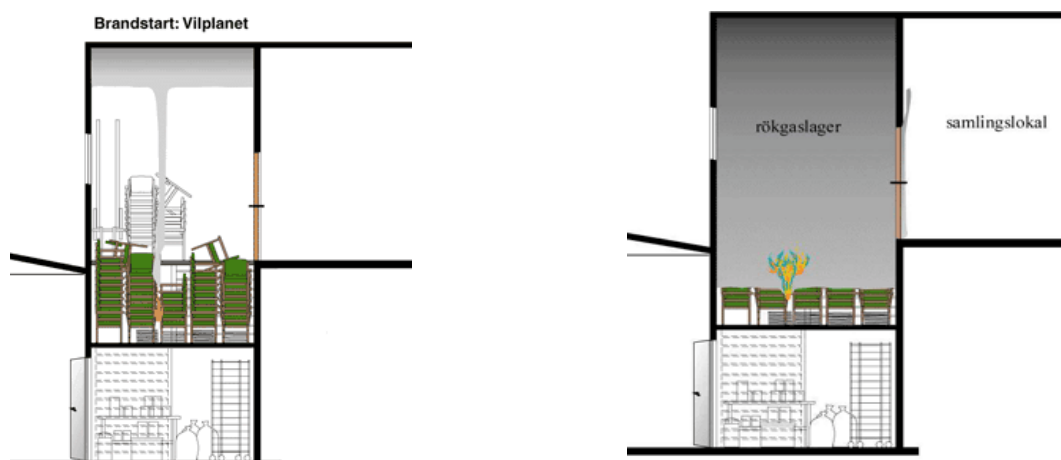


Figure 8. Flashover in disco.

To get an understanding of the fire development it was decided to reconstruct the fire on a scale 1:4. From these model scale tests a clear picture could be made.

The fire must have started in the middle of the stairwell on the landing between the two flights of steps, and the **fire must have been ignited only 10 to 20 minutes before the upper door was opened. The lower door must have been open at that time. Therefore a so called chimney effect could develop as the fire grew and the staircase heated up, and large amounts of smoke could stream later into the disco.**

Fire tests with the chairs in question showed that the oxygen available in the stairwell would only allow the fire to burn for a limited time. Then it would extinguish itself due to lack of oxygen. A series of drawings on how the fire must have developed are shown in figures 9 a to e.



Figures 9 a & b. The fire would have self extinguished, due to lack of oxygene, unless the door to the disco opens.

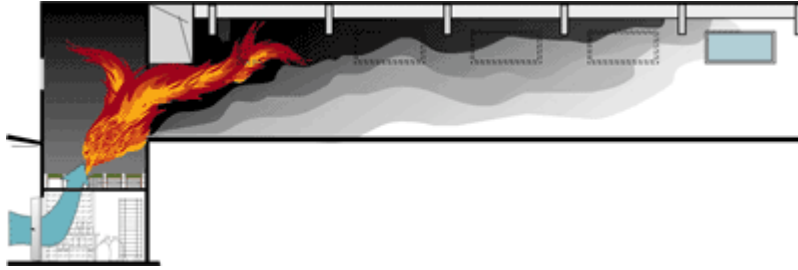


Figure 9 c. The discotheque was filled with smoke within a few minutes.



Figure 9 d. The flames filled the entire door opening and ignited the floor.



Figure 9 e. The floor was the main contribution to the vigorous fire; flames shot out from the side windows.

As a matter of fact the model tests showed that it was the combustible floor covering that made the fire develop as vigorously as it did. Very little was otherwise combustible in the discotheque. The smoke spread into the disco and the filling process was video recorded by three cameras. It took only two minutes in real time until the smoke coming out of the stairwell reached the entrance at the other end of the building. Then the smoke got denser and after five minutes lethal concentration of CO was registered at normal breathing heights.

2.3.3 Summary

The physical modelling of the fire proved to be very successful. Based on the experiments, convincing statements could be given to the police as to where and when the fire started. These statements have proven to be important in solving the case. However from the active fire safety point of view, **the facts that no smoke detection had been installed and that escape routes were unsafe have to be incriminated.**

2.4 Great fire, Windsor Tower Madrid - 12.2.2005

Successive events occurring on this tower of 100m with 32 floors

- Fire broke out on Saturday evening 12.2.2005 at 22h on 21st floor [8].....
- At 22h30 the fire brigade called arrives within 4 minutes, but does not intervene at this level as the fire has already spread to 5 floors and so is impossible to control.....
- At midnight the fire has spread to all floors above level 17.....
- On Sunday morning, at 1h15, the north façade down to level 17 falls off.....
- At 3 to 5am parts of the east and west façades collapse.....
- At 5.30am outer concrete columns and floor slabs collapsed on the upper 15 floors (see figure 10). This encourages the fire to spread below the 17th floor.....
- At 7am the fire reaches the 4th floor.....
- At 14h30 the fire reaches the 2nd floor.....
- At 17h the fire is fully extinguished, but the building is so much damaged that it is beyond repair and so will be pulled down

The reasons for this blaze are numerous but it may be underlined that

- **no compartmentation was foreseen** neither at the floor connection to the aluminium framed façade [4], nor inside near the stair and elevator zone; this permitted an easy spread to upper floors. But the lack of fire stopping screens between the floor slabs and the façade created significant gaps, so that debris from the burning floor could drop down and ignite also the next floors below;

- **no sprinklers were installed for this 100m high building**, and water could only be thrown up to $\approx 20\text{m}$ by the fire brigade (see figure 11).

If that fire would however have broken out during labour hours, the number of casualties and fatalities could have been quite enormous, as a consequence of the quick fire development and the inexistence of adequately protected evacuation paths and smoke extraction systems.

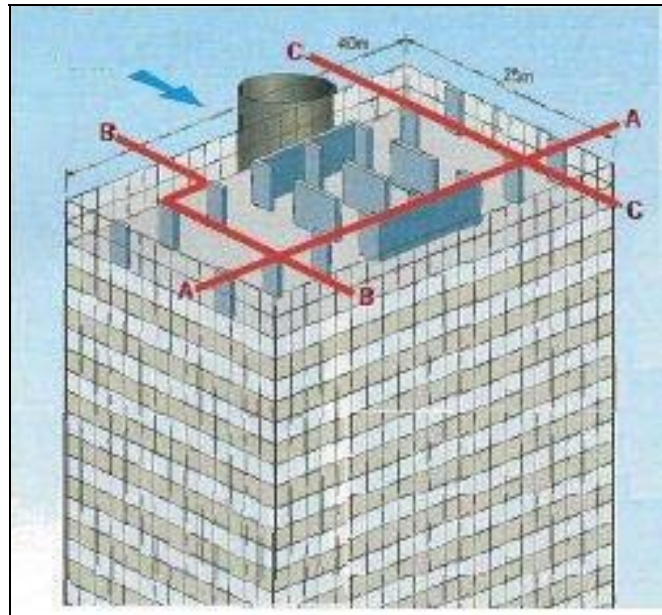


Figure 10. Structural system with line of failure AA, at 1.15am when the north façade falls off down to level 17, lines of failure BB and CC, at 3 to 5am when parts of the east and west façades collapse.



Figure 11. The remnant of a building, when active fire safety is ignored.

2.5 Endless list.....

Great fire, Mont Blanc Tunnel - 24.3.1999 39 fatalities

Great fire, Funicular railway tunnel Kaprun / Austria - 11.11.2000.....155 fatalities

Fire, Underground Parking Aerogare Roissy - 9.1.2004.....

Great fire, Commercial Centre Asuncion / Paraguay - 2.8.2004.....300 fatalities

Fire, Underground Parking Gretzenbach / Suisse - 27.11.2004.....7 fatalities

Great fire, Tunnel de Fréjus - 4.6.2005.....2 fatalities

REFERENCES

- [1] Charles Davy; Historical Depictions of the 1755 Lisbon Earthquake. Vol. V, Modern History Sourcebook Italy, France, Spain, and Portugal, pp. 618-628. Houghton Mifflin, Boston, 1914.
- [2] Chicago Historical Society; The Great Chicago Fire. Chicago, Rand McNally, 1971.
- [3] Weinspach P.M. et al / Unabhängige Sachverständigenkommission; Analyse des Brandes am 11.4.1996, Empfehlungen und Konsequenzen für den Rhein-Ruhr-Flughafen Düsseldorf, 14.4.1997.
- [4] Merker, Kotthoff; Untersuchung der Wirksamkeit von Weitwurfsprinklern als Brandschutzmassnahme zur Verhinderung der Brandübertragung an einer Doppelglasfassade der Fa. Gartner. Untersuchungsbericht Nr UIIV/ 99-116 für Allianz Grundstücks GmbH, Materialforschungs-und Prüfungsanstalt für das Bauwesen Leipzig e.V., Leipzig, 14.06.2000.
- [5] Wickström Ulf; SP reconstructed the Göteborg Disco fire. SP Fire Technology, BrandPosten, 22.6.2000.
- [6] Neves Cabrita I., Valente Joaquim, Ventura Joao; Analysis of significant fires and Statistical analysis of fire occurrence. FIRE - TECH, European study into the Fire Risk to European Cultural Heritage, 3rd Draft final report, pp. 76-78 / Fifth Framework Programme, Research European Commission, 2003.
- [7] Schorow Stephanie; Boston on Fire: A History of Fires and Firefighting in Boston, Commonwealth Editions, 2003.
- [8] NCE; Lack of fire stops blamed for speed of Madrid tower inferno. New Civil Engineer, Magazine of the Institution of Civil Engineers, p.5 to 7, 17.2.2005.

CHAPTER IX - AVAILABLE SOFTWARE

Jean-Baptiste Schleich¹

¹ University of Technology Aachen, University of Liège

Summary

The software programs described hereafter are freely available on a CD added to this Handbook 5 on the "Design of Buildings for the Fire situation".

In the corresponding application folders numerous examples are presented, in order to help the user in his effort of getting acquainted to that software. However in order to get assistance the corresponding user might refer to and directly contact the main author of Handbook 5, whose coordinates are indicated on the CD.

Furthermore useful background documents, corresponding theoretical developments and user manuals are given .

Because of the complexity of the calculation methods, these software packages are only intended for professional users active in the sector of civil engineering, who are fully aware of the possibilities, limits and its adequacy thereof for specific practical cases.

The use of this software is of course under the full responsibility of the user himself, whereas the main author of Handbook 5 can not be held responsible for any consequential damages, in particular those resulting from, either an incorrect or inappropriate use or a use made for an inadequate or inappropriate purpose, or either from possible misinterpretations by, wrong functioning of or even mistakes in the software.

1 FIRE RESISTANCE MODELS

1.1 Simple calculation models

1.1.1 Model "AFCB"

The model "AFCB" permits the calculation of the sagging and hogging moment resistances of a partially concrete encased steel beam connected to a concrete slab and exposed to fire beneath the slab according to the standard temperature-time curve [3].

This model corresponds to Annex F of prEN1994-1-2 [14].

1.1.2 Model "AFCC"

The model "AFCC" is a balanced summation model for the calculation of the fire resistance of composite columns with partially concrete encased steel sections, for bending around the weak axis, exposed to fire all around the column according to the standard temperature-time curve [1, 2].

This model corresponds to Annex G of prEN1994-1-2 [14].

1.1.3 Model "HS-CC"

The model "HS-CC" is for concrete filled hollow sections exposed to fire all around the column according to the standard temperature-time curve.

This model corresponds to Annex H of prEN1994-1-2 [14].

1.1.4 Nomogram

The Nomogram allows to design protected or not protected steel beams or steel columns exposed to fire according to the standard temperature-time curve [4].

This procedure corresponds to prEN1993-1-2 [13] and is presented in Chapter I, page 63 to 67 of this Handbook 5.

1.2 Advanced calculation models

These models may be used in association with any temperature-time heating curve, provided that the material properties are known for the relevant temperature range. Furthermore they are used for individual members, for subassemblies or for entire structures, and are able to deal with any type of cross section.

Hence advanced calculation models are much more complex, so require a given degree of knowledge and expertise and consequently may no more be used free of charge. For that reason no advanced calculation model has been incorporated in this CD.

2 FIRE DEVELOPMENT MODELS

2.1 Simplified fire model AA/EC1-1-2

The parametric temperature time-curves, given by the Annex A of EN1991-1-2 [9], constitute a simplified fire model, which may be used at least in the frame of a predesign. The corresponding theory is illustrated in the background document [7] and is presented in Chapter I, page 36 to 38 of this Handbook 5.

2.2 Advanced fire model OZONE 2.2.2

This software constitutes an advanced fire model according to Annex D of EN1991-1-2 and is illustrated in the background document [8]. It permits the combination of a localized fire source with a two zone situation, as well as the possible transition from a two zone to a one zone situation. The development of this two zone model called "OZONE" has been undertaken at the University of Liège [10, 11, 12] and is presented in Chapter I, page 39 to 42 of this Handbook 5 .

3 PROBABILISTIC MODEL VaP 1.6

This software permits to analyse a limit state function based on a number of variables following different types of distributions. The software called VaP "Variables Processor" was developed by Professor Jörg Schneider at the ETHZ [6] and predicts a.o. the failure probability $p_f = \Phi(-\beta)$ connected to the physical aspect described by the limit state function, as well as the corresponding safety index β [5].

REFERENCES

- [1] Jungbluth O., Hahn J.; Traglastenkatalog für ARBED AF30/120 Verbundstützen auf Walzträgerbasis. Trade ARBED, Luxemburg, 1982.
- [2] ECCS-TC3; Calculation of the fire resistance of centrally loaded composite steel-concrete columns exposed to the standard fire, Technical Note N° 55/ECCS. Brussels, 1988.
- [3] Cajot L.G., Schleich J.B., Hass R.; The fire design of composite beams according to the Eurocode 4, Part 10, Structural fire design. Nordic Steel Colloquium, Odense. Danmark, 9-11.9.1991.
- [4] ECCS-TC3; Fire resistance of steel structures-Nomogram, Technical Note N° 89, Brussels, 1995.
- [5] Schneider, J.; Introduction to safety and reliability of structures. Structural Engineering Documents, N°5, International Association for Bridge and Structural Engineering, IABSE, Zurich, 138 p., 1997.
- [6] Schneider J.; VaP, Variables Processor. Institut für Baustatik und Konstruktion, ETHZ, Zürich, 15.2.1999.
- [7] CEN; Background Document CEN/TC250/SC1/N298A - Parametric temperature-time curves according to Annex A of EN1991-1-2, 9.11.2001.
- [8] CEN; Background Document CEN/TC250/SC1/N299A- Advanced fire models according to 3.3.2 of EN1991-1-2, 9.11.2001.
- [9] EN1991-1-2, Eurocode 1 – Actions on structures, Part 1.2 – Actions on structures exposed to fire. CEN Central Secretariat, Brussels, DAV 20.11.2002.
- [10] Schleich J.B., Cajot L.G.; Natural fire safety concept. ECSC Research 7210-SA/522 etc., B-D-E-F-I-L-NL-UK & ECCS, 1994-98, Final Report EUR 20360EN, 2002.
- [11] Cadorin J.F.; Compartment Fire Models for Structural Engineering. Thèse de doctorat, Université de Liège, 17.6.2003.
- [12] Schleich J.B., Cajot L.G.; Natural Fire Safety Concept / Full scale tests, Implementation in the Eurocodes & Development of userfriendly design tools. ECSC Research 7210-PR/060 etc., D,F,FI,L,NL & UK, 1997-2000, Final Report EUR 20580EN, 2003.
- [13] CEN; prEN1993-1-2, Eurocode 3 – Design of steel structures, Part 1.2 – General rules – Structural fire design. CEN Central Secretariat, Brussels, Stage 49 draft, June 2004.
- [14] CEN; prEN1994 -1-2, Eurocode 4 – Design of composite steel and concrete structures, Part 1.2 – General rules – Structural fire design. CEN Central Secretariat, Brussels, Stage 49 draft, December 2004.